The University of Sheffield

Thesis Title

An investigation of the PsbS protein isolated from spinach chloroplast membranes

Author:	Mark Kevin Aspinall-O'Dea
Degree for Submission:	Doctor of Philosophy (PhD)
Department:	Molecular Biology and Biotechnology
Date of Submission:	September, 2004

Abstract

Dissipation of excess light energy in plant photosynthetic membranes plays an important role in the response of plants to the environment, providing short-term balancing between the intensity of sunlight and photosynthetic capacity. The carotenoid zeaxanthin and the photosystem II subunit PsbS play vital roles in this process, but the mechanism of their action is largely unexplained. This thesis reports a novel procedure for the extraction of the PsbS protein from spinach thylakoids, including a detailed account of the developmental process and characterisation of the isolated protein. The ability of the PsbS protein to bind xanthophyll cycle carotenoids *in vitro* was assessed, leading to the observation that the isolated protein was able to bind exogenous zeaxanthin, the binding resulting in a strong red shift in the absorption spectrum, and the appearance of characteristic features in the resonance Raman spectrum and a distinct circular dichroism spectrum, indicating pigment–protein, as well as specific pigment–pigment, interaction. A strong shift in the absorption spectrum of PsbS phenylalanine residues after zeaxanthin binding was observed. It is concluded that zeaxanthin binding to PsbS is the origin of the well known energy dissipation-related 535-nm absorption change. The ability of this PsbS-zeaxanthin complex to affect the rate of chlorophyll fluorescence quenching of the major LHCII antenna protein is detailed, revealing an increase in the rate of quenching, whilst the magnitude of quenching remained constant. The altered properties of zeaxanthin and PsbS after *in vitro* reconstitution and their subsequent effect on LHCIIb provide the first direct indication about how they regulate energy dissipation.

Acknowledgements

This PhD thesis does not simply represent the collective work of the last four years, as this goal has been the focus of my family and myself since I was nine years old. Throughout that time my family have supported me in everyway imaginable, having made huge sacrifices in order to give me the best possible start in life. It is safe to say they have succeeded; I will always be indebted to them. To mum and dad, this has only been made possible by your unfaltering love and support; I hope this makes you proud, as it is your achievement too. To my nan, who has been there even when others have not, I will always love you. To uncle Arthur, thank you for all your help over the years, I have always been grateful.

Professor Peter Horton gave me an opportunity; he had faith in my abilities and that is something I will always be thankful for. Your help in completing this thesis has been invaluable. A special mention should go to Mark Wentworth; after five years I consider you a friend, and through your knowledge and support you have made my life easier over that time. Also Alexander Ruban, after many a stimulating conversation I believe you have helped me to become a better scientist, if not a better person. Thank you both. To Pam Scholes, always there when I needed help, and incredibly you always seemed to provide a solution. I would also like to mention Dr Chi Wong, for his assistance during the final stages of my PhD, my examiners for taking the time to read this thesis, and the BBSRC for funding this project. Finally, thanks to the colleagues I have spent much of the last four years with. Many of you are now close friends, and in some part you have all contributed to this thesis. Good luck in the future, I wish you all the very best.

Mark Aspinall-O'Dea

"You can imagine anything you don't have. Even the future. The future more than anything"

Father of Walter de Silva
Chief Designer - Audi

Abbreviations

ATP	-	Adenosine triphosphate
CAB	-	Chlorophyll *a/b* binding proteins
^{3}Car	-	Triplet state carotenoid
CF_o	-	ATP-synthase integral membrane complex
CF_1	-	ATP-synthase extrinsic stroma exposed complex
Chla	-	Chlorophyll *a*
^{3}Chla	-	Triplet state chlorophyll *a*
Chlb	-	Chlorophyll *b*
CK2	-	Caesin Kinase II
Cyt b_{559}	-	Cytochrome b_{559} complex
Cyt b_6f	-	Cytochrome b_6f complex
DCMU	-	3-(3,4-dichlorophenyl)-1, 1-dimethylurea
Deriphat 160	-	Disodium *N*-lauryl-β-iminodipropionate
DTT	-	Dithiothreitol
ELIPs	-	Early light inducible proteins
FD	-	Ferredoxin
FNR	-	Ferredoxin-$NADP^+$ Reductase
ΦF	-	Fluorescence yield
LHCII	-	Photosystem II light harvesting antenna system
LHCIIb	-	Major light harvesting complex
MGDG	-	Monogalactosyldiacylglyceride
Mn	-	Manganese
$NADP^+$	-	Nicotinamide adenine dinucleotide phosphate
NADPH	-	Nicotinamide adenine dinucleotide phosphate (reduced)
NPQ	-	Non-photochemical quenching of chlorophyll fluorescence
$^1O_2^*$	-	Singlet state oxygen
OEC	-	Oxygen evolving complex
^{3}P680	-	P680 triplet chlorophyll
PbRC	-	Bacterial reaction centre
PC	-	Plastocyanin
PG	-	Phosophatidylglycerol
ΔpH	-	Change in transthylakoid pH gradient
Pheo	-	Pheophytin
pI	-	Isoelectric point

PSI	-	Photosystem I
PSII	-	Photosystem II
PQ	-	Plastoquinone
PQH_2	-	Plastoquinol
RC	-	Reaction centre
qE	-	Rapidly relaxing component of NPQ
qI	-	Irreversible/very slowly relaxing component of NPQ
qN	-	Non-photochemical quenching
qT	-	Slowly relaxing component of NPQ
SDS-PAGE	-	Sodium dodecyl (lauryl) sulfate - polyacrylamide gel electrophoresis
T½	-	Half-time
Tyr_z	-	Photosystem II D1 protein, Tyrosine Z amino acid
VDE	-	Violaxanthin deepoxidase
WT	-	Wild type
ZE	-	Zeaxanthin epoxidase

Contents

	Abstract	i
	Acknowledgments	ii
	Quotation	iii
	Abbreviations	iv
	Contents	vi

General Introduction – Chapter One

1.	Introduction	9
1.2	Photosynthetic phases – 'light' and 'dark' reactions	10
1.3	An overview of electron transport in higher plants	11
1.4	Photosystem II	12
	1.4.1 Reaction Centre (PSII)	12
	1.4.2 Inner (distal) antenna and PSII-core complex	14
	1.4.3 Oxygen-evolving complex	15
	1.4.4 S-state model of oxygen evolution	16
	1.4.5 Spatial organisation of PSII electron transport chain cofactors	16
1.5	PSII light harvesting antenna	18
	1.5.1 Major antenna complex – LHCIIb	19
	1.5.2 Minor antenna complex – CP29	25
	1.5.3 Minor antenna complex – CP26	27
	1.5.4 Minor antenna complex – CP24	28
	1.5.5 Related Lhcb proteins – PsbS	28
	1.5.6 Related Lhcb proteins – LHCIIe/Early light induced proteins (ELIPs)	28
	1.5.7 Macromolecular organisation of the Photosystem II antenna	28
1.6	Cytochrome bf complex	31
1.7	Photosystem I	31
	1.7.1 Photosystem I reaction centre core	32
	1.7.2 Photosystem I stromal side subunits	32
	1.7.3 Photosystem I lumenal side subunits	33
	1.7.4 Additional PSI components – PsaH, PsaL and PsaO Cluster	33
	1.7.5 Additional PSI components – PsaK and PsaG	34
	1.7.6 PSI structure	34
1.8	ATP-synthase complex	36
1.9	Photosynthetic regulation	36
	1.9.1 Cyclic electron transport	37
	1.9.2 State transitions	37
	1.9.3 Carotenoids	37
1.10	Photoprotection in higher plants	38
	1.10.1 Chlorophyll fluorescence yield and quenching	39
	1.10.2 Non-photochemical component of chlorophyll fluorescence quenching	40
1.11	The xanthophyll cycle	41
	1.11.1 qE – an historical overview	42
	1.11.2 qE – the site of energy dependent quenching	43
	1.11.3 Relationship between qE and the xanthophyll cycle	44
	1.11.3i Direct quenching mechanism: molecular gearshift model	45
	1.11.3ii Indirect quenching mechanism: allosteric qE model	46
	1.11.4 Genetic Analysis	50
1.12	PsbS	52
1.13	Aims	56

Materials & Methods – Chapter Two

2.1	General laboratory chemicals	58
2.2	Plant material	58
2.3	PSII membrane preparation (BBY particles)	58
2.4	Preparation of PSII antenna complexes by iso-electric focusing (IEF)	59
	2.4.1 Gel preparation	59
	2.4.2 Pre-focusing of the gel	59
	2.4.3 Sample preparation	60
	2.4.4 Loading and running the sample	60
	2.4.5 Sample elution – pH 3.5-5	60
	2.4.6 Sample elution – pH 5.0-7.0/3.0-9.0	60
2.5	Preparation of PSII PsbS protein from BBY particles	60
2.6	Chloroform/methanol extractions	61
2.7	DCCD binding	61
2.8	Isolation, purification and identification of plant carotenoids	61
	2.8.1 Large-scale pigment extractions	62
	2.8.2 Preparation of standard thin layer chromatography (TLC) plates	62
	2.8.3 TLC tank preparation	62
	2.8.4 TLC purification of extracted carotenoids	63
	2.8.5 Carotenoid identification	63
	2.8.6 Identification of violaxanthin by its isomerisation into auroxanthin	64
2.9	Sucrose Gradients	64
2.10	Measurement of the *in vitro* chlorophyll fluorescence quenching of isolated PSII antenna complexes	65
2.11	SDS-polyacrylamide gel electrophoresis (SDS-PAGE)	65
2.12	Deriphat polyacrylamide gel electrophoresis (native green gels)	66
2.13	Staining of polyacrylamide gels	66
	2.13.1 Silver stain	66
	2.13.2 Coomassie brilliant blue staining	67
2.14	Drying polyacrylamide gels	67
2.15	Western blotting	67
	2.15.1 Electro-blotting and antibody labelling	67
	2.15.2 Antibody detection using ECL ™ detection kit (Amersham)	68
2.16	Concentration using Centricon® centrifugal filter devices	68
2.17	Determination of chlorophyll concentration	68
2.18	Absorption spectroscopy	69
2.19	Circular dichromism (CD)	69
2.20	Resonance Raman spectroscopy	69
2.21	PsbS sequence analysis	69
	2.21.1 Reverse phase HPLC	70
	2.21.2 Mass spectrometry	70
2.22	Colloidal blue staining (Novex)	70

PsbS Isolation and Characterisation – Chapter Three

3.1	Introduction	72
3.2	Isolation of a 22kDa polypeptide by iso-electric focusing (IEF)	73
3.3	Selective solublisation of PsbS	87
3.4	Optimisation of Na-Cholate extraction	90
3.5	Determination of the primary sequence of the 22kDa extracted protein	94
3.6	Absorption spectra	94
3.7	Analysis of secondary structure by circular dichromism	96
3.8	DCCD binding properties of PsbS	99
3.9	PsbS homodimer	100
3.10	Discussion	102
3.11	Concluding remarks	103

Analysis of PsbS-Zeaxanthin Interactions – Chapter Four

4.1 Introduction 104
4.2 Spectral characterisation of Xanthophyll-Cycle carotenoids 104
4.3 Development of an effective reconstitution technique 105
4.4 Reconstitution of the PsbS protein 109
4.4.i Reconstitution – pigment/protein ratio effect at low component concentration 109
4.4.ii Reconstitution – effect of temperature 111
4.4.iii Reconstitution – pigment drying using solvents 113
4.4.iv Reconstitution – use of high component concentrations 114
4.5 Analysis of PsbS interaction of Antheraxanthin and Violaxanthin 118
4.7 Analysis of reconstituted PsbS interaction with LHCII components using *in vitro* fluorescence quenching technique 119
4.7.1 Introduction 119
4.7.2 Fluorescence Quenching 120
4.8 Discussion 125

General Discussion – Chapter Five

5.1 Introduction 129
5.2 PsbS – the relationship with pH 129
5.3 PsbS – the relationship with the xanthophyll cycle 130
5.4 PsbS – a model for the role of PsbS in qE 131
5.5 Conclusion 133

References – Chapter Six

6 References 136

Appendix – Publications

7 Publications 157

Chapter One

General Introduction

General Introduction

1. Introduction

Photosynthetic organisms require quanta of light energy to drive the conversion of inorganic H_2O and CO_2 into complex organic sugars. The process of oxygenic photosynthesis enables this through the reduction of $NADP^+$ coupled to oxygen evolution. It is thought to be an important factor in the evolution of multicellular eukaryotic organisms, as it provides almost all the reduced carbon required for sustainable life, along with the vast majority of molecular oxygen predominantly employed as the terminal electron acceptor in respiration.

The photosynthetic machinery in plants is located in specialised organelles known as chloroplasts. This organelle consists of three membranes, two forming a smooth outer envelope, which surround the elaborately folded inner membrane known as the thylakoid. The aqueous phase known as the stroma is found between the thylakoid and the outer membranes, and it contains the enzymes required for carbon fixation. The differentiation of the thylakoid membrane into granal and stromal regions (also referred to as stacked/appressed and unstacked/non-appressed regions, respectively) is a morphological reflection of the non-random distribution of the photosystems II and I between the appressed and non-appressed domains known as lateral heterogeneity.

The thylakoid consists of a continuous membrane organised into a 3 dimensional network with a single interior aqueous phase known as the lumen. Numerous models have been proposed for thylakoid structure, initially being derived from the early electron microscopy performed during the 1960s (Weier., 1963), with more recent versions proposed to illustrate lateral heterogeneity in the thylakoid membrane (Andersson & Anderson., 1980). To a greater or lesser extent, all of these models fail to accurately depict the thylakoid membrane. The generally accepted model was proposed by Paolillo., (1970), and later confirmed by Brangeon & Mustárdy., (1979). It displays the thylakoid membranes with multiple right-handed helices of stroma lamellae wrapped round a cylindrical grana forming a contiguous system. Recently, a computerised model has been generated (Figure 1.1), based upon electron micrographs from serial sections of granum-stroma assemblies (Mustardy & Garab 2003). The functional justification of the thylakoid architecture is the lateral heterogeneity of the appressed and non-appressed regions within the thylakoid membrane where the protein environment varies considerably. Photosystem I and ATP synthase dominate the unstacked regions of the membrane whilst the majority of Photosystem II is located in the granal stacks, providing a balance of energy between the two photosystems. The abundance

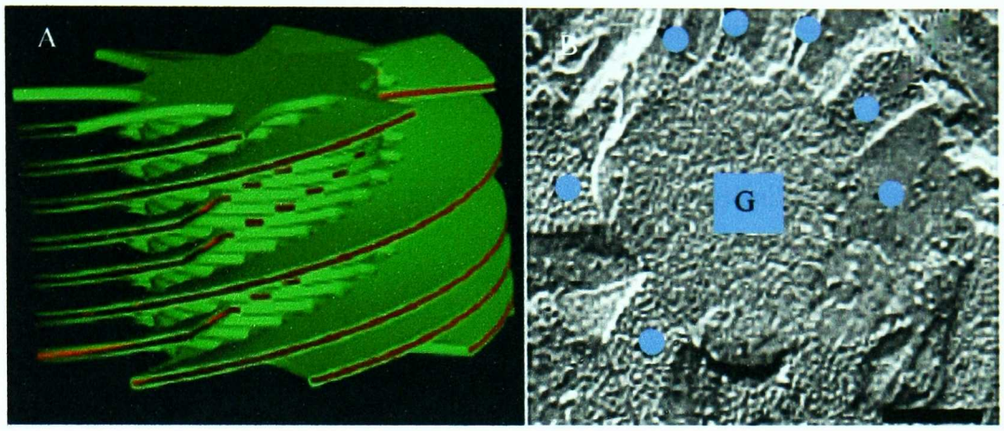

Fig 1.1 – Computer representation of the thylakoid membrane modified from Mustardy & Garab 2003. A: Depicts the helical arrangement of stroma membranes around the granum. B: Electron micrograph of thylakoid G – grana, Blue circles – stroma membranes.

of LHCII in the granum has led to suggestions that these antennae complexes play a structural role in the thylakoid.

1.2 Photosynthetic Phases – 'Light' and 'Dark' Reactions

The first of the two photosynthetic phases require photons of light energy to produce NADPH and ATP, through a series of biochemical events known as the light reactions, which occur in the chloroplast thylakoid membranes. Numerous multi-subunit pigment-protein complexes bind both chlorophyll and carotenoid molecules, along with other cofactors, in a specific orientation that maximises the efficiency of light capture and the subsequent transfer of this energy along the electron transport chain.

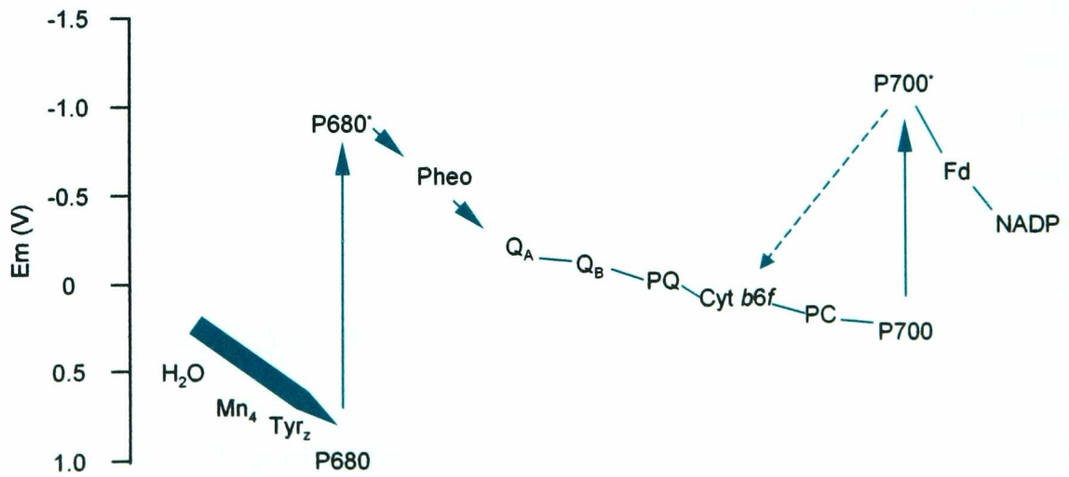

Figure 1.2 – The Z-scheme for photosynthetic electron transport. Unbroken line, linear electron transport. Dashed line, cyclic electron transport.

The vast majority of these pigments function to harvest light energy and increase the effective surface area for light absorption. The excitation energy is rapidly transferred to the reaction centres of the two photosystems where it drives charge separation and effects the release of an electron, which is passed along a series of electron carriers as illustrated in the Z-scheme. Higher plants transfer electrons from H_2O to ferredoxin, the latter being able to reduce $NADP^+$ to NADPH due to its reduction potential of approximately –0.42 V. Simultaneously, protons are transferred across the thylakoid membrane from the stroma to the lumen, creating a proton motive force employed by ATP synthase to drive ATP synthesis.

The second of the two phases of photosynthesis occur in the stroma and are known as the 'dark' reactions, utilising the NADPH and ATP produced during the 'light' reactions to assimilate CO_2 into carbohydrate.

1.3 An Overview of Electron Transport in Higher Plants

Charge separation occurs following excitation of the PSII reaction centre chlorophyll P680 and an electron is passed onto Q_A via a molecule of pheophytin, forming the highly oxidised species, $P680^+$. $P680^+$ is reduced by extraction of an electron from a tyrosine residue on the D1 subunit of PSII. An electron obtained from the splitting of water in the oxygen-evolving complex subsequently reduces the tyrosine residue.

The electron on Q_A is passed onto a molecule of plastoquinone bound to the Q_B site which, after accepting a second electron, becomes protonated and is then released as plastoquinol (PQH_2). Electrons from plastoquinol are then passed via the cytochrome b_6f (cyt b_6f) complex to a second mobile electron carrier called plastocyanin (PC). A second charge separation event within the reaction centre of PSI (P700) liberates a second electron which is passed along a series of carriers to the terminal electron acceptor ferredoxin (Fd). Ferredoxin is then used to drive the reduction of $NADP^+$ to NADPH by the Ferredoxin-$NADP^+$ oxidoreductase (FNR). An electron from plastocyanin finally reduces the PSI special pair chlorophyll $P700^+$ back to P700.

Translocation of protons across the thylakoid membrane occurs concomitantly with the vectoral transport of electrons from water to $NADP^+$. The pH gradient is formed by the production of protons through water splitting in the oxygen-evolving complex of PSII and lumenal proton release occurs following the oxidation of plastoquinol to plastoquinone (PQ)

by the cyt b_6f complex. The proton motive force generated by the proton gradient across the thylakoid membrane is subsequently used by the ATP synthase to form ATP.

1.4 Photosystem II

Photosystem II (PSII) is a multisubunit protein-cofactor complex found abundantly in the appressed (granal) regions of the thylakoid membrane. It functions as a water-plastoquinone oxidoreductase (for reviews see Hankamer et al. 1997; Barber 1998), with a complement of at least 28 subunits which collectively form the four principal components of PSII:

1. Reaction Centre
2. Inner (distal) antenna and RC-core Complex
3. Oxygen Evolving Complex (OEC)
4. Peripheral Antenna

1.4.1 Reaction Centre (PSII)

Found at the heart of PSII, the Reaction Centre (RC) incorporates the chloroplast encoded D1 and D2 polypeptides (*psb*A and *psb*D genes respectively) which form a heterodimer. The cofactors involved in charge separation and electron transport bind to the RC's dimeric core, and these include the primary electron donor P680 reaction centre chlorophylls, the primary electron acceptor, a molecule of pheophytin *a*, the PQ secondary electron acceptors Q_A and Q_B, and finally a non-haem iron molecule. The remaining reaction centre components consist of the cyt b_{559} 9kDa α and 4kDa β subunits, encoded by the chloroplast *psb*E and *psb*F genes, respectively. These polypeptides are known to ligate a single haem group, however, the function of cytochrome b_{559} still remains unclear. Current opinion point toward a photoprotective role by charge recombination during photoinhibitory periods (Whitmarsh & Pakrasi 1996). Lastly, cross-linking experiments (Tomo et al. 1993; Shi et al. 1999) and a high resolution electron density map (Zouni et al. 2001) have located the low MW PsbI and PsbX proteins close to the reaction centre D2 and cytochrome b_{559} proteins. The functions of these proteins are presently unknown.

Previous studies provided by electron microscopy of intact, active PSII at 15-30Å resolution (Nield et al. 2000), and electron crystallography on 2-D crystals of PSII-fragments at 8Å resolution, which lacked water oxidising activity, have recently been superseded by the x-ray crystal structures of PSII. The first, of the PSII structures is from *Thermosynechococcus*

elongatus (formerly *Synechococcus elongatus*) at 3.8Å resolution and consisted of 36 transmembrane helices (Zouni et al. 2001), and the second, from *Thermosynechococcus vulcans* at 3.7Å resolution that provided structural detail of major large PSII constituents not identified in the previous structure (Kamiya & Shen 2003). Significant detail has been observed regarding the spatial organisation of protein subunits, and cofactors, on the basis of crystal structures fully active in water oxidisation (Shen & Kamiya 2000; Kuhl et al. 2000; Zouni et al. 2001). The transmembrane α-helices of the PSII reaction centre D1-D2 heterodimer exist as two 5-helix groups arranged in interlocking semi-circles in the form of a handshake motif. It is thought that some of the D1 regions are close enough to the Mn-cluster to provide coordination for it, whilst helix A of D2 is in close proximity to the α and β subunits of cyt b_{559} (Kamiya & Shen 2003). The stromal side of the D2 protein is the location of the Q_A binding site (Barry et al. 1994; Svensson et al. 1996; Xiong et al. 1998) which tightly binds the PQ molecule. The Q_B binding site located on the D1 subunit was found unoccupied in the model presented by (Zouni et al. 2001). It is thought that the PQ bound to Q_B is disassociated during preparation of the crystals (Zouni et al. 2001).

The α-helical arrangements of the PSII-RC D1 and D2 subunits are structurally and functionally related to the light (L) and medium (M) subunits of the bacterial reaction centre (PbRC) (Michel & Deisenhofer 1988; Nitschke & Rutherford 1991; Rhee et al. 1997; Rhee et al. 1998; Hankamer et al. 1999; Zouni et al. 2001; Jordan et al. 2001; Kamiya & Shen 2003). A high resolution crystal structure at 3Å has been determined for the PbRC (Deisenhofer et al. 1985) and subsequently improved to ~2.5Å (for review see Fyfe & Jones 2000). This resemblance is also seen with the five carboxy-terminal helices of PsaA and PsaB in PSI (Schubert et al. 1998).

The stoichiometry of the cytochrome b_{559} subunit in relation to the PSII-RC is a highly controversial issue, which has yet to be concluded. The current structural models by (Zouni et al. 2001) and (Kamiya & Shen 2003) have identified only one cyt b_{559} subunit per reaction centre (by virtue of its haem iron) located in the position proposed by (Rhee et al. 1998) and (Rhee et al. 1997). In support of this data, a ratio of 1.25:1 cyt b559 to D1 polypeptide has been proposed by (Yruela et al. 2003) in a recent study, which highlights the variations of cyt b_{559} content in PSII preparations depending on the procedures used. The α and β subunits of cyt b_{559} form single transmembrane α-helices, and are distinguished by virtue of the longer α-subunit C-terminus which extends into the lumen.

1.4.2 Inner (distal) Antenna and PSII-core Complex

The reaction centre is surrounded by the other PSII subunits and the PSII-core is the minimal unit required for oxygen evolution. It is known to include the chlorophyll *a* (chla) binding inner (distal) antenna proteins CP43 and CP47, encoded by the chloroplast *psb*C and *psb*B genes respectively, the oxygen evolving complex (OEC) and a number of small polypeptide subunits thought to have either structural or regulatory roles.

The inner antenna system has been shown to bind 26 chla molecules (Zouni et al. 2001; Kamiya & Shen 2003) close to the lower limit of the range proposed by (Ghanotakis et al. 1999), whilst being significantly less than the 40 – 50 molecules predicted by (Bassi et al. 1996). CP43 and CP47 are also thought to bind the carotenoids β-carotene and potentially lutein (Bassi et al. 1996) however current structural data cannot confirm this (Zouni et al. 2001; Kamiya & Shen 2003). The topology of CP43 and CP47 suggested that both proteins consisted of 6 transmembrane helices (Vermaas et al. 1987; Bricker 1990) and initial confirmation with respect to CP43 was provided by (Sayre & Wrobelboerner 1994). With the advent of the 8Å structure of the PSII reaction centre from spinach, this prediction was confirmed for CP47, which could be clearly seen to contain 6 transmembrane helices (Rhee et al. 1997; Rhee et al. 1998). During the same period (Harrer et al. 1998) used crosslinking techniques to show that the homologous inner antenna proteins flank both sides of the reaction centre D1-D2-b_{559} complex, whilst upon acceptor-side photoinhibition of PSII D1 and CP43 were specifically crosslinked (Ishikawa et al. 1999). The crystal structures by (Zouni et al. 2001) and (Kamiya & Shen 2003) confirmed that both CP43 and CP47 consist of 6 transmembrane α-helices arranged as a trimer of dimers. The assignment is consistent with the fact that CP47 binds more chla molecules than CP43 (Kamiya & Shen 2003), however both subunits co-ordinate the antenna chla in the open space between the dimers. The centre-to-centre distances between pairs of nearest chlorophylls are in the range of 8.5-13.5Å (Zouni et al. 2001). These pigments form two layers close to the stromal and lumenal sides of the membrane in each subunit. This is consistent with the observation by (Barry et al. 1994) that the majority of conserved histidines (12 in CP43 and 8 in CP47) are located toward the stromal and lumenal ends of the proteins. Furthermore, the inner antenna proteins are structurally similar to each other (particularly in the transmembrane regions) whilst sharing homology with the six N-terminal α-helices of PsaA and PsaB in PSI (Rhee et al. 1997; Rhee et al. 1998; Schubert et al. 1998; Jordan et al. 2001).

The luminal regions of CP43, CP47, D1 and D2 together with the three extrinsic OEC proteins form a shield around the Mn-cluster (discussed below). Current structural models

show the lumenal part of CP47 in close proximity to those of D2, the 33kDa PsbO subunit and the 12kDa subunit found in cyanobacteria. It has been suggested that possible interactions between these proteins could form important binding sites for the OEC (Kamiya & Shen 2003) and have a role in chloride sequestration (Bricker & Frankel 2002). The crystal structure presented by (Kamiya & Shen 2003) has improved upon the 9Å map provided by (Hankamer et al. 1999), and shown the large E loop of CP47 to be particularly close to the extrinsic PsbO protein. This finding supports the numerous reports proposing potential association and interaction between these proteins (Seidler 1996; Enami et al. 1997; Bricker & Frankel 2002), and the possibility that CP47 could act to stabilise the oxygen-evolving complex (Green & Durnford 1996). CP43 is shown to be closely co-ordinated with the D1 protein of the PSII core (Zouni et al. 2001; Kamiya & Shen 2003) and a number of studies have proposed that CP43 acts as the protease, which cleaves the D1 protein during photoinactivation (Salter et al. 1992; Giacometti et al. 1992). It is thought that the presence of PsbO suppresses the contact between the D1 protein and CP43 (Henmi et al. 2003).

Additionally, a number of small polypeptide subunits of between 4 – 10 kDa form part of the PSII-core complex. The small MW proteins PsbH, PsbK and PsbL have all been implicated in the stabilisation of the PSII dimer, however no consensus regarding these subunits has been reached (Zouni et al. 2001; Kamiya & Shen 2003) and further study is required to better establish their function in relation to PSII. An antisense approach has been used to determine the role of the PsbW protein in *Arabidopsis thaliana*. This technique generated mutants, which displayed PSII dimer destabilisation along with a more general destabilisation of PSII itself (Shi et al. 2000). Finally, an unusual example of a polyprotein has been discovered in relation to the PsbY-1 and PsbY-2 proteins in *Arabidopsis thaliana* (Thompson et al. 1999), both encoded by the same gene. A single preprotein is imported into the chloroplast where it is processed into two integral membrane proteins with the same topology. The function of this polyprotein remains to be ascertained however *in vitro* studies have shown the protein to possess manganese binding capability and arginine metabolising activity (Gau et al. 1998).

1.4.3 Oxygen-evolving Complex (OEC)

The OEC is responsible for water hydrolysis in PSII. It is located on the lumenal surface of the thylakoid membrane and is comprised of a cluster of four manganese atoms bound to the D1/D2 heterodimer surrounded by the extrinsic 33, 23 and 17 kDa peptides. Combined

these form the catalytic site of the complex. PSII components have been shown to evolve O_2 if supplied with high Ca+Cl concentration (Bricker 1992) whilst extrinsic components stabilise the Mn-cluster enabling PSII to evolve O_2 at physiological Ca+Cl concentration. (Ono & Inoue 1984; Bricker & Ghanotakis 1996).

PsbO is the 33 kDa subunit of the OEC found in all oxygenic organisms (Bricker & Ghanotakis 1996), and is encoded by two nuclear *psb*O genes in *Arabidopsis thaliana*. The two isoforms of PsbO separate differently on SDS-PAGE due to differences in pI. The mature products of *psb*O have predicted molecular mass of 26536 Da and 26 542 Da respectively. As the largest PSII lumenal subunit PsbO is the critical component required for Mn-cluster stability (Ono & Inoue 1984), whilst binding Ca^{2+} and Cl^- essential for efficient water oxidation (Bricker & Ghanotakis 1996).

1.4.4 S-state Model of Oxygen Evolution in PSII

Experiments using a series of short (10 μs) saturating flashes on dark adapted chloroplasts showed that oxygen evolution was maximal after every fourth flash. This clearly demonstrates that 4 independent photo-oxidation steps are required to oxidise water and release molecular oxygen. (Kok et al. 1970) suggested a kinetic model called the S-state model to explain this observation. It suggested that each PSII reaction centre behaves as an independent unit. The model also suggests that the manganese cluster exists in one of five different oxidation states (called S_0-S_4). The model proposes that four separate charge separation events in the reaction centre of PSII sequentially removes four electrons from the Mn cluster and that S_4 is an unstable activated complex, which releases molecular oxygen and resets the cycle back to S_0 (Kok et al. 1970). Recent structural data has found the Mn cluster to consist of five manganese atoms, which are ligated to the polypeptide backbone at 4 to 5 locations (Kamiya & Shen 2003).

1.4.5 Spatial Organisation of PSII Electron Transport Chain Cofactors

The recent structural models from (Zouni et al. 2001) and (Kamiya & Shen 2003) have provided detailed information regarding the spatial organisation of chlorophylls and other cofactors with the PSII-RC. The components of the electron transport chain form two symmetrical branches assigned to the reaction centre heterodimeric core proteins D1 and D2, by analogy with the arrangement of the α-helices in the L and M subunits of the PbRC.

The D1-D2 heterodimer has been shown to bind six chlorophyll and two pheophytin molecules, whilst CP43 appears to bind 13 chlorophylls with the location of one molecule altered between the two species *Thermosynechococcus elongatus* and *Thermosynechococcus vulcans* used for structural studies (Zouni et al. 2001; Kamiya & Shen 2003). However, CP47 has been found to bind an additional chlorophyll molecule in *Thermosynechococcus vulcans* bringing its total to 17 rather than the 16 found by (Zouni et al. 2001).

Two chlorophyll *a* molecules P_{D1} and P_{D2} have been highlighted as potential candidates for P680. Lumenally located, they are arranged parallel in relation to each other and perpendicular to the membrane plane (Zouni et al. 2001; Kamiya & Shen 2003). The large separation of these chlorophyll molecules provides only weak excitonic coupling, and, as such, they are regarded as monomeric in nature. The unpaired electron in $P680^{\bullet+}$ is probably located on the D1 protein which lies in close proximity to Tyr_z, the immediate electron donor to the cationic radical (Zouni et al. 2001).

The crystal structure by (Zouni et al. 2001) found two spectroscopically unidentified chlorophyll *a* molecules Chl_{D1} and Chl_{D2}, termed accessory chlorophylls, located on the stromal side of the membrane and tilted 30° against its plane, like that of the PbRC (Zouni et al. 2001), separation of which correlates well with that of $Pheo_{D1}$-$Pheo_{D2}$. The reaction centre chlorophylls appear to display stronger interactions than those between the reaction centre chlorophylls and accessory chlorophylls (Kamiya & Shen 2003). The current structural models favour the "multimonomer" model proposed by (Barber & Archer 2001) and (Diner & Rappaport 2002) for PSII.

In the electron transport chain two pheophytin molecules, $Pheo_{D1}$ and $Pheo_{D2}$, follow the accessory chlorophylls. Q_A is found 12Å from $Pheo_{D1}$ and 10.5Å from the non-haem iron of PSII (Zouni et al. 2001). $P680^{\bullet+}$ is located ~27Å from $Q_A^{\bullet}$ as shown by paramagnetic resonance (Zech et al. 1997) and the crystal structure by (Zouni et al. 2001). As previously mentioned the Q_B site has been found unoccupied in the current structural models. An additional two chlorophyll *a* molecules were assigned to the spectroscopically identified species $Chlz_{D1}$ and $Chlz_{D2}$ (Zouni et al. 2001), coordinated by His 118 in D1 and His117 in D2 (Schelvis et al. 1994; Ruffle et al. 1998). The Cyt b_{559} haem-iron located 27Å apart from $Chlz_{D2}$ and ~8Å from the stromal side of the membrane (Zouni et al. 2001).

The most recent crystal structure of PSII suggests that secondary electron transfer may preferentially involve the cyt b_{559}-Car-RC pathway, and that electron transfer involving $Chlz_{D2}$-Car-RC may also be possible (Zouni et al. 2001; Kamiya & Shen 2003). This

proposal does not, however, take into account the redox potentials of the various components within the reaction centre (Kamiya & Shen 2003), and as a result an alternative pathway could prove to be more efficient. Moreover, the location of these carotenoids near to the reaction centre chlorophylls could enable them to contribute to excess energy dissipation during periods of light stress in order to maintain photosynthetic efficiency.

1.5 PSII Light harvesting Antenna

The primary light harvesting pigments in the thylakoid membranes of higher plants are chlorophylls *a* and *b*. Recent structural data shows the precise orientation these chromophores assume within the antenna system (Kuhlbrandt et al. 1994; Liu et al. 2004) in order to perform the functions of light harvesting and photoprotection. Early theories, however, proposed that chlorophyll molecules would be free unbound constituents of the thylakoid membranes lipid matrix, leading to the suggestion that the first experimentally observed chlorophyll-protein complexes were artefacts resulting from the non-specific association of chromophores with solublised membrane proteins. To challenge these theories a number of groups employed different solublisation and electrophoresis techniques that enabled them to isolate the majority of chlorophyll present in the thylakoid membrane ligated to specific binding proteins (Thornber 1975; Anderson et al. 1978). These findings were further supported by (Markwell et al. 1979) who, using the zwiterionic detergent deriphate 160 (disodium *N*-lauryl-β-iminodipropionate), found all thylakoid membrane chlorophylls specifically bound to a number of different chlorophyll-protein complexes, each having a different pigment content and size.

These complexes are collectively known as the chlorophyll a/b binding (CAB) proteins, which bind ~50% of thylakoid chla, all chlb and the majority of xanthophyll carotenoids in the thylakoid membrane (for reviews see Thornber et al. 1993; Jansson 1994; Bassi et al. 1996; Green & Dunford 1996). Difficulties in studying individual proteins from the CAB family emerged upon the discovery that the apparent molecular weights of all these proteins were found in the range of 20-30 kDa on SDS-PAGE, whilst structural similarities lead to cross-reactivity of anti-CAB antibodies. Overcoming these issues has involved the isolation and characterisation of genes encoding CAB polypeptides from a wide variety of plant species, along with enhanced protein isolation and micro sequencing techniques. More than 20 CAB genes have been characterised (for review see Jansson 1999), and divided into two groups known as *lhca* and *lhcb*. The former gene group encode for PSI antennae complexes as described in section 1.7, whilst the latter are primarily associated with PSII and will be described below.

	Lutein	Neoxanthin	Violaxanthin
LHCIIb	2	1	Trace – 0.5
CP29	0.7 – 2.0	0.5 – 1.0	1.0 – 2.0
CP26	1.0 – 2.0	0.5 – 1.0	0.5 – 1.0
CP24	1.5 – 2.8	0 – 1.0	0.5 – 1.0

Table 1.1 – Carotenoid composition of individual LHCII antenna complexes. Data was compiled using Thornber et al. (1993); Ruban et al. (1994a); Phillip & Young (1995); Bassie et al. (1996); Liu et al. (2004) and is expressed as number of molecules of carotenoid per LHCII monomer.

The light harvesting antenna of PSII exists as two distinct pigment-protein groups, the first of which are characterised by the chla binding proteins CP43 and CP47 forming the PSII core in conjunction with the RC (section 1.4.1). Surrounding the PSII core are a group of proteins which form the peripheral antenna of PSII, binding both chla and chlb along with the carotenoids lutein, neoxanthin and the xanthophyll cycle component violaxanthin (Thornber et al. 1993; Ruban et al. 1994b; Bassi et al. 1996; Ruban & Horton 1999; Ruban et al. 2001a; Liu et al. 2004). The Lhcb polypeptides can be divided into two groups, the major light harvesting polypeptides Lhcb1 – 3 that form trimeric LHCIIb, and the monomeric minor antenna CP29 (*lhcb4*), CP26 (*lhcb5*) and CP24 (*lhcb6*).

1.5.1 Major Antenna Complex – LHCIIb

The major chl a/b binding antennae complex of PSII, LHCIIb constitutes more than 40% of the photosynthetic membrane protein and binds ~50% of the total chl present in the thylakoid membrane. Oxygenic photosynthesis is largely reliant upon the efficiency and adaptability of this complex to collect light energy and deliver it to the reaction centres of PSII (review Horton et al. 1996). LHCIIb consists of three polypeptides Lhcb1, Lhcb2 and Lhcb3 of 28, 27 and 25 kDa (Jansson 1999). The complex is thought to exist in a trimeric state *in vivo*, with a molecular weight of ~72 kDa (Peter & Thornber 1991).

LHCIIb has a chl a/b ratio of 1.3 –1.4 (Thornber et al. 1993; Ruban et al. 1994b; Sandona et al. 1998; Ruban et al. 1999), and some years ago a structural model was released indicating the positions of 12 chls, three transmembrane helicies and two of the four known xanthophylls (Kuhlbrandt et al. 1994). The xanthophyll complement per monomer of LHCIIb consists of 2 lutein molecules, a neoxanthin molecule and a transient

substoichiometric amount of violaxanthin (Thornber et al. 1993; Bassi et al. 1996; Ruban et al. 1999).

The structural model described above emerged as a result of electron microscopy on 2D crystals of the LHCIIb protein at 6Å (Kuhlbrandt & Wang 1991), which reinforced a previous prediction from (Green et al. 1991), that each LHCIIb monomer contained three transmembrane α-helices, A – C. Additionally, the monomeric protein was shown to bind between 12 – 15 molecules of chlorophyll with a spacing arrangement indicative of delocalised coupling energy transfer with the complex, whilst employing the Förster mechanism between adjacent complexes (Peter & Thornber 1991). In additional to the carotenoid molecules described above (Ruban et al. 1999) a tightly bound phospholipid component is present in the complex (Nuβberger et al. 1993).

In 1994, a detailed analysis of LHCIIb structural components came in the form of a 3.4Å map from pea (Kuhlbrandt et al. 1994) which showed the intertwining relationship between helix A (43Å) and helix B (51Å) caused by their tilt from the membrane normal. This led to the proposal that a pair of salt bridges capable of stabilising the tertiary structure of the complex exist between two ion pairs (glutamate 65 - arginine 185 and glutamate 180 - arginine 70) located in close proximity to each other as the two helices cross. The third helix (C) proposed by (Green et al. 1991) was found to be the shortest at 31Å in length lying perpendicular to the membrane plane.

The 3.4Å crystal structure describes magnesium ligands for 9 – 12 chlorophyll molecules, with twelve actually visible in the map (Kuhlbrandt et al. 1994). Based upon the chl a/b ratio of the complex, these chromophores were tentatively assigned to 7 chla and 5 chlb and it is thought at least two of these chlorophyll molecules assume unique conformations relative to the other LHCs (Pascal et al. 2000). Site-directed mutagenesis has been used to further eludicate the positions of these chlorophylls in LHCIIb. Although some of these mutants lost more than one chlorophyll molecule and/or more than one type of chlorophyll, the results of these *in vitro* studies unanimously described two groups of four specific binding sites for chla and chlb molecules respectively. The remaining sites exhibiting little selectivity or alternatively were not assigned (Yang et al. 1999; Rogl & Kuhlbrandt 1999; Remelli et al. 1999). More recently a 3D crystal structure of LHCIIb has been solved with 2.72 Å resolution and provides the first x-ray structure of LHCIIb (isolated from *Spinacia Oleracea*) in an icosohedral proteoliposome assembly at atomic detail. Ninety-four percent of the polypeptide chain has been traced along with the accurate locations of 14 chlorophylls unambiguously assigned as 8 chla and 6 chlb. The resulting Chl a/b ratio of 1.33 is

consistent with previous biochemically determined values (Peter & Thornber 1991; Ruban et al. 1999).

Helix D inter-related through an internal pseudo-C_2 axis with an additional short helix, amphipathic in nature, has been located in the BC loop region. A fifth helix, E, is inclined 30° from the membrane normal and displays a length similar to that of helix D (Liu et al. 2004). The corresponding EC loop forms two antiparallel strands, stabilised by an ionic pair (Asp 111 and His 120) located on opposite strands along with a number of hydrogen bonds (Liu et al. 2004).

The monomer interface, or trimerisation region, of LHCIIb trimers is constructed from the amino-terminal domain and carboxyl terminus of the protein monomer, along with the stromal end of helix B, several helix C hydrophobic residues and cofactors associated with these regions of LHCIIb. The trimer core is formed by a total of six chlorophylls, two from each monomer (Liu et al. 2004). The most recent structural data regarding LHCIIb demonstrates the degree to which hydrogen bonding dominates monomer interaction within the trimeric complex, in addition to the structural role of phosphatidylglycerol (PG) in trimer stabilisation. Removal of the first 49 – 51 residues from the LHCIIb polypeptide by proteolytic cleavage results in a loss of PG and consequently, complete trimer dissociation (Liu et al. 2004). This phenomenon has previously been demonstrated by phospholipase A_2 hydrolysis of LHCIIb PG (Nuβberger et al. 1993).

The central ligands for 14 chls were identified as seven amino acid residues, two backbone carbonyls, four water molecules along with the phosphodiester group of a PG (Liu et al. 2004). The coordination mode of chla 611 to the latter is the second case of its kind since its discovery in PSI (Jordan et al. 2001; Liu et al. 2004). The opposite side of the phosphodiester group forms a hydrogen bond with Tyr 44 and an ionic bond with Lys 182. The hydrogen bonding effect between the polypeptide backbone (NH group/side chains) and chl b C7-formyl groups along with the C13'-keto groups of several chls strengthen pigment-protein linkage (Liu et al. 2004) and influence the absorption characteristics of the chromophores as previously shown (McLuskey et al. 2001). The C7-formyls of all chlb molecules except chlb 601 are selectively hydrogen bonded to the polypeptide or to the coordinated water of chlb 607. The amide side chain of Gln 131 is thought to selectively bind chlorophylls to LHCIIb (Bassi et al. 1999) (Remelli et al. 1999). This amino acid interacts with three chlb molecules, firstly through the C=O hydrogen bond interaction with the coordinated water of chl b 606, and then with two additional hydrogen bonds formed by NH_2 interaction with the C7-formyls of chl b 607 and chl b 609. As a result three chl b

molecules form a close proximity cluster in this region, an effect that could facilitate efficient energy transfer between these chls (Liu et al. 2004). Selectivity of these sites is thought to be based on the recognition of the relatively small structural differences between the methyl group of chla and the formyl group of chlb (Hobe et al. 2003). Recently, a systematic study of chl a/b binding site selectivity in recombinant LHCIIb was performed using a detergent exchange method to reconstitute protein (Hobe et al. 2003), and the relative affinities of chla and chlb binding sites were calculated from titration curves (Hobe et al. 2000). This method revealed five sites which exclusively bind chlb and a sixth site presenting a slight preference to this chromophore. The remaining six binding sites were found to favour chla, however, they were shown to tolerate chlb when presented in large excess *in vitro* (Hobe et al. 2003). It has been proposed that hydrophobic repulsion or steric hindrance may be the factors affecting chlb binding to chla sites as the environment surrounding the C7-methyl groups of chla molecules is mostly nonpolar (Liu et al. 2004). The data provided by (Hobe et al. 2003) suggests an explanation for the rather consistent chl a/b ratio observed in native LHCIIb, as this shows chla to be essential for the reconstitution of stable protein. In spite of this the 2.72 Å crystal structure observed no mixed binding sites for the 14 chlorophylls present in the complex (Liu et al. 2004), suggesting that the mixed occupancy observed during reconstitution (Remelli et al. 1999; Rogl & Kuhlbrandt 1999; Yang et al. 1999) does not occur during assembly *in vivo*.

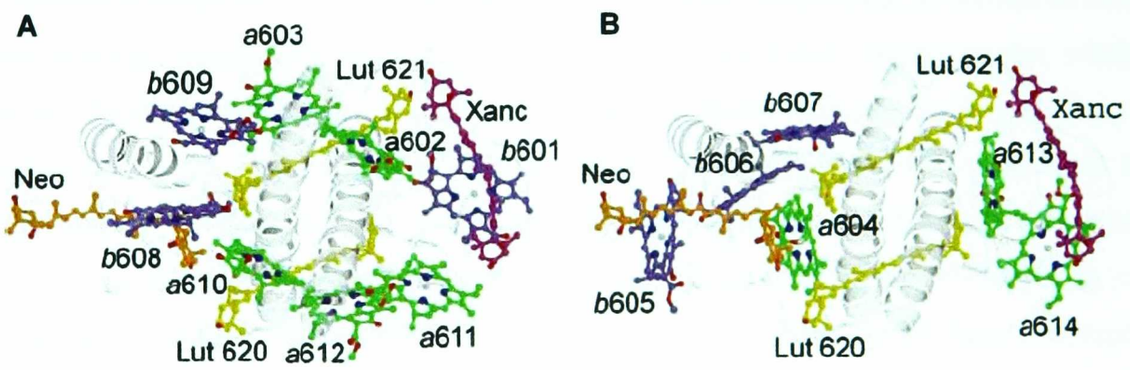

Figure 1.3 - Pigments in the LHC-II monomer adapted from Liu *et al.*, 2004. A, Pigment pattern in a monomer at the lumenal side of the thylakoid membrane. B, Pigment pattern in a monomer at the stromal side of the thylakoid membrane. Green, Chla; blue, Chlb; yellow, lutein; orange, neoxanthin; magenta, xanthophyll-cycle carotenoids.

The chlorophyll components of LHCIIb exist in two layers within the complex, distributed vertically, with each layer in close proximity to the stromal or lumenal surface (Fig 1.3A). In monomeric LHCIIb the stromal surface chlorophyll layer consists of 8 chls (5 chla and 3 chlb) surrounding the central helices A and B forming an elliptical ring (Fig 1.3B). The

average chlorophyll centre-to-centre distance is 11.26 Å (maximum 12.79 Å/ minimum 9.74 Å), and each chlorophyll is related to its symmetrical opposite via an internal pseudo-C2 axis (Liu et al. 2004). The lumenal layer consists of six chlorophylls (3 chla and 3 chlb) which form two independent clusters, the first comprising all three chlb molecules and an additional chla. The centre-to-centre distance between chlb 606 and chlb 604 in this cluster is the smallest within the LHCIIb complex at 8.05 Å. The second cluster exists as a chla dimer, with the shortest inter-layer chlorophyll-chlorophyll distance present between chlb 609 and chlb 606 at 13.89 Å (Liu et al. 2004).

The crystal structure shows an enrichment of chlb around helix C at the monomer interface with all six chlb molecules present, five from one monomer and an additional molecule (chlb 601) from a neighbouring monomer. The shortest inter-chlorophyll distance between adjacent monomers is 11.79 Å, highlighting a critical role for this chlb region in maintaining an energy equilibrium inside functional trimers (Liu et al. 2004).

The stromal chlorophyll layer extends into the trimeric complex, with 24 chlorophylls organised into two irregular circular rings. An inner ring located in the trimer core comprising six chla molecules is thought to be important during inter-monomer energy transfer. The subsequent outer ring consists of 9 chla and 9 chlb molecules arranged in a mosaic pattern of 3 chlb molecules alternating with 3 chla molecules. The arrangement of the stromal chlorophyll layer favours absorption of incident quanta from all directions over a broad spectral region, and the subsequent transfer of excitation energy to the putative terminal fluorescence emitter chla 612, at a highly efficient rate and in as few steps as possible (Liu et al. 2004). Energy transfer between lumenal clusters is significantly less efficient due to the large separation distances involved. Instead, these clusters are thought to act as upstream energy collectors transmitting excitation energy to stromal chlorophylls in an independent manner. The energy collected by the stromal chlorophyll layers is rapidly focused on chla 612 and chla 611 allowing transmission to neighbouring LHCs or reaction centres.

Two central all-*trans* luteins are bound on both sides of the A – B helix supercoil in narrow hydrophobic cavities, forming a cross-brace. The β-rings of these lutein molecules are orientated towards the lumenal surface whilst the ϵ-rings are directed towards the stromal surface. The polyene chains of luteins 620 and 621 are inclined with respect to the membrane normal by 59° and 62°, respectively. Both ring-shaped end groups of these two carotenoids interact through van der Waals forces and hydrogen bonds with four internal homologous polypeptide segments located on the stromal and lumenal ends of the A – B

helix supercoil (Bassi et al. 1997). These lutein molecules are located at the L1 and L2 carotenoid binding sites of LHCIIb (for review Bassi & Caffarri 2000). When LHCIIb is in its monomeric form the 0-0, 0-1 and 0-2 transitions for these lutein molecules have been identified as 495, 466 and 437 nm respectively, and a ½ maximum broadening of the 495 nm absorption band suggests that slight differences exist in relation to environment and configuration of the two lutein molecules (Ruban et al. 2000). A decrease in lutein absorption is seen upon trimerisation, along with the appearance of a red-shifted 510 nm band thought to result from protein influence or interaction with other pigment-protein complexes (Ruban et al. 2000). The presence of Lutein in the L1 site is a common feature in Lhca and Lhcb proteins (Bassi & Caffarri 2000), and has been found to be of critical importance for the reconstitution of stable LHCIIb (Bassi et al. 1999; Croce et al. 1999b) (Niyogi et al. 1997b). Binding of the carotenoid to the L1 site is sufficient to sustain more than 90% of the complexes $^{3}Chl^{*}$ quenching capability (for review see Bassi & Caffarri 2000). The L1 site has been found to lack the ability to exchange a bound chromophore.

Located in the chlb rich around helix C is the third carotenoid 9'cis neoxanthin, found inclined 58° from the membrane normal supporting previous evidence by (Croce et al. 1999a). The epoxycyclohexane ring of neoxanthin hangs over the chlorin ring of chla 604 and hydrogen bonds to Tyr 112 via its C3'-hydroxyl group. Side chains from the helix C amino acid residues Leu 134, Met 135 and Val 138 along with Trp 71 from helix B and the phytyl chains and chlorin rings of chlb 606 and 608 form a highly selective hydrophobic binding site for a hook shaped neoxanthin chain, allowing the cyclohexane ring of the carotenoid to extend into the solvent region. Neoxanthin has been found to occupy the N1 site of LHCIIb under all growth conditions (Bassi & Caffarri 2000) and its electronic transitions located at 486, 457 and 430 nm (Ruban et al. 2000). Reconstitution experiments using a recombinant form of LHCIIb with Neoxanthin yield highly unstable protein complexes that suffer from instability at increased temperatures along with a decreased resistance to proteolytic attack (Hobe et al. 2000). Evidence of pigment exchange in the N1 binding site has been seen in a number of species (Bungard et al. 1999), whilst being shown to preferentially bind 9-cis-5, 6-epoxy carotenoids such as neoxanthin and 9-cis-violaxanthin (Snyder et al. 2004). Six chla molecules are located in favourable positions with respect to Lutein for efficient downhill singlet energy transfer from Lutein → chla, with other data indicating that such excitation energy is transferred from Lutein exclusively to chla (Gradinaru et al. 1998), whilst the transfer of energy from Neoxanthin to chlb 606 and chlb 608 is deemed highly plausible (Liu et al. 2004). The crystal structure by (Liu et al. 2004) concludes that all three carotenoid pigments function as effective accessory LH antenna

components, acting in the blue-green spectral region to complement chl a/b absorption, as well as their structural and photoprotective roles.

At the monomer – monomer interface a carotenoid with all-*trans* configuration is found with a 34° incline from the membrane normal in what is thought to be the V1 carotenoid binding site. The hydrophobic binding pocket exists at the interface of several chlorophylls, along with hydrophobic residues from the polypeptide and PG. Part of the carotenoid polyene chain and one of its end groups is accommodated within the pocket, whilst the second of the carotenoid end groups protrudes outwards and faces the chlorin plane of the stromally located chlb 601. Evidence suggests that this is a mixed binding site containing different xanthophyll – cycle carotenoids, supported by the fact that the lumenal end group of the carotenoid points to the cavity formed around a local C3-axis, thought to be the docking site for VDE (Hieber et al. 2000). Early reports suggested that the V1 site could only bind Violaxanthin (Verhoeven et al. 1999), however, more recent data suggests that, with the exception of Neoxanthin, all xanthophylls could participate in the V1 pool with the proposed order of affinity to be Antheraxanthin > Violaxanthin > Lutein > Zeaxanthin (Caffarri et al. 2001). It has been proposed that the V1 site represents a reservoir of readily available Violaxanthin for use in the xanthophyll cycle, and is supported not only through structural data but also by the observation that xanthophyll cycle chromophores tightly bound to minor antenna are unaccessible to VDE (Farber et al. 1997; Ruban et al. 1999).

1.5.2 Minor Antenna Complex – CP29

Isolation of this complex from a variety of species has shown a variation in its molecular weight of between 29-31 kDa. Sequencing studies involving the CP29 polypeptide were hindered due to the complex being N-terminally blocked, however, partial sequences have been obtained for CP29 fragments from spinach (Henrysson et al. 1989), tomato and barley (Morishige & Thornber 1992) identifying the complex as an *lhcb4* gene product.

At ~257 amino acids in length the CP29 protein forms the largest of the PSII antenna complexes (Bassi et al. 1996), due to a 42 amino acid insertion prior to the first predicted helix, in a region highly conserved within the other *lhcb* genes (Bassi et al. 1996; Jansson 1999). Lhcb4 is predicted to bind 8 chl molecules (Bassi et al. 1996), thought to consist of 6 chla and 2 chlb molecules based upon the observed chl a/b ratio of 3.0. One of these chlb molecules and up to five chla molecules have been shown to adopt similar binding conformations to the chromophores of LHCIIb they are thought to correspond with (Pascal et al. 2000). The carotenoids within the complex are lutein, neoxanthin and violaxanthin,

however, the carotenoid composition of CP29 has been shown to vary considerably (Table 1.1). This observation is thought to reflect differences in the isolation procedures employed. Reconstitution experiments involving CP29 derived from E-coli have shown the chlorophyll-binding sites to be non-specific in nature, whilst lutein has again been shown to be essential for reconstitution and the correct folding of a light harvesting polypeptide (Giuffra et al. 1996).

In addition to these chromophores, CP29 has been shown to bind a Ca^{++} ion on the lumenal B – C loop (Jegerschold et al. 2000) where it is proposed the ion compensates for the charge on glutamate 166 enabling the acidic residue to ligate chlorophyll (Jegerschold et al. 2000). CP29 has also been shown to bind the carboxyl-modifying agent dicyclohexylcarbodiimide known as DCCD (Walters et al. 1994; Ruban et al. 1998a) on residue 166 (Pesaresi et al. 1997) suggesting the complex has an important function in photoprotective energy dissipation within the PSII antenna (Sandona et al. 1998).

Phosphorylation of the CP29 antenna complex has been shown to occur in plants subjected to low temperatures (Bergantino et al. 1995). The level of PSII photoinhibition demonstrated in these plants suggests that phosphorylated CP29 complexes may have a photoprotective role during cold stress (Bergantino et al. 1995). This theory is supported by data showing an increased level of photoinhibition under stress conditions in cold-sensitive maize lines lacking the ability to phoshorylate CP29 (Mauro et al. 1997). Phosphorylation occurs on threonine 83, an amino acid residue located within a region lacking any homology to the other light harvesting complexes (Testi et al. 1996). The recognition site possesses the general requirements for an animal casein kinase II (CK2) motif making this phosphorylation site unique amongst chloroplast proteins, which has led to the suggestion that phosphorylated CP29 is the first step in a signal cascade designed to respond to photoinhibitory conditions (Testi et al. 1996). Additional evidence exists that phosphorylation leads to conformational change within the complex that could alter energy transfer efficiencies between CP29 and the reaction centre of PSII, in a process that would move the equilibrium of PSII excitation energy away from reaction centres and towards the antenna system for safe dissipation (Mauro et al. 1997).

Functional analysis of CP29 from *Arabidopsis thaliana*, using an antisense approach (Andersson et al. 2001) has achieved very efficient downregulation of the polypeptide despite the fact that Lhcb4 is encoded by three different genes producing isoforms of CP29. Apparently the three genes are sufficiently similar to allow simultaneous RNA interference of all three mRNAs. Growth of plants lacking CP29 was not affected, and pleiotropic effects

on other photosystem subunits were restricted to Lhcb6 (CP24). In addition there was a slight decrease in PSII quantum yield, whilst oxygen evolution per leaf area was unaffected (Andersson et al. 2001). However, the latter should be related to the observation that PSII content was increased in the CP29 antisense plants by a factor of 15% when grown in high light (Andersson et al. 2001).

1.5.3 Minor Antenna Complex – Lhcb5 (CP26)

This complex reportedly exists as two apo-proteins of 29 and 26.5 kDa respectively (Thornber et al. 1993), with a mature polypeptide length of 247 amino acids (Bassi et al. 1996). Like its relative CP29, this polypeptide is N-terminally blocked, however, partial sequencing of the protein determined its corresponding gene as *lhcb5* (Bassi et al. 1996). Observed comparisons between chlorophyll binding residues of CP26 and LHCIIb suggest that the former binds 9 chlorophylls in total (Bassi et al. 1996), represented by 6 chla and 3 chlb molecules based upon the chlorophyll a/b ratio of 2.0. Reconstitution experiments using recombinant CP26 have shown that three of these chromophore binding sites preferentially select chla molecules, one of them being essential for protein folding (Croce et al. 2002). Additional evidence suggests that the one additional chlb molecule present in CP26, compared to CP29, is located in the B2 site of the complex (Croce et al. 2002).

The carotenoid complement of Lhcb5 includes lutein, neoxanthin and violaxanthin, however the variations in isolation procedures have shown disparity in the ratios observed (Table 1.1). Nevertheless, protein reconstitution has identified two xanthophyll-binding sites; the first (L1) is essential for protein folding and specifically binds the carotenoid lutein (Croce et al. 2002), a molecule that appears to be intrinsically involved with this process. The second site (L2) has a lower specificity *in vitro*, being able to bind any of the xanthophyll species present in thylakoids (Croce et al. 2002), however there is no evidence this occurs *in vivo*.

Like CP29, this complex has been found to bind the carbonyl-modifying agent DCCD (Walters et al. 1996) at positions 116 and 224 (both glutamate residues), suggesting that this protein may also be important in photoprotective energy dissipation within the peripheral antenna of PSII. However, an antisense-*lhcb5* line of *Arabidopsis thaliana* displays growth characteristics similar to that of wild type plants, with no pleiotropic effects in relation to other light harvesting subunits (Andersson et al. 2001). A decrease in PSII quantum yield was detected similar to that of *lhcb4*-antisense plants, however, oxygen evolution per leaf area was marginally increased under high light. PSII content was again observed to increase (by a factor of 30%) under these growth conditions (Andersson et al. 2001).

1.5.4 Minor Antenna Complex – CP24

The smallest antenna complex within PSII is CP24, the molecular mass of which is 21 kDa (Thornber et al. 1993) and consists of only 212 amino acid residues (Bassi et al. 1996). It has been possible to identify this protein as a product of the *lhcb6* gene using direct N-terminal sequencing (Morishige et al. 1990). With a chl a/b ratio of 1.0, CP24 has been shown to bind five molecules of chla and five molecules of chlb (Bassi et al. 1996), along with the carotenoids lutein, violaxanthin and potentially neoxanthin (Table 1.1) whilst the complex has been shown to have a capacity for xanthophyll exchange during the xanthophyll-cycle which is only marginally less than that of CP26 (Morosinotto et al. 2002).

1.5.5 Related *Lhcb* Proteins – PsbS (CP22)

PsbS is a 22 kDa *Lhcb* related protein, which forms the focus of this thesis and as such will not be discussed in detail here. Previous work reported that PsbS is important in the assembly of PSII (Hundal et al. 1990). The protein is predicted to have four membrane spanning helicies based upon hydrophobicity plots (Wedel et al. 1992; Kim et al. 1992; Wallbraun et al. 1994) and may bind chlorophyll a and b (Funk 1995b). Work on the *Arabidopsis thaliana npq4* mutant has suggested that the PsbS protein may have an important role in photoprotection (Li et al. 2000), see section 1.12.

1.5.6 Related *Lhcb* Proteins – LHCIIe/Early Light Induced Proteins (ELIPs)

(Peter & Thornber 1991) reported the existence of a 13kDa chlorophyll a/b binding protein (LHCIIe) which was enriched in xanthophyll cycle carotenoids, but to date this has yet to be confirmed. One possible explanation for this is that LHCIIe represents a member of the LHC-related ELIPs or early light induced proteins, which have molecular weights between 14 – 17 kDa. These proteins are expressed in dark-adapted plants following exposure to light (Adamska 1997; Jansson 1999) and may be involved in chlorophyll biosynthesis (Adamska 1997) and are suggested to have a photoprotective function.

1.5.7 Macromolecular Organisation of the Photosystem II Antenna

Light harvesting antenna complexes from PSII are precisely orientated in the PSII macrostructure forming PSII supercomplexes (Boekema et al. 1999b; Boekema et al. 1999a; Nield 2000), consisting of the major trimeric complexes LHCII (Kuhlbrandt et al. 1994; Liu

et al. 2004), and three minor monomeric complexes (Peter & Thornber 1991). Individual antenna complexes are essential for photosynthetic regulation and the harvesting of sunlight (Jansson 1994; Paulsen 1995; Horton et al. 1996), however, the relationship between these functions and the molecular architecture of the antenna system remain unresolved. Numerous groups have proposed models detailing PSII structural design in an attempt to uncover the interactive properties of antenna complexes. Initial representations were based upon 2-D electrophoresis of solublised PSII particles and cross-linking studies (Peter & Thornber 1991; Bassi & Dainese 1992; Thornber et al. 1993; Jansson 1994). The common feature running through these models was the existence of a PSII dimer with the minor antenna (CP29, CP26, CP24 and potentially Lhcb3) linking the PSII core and inner antenna with the peripheral antenna consisting of LHCIIb. Subsequently a direct method for the analysis of PSII-macrostructure was employed using the techniques of electron microscopy and single particle analysis (for review see Hankamer et al. 1997), resulting in two models being proposed for the PSII unit, derived from a 20 Å electron density projection map from isolated PSII particles (Hankamer et al. 1997; Boekema et al. 1998), and cross-linking studies (Hankamer et al. 1997).

Cross-linking studies have been further employed in order to locate the minor antenna complexes, and have shown CP29 to be in close proximity to CP43 and CP47, with CP26 positioned adjacent to CP43 (Hankamer et al. 1997). The location of CP26 has been directly observed in antisense plants using transmission electron microscopy aided by single-particle image analysis (Yakushevska et al. 2003). The size of LHCIIb, based on the electron density map from the 3.4 Å crystal structure (Kuhlbrandt et al. 1994), suggests the complex must lie within the top right hand corner of each PSII monomer (Fig 1.4b). The first 3-D structure of the PSII supercomplex from higher plants has been obtained by single particle analysis of images obtained using cryoelectron microscopy (Nield et al. 2000). In addition, the supercomplex structure of PSII derived from *Arabidopsis thaliana* has been determined, and shares the common dimeric structure found in other species, albeit at a resolution insufficient for the identification of individual subunits (Yakushevska et al. 2001).

A structure and function study of Lhcb2 has been performed using an antisense approach against the *lhcb2* gene (Ruban et al. 2003; Andersson et al. 2003). This led to effective downregulation of the three isoforms of Lhcb2 along with the five isoforms of Lhcb1 at the mRNA level, and the complete inhibition of synthesis of Lhcb2 at the protein level. As a consequence, LHCIIb trimers normally formed from these proteins were absent, however the stacking of thylakoid membranes, thought to rely upon interaction between LHCII proteins was undisturbed in transformants (Andersson et al. 2003). In addition, PSII isolated from

these antisense plants (Fig 1.4) were of normal size and shape (Ruban et al., 2003). In an attempt to explain these results it was observed that trimers composed of Lhcb5 and Lhcb3 were present in the absence of Lhcb1 and Lhcb2, and although not found in wild-type plants, they appear to function very much like normal LHCIIb trimers showing only a slight reduction in antenna size and a 2% decline in quantum yield (Andersson et al. 2003). A 10-15% reduction in photosynthetic rate per leaf area was attributed to an observed decrease in chlorophyll content over the same area, rather than a deficiency in the newly formed complex (Andersson et al. 2003). The lack of an N-terminus threonine residue in Lhcb5 and Lhcb3 (compared to Lhcb1 and Lhcb2) prevented state transitions in the antisense plants (Ruban et al. 2003).

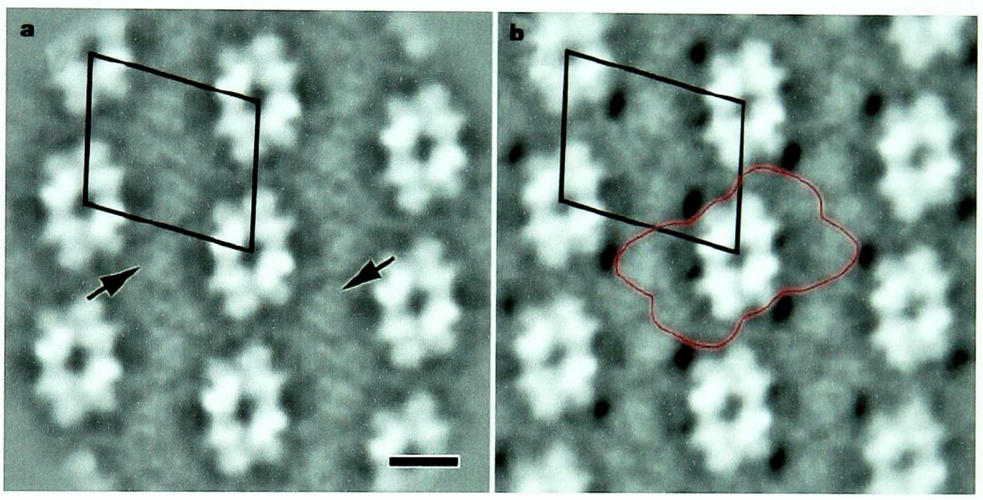

Figure 1.4 - Two-dimensional crystalline PSII complexes from Arabidopsis wild-type and Lhcb2 antisense plants modified from Ruban et al. (2003). a, Sum of 600 aligned crystal fragments from Arabidopsis Lhcb2 antisense plant with the unit cell (24.0 x 21.8 nm) and two trimers (arrows) indicated. b, Sum of 450 aligned crystal fragments from Arabidopsis wild-type with the unit cell (25.6 x 21.4 nm) and an outline of the fitting of the $C_2S_2M_2$ supercomplex (red line) indicated. Scale bar, 10 nm.

Mildly solublised membranes subjected to single particle analysis have been used to characterise PSII 'mega-complexes' (Boekema et al. 1999a; Boekema et al. 1999b), which contain all the minor antenna complexes and up to three LHCIIb trimers per PSII-core unit, with the designation of strong (S), medium (M) and loose (L) binding sites depending upon trimer occupancy. Additionally, a naturally occurring heptameric association of LHCIIb trimers has been characterised from partially solublised PSII membranes (Dekker et al. 1999). These membranes have frequently been observed to show crystalline macrodomains, with PSII organised in rows of large spaced or small spaced crystals (Boekema et al. 2000). Image analysis of the crystals revealed that the C_2S_2 and C_2S_2M supercomplexes form the basic components of the small-spaced and large-spaced crystals, respectively.

1.6 Cytochrome *bf* Complex

The Cytochrome b_6/f (cyt b_6/f) complex functions as a plastoquinol-plastocyanin oxido-reductase in higher plants acting as the electronic connection between PSII and PSI (Allen 2003). Forming a dimer in the thylakoid membrane (Cramer et al. 1997), the complex contains nine subunits per monomer in higher plant chloroplasts four of which are redox active polypeptide subunits. Firstly, cytochrome *f* (cyt *f*) is a polypeptide product of the *pet*A gene, the apoprotein has a molecular mass of 30 – 33 kDa and binds a single molecule of haem *c*. Cytochrome b_6 (cyt b_6) is the 23 kDa product of the *pet*B gene that forms an apoprotein binding two *b* - haem molecules, whilst the 20 kDa apoprotein of the *pet*C gene, Rieske Fe-S protein, binds a single 2Fe-2S centre. Lastly, Ferredoxin:$NADP^+$ oxidoreductase (FNR) is a nuclear encoded apoprotein with multiple isoforms of the *pet*H gene in *Arabidopsis*.

A fifth major polypeptide known as subunit IV forms part of the cyt b_6/f complex, and shows sequence homology with the C-terminus of cytochrome *b* from the mitochodrial cytochrome bc_1 complex (Widger et al. 1984). In addition several small hydrophobic subunits in the complex are thought to be required for assembly and/or stability of the complex. This has been shown for the *pet*G and *pet*N gene products (Berthold et al. 1995; Hager et al. 1999), and has been shown to contain a molecule of chlorophyll and β-carotene (Huang et al. 1994; Pierre et al. 1995; Zhang et al. 1999) along with its redox active cofactors. The isolated complex has been found to be active *in vitro* in both monomeric and dimeric states (Chain & Malkin 1991), whilst forming the previously described dimer *in vivo*. As has already been established (section 1.3) the cyt b_6/f complex supports the formation of the trans-thylakoid proton gradient through the action of the proton motive Q-cycle. This involvement leads to the translocation of four protons in a lumenal direction across the thylakoid membrane, per plastoquinol molecule oxidised to plastoquinone by the cyt b_6/f complex.

1.7 Photosystem I

This large macromolecular intrinsic membrane protein is primarily located in the non-appressed stromal lamellae regions of the thylakoid membrane. Its main function as a plastocyanin-ferredoxin oxidoreductase (Scheller & Moller 1990), terminates the photosynthetic electron transport chain.

1.7.1 Photosystem I Reaction Centre Core

This catalytic core is composed of a heterodimer of the 83 kDa PsaA and 82.4 kDa PsbB proteins which are homologous in their primary sequences and the topgraphic organization of their transmembrane helices (for review see Chitnis 2001). PsaA and PsaB proteins bind the majority of the chlorophyll including the P700 special pair chlorophyll, a member of which has been shown to be chlorophyll *a* molecule (Jordan et al. 2001). The heterodimer core also binds all the carotenoid molecules, both phylloquinone molecules and the F_X Fe-S cluster (for review see Chitnis 2001). The remaining PSI subunits are arranged around the heterodimeric core, and are spatially organized toward the stromal and lumenal sides of the thylakoid membrane.

1.7.2 Photosystem I Stromal Side Subunits

The proteins PsaC, PsaD, and PsaE form the stromal peripheral domain of Photosystem I. This domain contains the terminal electron donors, the ferredoxin-docking site and the ferredoxin-$NADP^+$ oxidoreductase (FNR). In addition, this domain is thought to stabilise the reducing side of PSI (for review see Scheller et al. 2001).

The 9 kDa peripheral protein PsaC is closely associated with the PSI PsaA and PsaB heterodimer, and combined, these three subunits, are responsible for binding all the cofactors of the electron transfer system. PsaC binds the remaining two 4Fe-4S clusters which form the terminal electron accepters F_A and F_B (Krauss et al. 1993; Krauss et al. 1996; Chitnis 2001).

It has been established that PsaD contains specific residues involved in the binding of ferredoxin (for review see Chitnis 2001). The protein has a predicted mass of 15.6 kDa and recent studies support the theory that PsaD acts to stabilise the other peripheral subunits and PSI itself (Chitnis et al. 1989). PsaE is the last stromally orientated subunit of the peripheral domain with a predicted mass of 8 kDa, it too is thought to be involved with the binding of ferredoxin (Rousseau et al. 1993; Chitnis 2001). Other possible functions include the stabilisation of the PsaC – PSI core interaction, which would facilitate the efficient transfer of electrons from F_X to F_A and F_B (Weber & Strotmann 1993). Two *psa*E genes have been found in *Arabidopsis thaliana* and studies involving an insertional knock-out of one of these genes caused a 60% decrease in PsaE levels compared to wild type (Varotto et al. 2000).

1.7.3 Photosystem I Lumenal Side Subunits

The photo-oxidaton of plastocyanin occurs on the lumenal side of PSI. The role of the PsaF protein, in this event, has been studied for some time, and it had been proposed that the 18 kDa protein contained the plastocyanin-docking site. Studies by (Haehnel et al. 1994) using site directed mutagenesis supported this theory, whilst PsaF-platocyanin interaction was confirmed in a nuclear mutant of *Chlamydomonas* (Farah et al. 1995). PsaF in plants has a multifunctional role, firstly responsible for interaction with PC, as evidenced by the reduction of the electron transport rate in the absence of this subunit (Haldrup et al. 2000). Secondly, PsaF appears to promote efficient energy transfer between the peripheral antennae and the PSI core, which is more susceptible to photodamage in the absence of this protein. PsaF has been shown to cross-link with the stromal subunit PsaE (Jansson et al. 1996).

Photosystem I lacking PsaF possessed a normal subunit complement with the exception of PsaN (Jansson et al. 1996). The 9.8 kDa subunit is the final component of the lumenal side of PSI and has been studied with a cosuppression approach (Haldrup et al. 1999). Plants lacking detectable amounts of PsaN showed no significant difference compared to wild type in terms of growth and photosynthesis. The function of the PsaN subunit is still unknown.

1.7.4 Additional Photosystem I Components - *The PsaH, PsaL, PsaO Cluster*

In cyanobacteria the PsaL subunit is involved in the trimerisation of PSI (Chitnis & Chitnis 1993), however, in plants, the photosystem has only been found in monomeric form. PsaL is found associated with the PsaH and PsaO subunits (absent in cyanobacteria) interactions between which have been evidenced by crosslinking studies (Jansson et al. 1996). PsaH deficient plants showed that essentially all state transitions (see section 1.9.2) were absent (Lunde et al. 2000). The absence of PsaH causes the phosphorylation state of LHCII to increase whilst remaining attached to PSII and the PSI antenna size to remain fixed during state 1-state 2 transition. It is thought that LHCII binds to PSI in the facinity of PsaH during state 2.

PsaL and PsaO are found in close proximity to PsaH, however, it has proven difficult to clarify the specific individual functions of these subunits to date. Pigment analysis of *Arabidopsis* plants lacking PsaL (and resultantly a proportion of PsaH and PsaO) suggested that this protein cluster binds 5 chlorophylls with absorption maxima near 688 and 667 nm (Ihalainen et al. 2002). It is thought that these chlorophylls could be implicated in the connection of the PSI core antenna systems with LHCII during state 2.

1.7.5 Additional Photosystem I Components – *PsaK and PsaG*

These subunits have a finite sequence similarity thought to have resulted from a gene duplication, and, it has been suggested, that they provide interaction between the core and peripheral antenna proteins, however, to date there is no evidence of specific functional similarity (Scheller et al. 2001). Absence of PsaK results in decreased levels of Lhca2 and Lhca3 in addition to a reduction in state transitions (Varotto et al. 2002; Jensen et al. 2002). Pigment analysis on plants lacking PsaG indicated that this subunit binds ~2 molecules of red-shifted β-carotene (Ihalainen et al. 2002) similar to that seen in PsaD and PsaF. PsaG is thought to provide dynamic regulation of PSI activity under normal growth conditions.

1.7.6 Photosystem I Structure

PSI and PSII form part of the photosynthetic reaction centre superfamily, which is divided into two distinct groups, based upon the terminal electron acceptors employed, type I Fe_4S_4 clusters and type II quinone (for review see Nitschke & Rutherford 1991). The original crystal structure model of trimeric PSI at 6Å was produced in 1993 and isolated from *Synechococcus* sp. (Krauss et al. 1993), and was subsequently superseded by a 4Å map of a type I PSI reaction center isolated from *Synechococcus elongatus* (Krauss et al. 1996; Klukas et al. 1999). Recently published work at 2.5Å atomic resolution (Figure 1.5) has provided the most complete structural detail regarding PSI in relation to the role of its protein subunits in binding cofactors, and the interactions between cofactors (Jordan et al. 2001). Isolated cyanobacterial PSI exists as a trimer with a three-fold rotational axis perpendicular to the membrane plane. At the 'trimerisation domain' PsaL is seen to form the majority of contacts between the monomers (Jordan et al. 2001). Each monomer consists of at least 11 different protein subunits coordinating more than 100 cofactors. The large subunits PsaA and PsaB are related by a pseudo-C_2 axis located at the center of the PSI and consist of 11 helices each (Krauss et al. 1996). The electron transport components were shown to be surrounded by a protein core consisting of 10 helices, 5 each from PsaA and PsaB (Krauss et al. 1996). These cofactors are arranged in two branches along the pseudo-C_2 axis, with most of the antenna Chl *a* molecules, carotenoids and lipids bound to PsaA and PsaB. As previously mentioned (section 1.4.1) the C-terminal domains of PsaA and PsaB are structurally similar to the D1 and D2 reaction center subunits of PSII. In contrast with the latter, the C-terminus domains of PsaA and PsaB cannot be considered as pure reaction center domains (Schubert et al. 1998) due to the concentration of antenna Chla coordinated by PsaA (12 chla) and PsaB (13 chlb). Inaddition, the central region of the PSI core antenna contains a total of 43 Chla molecules in stark contrast to the equivalent region of PSII (Jordan et al. 2001).

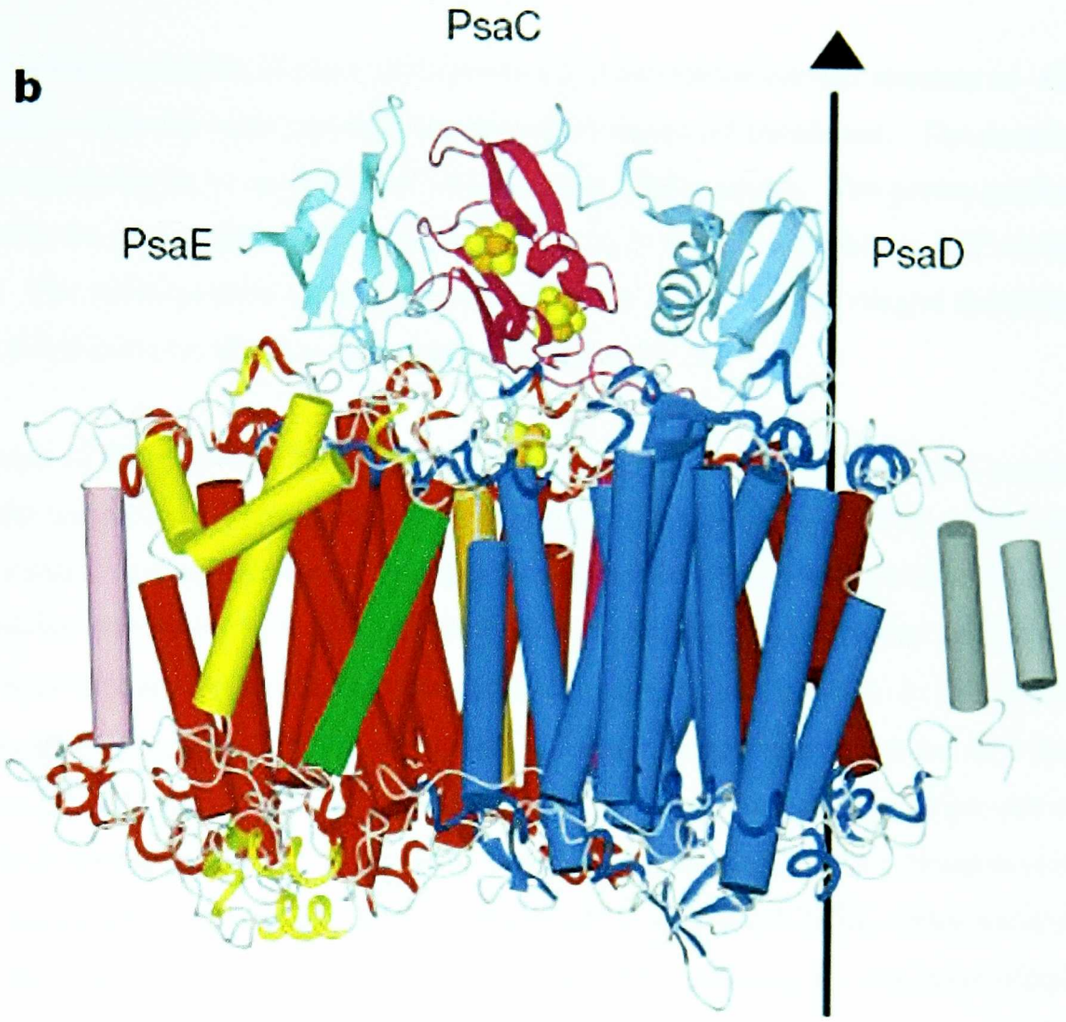

Figure 1.5 - Structural model of PS I trimer at 2.5 Å resolution as adapted from Jordon *et al.*, 2001. Side view of the arrangement of all proteins in one monomer of PSI, PsaA (blue), PsaB (red), and the stromal subunits PsaC (pink), PsaD (turquoise), PsaE (green) and the Fe_4S_4 clusters. View direction indicated by arrow at monomer II in 27a. The vertical line (right) shows the crystallographic axis.

However, the distribution of peripheral antenna Chla molecules on the N-terminal domains of PsaA and PsaB show strong resemblance to the PSII integral antenna proteins CP43 and CP47 (Jordan et al. 2001). Sequence similarity is found between CP43-PsaA and CP47-PsaB, which fold into comparable structures consisting of six transmembrane α-helices each (Zouni et al. 2001). These structural similarities between PSI and PSII are suggested to be a result of common evolutionary origin (Hankamer et al. 1999). The remaining membrane-intrinsic subunits are peripheral to the PSI-core and aide the coordination of antenna cofactors. The PSI structure indicates a possible lumenal docking site for cytochrome c_6 or plastocyanin and a stromal site for ferredoxin or flavodoxin, with the latter being formed by PsaC, PsaD and PsaE.

1.8 ATP-synthase Complex

The ATP-synthase complex of plant chloroplasts is a large macromolecular structure of ~600 kDa located within the non-appressed regions of the thylakoid membrane. The complex shows strong similarity to bacterial and mitochondrial ATP-synthase. The proton gradient generated by the photosynthetic electron transport pathway is used to synthesise ATP via this complex. The ATP-synthase has two distinct regions in the form of an integral membrane complex (CF_0) and an extrinsic stroma exposed complex (CF_1).

CF_0 consists of four different polypeptides (I-IV), which act in concert to channel protons through the membrane. Between 9-12 copies of subunit III are present which, along with subunits I and II, are required for CF_1 binding (Lemaire & Wollman 1989) whilst subunit IV is essential for activity (Feng & McCarty 1990). CF_1 contains the catalytic sites responsible for ATP-synthesis, and is formed from five different polypeptide subunits (α, β, γ, δ, ε) with a stoichiometry of $\alpha_3\beta_3\gamma\delta\varepsilon$. The α and β bind ADP and phosphate and convert ADP into ATP (Bar-Zvi et al. 1983) in a three stage process, involving the catalytic site present on each of the β subunit resulting β - γ interaction, enabling the release of ATP (Abrahams et al. 1994). This interaction is thought to occur as a result of γ-subunit rotation within the $\alpha_3\beta_3$ barrel of the complex (Sabbert et al. 1996; Noji et al. 1997), allowing the sequential release of ATP from the three active sites on the complex. This rotation is thought to be provided by the CF_0-III subunit, (which forms a ring like structure within the membrane), as a result of the protonation of key carboxyl group on a single subunit due to the proton motive force across the membrane. The δ-subunit links CF_0 and CF_1 and the γ-subunit appears to control proton-gating through the enzyme (Xiao & McCarty 1989; Engelbrecht & Junge 1990). The ε-subunit blocks catalysis in the dark preventing breakdown of ATP and may be involved on proton gating through interaction with the γ-subunit (Richter et al. 1984).

1.9 Photosynthetic Regulation

To sustain photosynthesis, the biochemical network of higher plants has developed into a highly flexible system in the face of changing environmental conditions, which can fluctuate both rapidly and over longer time periods. During high light conditions the rate of photosynthesis will reach saturation, at which point a number of processes act to ensure photosynthesis is maintained, some of which are described below.

1.9.1 Cyclic Electron Transport

During periods of stress when CO_2 fixation is low there is a lack of electron acceptors causing a collapse in linear electron flow between the two photosystems. Under such conditions, the generation of low pH in the thylakoid lumen is prevented and the prerequisite signal for the dissipation of excess light energy is not formed. This obstacle is overcome through a process of cyclic electron transport around PSI in a process that relays electrons between NADPH, ferredoxin, Cyt *bf*, plastoquinone and PSI.

1.9.2 State Transitions

This is a process by which an imbalance in the electron flow between PSII and PSI is restored. It involves the phosphorylation of LHCIIb in PSII complexes resulting in the mobile antenna disassociating from the latter and migrating to PSI through the thylakoid membrane. The question still remains, however, as to whether phosphorylated LHCIIb actually binds to PSI, if so where, and what regulatory role does PSI provide? Recent data indicates that the PSI-H protein (see section 1.7.4) may act to bind phosphorylated LHCIIb as plants lacking this component fail to perform state transitions. The enzymatic mechanism of this process is still unresolved. A number of candidates exist for the LHCIIb kinase protein which include the PSII-core associated kinase (Race & Hind. 1996), the four kinases (30, 55, 64 and 84 kDa) where the 55 kDa kinase has homology with a histidine kinase (Weber et al. 1998) and the recently identified TAK kinase (Snyder & Kohorn 1999; Snyder & Kohorn 2001).

1.9.3 Carotenoids

Carotenoids have multiple roles in oxygenic photosynthesis (for review see Owens, 1996). They can act as accessory light harvesters in support of chlorophyll in higher plants whilst being of particular importance to organisms that exist in environments which restrict the light available for chlorophyll absorption. The provision of defence against triplet chlorophylls and singlet oxygen species generated within the antenna system is the responsibility of the carotenoid molecules, which act to prevent photo-oxidative damage. This process involves the transfer of energy from triplet state chla (^{3}Chla) or singlet state oxygen ($^1O_2^*$) to a carotenoid molecule. In doing so, a triplet state carotenoid is formed (^{3}Car) which leads to the non-destructive thermal dissipation of this triplet energy by the carotenoid. Lastly, the carotenoid zeaxanthin, along with the xanthophyll cycle that

produces it, have an important role in the photoprotective dissipation of excess excitation energy during periods of light stress.

1.10 Photoprotection in Higher Plants

The exposure of plants to conditions of excess light intensities can lead to increased production of damaging reactive oxygen species as by-products of photosynthesis. As a result, plants have evolved both biochemical and physiological responses to light that enable optimisation of photosynthesis and continued growth. The regulation of light harvesting is required in order to balance the absorption and utilisation of light energy and prevent photo oxidative damage. Under conditions of excess light, plants employ protective non-photochemical mechanisms that quench singlet state chlorophylls and dissipate excitation energy as heat. Beyond the point of photosynthetic saturation, the antenna pigments of PSII continue to absorb light energy leading to an increase in the excitation density within the antenna, in a manner that is linearly proportional to the intensity of absorbed light. The result is an over reduction of PSII and increased photoinhibitory damage to reaction centre pigments and proteins. Such increases in the excitation density can result in triplet-state excitation of chlorophyll *a* within the antenna which can transfer energy to ground state O_2 to generate singlet oxygen ($^1O_2^*$), which can in turn lead to further damage to the pigments and proteins in the thylakoid membrane.

The specific inactivation of PSII and photoinhibition arises from electron transfer in the RC through one of two mechanisms, referred to as either the 'acceptor' or 'donor' side mechanism (Andersson & Barber 1996). The acceptor side mechanism results in the over reduction of the plastoquinone pool and the Q_A site. This causes the recombination of the $P680^+Pheo^-$ radical pair and the formation of the P680 triplet-state chlorophyll ($^3P680$). This can then react with molecular oxygen forming $^1O_2^*$ which, in turn, damages the chlorophylls and amino acids of the reaction centre (Andersson & Barber 1996). The rate of electron donation from P680 in the donor side mechanism exceeds the rate of electron removal from water and increases the lifetime of the $P680^+$ species causing a build up of this cation. The high redox potential of $P680^+$ required for the oxidation of water is great enough to oxidise the surrounding pigments and amino acids within the reaction centre (Barber & Andersson 1992; Andersson & Barber 1996). Damaged reaction centres can themselves release chlorophyll molecules and free radicals causing wide spread damage to other components of the thylakoid membrane. Repairing reaction centres requires the disassembly of PSII, the proteolysis of the damaged components and the subsequent synthesis and incorporation of a

new D1 (Andersson & Barber 1996). If the rate of damage begins to exceed the rate of repair, inactive PSII reaction centres accumulate in the thylakoid membrane resulting in decreased photosynthetic efficiency and the plant is said to be photoinhibited.

1.10.1 Chlorophyll Fluorescence Yield and Quenching

This excess energy is dissipated as heat via a number of mechanisms, which, collectively, reduce the quantum efficiency of PSII. They can be detected as non-photochemical quenching of chlorophyll fluorescence (NPQ). The electrons of chlorophyll molecules absorbing photons of light energy are promoted from the S_0 ground state to one of a number of higher energy levels, which results in rapid decay to the first excited state S_1 and the conversion of electronic vibrational energy into heat. Electrons at S_1 will decay to S_0 over time and release their absorbed energy as fluorescence. However, chlorophyll molecules within a photosynthetic membrane are influenced by a number of competing processes all of which can return an S_1 electron back to its ground state. These processes are listed below:

1. Re-emitted energy as fluorescence (k_F)
2. Inter-chlorophyll energy transfer (k_T)
3. Energy usage in photochemistry (k_P)
4. Energy dissipation through non-radiative processes as heat (k_D)

The fluorescence yield (ΦF) of any chlorophyll (whether a single molecule or a group of molecules) consists of the remaining energy after competition with all the above processes. This energy is re-emitted as light. The quenching of the fluorescence yield occurs in two distinct ways. Firstly, through photochemical quenching of chlorophyll fluorescence (qP or qQ), caused by an increase in k_P which can be used to gauge the redox state of Q_A. Secondly, through processes that stimulate non-photochemical quenching of chlorophyll fluorescence (qN or NPQ) due to an increase in k_T or k_D and is detailed below.

The photochemical and non-photochemical components of chlorophyll fluorescence quenching have been studied using numerous techniques. Initially, (Krause et al. 1981) blocked qP using 3-(3,4-dichlorophenyl)-1,1-dimethylurea (DCMU) whilst light doubling techniques (Bradbury & Baker 1981) enabled the separation of qN and qP. In (Quick & Horton 1984) used modulated fluorescence techniques, which employed saturating pulses to measure quenching and directly probe the relative contributions of qP and qN.

1.10.2 Non-photochemcial Component of Chlorophyll Fluorescence Quenching

Non-photochemical quenching of chlorophyll fluorescence is symptomatic of the regulation of energy dissipation by the light harvesting antennae of PSII. NPQ can be divided into at least three different components based on their relaxation kinetics in darkness, after a period of illumination, and their response to a number of different uncouplers and inhibitors (Horton & Hague 1988; Walters & Horton 1991).

1.10.3 Rapidly Relaxing qE

qE state is the major and most rapid component of NPQ in most algae and plants and is referred to as the pH- or energy-dependent component (Briantais et al. 1979). It has a dark relaxation half-time ($T_{1/2}$) of ~30 seconds (Walters & Horton 1991), and the level of qE has been shown to closely correlate with the conversion of violaxanthin to zeaxanthin through the action of the xanthophyll cycle (see section 1.11) in numerous plant species (Demmig-Adams 1990).

1.10.4 Slowly Relaxing state qT

This component relaxes in minutes. Under low light conditions qT is attributed to the state 1 to state 2 transition associated with energy redistribution between PSII and PSI. Chlorophyll fluorescence quenching due to qT is thought to arise due to the phosphorylation of LHCIIb (Allen 1992) since it is sensitive to the phosphatase inhibitor NaF (Horton & Hague 1988). The total contribution to fluorescence quenching from the state transition is ~20%, decreasing in high light (Horton & Hague 1988). However, during periods of prolonged high light stress the total amount of 'qT' has been shown to increase due to a slow relaxation component of qE (Lee et al. 1990; Walters & Horton 1991).

1.10.5 Irreversible or Very Slowly Relaxing State qI

The third component of NPQ, qI has the slowest relaxation and is the least defined. It consists of two distinct components; the first is sensitive to protein synthesis inhibition and is related to photoinhibition of photosynthesis whilst, the second, appears to be a photoprotective mechanism, forming a sustained quenching in the antenna (Lee et al. 1990; Walters & Horton 1991; Gilmore & Bjorkman 1994). Such prolonged quenching of chlorophyll fluorescence is supported by a number of elements including the maintenance of thylakoid ΔpH in the dark by ATP hydrolysis (Gilmore & Bjorkman 1994); the long-term

retention of zeaxanthin (for review see Demmig-Adams & Adams 1996), and a stable protonation site (Ruban & Horton 1994).

1.11 The Xanthophyll Cycle

The xanthophyll cycle was first characterised by (Yamamoto et al. 1962) as the two-step de-epoxidation of violaxanthin to zeaxanthin via an intermediate molecule antheraxanthin. Situated within the chloroplast this cycle has been found to be organised across the thylakoid membrane with the de-epoxidation reaction (violaxanthin → zeaxanthin) lumenally located whilst the epoxidation reaction (zeaxanthin → violaxanthin) occurs on the stromal side of the membrane (Yamamoto et al. 1999). Violaxanthin de-epoxidation occurs in the light and is catalysed by the enzyme violaxanthin de-epoxidase (VDE).

VDE has been purified from spinach using a combination of gel filtration and anion chromatography (Arvidsson et al. 1996) and from lettuce using lipid-affinity precipitation with monogalactosyldiacylglyceride (MGDG) (Rockholm & Yamamoto 1996). The enzyme from both species was found to have an apparent molecular weight of approximately 43 kDa on SDS-PAGE. Successful cloning of the first cDNA encoding VDE from lettuce was performed in *Ecoli* resulting in the expression of a fully functional enzyme (Bugos & yamamoto 1996). Its activity is controlled by the lumenal pH of the thylakoid, with a maximum activity between pH 4.8 – 5.2 whilst being completely inactive above pH 6.3 (Eskling et al. 1997). Additionally, the enzyme also requires the presence of ascorbate (Neubauer & Yamamoto 1994) and the thylakoid lipid MGDG for maximal activity.

During periods of dark or weak illumination the xanthophyll cycle is completed in a reaction catalysed by the enzyme zeaxanthin epoxidase (ZE). To date, it has not been possible to isolate the enzyme directly, however cDNA's encoding ZE have been cloned from *Nicotina plumbaginifloria* (Marin et al. 1996), pepper (Bouvier et al. 1996) and tomato (Burbidge et al. 1997) enabling the synthesis of fully functional ZE in *E.coli*. As with VDE, zeaxanthin epoxidase displays a strong pH dependency, with optimum activity occurring around pH 7.0 – 7.5 (Siefermann & Yamamoto 1975). Additional components are required for the reaction including molecular oxygen (Takeguchi & Yamamoto 1968), and the cofactors NADPH (Siefermann & Yamamoto 1975), FAD (Büch et al. 1995) along with the presence of ferredoxin or 'ferredoxin like' reductants (Yamamoto et al. 1999).

The role of the xanthophyll cycle in the dissipation of excess excitation energy will be detailed in section 1.11.3. Additionally, the cycle has been implicated in a number of other

important roles. It has been demonstrated that an association exists between the peroxidation and degradation of thylakoid lipids in pea and high light stress (Havaux et al. 1991), whilst the inhibition of zeaxanthin formation by dithiothreitol (DTT) exacerbates light-induced lipid damage. In support of this evidence, analysis of the zeaxanthin-deficient *Arabidopsis thaliana npq1* mutant showed an elevated level of thylakoid lipid damage under high light stress when compared to WT, whilst the *npq4* mutant plants, capable of zeaxanthin synthesis but lacking the rapidly reversible component of NPQ, displayed a transient increase in lipid damage with full recovery in a 24 hour period. Over expression of the *chy*B gene encoding the β-carotene hydroxylase enzyme (a component of the zeaxanthin biosynthetic pathway) in *Arabidopsis thaliana*, results in a specific two fold increase in the size of the xanthophylls cycle pool (Davison et al. 2002). These plants possess an increased tolerance to high light conditions, showing a reduction in lipid peroxidation, along with decreased leaf necrosis and antherocyanin levels. Such evidence highlights a strong link between zeaxanthin and the protection of thylakoid lipids from photodegredation.

The fluidity of the thylakoid membrane in the peripheral region of the hydrophobic core has been shown to be sensitive to the light-induced formation of zeaxanthin (Gruszecki & Strzalka 1991). The presence of zeaxanthin reduces the fluidity of the membrane and protects against heat-induced increases in lipid bilayer permeability (Gruszecki & Strzalka 1991; Havaux et al. 1996). These observations suggest the xanthophyll cycle helps to regulate membrane stability *in vivo*.

1.11.1 qE – An Historical Overview

Chlorophyll fluorescence quenching was originally thought to be unrelated to photochemistry (Murata & Sugahara 1969), however further investigation using DCMU discovered that this quenching could be inhibited/abolished by uncouplers such as nigericin and NH_4Cl (Wraight & Crofts 1970). This led to the suggestion that pH gradient formed across the thylakoid membrane during photosynthesis was related to light-induced quenching of chlorophyll fluorescence (Wraight & Crofts 1970), and was supported by data which found the fluorescence yield of intact chloroplasts to be largely dependent on the high-energy state of the thylakoid (Krause 1973). A linear correlation between chlorophyll fluorescence quenching and the intra-thylakoid proton concentration of broken pea chloroplasts was found by Briantais *et al*, (1979), and it was shown that abolition of the proton gradient using the uncoupler gramicidin led to complete reversal of quenching. This provided indisputable evidence of the link between 'energy dependent' chlorophyll fluorescence quenching qE and the ΔpH gradient across the thylakoid membrane and added

support to the idea that it was the pH gradient, across the thylakoid membrane, which is necessary for the induction of chlorophyll fluorescence quenching.

The formation of a ΔpH can be achieved in the dark using ATP hydrolysis which has been shown to induce chlorophyll fluorescence quenching, suggesting that light itself is not directly responsible for qE formation (Gilmore & Yamamoto 1992). The role of qE in photoprotection emerged after it had been observed that increases in light intensity resulted in a decreased steady state quantum yield (ϕ_s), whilst qP remained largely unchanged (Weis & Berry 1987), indicating that the reduction in quantum yield was not a result of negative feedback from reduced photosynthetic electron transport chain components, but due to increased dissipation of excess excitation energy. The function of qE, therefore, is to down regulate PSII preventing reduced Q_A accumulation and, in doing so, averting the subsequent photoinhibition of PSII (see section 1.4) during high light stress (Weis & Berry 1987; Krause & Weis 1991). Energy dependent quenching of chlorophyll fluorescence has been shown to correlate closely with the formation of zeaxanthin (Demmig-Adams 1990) implicating xanthophyll cycle as a component of qE regulation (Demmig-Adams & Adams 1996; Horton & Ruban 1999; Yamamoto et al. 1999; Wentworth et al. 2000).

1.11.2 qE – The Site of Energy Dependent Quenching

A considerable body of evidence exists that suggests, under most physiological conditions, the rapidly relaxing or qE component of NPQ occurs within the antenna rather than the reaction centre of PSII. The latter is thought to play only a minor role (if any) in qE contribution (Horton & Ruban 1992; Ruban & Horton 1995; Wentworth et al. 2000). The major observations, which support this theory, are as follows:

1. The qE inhibitor DCCD (Ruban et al. 1992a) has been shown to bind only the minor antenna polypeptides Lhcb4 (CP29) and Lhcb5 (CP26) (Walters et al. 1994; Ruban et al. 1998a). Recent evidence suggests that the PsbS (CP22) protein also binds DCCD (Dominici et al. 2002), however, the exact location of this polypeptide in PSII remains uncertain (Nield 2000).

2. Xanthophyll cycle carotenoids are located in the peripheral antenna, whilst qE and zeaxanthin levels observed *in vivo* closely correlate with each other (Demmig-Adams 1990).

3. Heat emission kinetics measured directly using laser-induced optoacustic spectroscopy show completion within 1.4 μs (Mullineaux et al. 1994). This time is significantly faster than Q_A^- and $P680^+$ recombination reaction (~120 μs) necessary to cause quenching within the reaction centre.

4. Preferential quenching of excitation energy within the antenna complexes has been observed during PSII analysis at 77K (Ruban & Horton 1995). Following the induction of qE, the spectrum of PSII resembled that of partially aggregated LHCII, with bands at 680 and 700 nm.

Taken together, this data strongly suggests that the antenna of PSII is the loci for qE related quenching. However, under certain physiological conditions, the reaction centre could also be involved, and, it has been shown, that reversible chlorophyll fluorescence quenching associated with the latter may occur as a consequence of low pH-induced Ca^{2+} release from the OEC (Krieger & Weis 1993). Such release is associated with a specific thermoiuminescence (TL) band around 50 °C, also seen in pea leaves under conditions in which reversible NPQ was observed (Johnson & Krieger 1994). Its absence however, in mature leaves indicates that reaction centre quenching could only occur under certain circumstances and would not normally contribute significantly to NPQ.

1.11.2 Relationship between qE and the xanthophyll cycle

Photosynthetic electron transport has been detailed in section 1.3 where the mechanism of proton translocation in the thylakoid, resulting in the formation of a ΔpH gradient, is outlined. As a consequence of this process, the lumenal pH of the thylakoid decreases and, in doing so, activates violaxanthin deepoxidase (see section 1.11) instigating the reversible conversion of violaxanthin into zeaxanthin. This decrease in lumenal pH also promotes qE formation resulting in excess excitation energy being dissipated within the antenna system. Currently two mechanisms have been proposed in order to rationalise the relationship between the xanthophyll cycle and the rapidly relaxing (qE) component of NPQ (for a review see (Horton & Ruban 1999). These hypostheses depend upon the structures and/or energetics of xanthophyll cycle carotenoids, however they have not yet been fully eludicated.

1. *Direct Quenching Mechanism* – the direct singlet-singlet downhill energy transfer from chlorophyll to carotenoid as the driving force behind fluorescence quenching.

2. *Indirect Quenching Mechanism* – regulation of antenna complex organisation by the xanthophyll cycle resulting in LHCII conformational changes that promote energy dissipation.

1.11.3.i Direct Quenching Mechanism: molecular gear shift model

This model proposes the direct quenching of chlorophyll excited states by the xanthophylls *via* singlet-singlet energy transfer resulting in the subsequent dissipation of excitation energy (Owens 1984).

Carotenoid energy diagrams display a minimum of two excited states designated as 2^1Ag (S_1) and 1^1Bu (S_2) based upon their symmetrical relationship. Direct transition from ground state (S_0) to the first excited state (S_1) is symmetrically forbidden for xanthophylls, however conversion between the second excited state (S_2) and the S_1 state is possible, and is employed by carotenoids as a means for energy transfer to chlorophyll molecules.

S_1 state energy levels have been approximated by employing energy gap law in a number of carotenoids upon measurement of S_1 (Frank et al. 1994). The S_1 state energy for zeaxanthin was 530 cm^{-1} lower than that of chlorophyll a (14700 cm^{-1}), whilst the S_1 energy of violaxanthin was greater than the latter at 15290 cm^{-1}. The energy level disparity between violaxanthin and zeaxanthin forms the basis of the molecular gear shift model (Owens 1984; Frank et al. 1994). Although only approximations, the fact that the chlorophyll *a* Qy band was found to be higher than the S_1 energy level of zeaxanthin suggested the latter would be energetically suitable for quenching excess excitation energy from chlorophyll *a* than the S_1 state of violaxanthin. Since the latter was significantly higher than that of chlorophyll a it would be more likely to act as a light harvesting pigment. Hence the molecular gear shift model proposes that violaxanthin would predominate under low light conditions as an accessory light harvesting pigment, whilst high light levels exceeding photochemical requirements would promote the conversion to zeaxanthin, enabling the dissipation excess chlorophyll excitation energy as heat.

However, advances in fluorescence spectroscopy allowed for direct measurement of violaxanthin and zeaxanthin S_1 energy levels (Polivka et al. 1999; Frank et al. 2000), and both studies concluded that S_1 energy level differences between xanthophylls were far lower than previously calculated (Frank *et al.*, 1994), making the differential effects of violaxanthin and zeaxanthin on chlorophyll fluorescence quenching more likely to involve

indirect factors rather than being solely due to the S_1 energy levels of the carotenoids (Polivka et al. 1999; Frank et al. 2000).

More recently *in vitro* studies using low temperature fluorescent spectroscopy have been employed to again attempt to accurately measure the S1 energy levels of the xanthophyll cycle carotenoids (Josue & Frank 2002). The results obtained are similar to work by (Frank et al. 1994), and it has been suggested that in order for the S_1-S_0 transitional energies observed at low temperature *in vitro* to change a protein, they would have to cause significant distortion of the carotenoid (Josue & Frank 2002). In spite of this, chlorophyll fluorescence quenching by zeaxanthin has never been directly observed, however, carotenoid cation radicals have been transiently observed after photoexcitation of bacterial light harvesting complexes (Frank & Brudvig 2004). This has led to the suggestion that electron transfer between carotenoids and chlorophylls could be a mechanism for quenching of excited states, and subsequent heat dissipation.

1.11.3.ii Indirect Quenching Mechanism: allosteric qE model

Fluorescence quenching has been observed in the absence of zeaxanthin in dark-adapted chloroplasts (Rees et al. 1989; Noctor et al. 1991), isolated LHCII complexes (Ruban & Horton 1994; Ruban et al. 1996) and in the *Chlamydomonas npq1* mutant (Niyogi et al. 1997a; Niyogi et al. 1997b) whilst the presence of zeaxanthin itself has been shown to amplify the level of qE at subsaturated H^+ concentrations (Rees et al. 1989). This data fails to support the idea of direct quenching by zeaxanthin and, as a result of the earlier work mentioned above, has led to the model proposed by (Horton et al. 1991) in which four key aspects related to the mechanistic process of NPQ are defined:

1. *Location* - energy dissipation occurs on one or more LHCII components
2. *Induction* - conformational change in single or multiple LHC components
3. *Control* - synergistic effect of targeted protonation and violaxanthin deepoxidation
4. *Dissipation* - thermal dissipation of excess excitation energy resulting from altered chlorophyll-chlorophyll interaction

This mechanism relies upon the structural and physical differences of the xanthophyll cycle carotenoids to mediate structural changes within the LHCII antenna, resulting in the thermal dissipation of excitation energy (Horton & Ruban 1999). It has been shown that the synergistic or allosteric nature of NPQ control can be characterised in enzymatic terms,

defining qE as a regulatory enzyme catalysed reaction (Horton et al. 1991; Horton et al. 2000). Confirmation that qE occurs in the light harvesting system (Ruban & Horton 1994), along with the discovery of potential protonation sites (Walters et al. 1996; Pesaresi et al. 1997) and the influence of the xanthophyll cycle, substantiate the proposed mechanism for indirect quenching of qE. The allosteric model provides a quantitative basis for qE based upon kinetic measurements on isolated thylakoids (for review see Horton et al. 2000). It is proposed that the reaction rate of qE is, in fact, the magnitude of quenching whilst the trans-thylakoid pH gradient provides a substrate for the reaction in the form of protons. The titration of H^+ concentration against qE in spinach chloroplasts has been shown to give rise to a sigmoidal response suggesting positive cooperatively in relation to proton binding (Noctor et al. 1991). The apparent pK of this reaction has been observed to vary (Krause et al. 1988), with pH shifts that can be systematically stimulated using modulators such as antimycin A and dibucaine (for review see Horton et al. 2000) which function to raise or lower the pH requirement for qE respectively. However, it is interesting to note that the inhibitory effect of Antimycin A is dependent upon the deepoxidation state of the antenna, and provides evidence of antagonism between qE effectors (Noctor et al. 1993). *In vivo* qE is regulated by the xanthophyll cycle where zeaxanthin has been shown to have a role in non-photochemical quenching (Demmig-Adams 1990). The activation of qE and a shift to lower lumenal pH always corresponds with violaxanthin deepoxidation and the formation of zeaxanthin (Horton et al. 1991), altering the properties of protonation, the dynamics of which approach those of 'Michaelis-Menton' kinetics. However, at saturating pH levels the maximum quenched level remains constant regardless of the presence of zeaxanthin, suggesting the latter acts to amplify qE *in vivo* (Rees et al. 1989; Noctor et al. 1991). The kinetics of qE formation in leaves have been shown to be biphasic in nature, possessing a rapid early phase in high light associated with ΔpH formation, and slower phase corresponding with the formation of zeaxanthin. The PSII antenna is thought to exist in two forms based upon the structural changes said to induce qE as a result of protonation and the deepoxidation of the xanthophyll cycle. Known as U (unquenched) and Q (quenched) forms respectively, they each have been observed to display different fluorescent lifetimes (Gilmore et al. 1995; Gilmore et al. 1998), and interaction between LHCII components give rise to positive cooperativity in relation to the transition from U $\rightarrow$ Q (for review see Horton et al. 2000).

This data supports two important predictions made by the allosteric model for qE. The first states that qE formation is absolutely dependent upon the formation of the trans-thylakoid pH gradient, whilst the second focuses on the protonation of specific residues within the antenna system. Collectively these processes result in a conformational change that brings

about quenching within the antenna (Horton et al. 1996). Further insights regarding the regulation of these processes have been obtained through observations involving LHCII behaviour *in vitro* (Ruban et al. 1994a; Ruban et al. 1996; Wentworth et al. 2000; Wentworth et al. 2001). Experiments using purified LHCII complexes in detergent have described highly fluorescent characteristics when held above the critical micelle concentration (CMC), which resemble that of the unquenched state. Dilution below the CMC results in the formation of a quenched species, and the rate of transition to such a state can be controlled through the application of known *in vivo* qE modulators such as Antimycin A and Dibucaine (Ruban et al. 1994a) as well as xanthophyll cycle carotenoids (Ruban et al. 1994a; Ruban et al. 1996). The application of DCCD has also been shown to inhibit such quenching *in vitro* (Ruban et al. 1996; Ruban et al. 1998b). All LHCII complexes emulate this behaviour, however the rate and magnitude of quenching is both accelerated and amplified for CP29 and CP26 when compared to LHCIIb under controlled conditions (for review see Horton et al. 2000). In all cases the kinetic characteristics displayed by LHCII complexes *invitro* fit the same second order rate equation found for qE *in vivo* (Ruban & Horton 1999; Wentworth et al. 2001; Ruban et al. 2001b), whilst the rate constant is modulated by the xanthophylls and effectors described above (Ruban et al. 1996). Carotenoid structure also plays an important role on the function of a given molecule in relation to qE modulation (Horton & Ruban 1999). Auroxanthin, the epoxy analogue of violaxanthin, affects quenching in a manner similar to that of zeaxanthin (Ruban et al. 1998b) as the epoxide of this carotenoid is located in the 5-8 position resulting in the end group being fixed in the plane of the carbon double bond chain. The positioning of the end group is inconsistent with that of violaxanthin, instead presenting similar structural characteristics to that of zeaxanthin.

The PSII light harvesting complex *in vivo* exists as a multi-subunit macromolecular aggregate (see section 1.5.7). In order to determine the mechanism of qE regulation it is necessary to ascertain whether the conformational changes responsible for qE induction occur within a single protein subunit or, alternatively, over LHCII as a whole. Initial experimental evidence found that large macromolecular protein aggregates formed under conditions used to promote quenching *in vitro* (Ruban & Horton 1992), the size of which could be modulated with controlled changes in detergent concentration (Ruban et al. 1997). It was proposed that zeaxanthin promotes the adoption of an aggregated state, whilst violaxanthin inhibits oligomer formation (Horton et al. 1991). However, more recent data has shed light on novel conditions under which zeaxanthin induced quenching can occur without protein aggregation (Wentworth et al. 2000), where it is assumed that xanthophyll-cycle carotenoids interact with the antenna proteins of PSII in a manner which optimises the frequency of contact with the external medium. Earlier work has shown that aggregation of

PSII antenna under quenching conditions gives rise to a qE absorbance spectrum at 683 nm with a 700 nm shoulder (Horton et al. 1991), the former displaying kinetic correlation to quenching upon the addition of zeaxanthin (Wentworth et al. 2000). This evidence suggests that the absorbance change around 680 nm eminates from a species that is either closely related to the quencher or is the quencher itself. The red-shift in peak maximum of fluorescence spectra from LHCIIb at 700 nm is due to protein aggregation. Control experiments using CP29 have shown that zeaxanthin is not responsible for this aggregated state, and, instead, acts to enhance the fluorescence yield of the complex (Wentworth et al. 2000). Additionally, qE has been shown to be closely associated with an absorbance change centred around 535nm (Noctor et al. 1993; Ruban et al. 1993b; Bilger & Bjorkman 1994), with the loss of qE in the *npq4* mutant of *Arabidopsis thaliana* (see section 1.11.4) resulting in a loss of absorption at 535nm (Li et al. 2000). This absorbance change has been shown to arise due to dramatic changes in the environment of the xanthophyll cycle carotenoid zeaxanthin (Ruban et al. 2002).

As already mentioned, previous work suggests that qE involves a conformational change within LHCII (Noctor et al. 1993; Ruban et al. 1993a; Bilger & Bjorkman 1994). Such changes are thought to underlie the process of fluorescent quenching both in the high light system, involving aggregation of isolated LHCII, and the low irradiance system, which simulates *in vivo* properties of excess light. This data suggests that the mechanism of conformational change may be the same in both systems, even though the driving force behind the structural changes are different (for review see Horton et al. 2000). Quenching has been observed to follow second order reaction kinetics (Wentworth et al. 2000) with modulators acting to alter the rate constant of the reaction (Wentworth et al. 2001), a trend also seen in chloroplasts and leaves (Ruban & Horton 1999; Ruban et al. 2001b). The hyperbolic kinetics of quenching support the theory that qE follows a second order reaction of the type $A + A \rightarrow 2A$. The fluorescent species found in the unquenched state is A, whilst 2A is the quencher found in the Q-state (for review see Horton et al. 2000). As a result of this model for the formation of 2A is predicted to follow first order reaction kinetics, corresponding to the absorbance change at 683 nm, which displays such kinetic behaviour in all *in vitro* experiments (Ruban et al. 1998b; Wentworth et al. 2000) and in isolated chloroplasts (Ruban et al. 1992b). If A is a chlorophyll molecule, then it follows that 2A could be a chlorophyll dimer (Horton et al. 2000; Wentworth et al. 2001).

All LHCb proteins posses a capacity to convert into a quenched state, however, *in vitro* studies cannot determine whether this potential is realised *in vivo*. To this end, genetic analysis has been employed to further explore the components involved in qE.

1.11.4 Genetic Analysis

Molecular genetics has been employed to improve our knowledge of photosynthesis, with a substantial amount of research undertaken in the area of light harvesting. Chlorophyll *b*-deficient mutants have been widely used to eludicate the genetic and biochemical control of chlb biosynthesis, as well as the function of the chromophore in the assembly of LHC proteins (Anderson et al. 1978; Eggink et al. 2001). Various Chl *b*-defiecient mutants have been identified in higher plants (Falbel et al. 1994), which differ both in the manner and location of the mutations (Lin et al. 2003). To develop a greater understanding of energy dissipation and the *in vivo* parameters controlling it, xanthophyll cycle components have been isolated in *Arabidopsis thaliana* that possess altered non-photochemical quenching characteristics. The *Arabidopsis thaliana* mutants described in below were derived from mutagenesis of M_2 seedlings with fast-neutron bombardment or 0.3% ethylmethane sulphonate (Niyogi et al. 1998; Li et al. 2000), and identified with chlorophyll fluorescence video imaging (Niyogi et al. 1998).

The inability of the *npq1* mutant to convert violaxanthin into zeaxanthin during periods of excess light (Niyogi et al. 1998) is due to a lack of VDE activity. As a result *npq1* plants exhibit significantly reduced NPQ levels highlighting the requirement for violaxanthin deepoxidation as a key contributor to qE. The component of qE retained in *npq1* mutants is not related to the xanthophyll cycle as it is thought that Lutein plays an important role in NPQ (Pogson et al. 1998). New alleles of *aba1* found in *npq2* mutants constitutively accumulate zeaxanthin, however, this alone is insufficient to generate qE in the absence of a ΔpH (Niyogi et al. 1998). The *Arabidopsis thaliana* mutant *npq4* displays an altered state of NPQ whilst maintaining a normal pigment content. The isolation of the *npq4* mutant was part of an attempt to identify the components necessary for qE (in addition to ΔpH and xanthophylls) and it was found to be specifically deficient in this NPQ component, whilst being able to produce zeaxanthin during high light at rates indistinguishable from wild type plants (Li et al. 2000). The *npq4* gene encodes the PsbS protein, a member of the LHC superfamily (Kim et al. 1992), and is discussed in section 1.12. The effect of PsbS gene dosage on pH and xanthophyll cycle mediated NPQ has been analysed using molecular and global time-resolved techniques, showing PSII chlorophyll *a* fluorescence lifetime distributions or steady-state intensities to be stiochiometrically related to the amount of PsbS protein (Li et al. 2002a). Over expression of the PsbS protein ultimately leads to an increase in qE. The precise mechanism by which the antenna system in higher plants detects lumenal ΔpH remains uncertain, however structural and genetic advances have greatly improved our knowledge of the proton transport mechanism in bacteriorhodopsin, with numerous side

chains actively involved in a protonation/deprotonation cycle (Grigorieff et al. 1996; Belrhali et al. 1999; Balashov 2000; Luecke et al. 2000). Recently, analysis of the quadruple glutamic acid mutant (4Glu) has concluded that two cation binding sites could exist in the extracellular region of bacteriorhodopsin (Sanz et al. 2001). It is thought these sites may form part of a proton transport pathway in which cations would be ligated by three Glu residues and a water molecule (Sanz et al. 2001).

Reaction centre properties have been observed to change in the *npq4* phenotype resulting in the formation of photochemically inactive, yet strongly quenching centres, which could potentially support a carotenoid or chlorophyll cation quencher (Peterson & Havir 2003). An *npq4-npq1* double mutant has been observed with the same characteristics as *npq4*, indicating that the latter mutation blocks the small amount of qE normally seen in *npq1* mutants. The characteristics of non-photochemical quenching in tobacco plants overexpressing VDE, PsbS and VDE+PsbS have been observed over a range of light intensities (Hieber et al. 2004). Analysis showed an increase in zeaxanthin formation and NPQ in plants over expressing VDE and PsbS respectively. The latter was observed to increase deepoxidation in addition to NPQ under low light conditions, a phenomenon thought to be caused by PsbS binding or inducing binding of zeaxanthin, causing the xanthophyll cycle equilibrium to shift towards higher deepoxidation states as a result of the limited capacity of the lipid matrix for xanthophylls (Hieber et al. 2004). The *Arabidopsis thaliana lut2* mutant, deficient in lutein, has been shown to induce NPQ at a rate slower than wild type plants, reaching a lower maximum extent (Pogson et al. 1998). When combined with the *npq1* mutant it has been shown than all qE is lost (Niyogi et al. 1998). Recent data suggests that lutein acts indirectly by organising LHCII (Lokstein et al. 2002) rather than specifically being involved in qE. The *npq1* mutant was originally isolated in *Chlamydomonas reinhardtii* (Niyogi et al. 1997a), and provided the first genetic evidence for the importance of zeaxanthin synthesis in non-photochemical quenching, whilst characterisation of the *lor1* mutant revealed the potential role for lutein in NPQ (Niyogi et al. 1997b).

It has been proposed that PGR5 is an essential component of the antimycin A sensitive cyclic electron transport system, involving the newly identified Cyt *bf* - FNR complex. *In vitro* biochemical studies have shed light on alternative pathways that contribute to ΔpH, whilst it has become apparent that only a proportion of the cyclic electron transport chain is antimycin A sensitive (Cleland & Bendall 1992; Scheller 1996). The ndh complex present in *Arabidopsis thaliana* is thought to support cyclic electron transport or proton transport. Contribution to the latter may also be accomplished via chlororespiration (for review see

(Peltier & Cournac 2002) as the terminal oxidase (PTOX), known to be essential for carotenoid synthesis (Carol et al. 1999), has been shown to have a substantial affect upon plastoquinone reoxidation when the gene from *Arabidopsis thaliana* is over expressed in tobacco (Joet et al. 2002).

1.12 PsbS

The PsbS subunit of PSII has become one of the most intensively studied components of the photosynthetic apparatus in recent times as a result of its role in protective energy dissipation during periods of excess illumination (Li et al. 2000). The following section will detail the current state of research into the PsbS protein, which forms the foundation for this PhD Thesis.

Research related to the oxygen-evolving complex of PSII by (Ljungberg et al. 1986) made use of oxygen evolving preparations isolated from spinach thylakoid membranes. Mild detergent treatment at pH 6.5 in the presence of 1M NaCl revealed the existence of an intrinsic membrane protein with an approximate molecular mass of 22 kDa (Ljungberg et al. 1986). This protein is the product of the nuclear encoded *psbS* gene and has various nomenclature in the literature. This initial work suggested PsbS was laterally segregated in the thylakoid membrane, being found almost entirely in the PSII rich appressed regions of the grana and all but absent from the unappressed regions (Ljungberg et al. 1986). These initial observations suggested that PsbS could be located in PSII core preparations, thereby inferring that the protein might form an integral subunit in the PSII core (Ghanotakis & Yocum 1986; Ljungberg et al. 1986; Marr et al. 1996). However, more recent studies involving cryoelectron microscopy and single particle analysis imply that the PsbS protein is not located in the PSII supercomplex (Nield 2000). By inference it was suggested to be present in the LHCII regions. In support of this it has been shown that PsbS is not located near the additional M-LHCII and CP24 subunits present in PSII-LHCII supercomplexes (Yakushevska et al. 2001).

As a result of preliminary work on the purified protein isolated from spinach, it was believed that the protein was hydrophobic in nature (Ljungberg et al. 1986). In 1992, amino acid sequence data highlighted four potential membrane-spanning regions giving rise to a very hydrophobic protein (Kim et al. 1992). This was later confirmed using topographic studies with trypsin digestion of the PsbS protein (Kim et al. 1994). Particle-induced X-ray

emission data generated with isolated polypeptides showed that the protein did not bind any metallic cofactors, and absorption spectroscopy in the visible region indicated a lack of pigments (Ljungberg et al. 1986; Bowlby & Yocum 1993). In addition, the behavior of the polypeptide during ion-exchange chromatography indicates that the protein has a pI greater that 6.5 (Ljungberg et al. 1986), which is supported by data from (Funk et al. 1995b) showing PsbS to have a pI 6.1 determined by isoelectric focusing using ampholine carriers (pH 4-6.5).

Analysis of sequence data from a cDNA clone encoding the 22kDa PsbS protein suggested that the protein was probably N-terminally blocked. The cDNA clone consisted of 1,012 nucleotides with an ORF encoding a 274 amino acid precursor of the spinach PsbS protein. It is thought that the mature protein includes at least 198 residues (Wedel et al. 1992; Kim et al. 1992). Sequence similarity exists between PsbS and other LHC proteins, which is comparable to that between LHC proteins and ELIPS (Wedel et al. 1992; Kim et al. 1992). The latter group of proteins are known not to bind any pigments (Green et al. 1991; Jansson 1999).

Current evidence regarding the pigment binding properties of PsbS has been obtained using various protein purification methods. The implementation of milder solublisation techniques (using octyl-thioglucopyranoside [0.6 %] and octyl-glucopyranoside [with a detergent/chlorophyll ratio of 30:1]) and native SDS-PAGE gels has yielded a protein with bound pigments (Funk et al. 1994). However, the chlorophyll binding properties of PsbS isolated under these, and other conditions, differ widely. Analysis showed an absorption peak at 674 nm and two maxima at 440 nm and 468 nm indicating the presence of chlorophyll *a*, whilst the shoulder at 650 nm inferred the presence of chlorophyll *b*. A chlorophyll a/b ratio of 1.8 and a chlorophyll-protein ratio of 3-4 were determined. 77 K fluorescence excitation spectra indicate that there was energy transfer from a pigment (possibly chlorophyll *b*) to chlorophyll *a*. In a further study it was suggested that the protein contained six chlorophyll *a* molecules along with one chlorophyll *b* and a carotenoid (Funk et al. 1995b). In this instance, the protein was purified using non-ionic detergents and isoelectric focusing. The PsbS apoprotein has also been shown to be stable in the absence of pigments (Funk et al. 1995a), a unique feature of the protein, since the tertiary structure of all other known PSII antennae proteins have been found to be unstable in the absence of pigments (Giuffra et al. 1996; Ros et al. 1998). Native PsbS preparations purified from chloroplasts or obtained by overexpression in bacteria have also been shown to lack any detectable bound chlorophylls or carotenoids under conditions in which Lhc proteins maintain full pigment binding (Dominici et al. 2002). Reconstitution with zeaxanthin (see

chapter four) results in the energy-dissipation related 535nm absorbance change shown *in vivo* to arise from the activation of 1-2 molecules of this pigment (Aspinall-O'Dea et al. 2002; Ruban et al. 2002). In addition, expression of the *PsbS* gene has been seen in etiolated spinach seedlings grown either in complete darkness or exposed to light of various qualities (Adamska 1996), whilst low-temperature effect on gene expression has been observed to be minimal under both field and laboratory conditions (Norén 2003).

The amino acid sequence of the Zea *mays* PsbS protein has been determined, allowing the subsequent development of an anti-PsbS antiserum targeted to a highly specific region on the stroma-exposed loop of the protein between the second and third helices (Bergantino et al. 2003). Immunoblot analysis of a variety of higher plant species (spinach, tobacco, rice, barley and carrot) revealed a 42 kDa band thought to be the result of a PsbS dimer. Two acidic residues (E122, E226) located on what is thought to be the lumenal side of PsbS have been shown to be essential for its function (Li et al. 2002b), and it has been proposed that protonation at these sites during periods of light stress could form a critical aspect of the mechanism responsible for excess energy dissipation. Analysis of structural homology between PsbS and CP29 has also revealed acidic residues on the two lumenal exposed loops, which have been shown to bind DCCD (Dominici et al. 2002), whilst light induced lumenal pH changes in intact chloroplasts and whole plants have been shown to associate with a reversible variation in the PsbS monomer/dimer ratio, with an acidic environment promoting monomerisation and interaction with the light harvesting complex, whilst an alkaline pH causes dimerisation and PSII core association (Bergantino et al. 2003).

As previously mentioned the *psbS* gene was found to have significant homology with the genes of the Lhcb family of proteins, which encoded the different members of the peripheral antennae complexes of PSII (Wedel et al. 1992; Kim et al. 1992; Green & Pichersky 1994). The *psbS* gene was also shown to have homology with genes encoding both the early light inducible proteins (ELIPS) and the fucoxanthin-chlorophyll *a/b* antennae proteins (Green & pichersky 1994). A recent review of light harvesting related proteins (LHCs, ELIPs and HLIPs) suggests that the original function of these proteins was the dispersal of absorbed light energy (Montane & Kloppstech 2000), a function now inextricably linked to PsbS. The hydropathy profile of PsbS was used to predict the folding pattern of the protein, the result of which suggested that, unlike the chlorophyll *a/b* binding peripheral antennae complexes which have three membrane spanning helices, PsbS has four (Wedel et al. 1992; Kim et al. 1992; Wallbraun et al. 1994). This prediction was confirmed by topological studies on the PsbS protein in an isolated from spinach (Wallbraun et al. 1994). In addition to the sequence for the spinach gene *X68552*, full length sequences are now available for the *psbS* genes of

tomato *U04336* (Wallbraun et al. 1994), rice (Iwasaki et al. 1997), *Arabidopsis AF134131* (Jansson 1999) and tobacco *X84225* (Kim & Pichersky 2004) and are all predicted to contain four membrane spanning helices.

Analysis of the *psbS* gene sequences derived from different species show that there are internal homologies between the first and third helices of the protein in a manner, which is similar to that, found in the Lhcb proteins (Wedel et al. 1992; Kim et al. 1992). In addition, the second and fourth helices were also found to show strong sequence similarities with each other (Wedel et al. 1992; Kim et al. 1992). The internal homology present within PsbS and its strong similarities to the light harvesting proteins of PSII has led to the theory that the protein arose following two successive gene duplications from an ancestral one-helix protein (Green & Pichersky 1994; Jansson 1999; Montane & Kloppstech 2000). The four-helix PsbS like protein then lost the majority of the C-terminal helix through a deletion event, giving rise to the three-helix chlorophyll *a/b* proteins of the PSII antennae (Green & Pichersky 1994; Jansson 1999; Montane & Kloppstech 2000). This theory suggests that a PsbS like protein predates the formation of the antennae of PSII. This idea is supported by the observation that a 22 kDa homologue of PsbS is present in the cyanobacterium *Synechocystis* 6803, which lacks the chlorophyll *a/b* binding antennae complexes (Nilsson et al. 1990).

The function of the PsbS protein is still unclear although initial work has suggested a number of functional and structural roles which have included the stabilisation of the acceptor side of PSII (Ghanotakis & Yocum 1986), and a possible docking site for the 23 kDa extrinsic protein of the oxygen evolving complex (Ljungberg et al. 1986). A possible role in chlorophyll binding has been inferred (Funk et al. 1994), with sequence data revealing strong homology between PsbS and the various LHC-gene products and the ELIPs (Wedel et al. 1992; Kim et al. 1992). An alternative view is that the protein may bind pigments in a transient fashion, and could act to chaperone newly synthesised pigment molecules to their target sites or act to bind excess pigments during turnover of chlorophyll binding proteins (Funk et al. 1994). However, the previously described role of PsbS in NPQ is most convincing, and forms the foundation of this thesis.

1.13 Aims

1. Extraction and purification of the Photosystem II PsbS protein, and characterisation of the basic structural features of the protein.
2. Analysis of PsbS binding properties in relation to xanthophyll cycle carotenoids
3. Study the effect of PsbS in relation to the *in vitro* fluorescence quenching of LHCII antenna proteins

Chapter Two

Materials & Methods

Materials and Methods

2.1 General laboratory chemicals

General Laboratory chemicals were obtained from Sigma and were AnalaR or the highest grade available unless stated otherwise.

2.2 Plant material

The Photosystem II light harvesting complexes used for the isolation of PsbS were isolated from market spinach *Spinacia oleracia* (L.) cv. Subito. This plant material was purchased fresh from a supermarket and stored at 4°C in the dark until required for use.

2.3 PSII membrane preparation (BBY particles)

The preparation PSII particles were carried out essentially using the method of Berthold et al. (1981). During preparation all solutions and glassware were kept on ice and all centrifugation steps were carried out at 4 °C. Up to 80 g of fresh leaves were used with midribs removed and finely chopped with a sharp knife before homogenising in 300 ml of slushy grinding medium (0.33 M sorbitol, 10 mM $Na_4P_2O_7.10H_2O$, 5 mM $MgCl_2$, 2 mM sodium D-iso-ascorbate, pH 6.5) with 2-3 short bursts from a Polytron (Kinematica GmbH). The homogenate is initially filtered through a double layer of muslin followed by 8 layers of muslin surrounding a central layer of highly absorbent cotton wool. Filtration was aided by gentle squeezing of the muslin and prior wetting with ice cold grinding medium. The sample was then centrifuged at 4,000 x g for 5 minutes (MSE Mistral, 6L), the supernatant discarded and the pellet resuspended in washing medium (0.33 M sorbitol, 10 mM MES, pH 6.5) before centrifugation for 7.5 minutes (4,000 x g). The resulting pellet was resuspended in 30 ml of resuspension medium (0.33 M sorbitol, 1 mM EDTA, 1 mM $MgCl_2$, 50 mM HEPES, pH 7.6) and osmotically shocked by the addition of 50 ml of breaking medium (5 mM $MgCl_2$, pH 7.6) with mixing. The osmotic potential was restored after 30 seconds by the addition of 50 ml of osmoticum medium (0.66 M sorbitol, 5 mM $MgCl_2$, 40 mM MES, pH 7.6). The thylakoids were then centrifuged for 10 minutes (4,000 x g) and the pellet resuspended in stacking medium (5 mM $MgCl_2$, 15 mM NaCl, 2 mM MES, pH 6.3). A 0.5ml aliquot was used for chlorophyll determination, described in section 2.x, with the remainder pelleted by centrifugation at, 4,000 x g for 10 minutes before resuspension to a final chlorophyll concentration of 3 mg/ml in stacking medium. The sample was left on ice in the dark for a minimum period of 45 minutes to

promote membrane stacking. Following this the sample was diluted with half its volume of 10 % (v/v) Triton X-100 in stacking medium to give a final detergent concentration of 3.33 % (v/v). The sample was then incubated on ice for 30 minutes with occasional inversions to help membrane digestion. Following this the digestion was stopped by dilution of the detergent with the addition of at least 6 ml of stacking medium. The sample was then pelleted by centrifugation for 30 minutes at 30,000 x g in a Beckman J2 centrifuge using the J2-21 rotor. The pellet was resuspended in particle wash medium (2 mM EDTA, pH 7.5) and the centrifugation repeated (30,000 x g, 30 minutes, 4 °C). The supernatant was discarded and the final pellet resuspended in dH_2O, for use on IEF, or SMC solution (0.4M sucrose, 50mM Mes-NaOH/pH 7.0, 20mM $CaCl_2$), at a final chlorophyll concentration of 2.5 mg/ml. Samples were flash frozen in liquid nitrogen and stored at –80 °C.

2.4 Preparation of PSII antennae complexes by iso-electric focusing (IEF)

IEF was carried out using a Multiphor II Electrophoresis system (Pharmacia) following the method of Bassi et al. (1991) modified by Ruban et al. (1994a).

2.4.1 Gel preparation

The flat bed gel tray (24.5 x 11.0 cm) was carefully cleaned prior to use. Electrode strips were prepared by soaking them in 2 % (w/v) ampholine solution (pH range 3.5-5.0/5.0-7.0/3.0-9.0, Sigma). Excess solution was removed with tissue and the strips placed at either end of the gel tray. 100 ml of slurry was prepared containing 2 % (w/v) ampholines (pH ranges 3.5-5.0/5.0-7.0/3.0-9.0, Sigma), 1 % (w/v) glycine, 4 % Ultrodex (Pharmacia) and 0.06 % (w/v) *n*-dodecyl β-D maltoside (Sigma). The slurry was carefully poured into the gel tray after which any surface bubbles were removed. Over a 2-hour period the gel was allowed to solidify through the evaporation of between 26-30 g of water, aided by a fan mounted above the gel tray. The anode and cathode were prepared in the following way. An electrode strip was soaked in either anode solution (5.6 % (v/v) H_3PO_4) or cathode solution (1 M NaOH), the excess removed by a tissue and the electrode strip carefully placed at either end of the gel on top of the other strips.

2.4.2 Pre-focusing of the gel

A 0.1 % (v/v) solution of Triton X-100 was applied to the surface of the Multiphor II cooling plate to improve heat transfer from the gel tray. The gel tray was then placed on the cooling plate and the

electrodes connected to the electrode strips. Prefocusing of the gel was carried out at ~8 W (13 mA, 600 V) for 1-2 hours.

2.4.3 Sample preparation

Approximately 45 minutes before the completion of the prefocusing procedure samples were prepared for IEF. 1ml of 3 % (w/v) *n*-dodecyl β-D maltoside was added to 2 ml of BBY particles (~2 mg total chlorophyll), to give a final detergent concentration of 1 % (w/v). The resulting solution was incubated in a sealed container on ice for 30 minutes with occasional stirring.

2.4.4 Loading and running the sample

The electrode holder was removed from the prefocused gel and the sample applicator applied approximately 2 cm from the cathode. The gel within the applicator was removed and mixed with the sample, after which the mixture was place back in the applicator and allowed to settle for 2-3 minutes. After this time the applicator was removed, the electrodes replaced and the sample was focused overnight (~20 hours, 8 W, 13 mA, 600 V).

2.4.5 Sample elution – pH 3.5-5

A thin spatula was used to collect each band into elution columns, from which antenna complexes were eluted with elution buffer (25 mM HEPES, 200 μM *n*-dodecyl β-D maltoside, pH 8.0) using a plastic pasteur pipette. PSII antenna complexes were either used fresh or aliquoted into 2.5 ml cryogenic storage ampoules (Nalgene) and flash frozen in liquid nitrogen and stored at - 80°C.

2.4.6 Sample elution – pH 5.0-7.0/3.0-9.0

Samples were collected every centimeter along the length of the gel (23 in total) for analysis. All samples were eluted as in 2.4.5 and stored at –80°C.

2.5 Preparation of PSII PsbS protein from BBY particles

This procedure is described in chapter 3 as part of method development.

2.6 Chloroform/methanol extractions

Protein extraction is achieved by mixing 0.4ml sample and 0.4ml MeOH in an 1.5 ml eppendorf tube (standard quality), followed by the addition of 0.2ml of chloroform. The mixture was then vortexed for a few seconds and centrifuged for 3 min at 13000 rpm using a bench top centrifuge (Mistral). This leaves three layers in the tube with water at the top, followed by the protein and finally chorophorm. Careful removal of water was followed by the addition of 0.3ml MeOH. The sample was then mixed. Centrifuge at 1300 rpm for an additional 3 min and discard the resultant supernatant. Dry the pellet and add 40µl dH_2O. Store at minus 20°C.

2.7 DCCD binding

A sample protein concentration of 150µg/ml is required. A total of 0.4ml of this sample was mixed with 5µl of DCCD [C^{14}] taken from a 10mM stock solution, giving a final concentration of 125µM. This was incubated at room temperature for 15 min and then extracted using the chlorophorm/methanol technique described in 2.7. Once completely dry the resultant pellet was dissolved using loading buffer (0.0625 M Tris/HCl (pH 6.76), 2 % (w/v) SDS, 5 % (v/v) β-mercaptoethanol, 10 % (w/v) glycerol (BDH), 0.001 % (w/v) bromophenol blue (FSA Laboratory supplies)) and heated at 90°C for 20 min. These samples are then either loaded onto a 17% polyacrylamide gel or stored at -20°C in a designated radioactive freezer.

2.8 Isolation, purification and identification of plant carotenoids

Plant carotenoids *in vivo* are stabilised by association with proteins. However extraction of these pigments can potentially cause damage, particularly to the extended series of conjugated double bonds. These pigments are susceptible to attack from a range of chemical and environmental factors including oxygen, heat, light and acids.

To minimise the exposure of the extracted pigments all work was performed as quickly as possible in subdued light. This was especially important during sample chromatography when the carotenoids were particularly susceptible to damage. Therefore, TLC was carried out in in an acid free, dark fume hood. Prevention of sample oxidation was ensured by pigment storage of at –20 °C, sealed in containers that had been thoroughly flushed with O_2 free N_2. All solvents used during the procedures were either the highest grade available.

2.8.1 Large-scale pigment extractions

Large quantities of plant material (using up to 1 kg fresh weight of starting material) are required in order to purify individual carotenoids. Fresh orange peppers were diced with their core removed and frozen in liquid nitrogen. This material was transferred to a 1 l glass beaker and ethanol (EtOH) was added to submerge the sample up to a depth on 1cm. This was then homogenised for 1-2 minutes with a hand held Polytron (PT 1200 CL, Kinematica GmbH), the resulting homogenate was covered in foil and stored overnight in the dark. After this period the homogenate was filtered using a Buchner funnel and Whatman filter paper (12.5 cm diameter) and the residue re-extracted with re-distilled ethanol for approximately 30 minutes. The sample was then re-filtered and the procedure repeated until all of the pigments had been extracted. The filtrate was then treated with a 6:1 ratio 50% KOH, and stored overnight in the dark. An equal volume of diethyl ether was added to the treated filtrate and the mixture transferred to a large separating funnel. Phase separation was achieved by the gradual addition of dH_2O. If phase separation did not occur concentrated NaCl (5 M) solution was added and the solution left. If separation still did not occur then additional EtOH was added until the phases began to separate. Once separation had occurred the aqueous phase was removed and the diethyl ether layer, which containing the extracted pigments was washed with dH_2O. The phases were again left to separate before the aqueous phase was removed, this procedure was repeated twice before the aqueous phase was finally removed and the dry diethyl ether layer collected. The diethyl ether was removed and the pigments dried at 40 °C using a rotary evaporator. Any remaining water was driven off by the addition of a small amount of EtOH. The sample flask was then flushed with O_2-free N_2 to remove oxygen, sealed and stored at –20 °C until needed.

2.8.2 Preparation of standard thin layer chromatography (TLC) plates

The glass support plates were thoroughly cleaned with ethanol prior to use. A single pellet of KOH was dissolved in 60 ml dH_2O, to which was added 30 g Kieselgel 60 F_{254} (Sigma). The mixture was gently stirred to produce a lump free slurry and a commercial plate spreader used to produce uniform 0.5 mm thick preparative TLC plates. The plates were then oven dried for approximately 2 hours at 120 °C. Dry plates were removed and allowed to cool prior to use.

2.8.3 TLC tank preparation

The chromatography tank was lined with filter paper and filled with approximately 100 ml of the diethyl ether. The tank was allowed to equilibrate for approximately 30 minutes prior to use.

2.8.4 TLC purification of extracted carotenoids

Dry pigments were re-dissolved in 100 % diethyl ether, then applied in a concentrated band to a TLC plate using a drawn out pasteur pipette. The band was allowed to dry and the plate quickly transferred to a prepared TLC tank (see above). The solvent system for standard TLC was 100 % diethyl ether. Development was stopped when the solvent front was almost at the top. The TLC tank was covered at all times during the development of the plate to prevent damage to the carotenoids from the light. Individual pigment bands were then removed from the plate using a small brush. The silica was transferred to a scinted glass funnel and 100 % diethyl ether used to elute the carotenoid. Violaxanthin was removed first due to its susceptibility to degradation on silica. Eluted carotenoids were blown down to dryness under a stream of O_2-free N_2. Repeating the TLC procedure until the carotenoid ran as a single discrete band purified individual carotenoids. The final sample of pure carotenoid was dried under O_2 free N_2 and stored in a sealed N_2 flushed container at - 20°C.

2.8.5 Carotenoid identification

A number of techniques were used in conjunction to identify particular isolated carotenoids. Initial identification was performed by room temperature absorption spectroscopy using a Carey 500 UV/Vis scanning spectrophotometer. Absorption spectra of samples were measured in 100 % ethanol and the 3 main carotenoid peak positions were then compared to published values (Young and Britton, 1993). TLC was then used to calculate the R_f values of individual pigments in a 100 % diethyl ether solvent system (see table 2.1). Identification of individual carotenoids was achieved by comparing the R_f values of the pigments to those obtained from purified standards, (provided by Prof. A.J. Young).

$$R_f = \frac{\text{Distance Moved by Pigment}}{\text{Distance Moved by Solvent Front}} \qquad \text{(Equation 2.1)}$$

Table 2.1 Standard carotenoid R_f values (100 % diethyl ether solvent system)

R_f values represent the mean ± the standard error from the mean from 4 individual runs

Pigment	R_f Value	
	Standard	Experimental
Violaxanthin	0.19	0.19 ± 0.01
Antheraxanthin	0.37	0.38 ± 0.03
Zeaxanthin	0.51	0.50 ± 0.03

2.8.6 Identification of violaxanthin by its isomerisation into auroxanthin

Violaxanthin (di-5,6-epoxide) is highly susceptible to attack by acids, leading to the formation of the difuranoid (5,8-epoxide) auroxanthin. This isomerisation displays a characterised blue chromatic shift of approximately 40 nm (see table 2.2), and can be used to aid identification of violaxanthin. The carotenoid to be tested was dissolved in ethanol and its absorption spectra measured using the Carey 500. Following this a few drops of 0.5 M HCl were added to the cuvette and the contents mixed. The absorption spectrum was again measured to identify any changes in peak positions.

Table 2.2 Peak positions of violaxanthin and auroxanthin in 100% ethanol

Peak	λ_{Max} (nm)	
	Violaxanthin	Auroxanthin
1	419	380
2	442	400
3	472	425

2.9 Sucrose Gradients

A seven step exponential gradient from 0.1M to 1M sucrose was used. Two 60 ml stock solutions of 0.1M and 1.5M respectively (buffered with 20mM HEPES/pH 8.0 containing 20μM DM) are prepared for a total of six tubes. 1.5ml of 0.1M sucrose was pipetted into each of the six tubes (9ml total). Subsequently, 9ml of the 1.5M stock solution was added to the 0.1M stock and mixed. Again, a total of 9ml of the latter stock are added to the tubes. This process must be repeated six times to form the gradient. Finally 0.6ml of 1.5M sucrose was added to help prevent any sample pelleting. 200 to 300μl of sample are loaded onto each tube and centrifuged at 200 000 x g in a SW41 rotor for 18 h at 4°C.

2.10 Measurement of the *in vitro* chlorophyll fluorescence quenching of isolated PSII antenna complexes

In vitro fluorescence quenching measurements were carried out on individual antenna complexes using the method described by Ruban et al. (1994b; 1996). A modified DW2/2 aqueous-phase oxygen electrode (Hansatech instruments Ltd.) was used as the sample chamber and this was linked to a PAM 101 fluorimeter (Walz instruments Ltd.) by means of a fibre-optic. The output channel of the PAM 101 was connected to an R-50 multi-channel chart recorder (Rikadenki) allowing real time measurement of the fluorescence yield. Chlorophyll fluorescence was excited repeatedly by light pulses of either 1.6 or 100 kHz produced by a light emitting diode (LED). The LED had a peak wavelength of 650 nm with a short pass filter that cut at 680 nm. A long pass filter was used on the detector side to filter out light with wavelengths less than 700 nm. The sample chamber was maintained at 20 °C throughout the experiment by an RTE-4 refrigerated water circulator (NESLAB).

IEF prepared antenna complexes were adjusted to a final chlorophyll concentration of approximately 60 mg/ml in elution buffer (25 mM HEPES, 200 mM DM, pH 8.0) prior to use. LHCII samples were diluted into 1.2 ml of assay buffer (20 mM HEPES, 10 mM MES, pH 8.0) with constant stirring to give a final chlorophyll concentration of 3 – 6 mg/ml. Chlorophyll fluorescence was monitored continuously after the addition of the sample to the sample chamber and the level of quenching was quantified as the difference in fluorescence divided by the amplitude of the quenched fluorescence, $(F- F')/F'$, where F is the level of fluorescence recorded for a sample diluted into 200 μM DM.

2.11 SDS-polyacrylamide gel electrophoresis (SDS-PAGE)

Polypeptide compositions of samples were analysed by fully denaturing SDS polyacrylamide gels, using the Biorad™ mini-protean II system. The concentration of the resolving gel used was dependent on the size of the proteins to be separated. A 15-17 % gel was routinely used for analysis of the PSII antenna complexes as 17 % gels were found to give good resolution of the Lhcb1-3 polypeptides of LHCIIb. Samples were denatured at 90 °C for 20 minutes in sample loading buffer (0.0625 M Tris/HCl (pH 6.76), 2 % (w/v) SDS, 5 % (v/v) β-mercaptoethanol, 10 % (w/v) glycerol (BDH), 0.001 % (w/v) bromophenol blue (FSA Laboratory supplies)) then loaded onto a 15-17 % gel (15-17 % (w/v) 30/0.8 acrylamide/bis-acrylamide, 0.375 M Tris/HCl pH 8.8, 0.1 % SDS) polymerised using 1 % (v/v), ammonium persulphate (APS) and 0.1 % (w/v) N, N, N', N'-tetramethylethylene diamine (TEMED, Biorad). The stacking gel used was 6 % 30/0.8 acrylamide/bis-acrylamide, 0.125 M Tris/HCl, pH 6.8, 0.1 % SDS, polymerised using 0.4 % APS and 0.16 % TEMED. The gel running buffer contained 25 mM Tris, 192 mM glycine and 0.1 % SDS. SeeBlue+2™ standards (Invitrogen) were used as molecular weight standards. Gels were run at 120-150 V for approximately 60 minutes, until the standard markers had run fully.

2.12 Deriphat polyacrylamide gel electrophoresis (native green gels)

Non-denaturing gel electrophoresis was carried out according to the method of Peter and Thornber (1991) using a water-cooled Midget Electrophoresis unit (LKB). Antenna complexes were taken directly after preparation by IEF along with the IEF loading origin and applied at approximately 2 μg Chl/lane onto a 4.5 % Deriphat polyacrylamide gel (4.5% (w/v) 20/1 acrylamide/bis-acrylamide, 12 mM glycine, 1.54 mM Tris/HCl pH 8.3, polymerised with 0.05 % (v/v) TEMED, 0.12 % (w/v) APS). The running gel buffer contained 0.2 % (w/v) Deriphat 160-C (sodium N-dodecyl β-iminodipropionate), 0.01 % SDS, 95.9 mM glycine, 12.4 mM Tris/HCl pH 8.3. Gels were cooled to 4 °C during running with a water circulator, and electrophoresed at 130 V for approximately 45 minutes.

2.13 Staining of polyacrylamide gels

A number of staining techniques were used depending on the function of the gel in question.

2.13.1 Silver Stain

Silver staining of gels using the Silver Stain Plus kit (Biorad) was employed to visualise low quantities of proteins present in some samples. The protocol used followed the manufacturer's instructions, except that the Development Accelerator solution was prepared freshly each time. All glassware and containers were thoroughly cleaned using nitric acid (50 % (v/v)), and then well rinsed with dH_2O prior to use. 5 ml Silver Complex solution, 5 ml Reduction Moderator solution and 5 ml Image Development solution were added to 35 ml of dH_20 in order. This mixture was then added to 50 ml of Development Accelerator solution (5.3 % (w/v) development accelerator reagent), mixed briefly and poured onto the gel. Gels were stained for 5 – 15 minutes depending on the intensity required with gentle shaking. The reaction was stopped by placing the gels in 5 % (v/v) acetic acid for approximately 15 minutes, after which they were rinsed in dH_2O before drying.

2.13.2 Coomassie brilliant blue staining

Gels were stained overnight with Coomassie brilliant blue stain (0.25 % (w/v) Coomassie brilliant blue-R250, 10 % (v/v) methanol (BDH), 7 % (v/v) acetic acid 83 % (v/v) dH_2O). Gels were de-stained for 2-10 hours in 10 % (v/v) methanol, 7 % acetic acid 83 % (v/v) dH_2O.

2.14 Drying polyacrylamide gels

Gels were dried between sheets of cellophane (Promega) using a gel drying kit (Promega). The cellophane sheets were dipped in dH_2O and the gel placed between them, ensuring that no air bubbles were present. The assembled gel-drying frame was then warmed in an oven (BioRad GelAir Dryer) until the cellophane and gel were completely dry.

2.15 Western blotting

Primary antibodies against the PSII antenna proteins Lhcb1, Lhcb2, Lhcb3, Lhcb4, Lhcb5, Lhcb6 (provided by Dr Stefan Jansson (Umeå)) and PsbS (provided by Dr Mark Wentworth (Sheffield)) were used for the western blot analysis of samples.

2.15.1 Electro-blotting and antibody labeling

Following separation of protein samples by SDS-PAGE the gels were then electro-blotted onto a Hybond-C™ (Amersham) membrane using a BioRad electroblotting system. For 2 gels the protein was transferred to the membrane at a current of 30 mA and 250 V for 50 minutes in western transfer buffer (72 g glycine, 15.15 g trizma base, 1 l methanol, 15 ml 10 % SDS, dH_2O to a final volume of 5 l). After transfer the membrane was blocked overnight at room temperature with gentle agitation in membrane blocking solution (150 mM NaCl, 10mM Tris-HCl, pH 7.5, 0.05 % Tween 20, 5 % dried milk powder). Following this it was rinsed 2 x 5 minutes at room temperature with gentle agitation using wash solution (150 mM NaCl, 10 mM Tris-HCl, pH 7.5, 0.05 % Tween 20). The primary antibody was diluted from 1:1000 to 1:10000 times (depending on the antibody and sample used) in blocking solution and added to the membrane, which was then incubated at room temperature with gentle shaking for 2 to 3 hours. The blot was then washed 3 x 5 minutes at room temperature with gentle agitation in wash solution. The secondary antibody (horse-radish peroxidase labelled anti-rabbit IgG; Amersham Life Science) was then added to the blot and incubated at room temperature for 50 mins with gentle shaking. Finally, the membrane was washed 3 x 15 minutes at room temperature with gentle shaking with wash solution.

2.15.2 Antibody detection using ECL™ detection kit (Amersham)

Antibody binding was detected using an ECL Western Detection Kit (Amersham Life Sciences) following the manufacturer's guidelines. To summarize, Reagents 1 and 2 were mixed in equal volumes and added to the membrane between two layers of polythene. After 1 minute of gentle agitation, excess fluid was drained, the bag sealed and the blot exposed to Kodak X-OMAT AR film for 30 minutes. Subsequent exposure times were estimated depending upon the intensity of the signal from the initial exposure.

2.16 Concentration using Centricon® centrifugal filter devices

Isolated antenna complexes were routinely concentrated using Centricon® micro-concentrators (Millipore) with a 10kDa limit. The reservoir (2 ml maximum volume) was filled with sample and then before centrifugation at 4,500 x g for up to 20 minutes in a bench top centrifuge (MSE Mistral 1000). After the initial spin the sample was resuspended using a pipette, additional sample added and the centrifugation repeated. This process was repeated until the sample was at the concentration

required. The concentrated sample was collected by applying the collection cap to the top of the reservoir, inverting the filter and centrifuging at 2,000 x g for 2 minutes.

2.17 Determination of chlorophyll concentration

Sample chlorophyll concentration was measured using the method of Porra et al. (1989). Pigments were extracted with 80 % (v/v) acetone and centrifuged at 3,000 x g for 5 minutes to remove debris. Sample absorption was measured at 663 nm (A_{663}), 645 nm (A_{645}) and 470 nm (A_{470}) using a Beckman DU650 spectrophotometer. Chlorophyll concentration and chlorophyll *a*/*b* ratio were estimated using the following equations.

$$[\text{Chl } a] = 12.7\,(A_{663}) - 2.69\,(A_{645}) \qquad \text{(Equation 2.2)}$$

$$[\text{Chl } b] = 22.9\,(A_{645}) - 4.68\,(A_{663}) \qquad \text{(Equation 2.3)}$$

$$\text{Total } [\text{Chl}] = 20.2\,(A_{645}) - 8.02\,(A_{663}) \qquad \text{(Equation 2.4)}$$

$$\text{Chl } a/b \text{ Ratio} = \frac{[\text{Chl } a]}{[\text{Chl } b]} \qquad \text{(Equation 2.5)}$$

2.18 Absorption spectroscopy

Temperature controlled absorption spectroscopy of samples were recorded using a Carey 500 UV/Visible scanning spectrophotometer. For standard measurements absorption spectra were scanned at 5 nm/sec from 350-750 nm for chlorophyll containing samples or 350-600 nm for isolated carotenoids. Absorption spectroscopy in the protein region was scanned at 5 nm/sec from 190-500 nm. Data analysis and manipulations were carried out using Grams/32 (Galactic Industries Corporation) software.

2.19 Circular dichromism spectroscopy (CD)

Temperature controlled CD spectroscopy of samples were recorded using a Jasco J810 spectropolarimeter. Spectra were scanned at 5 nm/sec from 750-190 nm. Data analysis and manipulations were carried out using Grams/32 (Galactic Industries Corporation) software.

2.20 Resonance Raman Spectroscopy

Low temperature resonance Raman spectra were obtained in a helium flow cryostat (Air Liquide, Paris, France) using a Jobin-Yvon U1000 Raman spectrophotometer equipped with a liquid nitrogen-cooled charge-coupled devices detector (Spectrum One, Jobin-Yvon, Paris, France). Excitation was provided by Coherent Argon (Innova 100) and Krypton (Innova 90) lasers (at 457.9, 476.5, 496.5, 488.0, 501.7, and 514.5 nm and at 528.7 and 413.1 nm, respectively) and a Liconix helium-cadmium laser (at 441.6 nm). The choice of this wavelength range was determined by the absorption profiles of the xanthophylls used. This work was kindly carried out by Dr A Ruban (Sheffield).

2.21 PsbS sequence analysis

Sequencing of the PsbS protein was carried out using reverse phase HPLC mass spectrometry technique, provided by Dr Chi Wong (Sheffield). PsbS samples were ran on a 17% polyacrylamide gel and stained using colloidal blue (Novex), see section 2.20. Bands thought to be PsbS were cut from the gel and placed in 2ml eppendorf tubes (standard quality), kept at 4°C.

2.21.1 Reverse Phase HPLC

A CapLC (Waters) HPLC machine was used with a PepMap C18 column (LC Packings, USA) at a flow rate of 200 nl/min. Two HPLC grade solvents were used. Solvent A (95% dH_2O, 4.9% acetonitrile and 0.1% formic acid) and Solvent B (4.9% dH_2O, 95% acetonitrile, 0.1% formic acid), with the following gradient:

1. 3 min at 100% solvent A
2. 33 min 100% solvent A to 80% solvent B.
3. 2 min 80% solvent B
4. 2 min 100% solvent A.

2.21.2 Mass Spectrometry

This used a QTOF micro (Waters) mass spectrometer, set for MS scan for doubly and triply charged peaks, then switched into MSMS mode for fragmentation (i.e. peptide sequencing). Data analysis used MassLynx version 4 software with the ProteinLynx Global Server.

2.22 Colloidal blue staining (Novex)

Colloidal blue staining was performed following the manufacturer's instructions for Tris-Glycine gels. The gels were covered in freshly prepared staining solution (55 % (v/v) dH_2O, 20 % (v/v) methanol, 5 % (v/v) stainer B solution, 20 % stainer A solution) and left to stain for 3-12 hours with gentle shaking. The stain was removed and the gels de-stained overnight with 200 ml of dH_2O.

Chapter Three

PsbS Isolation & Characterisation

3.1 Introduction

It is now established that whenever incident light exceeds the dissipative capacity of electron transport and carbon assimilation, there is an excess of excitation density, which can destabilise the photosynthetic apparatus, and result in its damage. Protection against such damage requires the dissipation of excess light energy, which is detected as the nonphotochemical quenching of chlorophyll fluorescence, qE (see section 1.11). The transthylakid pH gradient and the xanthophyll cycle act to regulate qE, with the relationship between the latter and PsbS observed by Li et al. 2000 when mutational studies involving *Arabidopsis thaliana* generated the *npq*4-1 mutant described in section 1.11.4. However, the mechanism by which PsbS and the xanthophyll cycle detect changes in transthylakoid pH and subsequently regulate qE remains largely unexplained. One obstacle which has hampered attempts to eludicate the role of PsbS in qE is its extreme hydrophobicity, which leads to problems of aggregation when using established methods of thylakoid membrane fractionation (Dominici et al. 2001). Studies by other groups (Ljungberg et al. 1986; Kim et al. 1992; Funk et al. 1994; Funk et al. 1995a) have yielded conflicting results with regard to the ability of PsbS to bind cofactors and pigments. Absorption spectra suggesting that this protein can bind pigments (Funk et al. 1994; Funk et al. 1995a) have not been consistent, giving rise to the suggestion that such data is a result of non-specific binding. It was thus evident that further work was required to isolate the PsbS protein in both a native and highly purified state. Research leading to the development of a rapid procedure for the preparation of PsbS from spinach PSII membranes (Aspinall-O'Dea et al. 2002) is described here, along with characterisation of the purified protein.

3.2 Isolation of a 22 kDa polypeptide by iso-electric focusing (IEF)

Earlier work has employed IEF to isolate native LHCII components from photosystem II BBY particles (Berthold et al. 1981) using the method previously described by Bassi et al. 1992 (modified as in Ruban et al. 1994b). Therefore, an investigation was carried out to discover if PsbS could be purified using the same methodology. Immunoblot analysis of samples generated by IEF (for method see section 2.15) determined that PsbS was focused at the loading origin, or Z-band, of the gel as shown in figure 3.1 (referred to as **a**). The loading origin has been defined as Z as it is the last possible band on any IEF. Using an ampholine range of pH 3.5 – 5 IEF resolves PSII antenna proteins at a pI of approximately 3 (Fig 3.1I, sections 16 – 22) resulting in the formation of five green bands depicted by the letters A – E. Band A is the most intense of the five as it contains LHCIIb

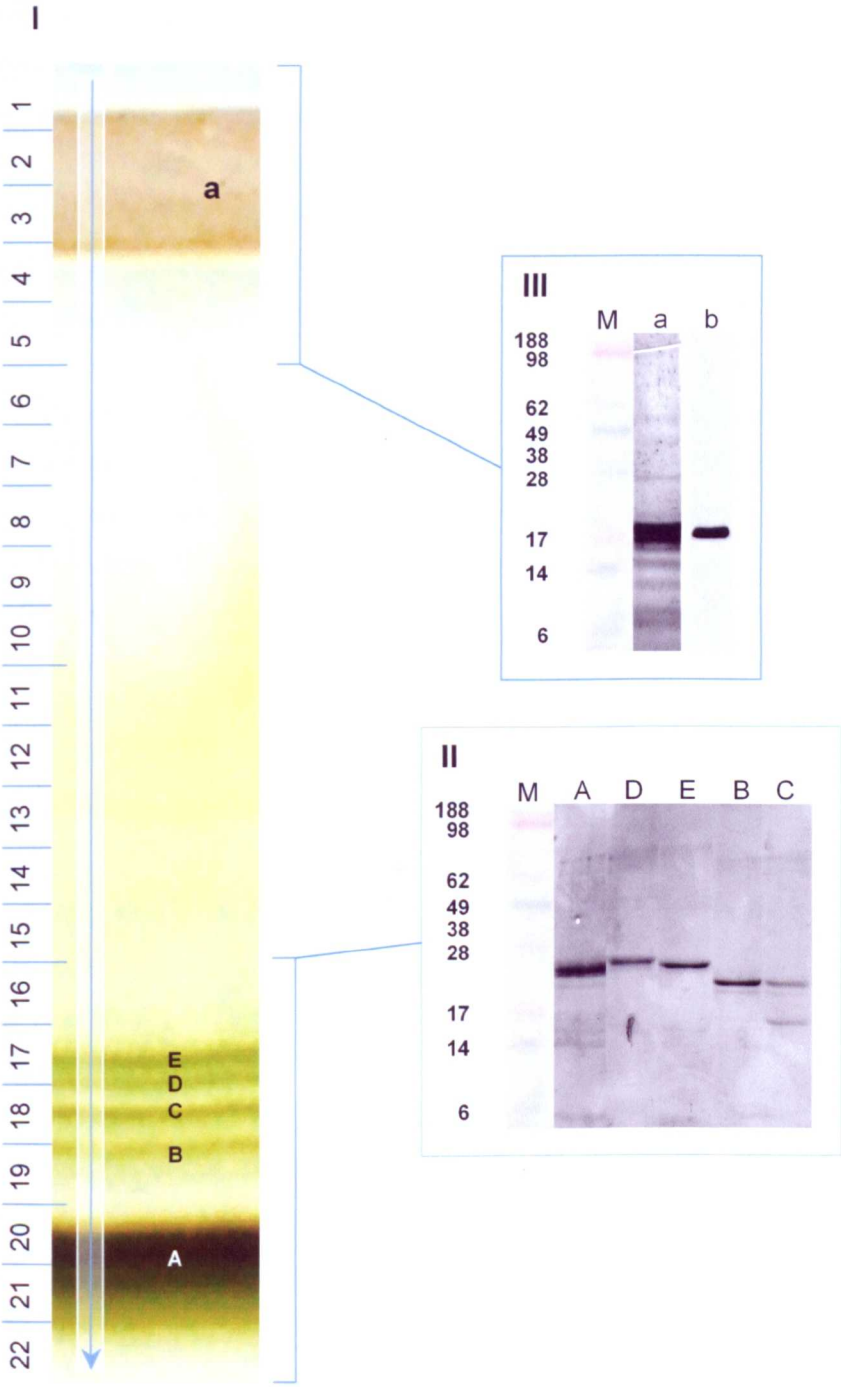

Figure 3.1 – IEF ampholine range pH 3.5-5. I, IEF gel loaded with digested BBY particles (2mg/ml). Arrow indicates the direction of decreasing pH. II, Silver stained SDS-PAGE gel loaded with LHCII antenna proteins, M Seeblu+2 marker (7μl), lanes A to E (10 μl) refer to the coloured bands on IEF labelled A to E. III, Silver stained SDS-PAGE gel loaded with sample from IEF section **a** (10μl). M, Seeblue+2 marker (7μl). **a**, as above, b, anti-PsbS immunoblot of **a**.

and the majority of chlorophyll present in the PSII particle preparation. This band is also seen to migrate the furthest. The next two bands (Fig 3.1I, bands B and C) represent the minor antenna complex proteins CP24 and CP26 respectively, with the former migrating slightly further than CP26 and displaying reduced chlorophyll intensity. Finally, bands D and E are formed by two protein species, CP29 and CP29'. These bands have comparable intensities and are thought to arise due to the phosphorylation of a percentage of the CP29 population in PSII. The IEF region denoted by the section 6 to 15 (Fig 3.1I) contains a large amount of carotenoid pigment along with the D1 and D2 PSII core proteins, whilst sections 1 – 5 contain a number of protein species including PsbS.

SDS-PAGE analysis of bands A to E (Fig 3.1II) confirmed the presence of the protein complexes described above, with lane A displaying a broad band containing LHCIIb after silver staining. Lanes D and E show CP29' to migrate slightly further on SDS-PAGE, probably due to a charge difference between the species. CP24 and CP26 can be seen in lanes B and C respectively, however the intensity of staining for the latter is significantly less. Analysis of sections 1 – 5 using SDS-PAGE and western blots revealed the location of PsbS on this IEF. All five sections were taken as one from the ampholine gel and concentrated using centricon® micro-concentrators (see section 2.15 for method). After silver staining the SDS-PAGE gel revealed nine distinct protein bands (Fig 3.1III, lane b). One high molecular weight band at ~40kDa could be resolved with an additional three bands grouped at around 20kDa. A band present at ~15kDa could be observed with an additional four low molecular weight bands below 10 kDa. Immunoblot analysis using an anti-PsbS antibody confirmed PsbS to be present at ~20kDa migrating the shortest distance of the three protein bands in that region (Fig 3.1III, lane c). Such observations are consistent with previous data suggesting that PsbS would focus at a pI greater than five (Ljungberg et al. 1986), which has been supported by analysis of samples prepared from flatbed IEF using the detergent octyl-glucopyranoside (Funk et al. 1995a). These preparations were derived from both etiolated and mature spinach plants, with the resultant *psbS* gene product shown to be located at the loading origin between pH 5.9 and 6.1 respectively.

A narrow pH range was employed between 5 and 7 (Fig 3.2), with the intention of focusing PsbS away from the loading origin at approximately pH 6. Analysis of the IEF showed that the central region of the ampholine gel was relatively free from pigments (Fig 3.2I, sections 5 – 15) with the major and minor PSII antenna components tightly focused at the end of the gel (Fig 3.2I, sections 21 and 22) preventing the resolution of individual minor antenna complexes. The loading origin retained the starch like consistency of earlier IEF runs as seen in figure 3.1Ia. SDS-PAGE analysis of samples A to D indicated that PsbS was not

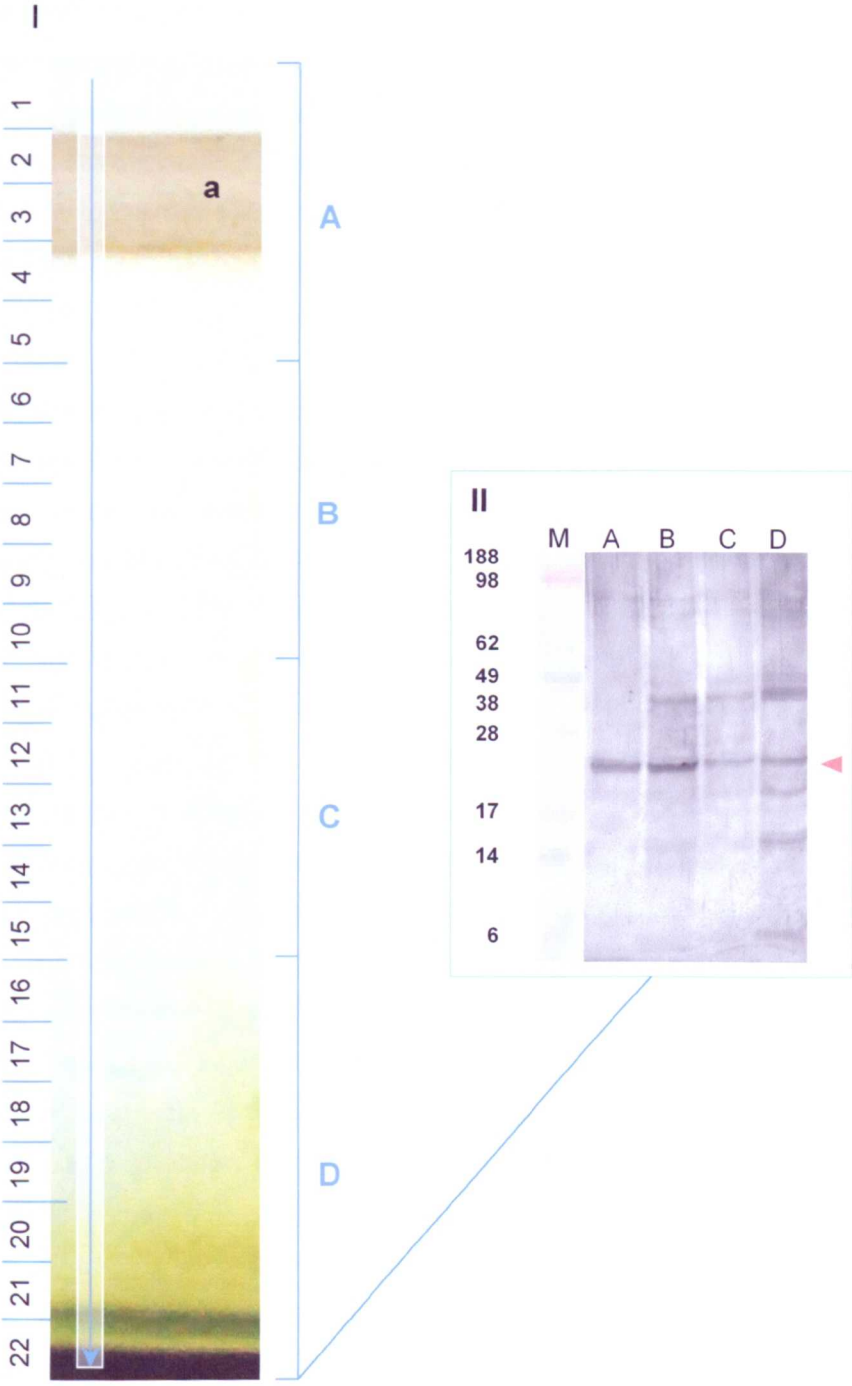

Figure 3.2 – IEF ampholine range pH 5.0-7.0. I, IEF gel loaded with digested BBY particles (2mg/ml). Arrow indicates the direction of decreasing pH. II, Silver stained SDS-PAGE gel loaded with samples A to D from IEF. M Seeblu+2 marker (7μl), lanes A to D (10 μl) refer to the sections on IEF labelled A to D (10μl). Red arrow indicates the location of the PsbS band on the gel.

focused and could be found across the entire gel, as shown in figure 3.2II were PsbS is denoted by a red arrow. Due to the intensity of the PsbS bands in lanes A and B (Fig 3.2II) it appeared the protein was predominantly located at this region on the corresponding IEF gel (Fig 3.2I), on or near the loading origin. In addition to PsbS, lanes B to C possess a number of other protein bands at approximately 18, 15 and >10 kDa along with PSII reaction centre and antenna proteins above the 22kDa PsbS band. The ampholine range between pH 5 and 7 was thought to be too narrow for effective focusing of the PsbS protein, however it was also possible that PsbS could not be resolved on IEF due to some inherent characteristic of the protein.

Analysing the first of these possibilities could easily be achieved through employing a wider pH range between 3 and 9 with the predicted pI of PsbS located far from the loading origin of the gel. Initial observations found that the LHCII antenna complexes were characteristically resolved around pH 3, with a broader focus of pigment throughout the latter half of the gel (Fig 3.3I). Four green bands can been observed in sections 20 to 22, which constitute PSII antenna complex proteins, however the resolution of the minor antenna proteins is significantly reduced from that seen in figure 3.1I, as shown by SDS-PAGE analysis in Fig3.3II. Lane 22 appears to contain LHCIIb almost exclusively, whilst the minor antenna complex proteins are poorly resolved between lanes 20 and 21. SDS-PAGE analysis of sections 1 to 19 determined that PsbS was only present in four of the first five sections taken from this IEF. It can be seen from the polyacrylamide gel shown in figure 3.3III that a significant amount of PsbS is present in lanes 2 and 3, which account for the loading origin (approximately pH 9) of the corresponding IEF (Fig 3.1I, **a**). The intensity of PsbS staining in lanes 4 and 5 is considerably less than in the latter two lanes, suggesting that the concentration of protein in these areas is relatively small. Interestingly, silver stains show sections 1 to 5 to almost solely contain PsbS, however it should be noted that the loading origin at section **a** is significantly cleaner than in previous IEF trials. The appearance of the loading origin depends upon the quality of market spinach used to prepare PSII particles, and this can be seen to vary widely between seasons, thus purity within the loading origin can not consistently be reproduced. It was evident that further purification of PsbS using isoelectric focusing may not be possible. The location of the protein was consistent across all three of the pH ranges employed during these experiments. However, the PsbS extracted from the loading origin could not be used for further study due to the presence of so many other polypeptides. Nonetheless, the Z-band did provide an excellent platform from which further purification of PsbS could be attempted using alternative techniques.

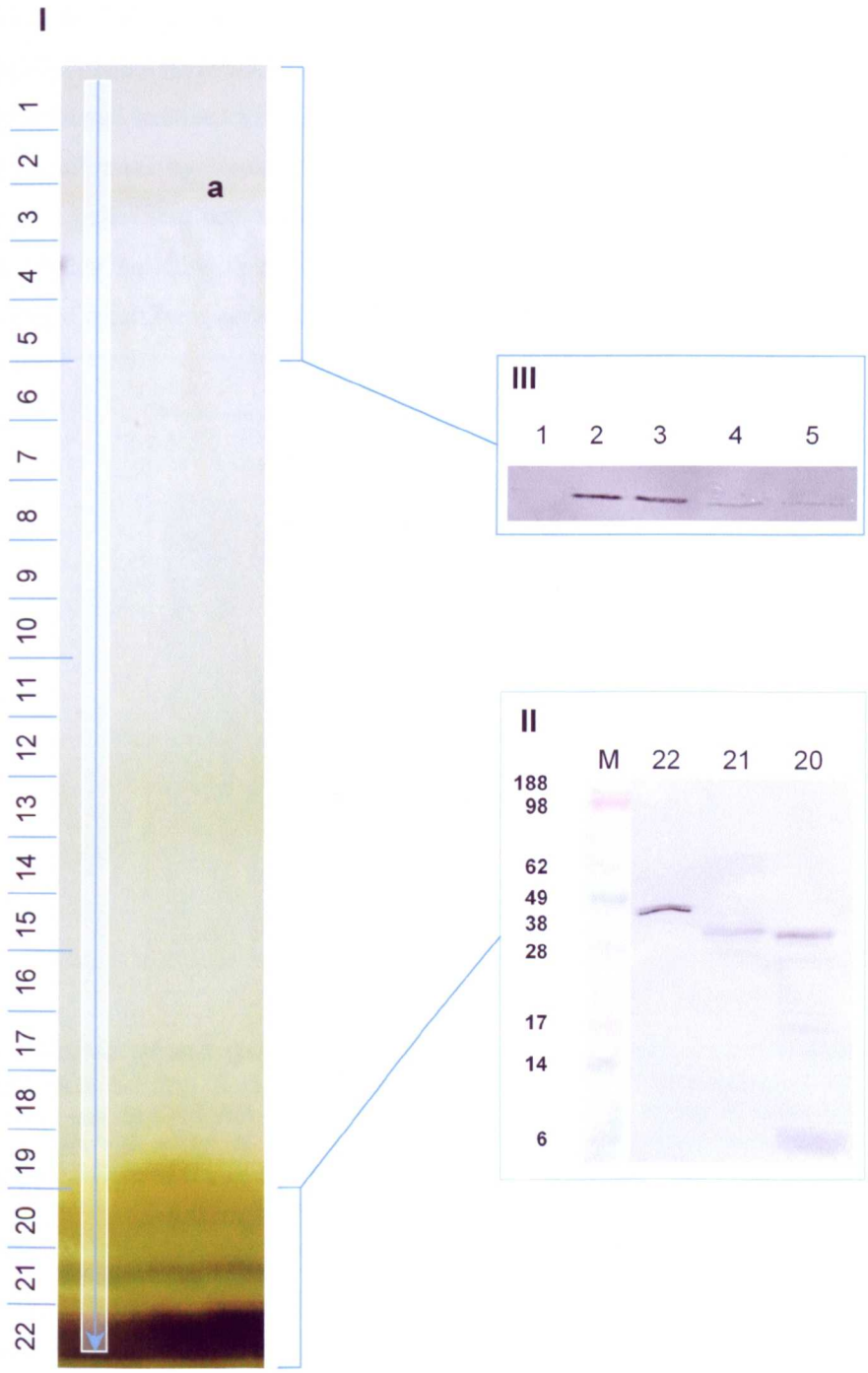

Figure 3.3 – IEF ampholine range pH 3.0-9.0. I, IEF gel loaded with digested BBY particles (2mg/ml). Arrow indicates the direction of decreasing pH. II, Silver stained SDS-PAGE gel loaded with LHCII antenna proteins derived from section 20 to 22 on the IEF. M Seeblu+2 marker (7μl), lanes 20 to 22 (10 μl). III, Silver stained SDS-PAGE gel loaded with samples from IEF sections 1 to 5. M, Seeblue+2 marker (7μl). Lanes 1 to 5 as described.

The experiments using IEF could be explained simply by the fact it is not possible to focus PsbS using this technique, however it was important to ensure that the protein was not immobilised in some way, for instance through aggregation due to its extreme hydrophobicity. PsbS enrichment had been observed in the Z-band sample extracted using an ampholine range between pH 3.5-5 (Fig 3.1I). Previous attempts to isolate the protein from PSII membranes by Funk et al. (1994) using octyl-thioglucopyranoside (OTG) had given rise to a pellet that possessed remarkable similarity to the Z-band extract from IEF. Treatment of this pellet with repetitive electrophoresis under non-denaturing conditions isolated a single green band containing the 22 kDa PsbS as shown by immunoblot analysis.

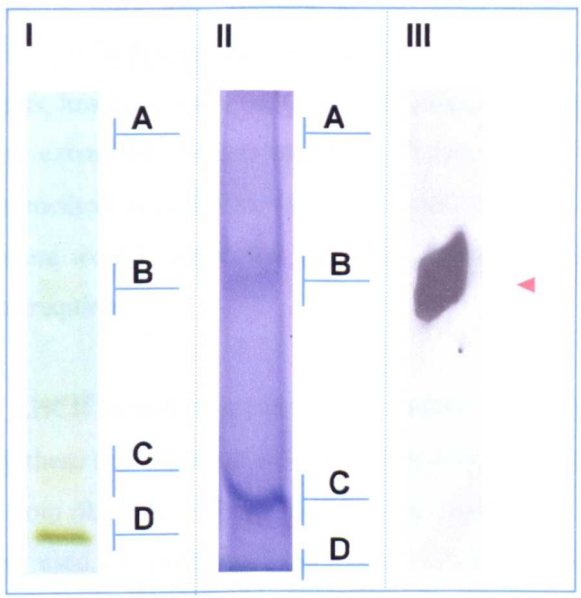

Fig 3.4 – Native green gel. I and II, Z-band preparation extracted with detergent mix (for method see section 2.x). 8ml sample loaded per lane separated on a 10% polyacrylamide gel by Deriphat-PAGE having 0.3ml 10% SDS added to reservoir buffer at 100V and 4°C for ~20 mins. A, PSII – RC core components. B, PsbS protein. C, Additional low molecular weight Z-band components. D, Free Pigment. II, same result as I with comassie blue stain. III western blot of I with anti-PsbS antibody at 1:2500 dilution.

The use of non-denaturing gel electrophoresis would enable the characterisation of the Z-band fraction and determine if PsbS (in a non-denatured state) could be resolved using PAGE. The use of this procedure when analysing PSII membranes from barley found the LHCII antenna proteins migrated between the reaction centre components and free pigment, with the latter travelling furthest in the gel (Peter and Thornber, 1991). Figure 3.4I displays a gel containing four pigmented bands designated A to D, which were tentatively assigned using the evidence described by Peter and Thornber, (1991). Thus, band A was thought to consist of reaction centre components, with free pigment denoted by band D. Band C is observed to travel almost as far as free pigment, thus accounting for low molecular weight

components in the Z-band. Therefore, it was possible that band B could contain PsbS, as this band appeared in a region of the gel normally occupied by LHCII antenna components during PSII membrane separation. The colouration of these bands would also indicate that a number of Z-band components could potentially bind pigments. Staining of the gel with coomassie blue (Fig 3.4II) did not indicate the presence of any additional protein bands absent from fig 3.4I, and consisted of four similarly positioned bands again designated A to D. It was not clear whether any of these represented PsbS, thus immunoblot analysis of the gel was performed, which determined that the protein was located within the second pigmented band (Fig3.4III) as had earlier been predicted. The configuration of the bands within the gel suggested that reaction centre components along with additional low molecular weight proteins were also isolated in the Z-band extract, albeit with less abundance than PsbS. This technique had shown that PsbS could be separated from the other Z-band components, however it was not a suitable basis with which to start large-scale protein purification and extraction for two reasons. Electro elution of PsbS from the gel would be an inefficient method of isolation, whilst the small loading volumes (8µl per lane) required for the procedure would reduce this efficiency further still, thus a more effective method of isolation was required.

Previous work with LHCII antenna proteins had employed sucrose density gradient centrifugation to purify these complexes after isolation by IEF Ruban et al. (1999), using an exponential gradient from 0.15 to 1.0 M sucrose (for method see section 2.9). This technique was therefore used for analysis of the Z-band. A total of eight Z-band fractions concentrated to ~500µl were required in order to achieve a chlorophyll concentration that could be visualised on the sucrose gradient (Fig 3.5). It is predicted that PsbS would be located slightly lower on the sucrose gradient than monomeric LHCII and higher than trimeric LHCIIb, which had been observed at sucrose densities of 0.3M and 0.43M respectively (Ruban et al. 1999). Additionally, PSII components were found at 0.51M sucrose with PSI located at 0.61M. Free pigment was observed at 0.21M sucrose. The sucrose gradient for LHCIIb trimers isolated by IEF can be seen to display four distinct coloured bands (Fig 3.5, tube I). Band A possesses very weak colourisation and is denoted as free pigment due to its presence at ~0.21M sucrose. The pale green band at 0.30M sucrose (band B) is occupied by LHCII monomers, whilst band C (0.43M) contains trimeric LHCIIb. The population of band D (0.48M) is unknown, however it is possible that it contains PSII components along with proteins damaged as a result of IEF. Tube II (Fig 3.5) displays a similar banding pattern to that of tube I, however the trimeric LHCIIb band observed in the latter is absent. The free pigment band at ~0.21M is paler than in tube I, with the overall chlorophyll content significantly reduced. Again, LHCII monomers

(specifically CP29) are located at 0.3M sucrose with an additional band at ~0.48M similar to that described in tube I, albeit with significantly reduced pigment content.

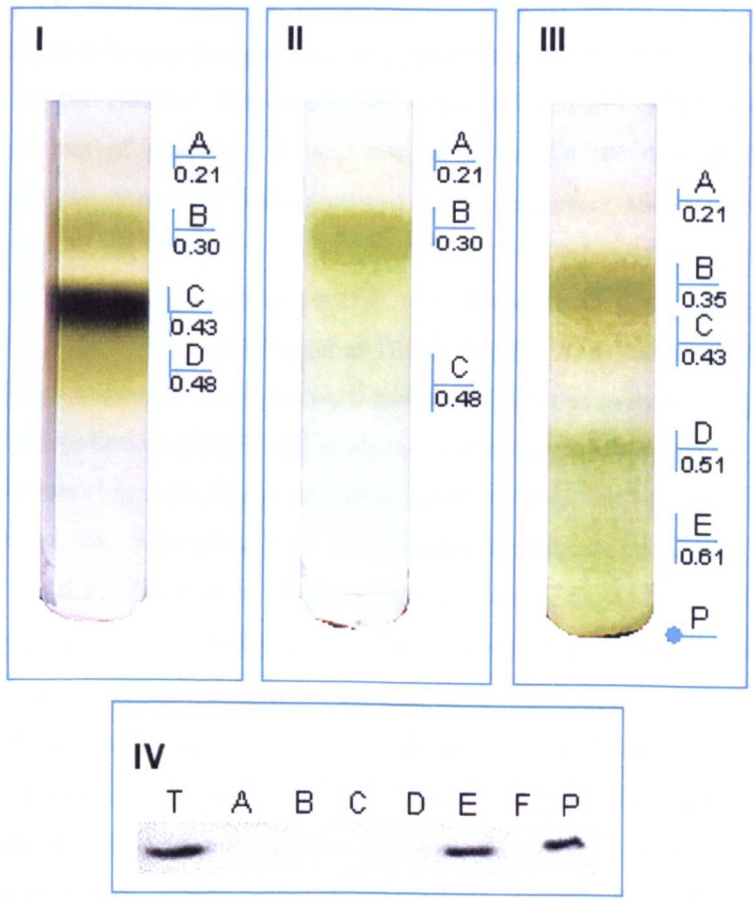

Fig 3.5 – Sucrose gradient analysis of IEF Z-band. Sucrose density gradient analysis of PSII-antenna components and Z-band isolated using IEF. I, LHCIIb trimer. II, CP29 monomer. III, Z-band. Free Pigment in all tubes designated as (A). (B) in tubes I and II is LHCII monomer (CP29/CP26). (C) tube I LHCIIb trimer. (D) tube I PSII. (C) tube II PSII. Tube III, (B) apparent monomer band, (D) pigment free region, (E) PSII, (F) PSI, (P) gradient pellet. IV, western blot analysis of tube III samples A – P with thylakoid control (T) using anti-PsbS antibody at 1:2500 dilution.

Tube three (Fig 3.5III) shows the gradient of the IEF Z-band to have five distinct coloured bands marked A-E, along with a pellet (P). A free pigment band had formed at 0.21M sucrose (band A) with a second band located at ~0.35M sucrose (band B), which was initially thought to contain PsbS due to the prediction described earlier. Additionally, band C (0.43M) had the appearance of the trimeric LHCIIb population in tube I, whilst bands E (0.51M) and F (0.61M) were both located at densities previously described for PSII and PSI components respectively (Ruban et al. 1999). However, observations derived from immunoblot analysis of the gradient fractions (Fig 3.5IV), indicated that PsbS was associated

with PSII (Band E), with a significant quantity of the protein in the gradient pellet (P) and completely absent from the remaining bands in the sucrose gradient.

The outcome of the sucrose gradient appeared to contradict earlier work involving non-denaturing PAGE, and it was thought that the concentration step employed to visualise the Z-band sample on the gradient had caused the hydrophobic PsbS protein to aggregate, or simply precipitate out of solution. It was also possible that the detergent used in non-denaturing PAGE (Deriphat-160) had solublised PsbS. If correct, the latter would indicate that incubation of PSII particles with 1% DM had failed to solublise the protein; this in turn could account for its inability to focus on IEF. To further explore these possibilities PSII particles treated with DM were centrifuged at 10 000 x g for 20 minutes prior to application on IEF to ensure all suspended particles were removed from the sample. Figure 3.6I shows the effect of centrifugation on the IEF gel analysed over an ampholine range of pH 3.5-5. As in earlier experiments (Fig 3.1I) five green bands could be observed between sections 17 and 22 (labelled A to E), indicating that centrifugation had not adversely affected the performance of the IEF. The region located between sections 6 and 16 could again be seen to contain a large quantity of carotenoid pigments, however the loading origin of the gel appeared significantly cleaner in figure 3.6I, due to the removal of starch and insoluble components from the sample applied. SDS-PAGE analysis of the antenna complexes (Fig 3.6II) revealed samples A – E possessed similar characteristics to those seen in figure 3.1II, with a broad LHCIIb band (Fig 3.6II, lane A), a slight disparity between the two CP29 species in lanes D and E, and a significantly reduced staining intensity for CP26 when compared to CP24 (lanes C and B respectively). An additional band at ~15kDa could also be seen in lane C. Analysis of sections 1 to 5 (Fig 3.6III, lane a) displayed a significant reduction in protein content when compared to figure 3.1III (lane a), whilst an anti-PsbS immunoblot confirmed the presence of PsbS in the loading origin, albeit at a greatly reduced concentration. When using a narrow ampholine range between pH 5 and 7, PsbS had been observed across the entire IEF gel. Figure 3.7I again appeared similar to an earlier gel (Fig 3.2I) with the LHCII antenna complexes poorly resolved at ~pH 5 (Fig 3.7I, section H), whilst the central region of the gel seemed largely devoid of pigments (Fig 3.7I, sections G and F). Here the loading origin also appeared cleaner after centrifugation. SDS-PAGE analysis of the IEF (Fig 3.7II) indicated that PsbS was now only present in lanes E and F, corresponding to the first half of the gel nearest the loading origin. A high molecular weight protein (~50kDa) is present in lanes F to H, with all LHCII antenna components located on lane H. The intensity of PsbS bands present in lanes E and F was significantly reduced when compared to the earlier gel (Fig 3.2II), whilst the total number of bands present had fallen dramatically. The third ampholine range employed in these experiments followed the same

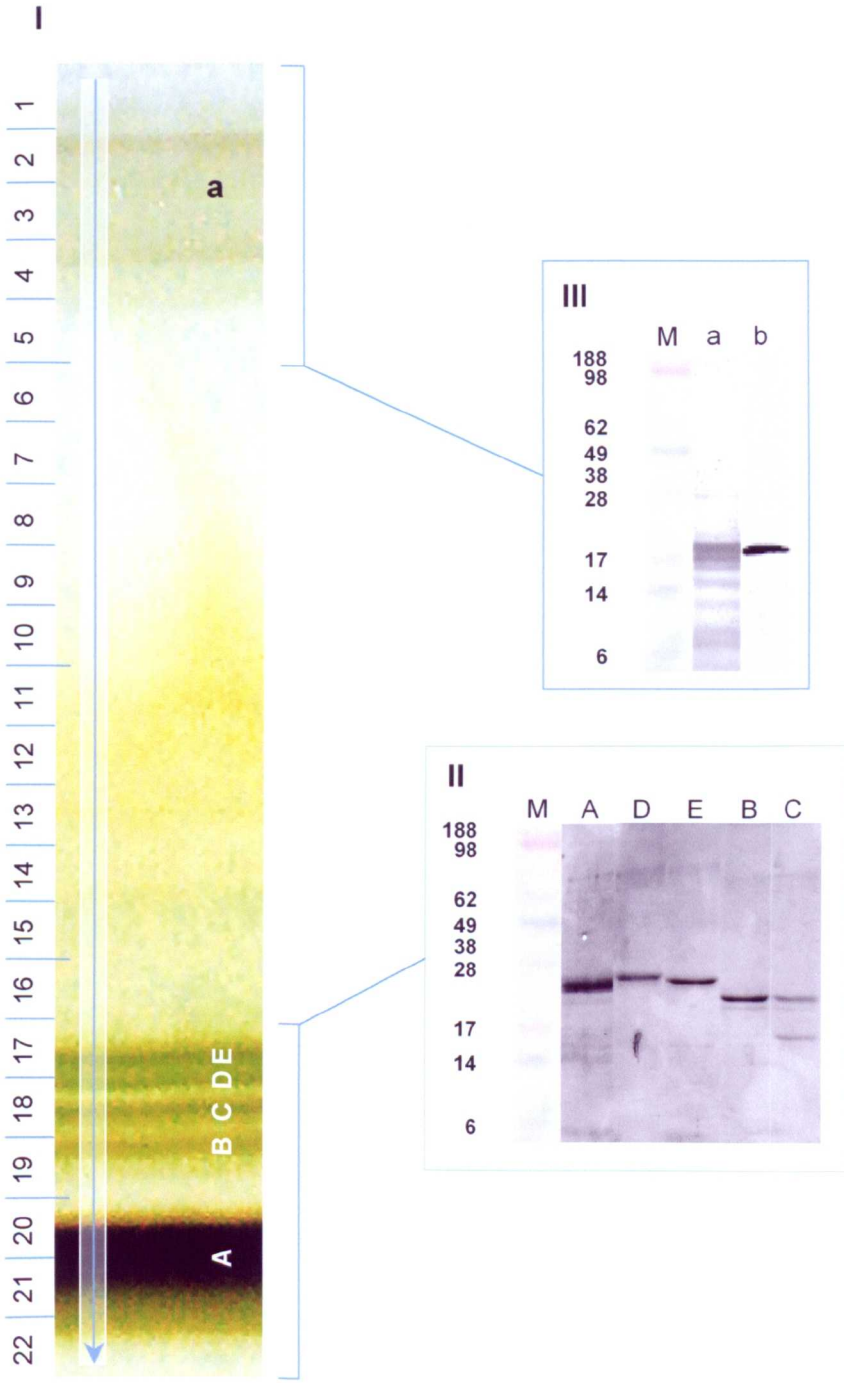

Figure 3.6 – IEF ampholine range pH 3.5-5. I, IEF gel loaded with digested BBY particles (2mg/ml), centrifuged at 10 000 x g for 20 min prior to application. Arrow indicates the direction of decreasing pH. II, Silver stained SDS-PAGE gel loaded with LHCII antenna proteins, M Seeblu+2 marker (7μl), lanes A to E (10 μl) refer to the coloured bands on IEF labelled A to E. III, Silver stained SDS-PAGE gel loaded with sample from IEF section **a** (10μl). M, Seeblue+2 marker (7μl). **a**, as above, b, anti-PsbS immunoblot of **a**.

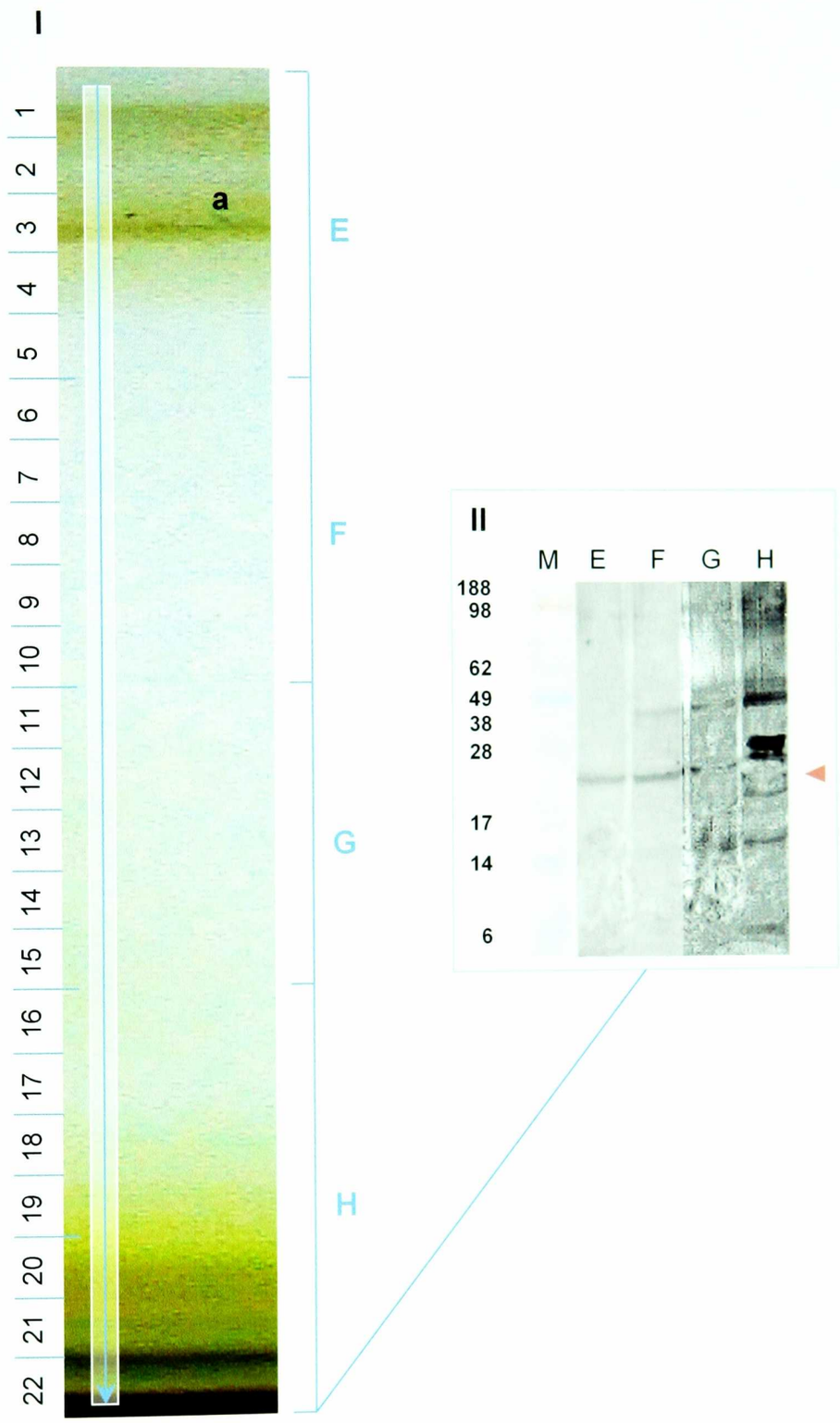

Figure 3.7 – IEF ampholine range pH 5.0-7.0. I, IEF gel loaded with digested BBY particles (2mg/ml), centrifuged at 10 000 x g for 20 min prior to application. Arrow indicates the direction of decreasing pH. II, Silver stained SDS-PAGE gel loaded with samples A to D from IEF. M Seeblu+2 marker (7μl), lanes A to D (10 μl) refer to the sections on IEF labelled A to D (10μl). Red arrow indicates the location of the PsbS band on the gel.

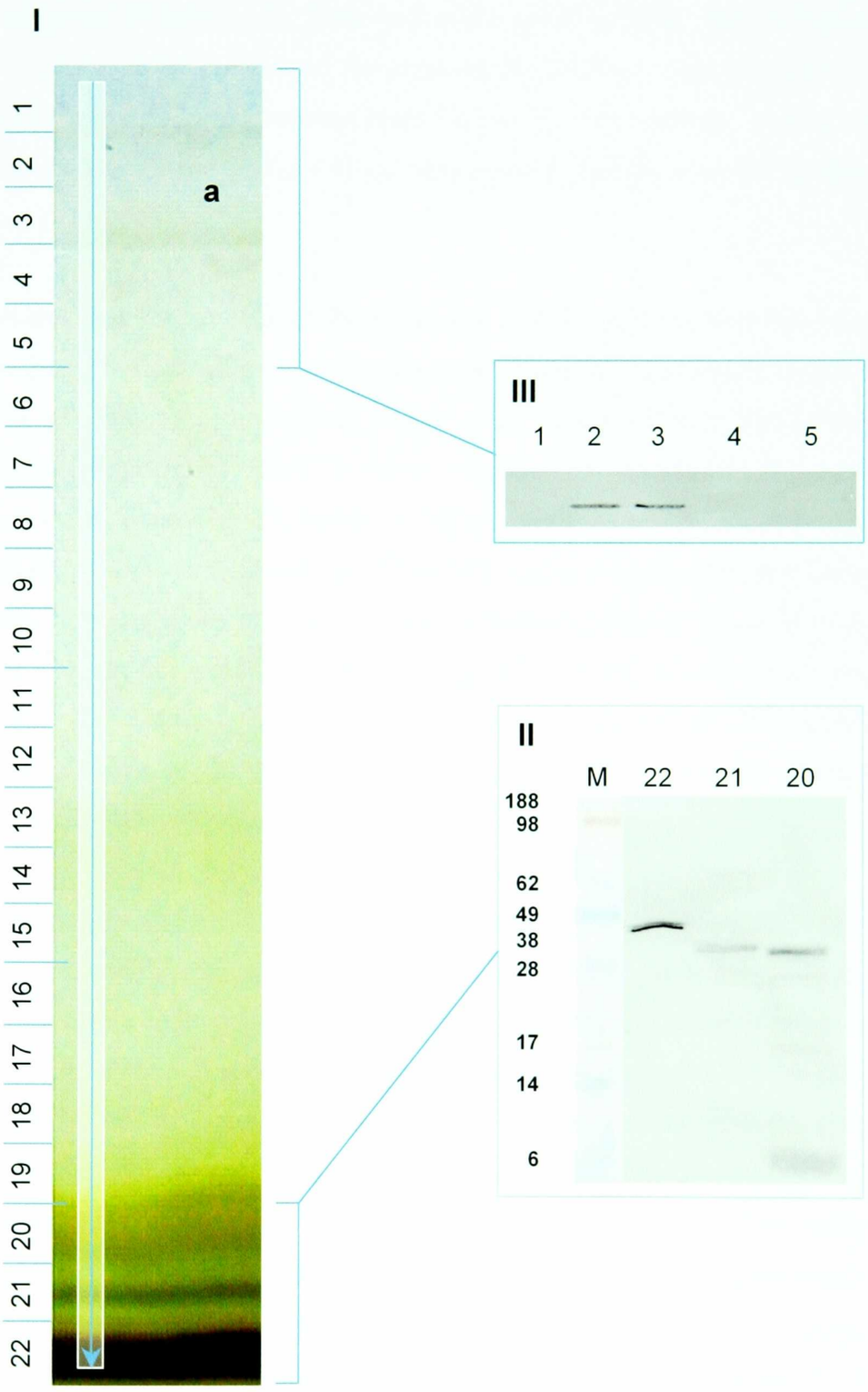

Figure 3.8 – IEF ampholine range pH 3.0-9.0. I, IEF gel loaded with digested BBY particles (2mg/ml), centrifuged at 10 000 x g for 20 min prior to application. Arrow indicates the direction of decreasing pH. II, Silver stained SDS-PAGE gel loaded with LHCII antenna proteins derived from section 20 to 22 on the IEF. M Seeblu+2 marker (7μl), lanes 20 to 22 (10 μl). III, Silver stained SDS-PAGE gel loaded with samples from IEF sections 1 to 5. M, Seeblue+2 marker (7μl). Lanes 1 to 5 as described.

trend (Fig 3.8I). LHCIIb could be located in section 22 of the IEF; with the minor antenna proteins poorly resolved between sections 20 and 21. Again, a broader focus of pigment could be observed throughout the latter half of the gel (Fig 3.8I). SDS-PAGE analysis of lanes 20 to 22 (Fig 3.8II) confirmed the presence of LHCIIb in lane 22, whilst the LHCII minor antenna were dispersed between lanes 20 and 21. Interestingly, however, PsbS was only present in lanes 2 and 3 (Fig 3.8III), corresponding exactly with the loading origin of the IEF.

It was evident that the amount of PsbS present in PSII particles had been significantly reduced as a result of centrifugation, with the remaining population largely unable to migrate through the gel, again suggesting that it was simply not feasible to focus PsbS on IEF. However, the observations made in these experiments could also be explained by considering the extreme hydrophobicity of the protein. It was possible that residual PsbS protein, present within the supernatant of the PSII particle preparation after centrifugation, was effectively 'sticking' to other hydrophobic membrane proteins. Thus, by increasing the duration of PSII particle incubation with 1% DM, this residual protein could be effectively washed off. To further investigate these proposed explanations, PSII particles were subjected to a series of increasing incubation periods, beyond the 30 minutes already employed for IEF sample preparation.

SDS-PAGE analysis of the pellet and supernatant derived from extracted BBY particles after centrifugation found that the pellet was highly enriched in PsbS (Fig 3.9), with the majority of high molecular weight proteins present in the supernatant. In order to determine the percentage yield of PsbS, it was assumed that PSII particles possessed 100% of the available PsbS protein. It was necessary that samples were loaded onto the SDS-PAGE gel on the basis of volume, not protein concentration. To achieve this the pellet, formed after centrifugation, was resuspended in buffer to 1ml, whilst the supernatant concentration using 10kDa centricon® micro-concentrators to the same volume. Of each sample, 200µl would be taken and diluted five times into loading buffer, insuring good mixing of sample prior to extraction. Once diluted, samples were denatured in the normal way (see section 2.11). The SDS-PAGE gel shown in figure 3.9I displays the result of each incubation period tested. Lanes A to C show the content of pellets formed after incubation for 40, 45 and 50 minutes respectively. Lanes D to E show the supernatant content over the same incubation periods. The striking feature of lanes A to C is an almost complete lack of protein bands above the ~22kDa PsbS band indicated by the red arrow. Additionally, these lanes display a number of low molecular weight bands. In each case, the level of band staining intensifies with increasing incubation period. Lanes D to F contain a large number of tightly packed protein

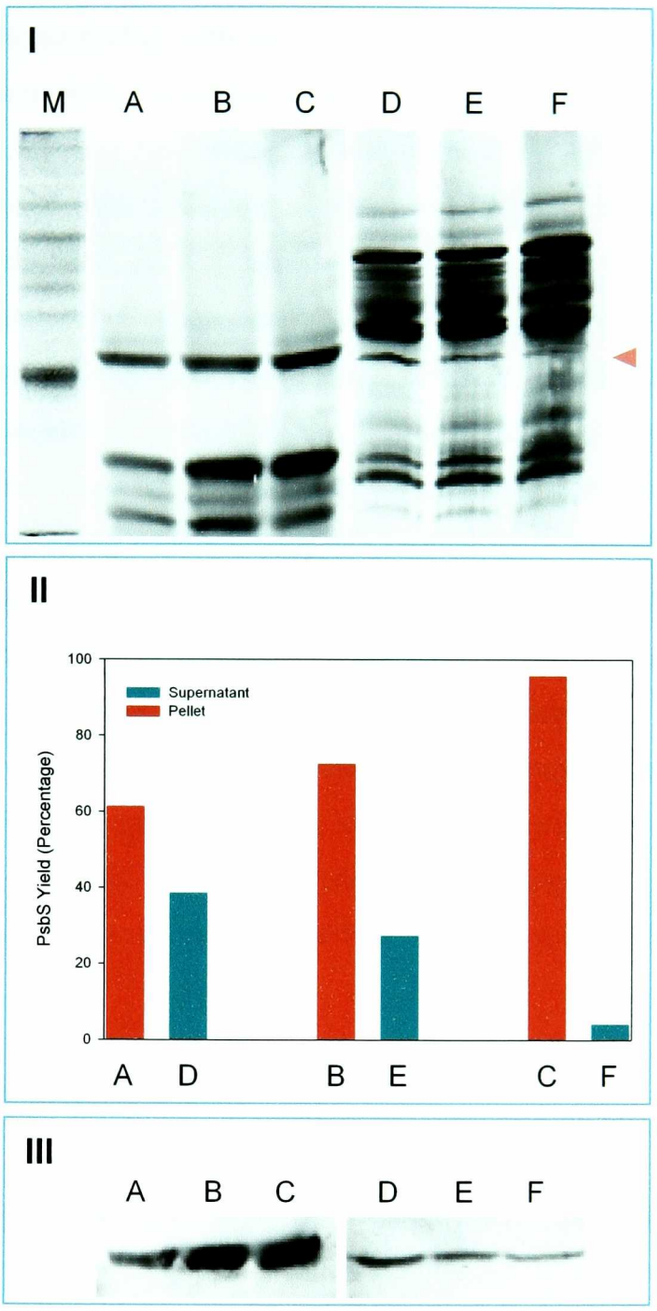

Fig 3.9 – DM optimisation. I, silver stain analysis of SDS-PAGE gel loaded with 10μl sample per lane treated with 5x loading buffer. M, molecular weight marker Seeblue+2 (invitrogen). A, BBY pellet after 40 min extraction with 1% DM. B, 45 min extraction pellet. C, 50 min extraction pellet. D, BBY supernatant after 40 min extraction with DM. E, 45 min extraction supernatant. F, 50 min extraction supernatant. Red arrow indicates position of 22kDa PsbS band in gel. II, densitometry data comparing concentration (density) of PsbS in BBY pellet and supernatant vs extraction time, A – D, 40 min extraction. B – E, 45 min extraction. C – F, 50 min extraction. Dark cyan (pellet) and light cyan (supernatant). III, western blot of I using anti-PsbS antibody at 1:2500 dilution.

bands above the ~22kDa PsbS protein, accounting for LHCII antenna and PSI core proteins. A number of bands can also be detected below 22kDa, with the staining intensity of two bands around 10kDa increasing with each incubation period. The high molecular weight proteins can be seen to follow a similar trend, whilst the PsbS protein appears to decrease over the same range. Some low molecular weight bands do not follow this trend, and can be seen to increase in both the pellet and supernatant. This phenomenon is thought to result from staining imperfections, as a sample with fewer proteins will stain differently to a sample with a large number of components. As a result, it is difficult to quantify the staining of specific bands between heterogeneous samples, however, densitometry analysis can reveal trends and provide an idea of protein yield. It is also possible, however, that these bands represent different proteins. Figure 3.9II shows the estimated PsbS yield for each incubation period, with column labelling corresponding to a lane on the SDS-PAGE gel (Fig 3.9I). The graph displays a steady increase in PsbS enrichment within the pellet from ~60% after 40 minutes to almost 95% after 50 minutes. Figure 3.6II shows an anti-PsbS immunoblot of these samples, and highlights the change in PsbS concentration within the pellet and supernatant respectively, and supports the densitometry analysis described above. Thus, incubation with DM can be used to remove most of PSII proteins from the pellet, leaving almost 100% of the available PsbS protein along with a number of low molecular weight proteins. This provides an excellent platform from which to selectively solublise PsbS using a different detergent.

3.3 Selective Solublisation of PsbS

A number of detergents had previously been employed when solublising and extracting intrinsic membrane proteins from the thylakoid including Triton X-100 (Ljungberg et al. 1986), OGP (Funk et al. 1994; Funk et al. 1995a) and Sodium Cholate (Bowlby and Yocum, 1993). Deriphat – 160 had been observed to solublise PsbS during non-denaturing electrophoresis (Fig 3.4). Thus deriphats ability to solublise PsbS, along with the others mentioned, would be used in an attempt to selectively extract the protein from the DM pellet. In each extraction, the DM-pellet was resuspended in 1ml of detergent buffer to maintain consistency with earlier experiments involving DM.

The results of these extraction experiments are presented in figure 3.10I. After extraction with 0.06% Triton X-100 in the presence of 1M NaCl (lane 2), the resultant supernatant appeared to posses a similar protein complement to that of the DM-pellet (lane 1), albeit at a significantly lower concentration. Densitometry analysis determined that the concentration of lower molecular weight proteins present in the supernatant appeared to be higher than that

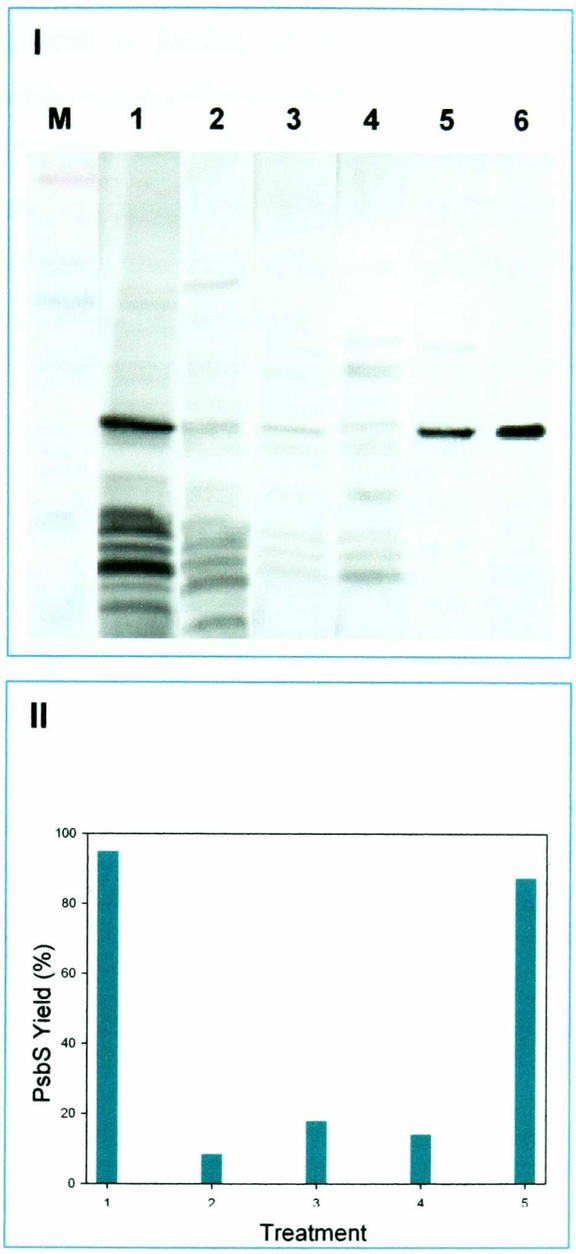

Fig 3.10 – Selective Solublisation of PsbS I, silver stain analysis on SDS-PAGE gel loaded with 10μl of sample per lane pre-treated with 5x loading buffer. M, molecular weight marker SeeBlue+2 (invitrogen). 1, DM-pellet control. 2 – 5 are detergent extractions of 1. 2, 0.6% triton X-100. 3, 1% deriphat – 160. 4, 0.6% OTG. 5, 0.5% Na-Cholate. 6, Western blot of 5 using anti-PsbS antibody at 1:2500 dilution. Samples 2 – 5 incubated with detergent, vigorously shaken for 5 mins and kept overnight at 4°C. II, densitometry analysis of bands resolved on SDS-PAGE gel. Total of 13 individual bands resolved across lanes 1 – 6. Blue box indicates absence on a particular band in that lane. Bands counted horizontally from top to bottom. III, Densitometry chart of band 6 (PsbS) showing the percentage purity of the band vs treatment. 1 – 5 relate to lanes 1 – 5 on I.

of PsbS (Table 3.1). In addition, the use of Triton seemed to efficiently extract a high molecular weight protein at ~50kDa (Fig 3.7I, lane2) which constituted ~11% of the total protein in that lane, with a number of lower molecular proteins present at similar concentrations. Extraction using a 1% deriphat–160 solution had a relatively minor effect upon incubation with the DM-pellet (Fig 3.7I lane 3). A number of proteins can be observed with molecular weights both higher and lower than 22kDa at bands 3, 7 and 9 – 11 (Table 3.1), extracted with roughly the same efficiency as PsbS (Table 3.1, band 6), thus no enrichment of the PsbS protein had occurred.

Bands	Lane					
	1	2	3	4	5	6
1	1	9				
2	2					
3			11	8	5	
4	1	7	9	19		
5	1	4	3	4		
6	20	9	19	16	92	100
7	12	8	12	8		
8	15	10	7	17		
9	13	13	13	5	3	
10	20	12	13	5		
11	7	15	13	18		
12	8					
13		13				

Table 3.1 – Densitometry analysis of detergent extractions. Total of 13 individual bands resolved across lanes 1 – 6. Blue box indicates absence on a particular band in that lane. Bands counted horizontally from top to bottom. III, Densitometry chart of band 6 (PsbS) showing the percentage purity of the band vs. treatment. 1 – 5 relate to lanes 1 – 5 on I.

The 50kDa protein present in lane 2 (Table 3.1, band 1) is absent in this extract, along with a low molecular weight component of ~10kDa (Table 3.1, band 13). Lane 4 is the result of an extraction with 0.6 % OTG, and appears to be remarkably similar to that of deriphat–160 with an overall extraction efficiency roughly half that of Triton. Bands 4, 8 and 11 are all present at similar concentrations to that of PsbS (Table 3.1, band 6). In addition, a number of other bands have been resolved and are also clearly present in lanes 1 to 3. Extraction with 0.5% Na-cholate (Fig 3.10, lane 5), in the presence of 250mM NaCl at pH 7 as described by Bowlby and Yocum, (1993) yielded a significant enrichment in PsbS. Analysis of the SDS-PAGE gel shows a single heavily stained band at 22kDa (~92%), along with a minor contamination from a higher molecular weight protein at about 35kDa (~5%) and a single low molecular weight protein (~3%). Incubation with anti-PsbS antibody (Fig3.10,

lane 6) determined that the 22kDa band was indeed PsbS. Figure 3.10II tracks that extraction efficiency of each treatment. The percentage yield of PsbS shown is calculated on the assumption that 100% of the protein is present in a PSII particle preparation, and 95% of this protein is present in the DM-pellet (Fig 3.10, lane 1). Thus, it can be concluded that Na-Cholate is 4 to 5 times more efficient at extracting the protein than the other detergents, providing an overall PsbS yield from PSII membranes of ~87%.

3.4 Optimisation of Na-Cholate extraction

The Na-Cholate incubation of the DM-pellet had been established as an extremely reproducible method for PsbS extraction, it was necessary to further optimise the extraction procedure in order to determine method of isolating PsbS could be developed that produced similar yield, whilst minimising the extraction period. It should be noted that only a five of the severn extraction variations used provided a positive result, and these are described in table 3.2.

Extraction Procedure	Duration	Protein Extraction
Shaking (ice)	5	Yes
Shaking (ice)	10	Yes
Pipette Mixing	5	No
Pipette Mixing	10	Yes
Resuspend (leave)	30	No
Resuspend (leave)	60	No
Resuspend (leave)	ON*	Yes
* ON – Over night (24 hr) incubation		

Table 3.2 - Extraction procedures. Description of the three extraction techniques have been employed, incubation duration and the extraction result (ie presence or absence of protein bands on SDS-PAGE gel).

Figure 3.11I shows the outcome of SDS-PAGE analysis for those methods, which supported any extraction at all. Mixing of the DM-pellet in the presence of Na-Cholate and NaCl on ice, using an automated shaker for 5 min (Fig 3.11I, lane 1) gave rise to a similar result as that described above (Fig 3.10, lane 5), albeit with a slight increase in the concentration of

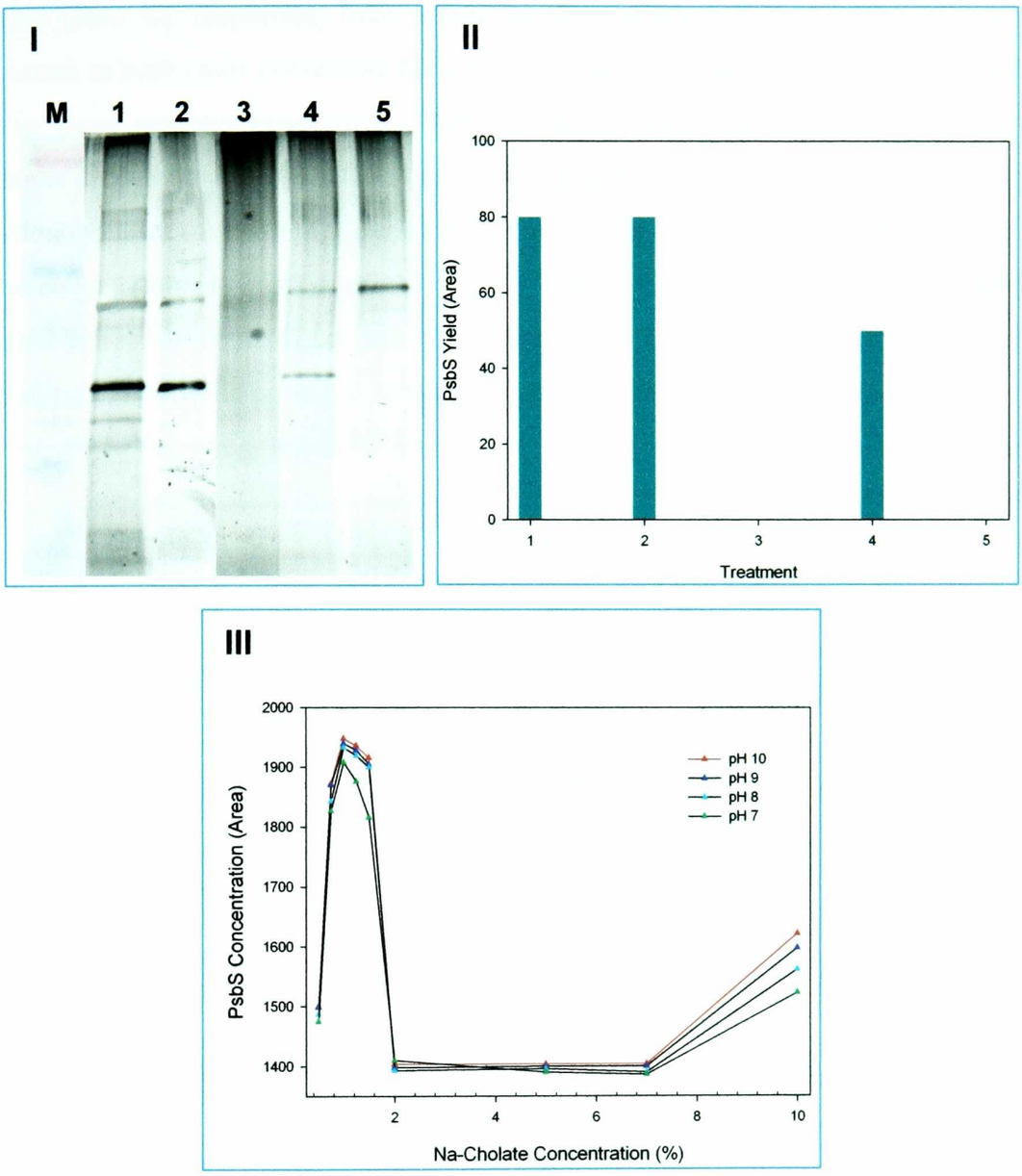

Figure 3.11 – Na-Cholate extraction optimisation. I, silver stain analysis on SDS-PAGE gel loaded with 10µl of sample per lane pre-treated with 5x loading buffer. M, molecular weight marker SeeBlue+2 (invitrogen). 1, extraction with vigorous shaking for 5 min. 2, extraction with vigorous shaking for 30 min. 3, extraction using Pasteur pipette for 5 min. 4, extraction using Pasteur pipette for 10 min. 5, extraction using overnight extraction at 4°C only. II, analysis of PsbS yield calculated using densitometry analysis. 1 – 5 related to lanes 1 – 5 on I. III, densitometry analysis of PsbS yield vs treatment. Inset colour coding for pH treatments.

impurities present in the supernatant. This period was increased to both 10 (not shown) and 30 mins (lane 2), displaying little affect on the volume of PsbS extracted, with the supernatant in both cases containing 80% PsbS (Table 3.3, lanes 1 and 2). The overall PsbS yield in these samples constituted ~90% of the protein originally present in the PSII membrane preparation (Fig 3.11II). The use of a pipette to mix the DM-pellet and detergent extraction medium over a 5 min period failed to extract PsbS (Fig 3.11I, lane 3), and could only manage minor extraction of the 35kDa band. Doubling of this time significantly improved extraction of PsbS and the 35kDa band (Fig 3.11I, lane 4), with each component constituting ~50% of the protein within the sample (Table 3.3).

Bands	Lane				
	1	2	3	4	5
1	7	15	100	50	97
2	1				1
3					1
4	80	80		50	1
5	1				
6	5				
7	3				
8		5			
9	2				
10	1				

Table 3.3 – Densitometry analysis of cholate extraction procedures. Total of 10 individual bands resolved across lanes 1 – 5 (Fig 3.11I). Blue box indicates absence on a particular band in that lane. Bands counted horizontally from top to bottom.

However, the yield was significantly less than that shown in both lane 1 and 2 (Figure 3.11II). Finally, overnight incubation at 4°C after initial mixing of the pellet with detergent failed to extract PsbS at all. Only the 35kDa protein could be resolved on silver stain (97%) along with a number of minor high molecular weight components. Thus, vigorous shaking on ice provided the most efficient method of agitation during incubation, enabling the rapid extraction of PsbS whilst maintaining a very high protein yield. The next stage of optimisation involved variations in detergent concentration and pH. Figure 3.11III details the effect of altering the detergent environment during extraction, with the most efficient extraction yield occurring between 0.75% and 1.5% Na-Cholate across all pH ranges. Once at 2% detergent concentration protein yield is significantly impaired until ~7% when levels steadily increase to the maximum concentration tested at 10%. However, it should be noted that at no point does the extraction yield increase beyond that of 1% Na-cholate. The effect of pH is negligible at lower detergent concentrations, whilst having a significant impact at

higher detergent concentrations. At all times extraction dependency on pH follows the same trend; to a greater of lesser extent increased alkalinity results on improved extraction yield.

Although effective, extraction with Na-Cholate delivers inconsistent results relating to the level of purity. Thus, the final purification step involves gel filtration (Fig 3.12) in order to separate PsbS from the other protein species that may be extracted along with it during incubation with Na-Cholate, whilst replacing the detergent with DM. This process employed a G-25 Sephadex column, with 1ml aliquots being collected ten seconds after the sample had completely entered the column. SDS-PAGE analysis shows that the contents of the optimised Na-Cholate extraction appear in aliquots 4 to 6 (Fig 3.12, lanes 4 to 6), however, PsbS is found in aliquot 6 with minor contamination from other proteins. When collected from the gel filtration column the sample is completely free from pigments and runs behind a green band containing the majority on the other protein components from the pellet extraction. Running aliquots 4 and 5 through the column again allows almost all the PsbS protein contained within them to be isolated, resulting in highly purified protein sample (Fig 3.12II, lane 6).

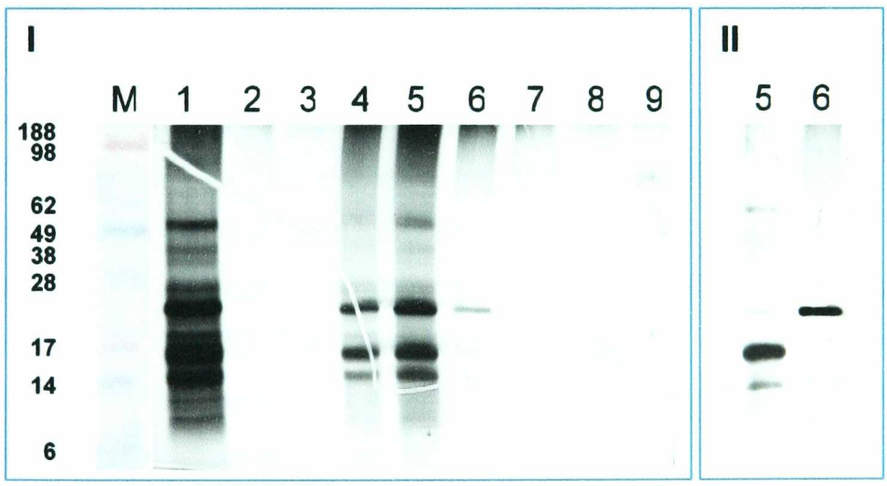

Fig 3.12 – Gel Filtration. M, SeeBlu+2 marker (7µl). Lane 1, Control sample Dm-pellet (10µl). Lanes 2 - 9 correspond to column aliquots 2 - 9 (10µl).

In order to determine if soluble PsbS could be focused using IEF, a sample of the purified proteins was applied to a gel with an ampholine range between pH 3 and 9 (Fig 3.13). The protein sample was incubated with coomassie blue prior to application to the gel so that the PsbS location could easily be determined. The loading origin of the gel is indicated by **a**, whilst the location of the PsbS protein is shown by **b.** Excess coomassie blue stain can be found at **c**. It can be concluded that soluble PsbS can be focused using IEF, and the protein species possesses a pI of ~6.

This data presents a very reproducible, rapid procedure for the extraction of the PsbS protein from PSII membranes and provides for investigation of PsbS structure and function. This first stage of investigation described below involves the characterisation of the protein, using biochemical and spectroscopic techniques.

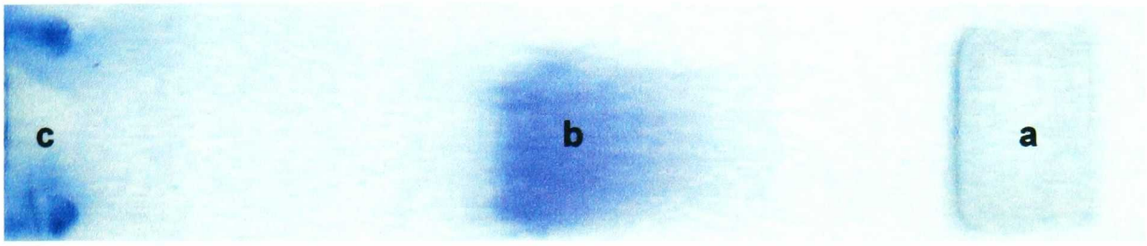

Fig 3.13 – Solublised PsbS IEF. IEF pH 3 – 9, contains PsbS sample (1ml) loaded after incubation with coomassie blue stain.

3.5 Determination of the primary sequence of the 22kDa extracted protein

The method used for the determination of this sequence is detailed in section 2.21. The 22kDa protein isolated from PSII particles proved to be identical in every aspect to the original PsbS sequence obtained from spinach (Kim et al. 1992; Wedel et al. 1992). Figure 3.14I displays the full PsbS polypeptide sequence including its 69 amino acid targeting sequence highlighted by the blue box between 001 and 069. The four predicted transmembrane helices are underlined in light blue, whilst the regions of protein that have been sequenced are shown in red. Additionally, the epitope for the anti-PsbS antibody is highlighted between helix two and three by a red box. The total number of matches scored when sequencing the 22kDa extract was 7, many of which overlapped, resulting in only three distinct sequenced regions in figure 3.12I. All 7 individual sequence matches are shown in figure 3.12II along with their start and end points.

3.6 Absorption Spectra

The absorption spectrum of the PsbS preparation shows that it contained no bound pigment; if the absorption spectrum shown in figure 3.15 is extended into the visible region, there is no recorded absorption from either carotenoid or chlorophyll. In contrast, a sample of LHCII

I

```
001  MAQAMLLMMP GVSTTNTIDL KRNALLKLQI QKIKPKSSTS NLFFSPLPSS

051  SSSSSTVFKT LALFKSKAKA PKKVEKPKLK VEDGLFGTSG GIGFTKENEL   HELIX 1
                                LK VEDGLFGTSG GIGFTKENEL
101  FVGRVAMIGF AASLLGEGIT GKGILSQLNL ETGIPIYEAE PLLLFFILFT   HELIX 2
     FVGR
151  LLGAIGALGD RGRFVDEPTT GLEKAVIPPG KDVRSALGLK TKGPLFGFTK   HELIX 3
                    FVDEPTT GLEK                  TKGPLFGFTK
201  SNELFVGRLA QLGFAFSLIG EIITGKGALA QLNIETGVPI NEIEPLVLLN   HELIX 4
     SNELFVGR
251  VVFFFIAAIN PGTGKFITDD EEED
```

Fig 3.14 – PsbS sequence analysis. I, shows the protein sequence for spinach PsbS (Kim et al. 1992; Wedel et al. 1992), bold red regions indicated sequenced protein. Sequence highlighted in purple is a precursor peptide. Helices 1 – 4 are underlined in blue (Kim *et al* 1992), and the sequence boxed in red is the spinach anti-PsbS antibody epitope (Aspinall-O'Dea et al. 2002). II, Seven PsbS sequence matches determined by ProteinLynx™.

II

Start	End	Sequence
079	096	(K) LKVEDGLFGTSGGIGFTK (E)
081	096	(K) VEDGLFGTSGGIGFTK (E)
097	104	(K) ENELFVGR (V)
164	174	(R) FVDEPTTGLEK (A)
191	200	(K) TKGPLFGFTK (S)
193	200	(K) GPLFGFTK (S)
201	208	(K) SNELFVGR (L)

at the same protein concentration would give an OD of ≈20 in the red region of the spectrum. The spectra can be used to further test the purity of the PsbS preparation. The published amino acid sequence of spinach PsbS indicates the presence of 17 phenylalanines and 1 tyrosine (Kim et al. 1992; Wedel et al. 1992), which can also be seen in the sequence analysis carried out for the extracted PsbS protein (Fig 3.14I). By using the extinction coefficients at 257 and 274 nm of 0.19 x 10^5 and 1.25 x 10^5 $M^{-1} \bullet m^{-1}$, respectively, a theoretical absorption ratio of phenylalanine to tyrosine of 2.5 is predicted. The absorption spectrum of the PsbS preparation was deconvoluted to show the contributions from phenylalanine and tyrosine (Fig 3.15), and these data gave a phenylalanine/tyrosine ratio of 2.0. A very minor contribution from tryptophan (not present in the PsbS sequence) at 288 nm is evident, but given the large extinction coefficient of this amino acid, the level of contamination by other proteins would appear to be minimal.

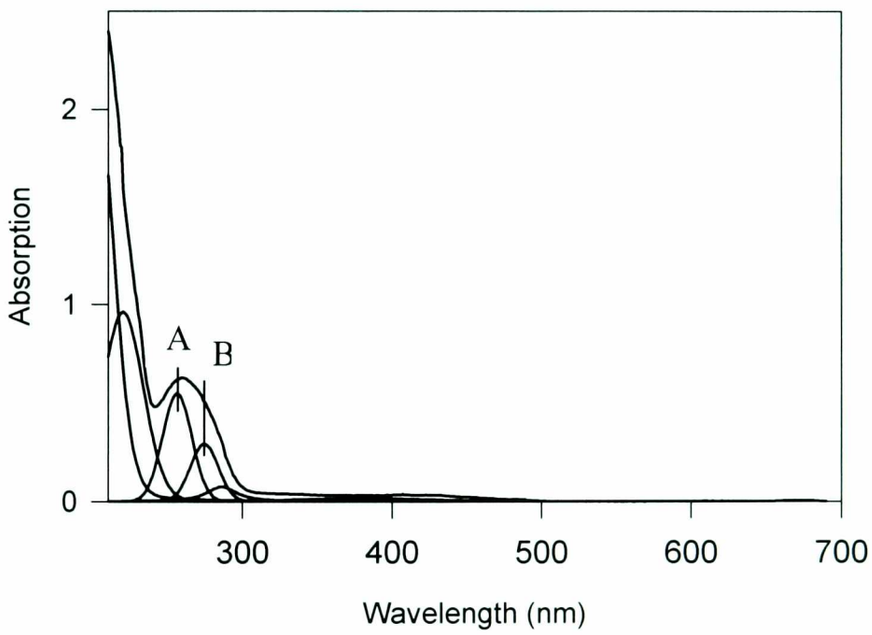

Figure 3.15 – Absorption spectra of the preparation of purified PsbS. The absorption was deconvoluted, revealing the bands at 257nm (A) and 274nm (B) arising from phenylalanine and tyrosine, respectively.

3.7 Analysis of secondary structure by circular dichromism

The CD spectrum of the PsbS preparation shows the presence of secondary α-helical structure with characteristic minima at 208 and 222 nm (Fig 3.16), providing evidence that the protein was not denatured and suggesting that it had been isolated in a native form. Protein denaturation (unfolding of helical structure) is induced at high temperature and is measured by a loss of CD. A temperature dependency analysis of the secondary structure for purified PsbS was carried out, and compared to LHCII. Figure 3.17A shows spectra for

LHCIIb at 10 and 70°C (after denaturation), with PsbS spectra shown at 10 and 90°C (Fig 3.17B) due to the proteins ability to retain helical structure at higher temperatures than LHCII antenna.

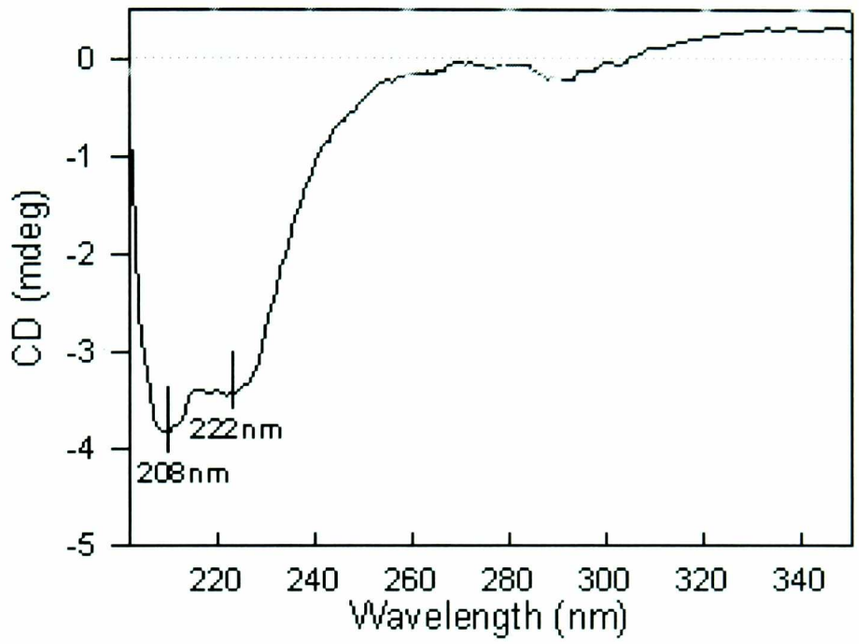

Figure 3.16 – CD spectra of the preparation of purified PsbS. Spectrum taken at room temperature shows minima at 208 and 222 nm, characteristic of α-helical structure.

The change in CD signal at 211nm with increasing temperature (Fig 3.17C) indicates that LHCIIb can retain helical structure up to 60°C, after which the signal diminishes sharply with all secondary structure lost at 90°C. In contrast PsbS secondary structure is unaffected up to 75°C, at which point the 211nm signal is reduced, but at a slower rate than LHCIIb. All structure is lost at 110°C, with approximately 50% of the total signal at 211nm lost between 100°C and 110°C. Figure 3.14D displays a similar effect at 222nm, however PsbS can be seen to lose signal from 70°C although the overall rate of structural decline is similar to that of the signal at 211nm. Again all structure is lost at 110°C.

Low pH also commonly denatures proteins. Figure 3.17E shows the loss of secondary structure of the PsbS protein at pH 4. This is a common feature in LHCII antenna proteins (personal communication Dr M Wentworth), however it should be noted that the pH changes potentially detected by PsbS *in vivo* would occur on the lumenal side of the protein and not across the entire structure as can be seen here. Thus, it is possible that the thylakoid

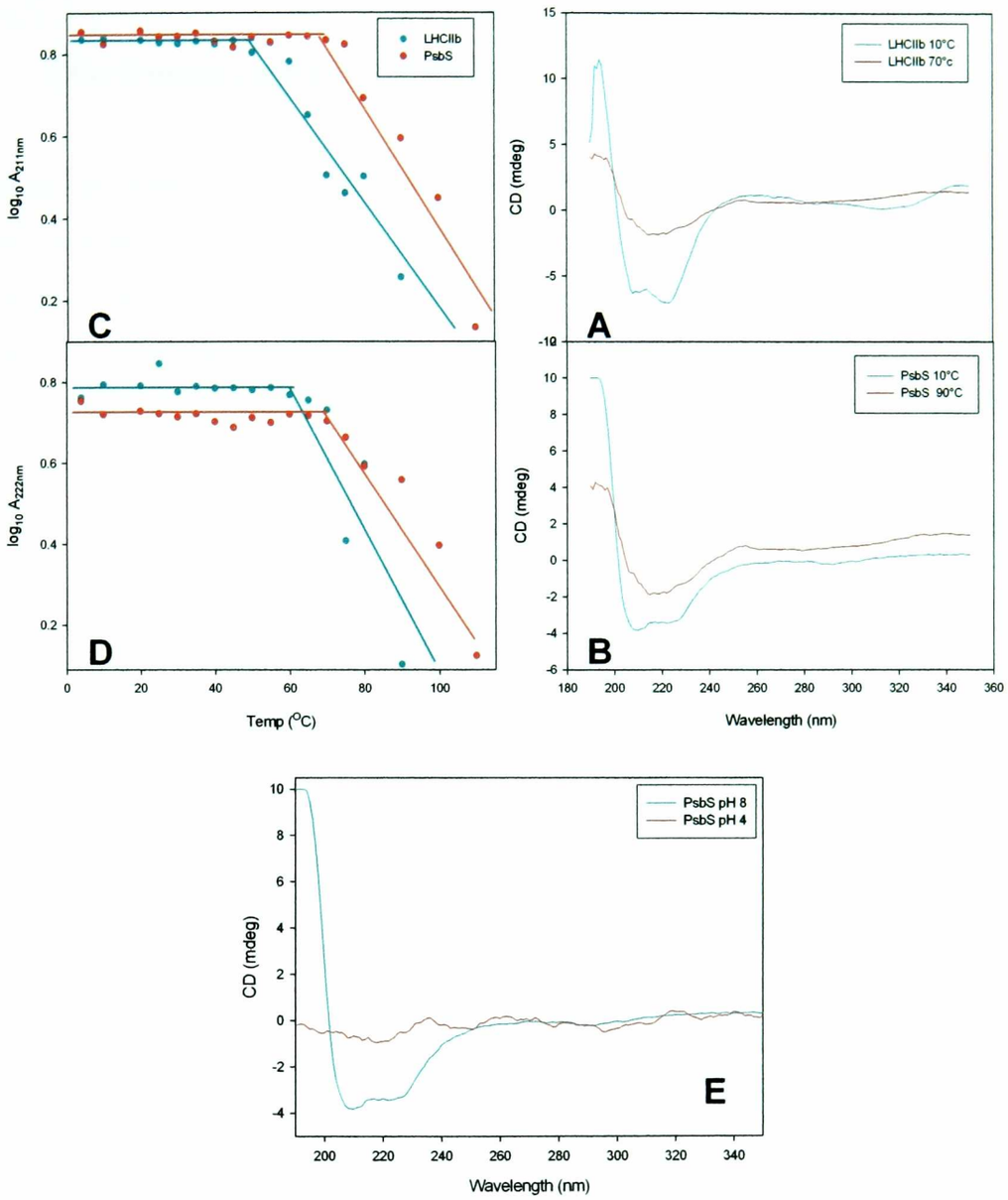

Figure 3.17 Analysis of PsbS Temperature and pH Kinetics. A, CD spectrum of LHCIIb at 10°C (dark cyan) and 70°C (red). B, CD spectrum of PsbS at 10°C (dark cyan) and 90°C (red). C, temperature vs $\log_{10}$ amplitude at 211 nm for PsbS (red), and LHCIIb (cyan). D, temperature vs $\log_{10}$ amplitude at 222 nm for PsbS (red), and LHCIIb (cyan). E, CD spectrum of PsbS at pH 8 (cyan) and pH 4 (red).

membrane in vivo supports PsbS, enabling it to retain helical structure at low pH levels than *in vitro*.

3.8 DCCD binding properties of PsbS

Biochemical analysis of purified PsbS from spinach chloroplasts and recombinant expression of the *Arabidopsis thaliana* protein in *E-coli*, have shown that structural homology exists between CP29 and PsbS in the form of acidic residues residing in each of the two lumenally exposed loop regions (Dominici et al. 2002). It is thought that these residues promote binding of DCCD to the PsbS protein. In CP29 these loops constitute a DCCD/Ca^{2+} binding domain, suggested to be involved in sensing low lumenal pH.

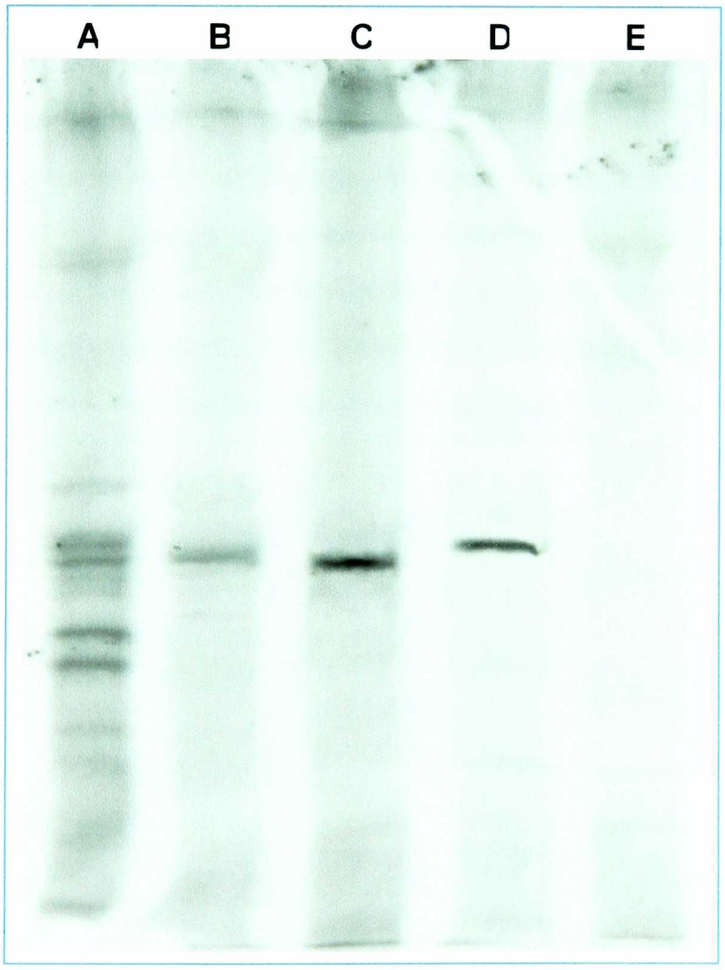

Figure 3.18 – DCCD binding analysis. Samples prepared as in section 2.7. 10μl loaded per lane. A, PSII particles. B, LHCIIb. C, CP26. D, CP29. E, PsbS.

Figure 3.18 shows the DCCD binding analysis for the spinach PsbS protein. Lanes A – D contain control samples of PSII particles, LHCIIb, CP29 and CP26 respectively. Lane A displays ~10 bands bound with DCCD including the PSII antenna proteins shown in lanes B

– D. The latter have only one band per lane with bound DCCD. Lane E contains purified PsbS, and shows no detectable binding. Further analysis of PsbS binding across the pH range 4 to 8 also failed to show DCCD binding (data not shown).

3.9 PsbS Homodimer

Recently, a 42kDa homodimer of the PsbS protein has been characterised in a number of species including spinach, tobacco, rice, barley and carrot (Bergantino *et al.*, 2003) by means of a highly specific antiserum with an epitope on the stroma-exposed loop between the second and third helices. The monomer/dimer ratio has been shown to vary with lumenal pH, with dimerisation prevalent under alkaline conditions and monomerisation under acidic conditions. This phenomenon has never been seen using the anti-PsbS antibody developed for the epitope shown in figure 3.14I. In an attempt to verify the ability of this antibody to detect the presence of a 42kDa band, thylakoid membranes were incubated under partially denaturing conditions to preserve any dimerised PsbS complexes. The incubation was performed in loading buffer at room temperature over a range of times from 2 to 20 minutes. A slightly alkaline pH was used (pH 8) to also promote homodimer formation. Figure 3.19 shows the gradual formation of the 22kDa protein band over time, however there appears to be a complete absence of other bands, most notably that of a 42kDa band.

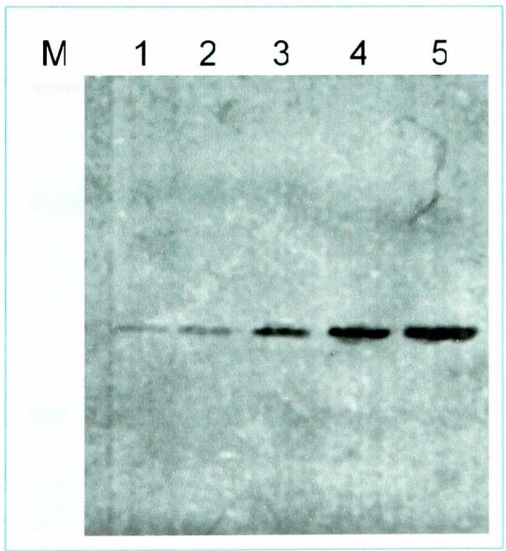

Figure 3.19 – Analysis of anti-PsbS antibody detection of 42kDa PsbS dimeric band. Western blot using anti-PsbS antibody at 1:2500 dilution. M, molecular weight marker SeeBlue+2 (invitrogen) 7ml loaded. All other lanes loaded with 10ml BBY sample in 5x loading buffer 1, 1 min incubation. 2, 2 min incubation. 3, 5 min incubation. 4, 10 min incubation. 5, 20 min incubation. All BBY samples incubated for the designated duration at 90oC in 5x loading buffer.

3.10 Discussion

The data shown in this chapter provides the first dedicated purification procedure developed for the PsbS protein. This rapid method has succeeded in extracting PsbS with a remarkably high yield and purity, in the complete absence of pigments. Such an effective method of isolation for this protein has never before been described, thus it is reasonable to conclude that a reproducible and unique method has been established as a result of this work.

Due to this success, the first stage of characterisation for the PsbS protein has been completed and provides unequivocal evidence that the 22kDa protein extracted is, indeed, PsbS. The purity of the PsbS protein has been analysed using biochemical and spectroscopic techniques, whilst densitometry analysis of SDS-PAGE gels indicates that isolated PsbS represents more than 90% of the species population in PSII particles. Quantitative analysis of protein UV absorption spectra confirmed the level of purity.

Analysis of the protein secondary structure has shown isolation of PsbS is achieved whilst maintaining helical structural within the complex, in the absence of pigments. The protein has previously been shown to be present in the leaves of etiolated spinach plants (Funk et al. 1995), a phenomenon unique to PsbS, as the remainder of the LHCII antenna family require chromophores and carotenoids for correct folding. This helical structure is maintained at relatively high temperatures when compared to LHCIIb, indicating that PsbS may be significantly more robust than other LHCII proteins. Structural integrity is lost very quickly between pH 5 and 4 when analysed *in vitro*. Such instability at low pH may not be surprising as physiological acidity peaks at approximately pH 5. However, as mentioned earlier it is also possible that *in vivo* the thylakoid membrane provides further support to the PsbS protein at lower pH levels.

Analysis of the DCCD binding properties for this protein shown to exist in a highly purified state with structural integrity maintained over a wide range of conditions, has failed to observe any interaction. Over the full physiological pH range DCCD has failed to bind this protein, an observation that contrasts with earlier work (Dominici et al. 2002). Although it is difficult to explain such inconsistencies it should be noted that the protein analysed here has been isolated using a significantly different method, and perhaps the binding of DCCD to PsbS is dependent upon interactions with other components such as LHCII proteins or, alternatively, even other PsbS proteins. Such interaction has been observed in the form of 42kDa PsbS homodimers (Bergantino et al. 2003), however analysis using the PsbS antibody developed for the experiments described in chapter 3 has failed to locate this dimer.

Analysis of the western blot in figure 3.20 shows a steady increase in PsbS detection at 22kDa as a result of increasing the incubation time for the sample. This increase can be explained in a number of ways; firstly, the increase in incubation time simply breaks down more of the PSII particles present in the BBY sample used, resulting in more solublised protein entering the gel. Secondly, the increased intensity of PsbS detection could be a result of homodimer collapse due to longer incubation with loading buffer. Figure 3.20 shows the predicted structure of monomeric PsbS in the thylakoid membrane (modified from Kim et al. 1992) with the 12 amino acid epitope of the anti-PsbS antibody located on the stromal side of the membrane (marked in red) in a loop region between helix two and three. Dimerisation of the PsbS protein could obstruct this region resulting antibody being unable to detect a dimeric form of PsbS.

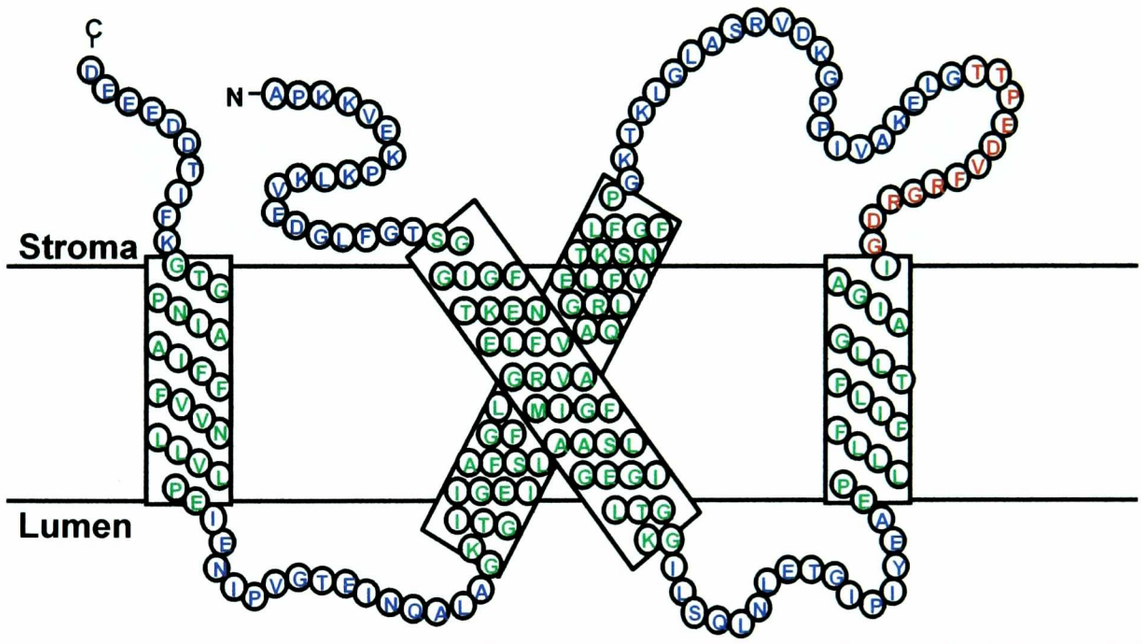

Figure 3.20 – Predicted helical structure of the spinach PsbS protein. Amino acids corresponding to transmembrane α-helices shown in green, loop regions shown in blue with the anti-PsbS antibody epitope highlighted in red. Thylakoid membrane is designated by the horizontal black lines with the stromal and lumenal sides indicated. Adapted from Kim et al. 1992.

3.11 Concluding Remarks

The data presented in this chapter has allowed a reproducible method for the extraction of soluble PsbS to be established and is detailed below, whilst figure 3.21 displays a flow diagram of the extraction proceedure. PSII membrane fragments were prepared from spinach thylakoid membranes essentially as described (Berthold et al. 1981). For PsbS preparation, the PSII membrane fragments (2 mg of total chlorophyll) were extracted with 1% *n*-dodecyl b-D-maltoside (DM), incubated on ice for 50 min, stirred occasionally, and centrifuged at 10,000 x *g* for 20 min. The pellet was extracted with 0.5% sodium cholate

(Sigma), pH 7.0/250 mM NaCl (Bowlby & Yocum 1993), incubated in the dark on ice with vigorous stirring for 5 min, and centrifuged at 10,000 x *g* for 10 min. The supernatant was passed through a Sephadex G-25 column, and eluted fractions containing PsbS were stored in a solution of elution buffer (25 mM Hepes, pH 8.0 (0.01% DM).

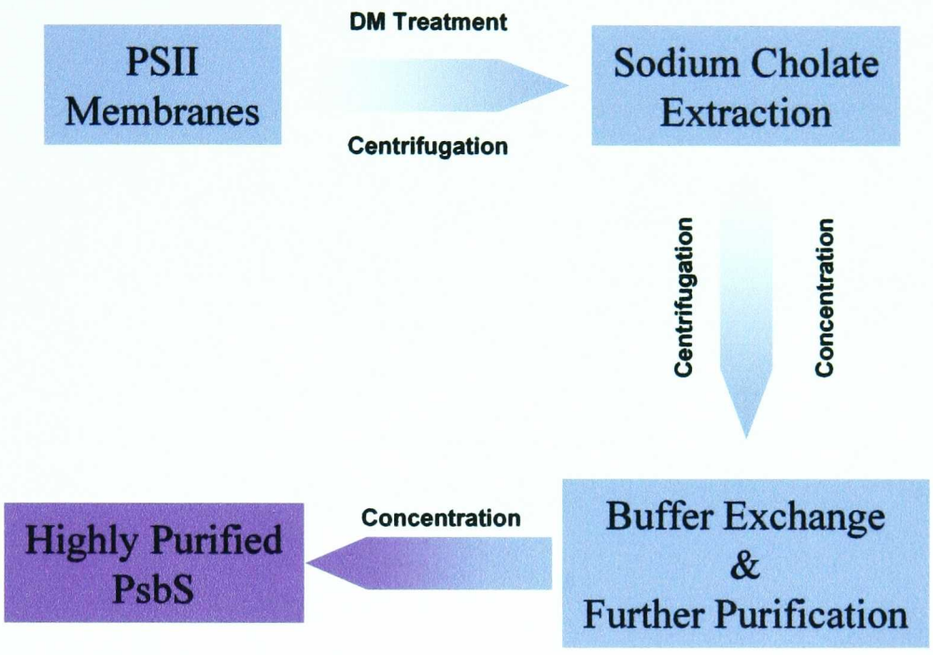

Figure 3.21 – Flowchart describing PsbS isolation proceedure.

The first characterisation of PsbS secondary structure is detailed here, with the protein shown to be stable under a number of conditions. The helical structure of the protein in the absence of pigments provides an ideal platform for further study, specifically in relation to its interaction with the xanthophyll cycle carotenoid zeaxanthin. In addition, it will be possible to determine the effect of the PsbS protein on other LHCII components using an *in vitro* fluorescence quenching assembly.

Chapter Four

Analysis of PsbS-Zeaxanthin Binding Interactions

Analysis of PsbS-Zeaxanthin Interactions

4.1 Introduction

Dissipation of excess excitation energy absorbed during photosynthesis by the light-harvesting antenna of plant PSII is detected as the non-photochemical quenching of chlorophyll fluorescence (qE), which is regulated by the transthylakoid pH gradient (ΔpH) and the xanthophyll cycle (see section 1.11). Conditions of excess light result in the accumulation of zeaxanthin (Demmig-Adams 1990). An absorption change with a wavelength maximum of ≈535 nm correlates with the formation of qE (Ruban et al. 1993b; Bilger & Bjorkman 1994) resulting from an unusually large red shift in the absorption spectrum of one or two molecules of zeaxanthin to ≈525 nm (Ruban *et al.*, 2002). This absorption change is thought to arise from the molecule binding to the specific site in PSII involved in qE regulation. PsbS is an essential component for qE (Li et al. 2000), and has been proposed as a candidate for the site of zeaxanthin binding in PSII. The extracted protein described in chapter 3 was used to probe the binding properties of PsbS in relation to zeaxanthin, which required the development of a new reconstitution technique.

4.2 Spectral characterisation of Xanthophyll-Cycle carotenoids

All three components of the xanthophyll cycle were employed in reconstitution experiments using extracted PsbS, to determine if conditions suitable for zeaxanthin binding would also favour specific interactions with either Violaxanthin, Antheraxanthin or both (section 4.5). It is essential to analyse the absorption spectra of freshly prepared pigments prior to their use in reconstitution experiments in order to determine the concentration of the sample, and ensure the pigment is in the required isomeric state. Table 4.1 presents the absorption maxima for each xanthophyll cycle component when dissolved in ethanol, and the characteristic absorption spectrum for zeaxanthin can be seen in Fig 4.1A, with maxima at 428, 454 and 482 nm. The absence of a *cis* peak at ≈350 nm indicates that the zeaxanthin sample exists in an all-*trans* conformation, essential for binding to LHC proteins. Violaxanthin and Antheraxanthin also display characteristic absorption spectra when dissolved in ethanol (Fig 4.1B and C), with peak maxima at 423, 447, 472 nm and 425, 450, 475 nm respectively. Again, this confirms that these samples have not been damaged, and specifically ensures that Violaxanthin has not been isomerised to Auroxanthin during extraction. The absorption spectrum of a given pigment can be shifted depending on the polarity of the solvent, as can been seen with zeaxanthin when

dissolved in diethyl ether (Fig 4.1D). This spectrum has peak maxima at 424, 450 and 478 nm, which directly correlate to those in table 4.1.

Pigment	Absorption Maxima (nm)			Solvent
	1-1	0-1	0-0	
Violaxanthin	426	453	483	Ethanol
Antheraxanthin	430	456	484	Petrol/Ethanol
Zeaxanthin	428	454	482	Ethanol
Zeaxanthin	424	450	478	Diethyl Ether

Table 4.1 – Characteristic absorption maxima for xanthophyll cycle components in ethanol (Young and Britton, 1993) and diethyl ether (experimental observation).

4.3 Development of an effective reconstitution technique

Characterisation of the PsbS protein extracted using the method described in Chapter 3a had suggested that the protein existed in a native state *in vitro* (Chapter 3b). This stability in the absence of pigments had previously been observed in etiolated spinach leaves (Funk 1995a), and presented a problem with using conventional reconstitution techniques. The latter rely upon the absolute requirement of pigments for protein folding, and have been employed studying both LHCIIb (Hobe et al. 2000; Hobe et al. 2003) as well as the minor antennae complexes CP26 and CP24 (Frank et al. 2001; Morosinotto et al. 2002). Although variations in technique exist, the basic process is to attempt refolding of a denatured protein (pigments removed) in the presence of controlled pigment ratios, relying upon the knowledge that a given protein can bind specific pigments. Prior to the experiments described in section 4.4, however, the evidence that PsbS could bind pigments was controversial (Funk et al. 1994; Funk 1995b), making reconstitution using traditional methods difficult.

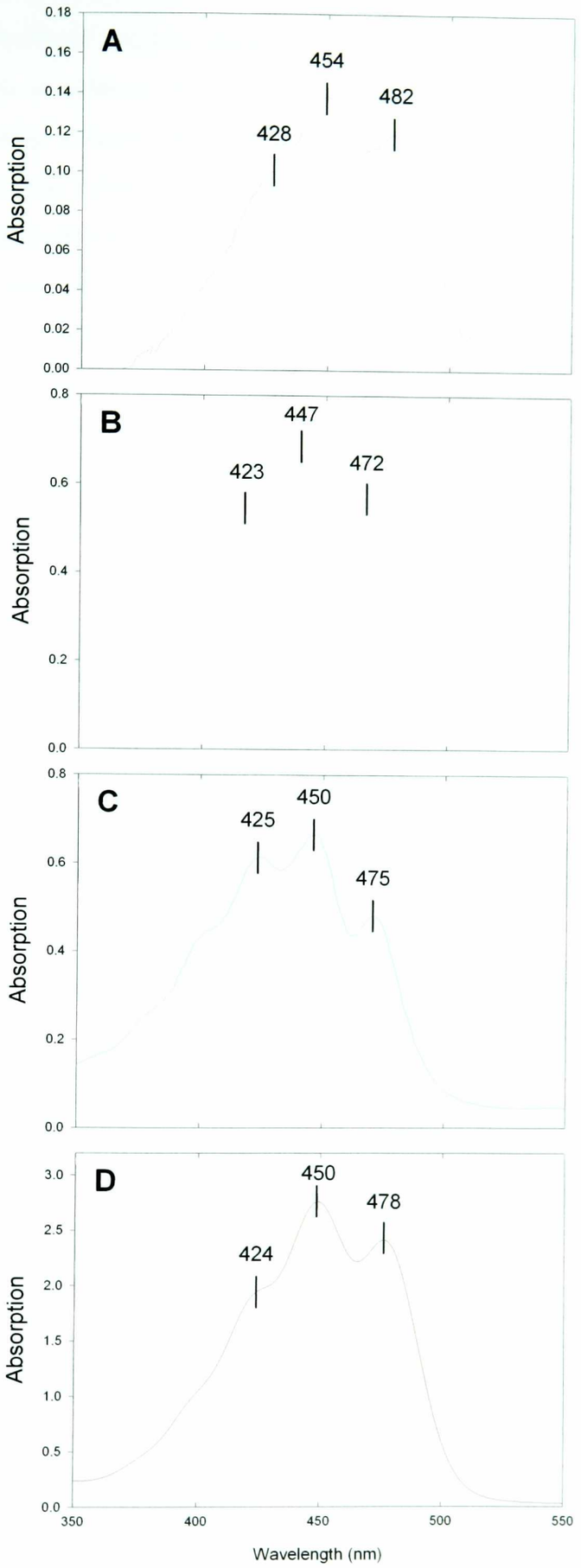

Figure 4.1 – Absorption spectra of Xanthophyll Cycle carotenoids. A, Zeaxanthin dissolved in absolute ethanol. B, Violaxanthin dissolved in ethanol. C, Antheraxanthin dissolved in ethanol. D, Zeaxanthin dissolved in diethyl ether.

The initial aim was to develop a method that ensured the pigment in question could be dissolved into the detergent buffered protein sample without causing aggregation of the carotenoid. Zeaxanthin dissolved in ethanol was initially added to the protein sample in an effort to reconstitute PsbS using a rapid and efficient procedure. Analysis showed that zeaxanthin dissolved in solvent could indeed be directly added to samples without precipitating the protein, or causing pigment aggregation. The absorption spectrum in figure 4.2 (trace 1) possesses peak maxima at 435, 451 and 485 nm, correlating well with those shown in table 4.1. The spectrum also appears to display broadening beyond the 0-0 transition, along with a small shoulder present at 407 nm. Unfortunately, the use of this method was later found to frequently cause zeaxanthin aggregation with a large peak maxima forming at 388 nm (Fig 4.2, trace 2), a characteristic feature of zeaxanthin aggregation (Ruban et al. 1993a).

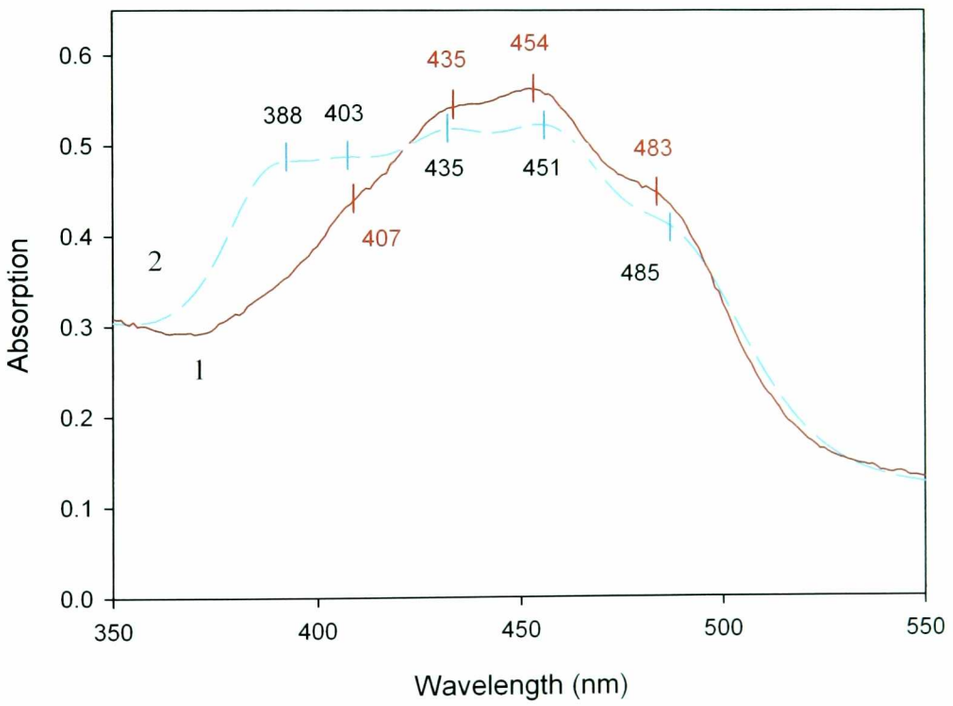

Figure 4.2 – Absorption spectrum of PsbS-zeaxanthin complex reconstituted using ethanol-dissolved pigment (1). Aggregated zeaxanthin spectrum formed after reconstitution using ethanol dissolved zeaxanthin (2).

Further analysis of this spectrum reveals that the 1-1, 0-1 and 0-0 transitions are consistent with spectrum 1, located at 432, 454, and 485 nm respectively. The small shoulder found at 407 nm (spectrum 1) is still visible at ≈4.3 nm in spectrum 2. Again there appeared to be a slight

broadening of the spectrum beyond the 0-0 transition. Due to this frequency pigment aggregation it was necessary to explore alternative methods of reconstitution.

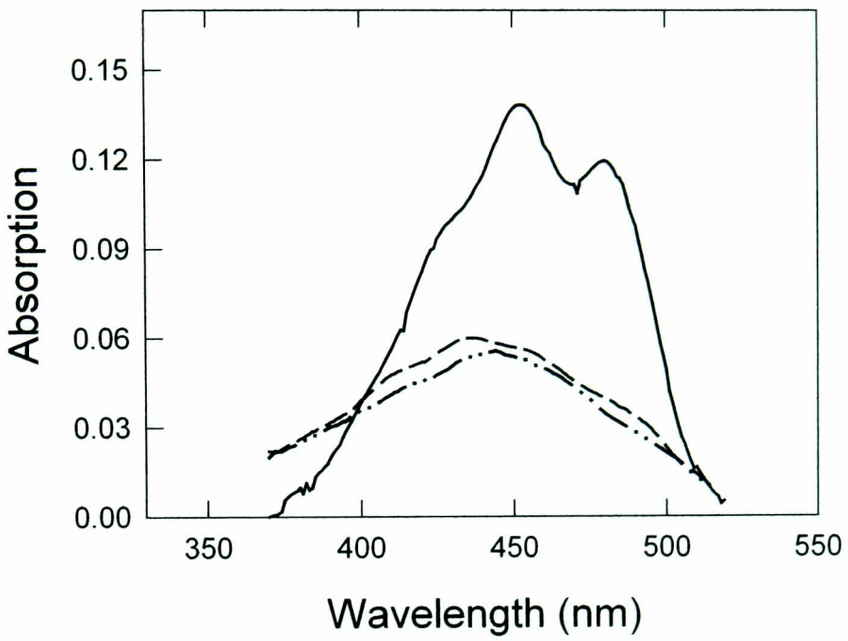

Figure 4.3 - Absorption spectra of zeaxanthin in ethanol (solid line) and in detergent buffer used in reconstitution experiments (dashed line) and BSA control (dash-dot line)

The second approach involved briefly incubating PsbS with zeaxanthin deposited as a dry film on the surface of a glass tube. Initial observations found that the zeaxanthin layer was rapidly absorbed by the PsbS sample and spectroscopic analysis determined that the pigment was in a stable, non-aggregated state. The absorption maxima of this spectrum were found to be similar to those in figure 4.2 (trace 1) at 434, 456 and 486 nm along with the shoulder at 407 nm, suggesting that quantitatively similar results could be obtained with both methods. It should be noted that aqueous buffer minus PsbS causes a quite different effect (Fig 4.3, dashed line), with very little pigment uptake detected resulting in a poor, largely featureless, spectrum when compared to zeaxanthin in ethanol (solid line). A similar result is found with the BSA control (dash-dot line). However, due to the uneven nature of the zeaxanthin layer (Fig 4.4 A), a pigment residue would still remain after incubation with PsbS, which could only be marginally reduced with extended sonication. This issue would significantly hinder accurate pigment:protein ratio calculations during reconstitution experiments, and would need to be overcome as this method effectively prevented pigment aggregation. To form a more uniform layer the pigment sample was vortexed whilst being dried under oxygen free nitrogen (Fig 4.4

effective at creating a smooth layer around the base of the glass (Fig 4.4 C). Pigment uptake was visibly improved using this method, with a significant reduction in pigment residue remaining in the tube.

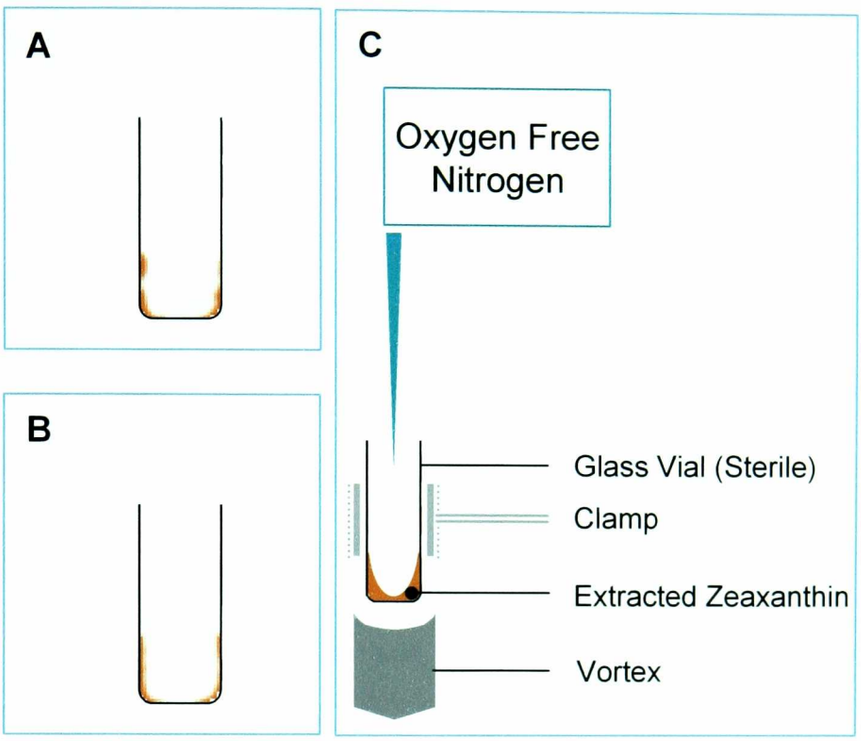

Figure 4.4 – Pigment drying procedure. Unevern distribution caused in the absence of vortex (A). Diagram of apparatus used during pigment drying (B). Uniform pigment layer resulting from vortex during drying procedure (C).

4.4 Reconstitution of the PsbS protein

Once a method had been developed that could reproducibly combine zeaxanthin and PsbS, the next stage was to test the hypothesis that PsbS would bind zeaxanthin leading to changes in the visible region of the spectrum, and shed light on the potential role involving the protein and the *in vivo* Δ535 nm shift (Ruban et al. 2002).

4.4.i Reconstitution – pigment/protein ratio effect at low component concentrations

In order to conserve materials, initial experiments were conducted using relatively low volumes allowing the concentration and, therefore, the quantity of raw materials needed for each experiment to be minimised. Initial analysis of PsbS binding properties in relation to zeaxanthin focused used a total of five different pigment/protein ratios to characterise the effectiveness of pigment uptake from the glass tube and, consequently observing any spectral changes taking place in the visible region as a result. Each incubation involved increasing molar ratios of

zeaxanthin compared with PsbS, which were calculated, based on the concentration of protein. Thus a 2:1 ratio would contain twice as much zeaxanthin as PsbS. These spectra are displayed in figure 4.5, with the 0-0, 0-1 and 1-1 transitions highlighted along with the ≈405 nm

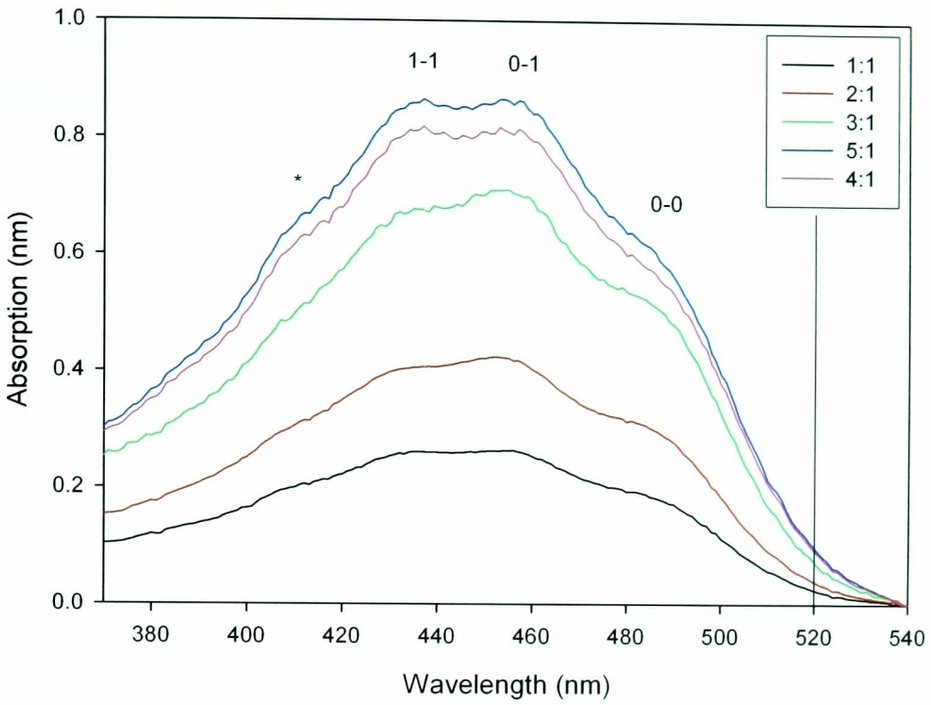

Figure 4.5 – Spectral analysis of increasing zeaxanthin concentration. Peak maxima for all spectra highlighted at 1-1, 0-1 and 0-0 transitions. Shoulder (≈405 nm) indicated by *. 520 nm marker shown by vertical line. Refer to key in upper right corner for description of each spectrum.

shoulder (*) mentioned previously. Peak maxima for each individual spectrum are summarised in Table 4.2. The structure of each spectrum is similar to that of the zeaxanthin control (Fig 4.1A), however, further analysis reveals variations, not only in the presence of PsbS, but also with increasing zeaxanthin concentration. The 1:1 ratio of pigment to protein (Fig 4.5, black trace) displays absorption intensity similar to that of the control (Fig 4.1A). Peak maxima are found at 434, 456 and 486 nm, correlating well with data shown in table 4.1, and are representative of the maxima for all five ratios (Table 4.2). Overall the spectrum is broader than that of zeaxanthin in ethanol and this observation is particularly characteristic of the region between 500 and 520 nm (Fig 4.5, #), and can be seen for all five spectra. It is possible, however, that this phenomenon results from light scattering caused by elements within the PsbS-zeaxanthin sample. The 2:1 ratio (red trace) is largely identical to that of spectrum one having roughly twice the absorption intensity of the latter, however the 0-1 transition appears to be slightly blue-shifted at 451 nm (Table 4.2). Spectrum 3 (green trace) follows a similar pattern with standard absorption maxima, whilst the increased absorption intensity of spectrum

4 (pink trace) is significantly less than that seen for earlier ratios; with the increase for the highest zeaxanthin ratio 5:1 (blue trace). In all spectra the shoulder at ≈405 nm remains constant (Table 4.2).

Ratio (Zeaxanthin:PsbS)	Absorption Maxima (nm)			* (≈405 nm shoulder)
	1-1	0-1	0-0	
1:1	434	456	486	407
2:1	434	457	488	406
3:1	434	453	486	406
4:1	434	451	484	407
5:1	437	456	490	407

Table 4.2 – Summary of absorption maxima and shoulder from spectra taken in Figure 4.5

The nature of these increases in absorption intensity indicates that pigment uptake is most efficient between the 2:1 and 4:1 ratios, indicating that zeaxanthin uptake can be saturated at higher pigment concentrations.

4.4.ii Reconstitution – effect of temperature

Earlier research using the pigment Astaxanthin has shown that temperature alone could profoundly affect the aggregate state of a carotenoid (Mori et al. 1995), and it was thought this may act to improve the effectiveness of any potential pigment binding. The reconstitution temperatures are maintained by incubating samples in a water bath and sustained during spectral analysis using a temperature controlled spectrophotometer. The temperature range used was from 4 to 40°C, and measurements were taken at key points previously shown to alter the visible spectrum of Astaxanthin (Mori' 95). A pigment/protein ratio of 2:1 was employed (Fig 4.6). Again the three transitions are highlighted along with the shoulder at ≈405 nm (*) and the marker at 520 nm (#). The spectra taken at 4 and 12°C display very little structure when compared with those taken at higher temperatures, with spectrum 2 (blue trace) showing only a marginal increase in pigment uptake, with both samples leaving significant residue behind after incubation. Peak maxima correlate with the zeaxanthin control figures (Table 4.3). Increasing the reconstitution temperature dramatically boosted pigment uptake (red trace), improving upon the original 2:1 ratio incubation performed at room temperature in section 4.4.i. The 0-0, 0-1

and 1-1 transitions all appeared to be red-shifted. Additionally, the ≈405 nm shoulder could be clearly seen.

Temperature (°C)	Absorption Maxima (nm)			* (≈405 nm shoulder)
	1-1	0-1	0-0	
4	430	452	484	409
12	433	455	487	406
21	436	458	493	409
28	437	459	495	408
30	439	461	494	411
35	435	460	492	409
40	437	460	490	408

Table 4.3 – Absorption Maxima determined during temperature controlled reconstitution experiments. Analysis of the shoulder at ≈405 nm.

At 28°C the spectrum changed significantly (dark red trace), with a significant reduction in pigment uptake, resulting in reduced absorption intensity. Table 4.3 shows that absorbance maxima for the latter transitions to be characteristic of zeaxanthin, with a shift in the 0-0 transition of ~7 nm.

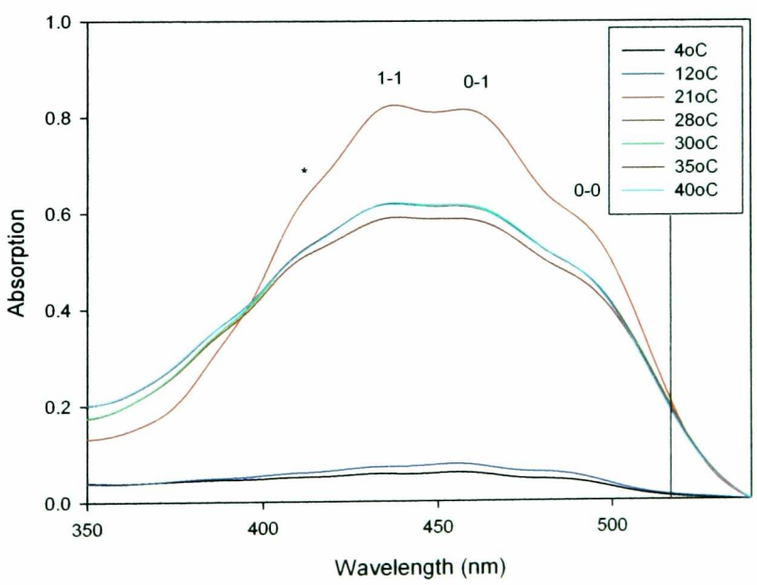

Figure 4.6 – Spectroscopic analysis of temperature controlled reconstitution. 4°C (red), 12°C (light green), 21°C (blue), 28°C (pink), 30°C (dark green), 35°C (grey) and 40°C (purple). Peak maxima at 1-1, 0-1 and 0-0 highlighted along with the shoulder at ≈405 nm and the 520 nm marker (vertical line).

A further increase to 30°C resulted in a slight increase in zeaxanthin uptake, however overall absorption remained lower than that found for 21°C. Again, the 0-0 transition was found to be red-shifted (Table 4.3). The incubation temperatures at 35 and 40°C are denoted by spectra 6 and 7 (Fig 4.7, dark red and light blue traces), both displaying identical pigment uptake, similar to that seen at 30°C. This data indicates that optimum pigment uptake is achieved at 21°C, with a pigment ratio of 2:1 zeaxanthin to PsbS.

4.4.iii Reconstitution – Pigment drying using alternative solvents

These results described above failed to generate the large absorbance shifts described *in vivo* (Ruban et al. 2002) and it was thought that the manner in which zeaxanthin was packed, once dry, could be hampering efforts to successfully achieve binding, a factor which could be affected by residual water deposits in the pigment sample. Thus, using an alternative solvent, zeaxanthin could be dried in such a way as to render it more amenable to binding at lower concentrations and temperatures. It was also possible that the nature of such binding could create spectral shifts similar to those reported *in vivo*. The use of different solvents was, therefore, designed to 'prime' zeaxanthin for uptake by PsbS.

Initially dry ethanol was dried using water-absorbing microbeads (Sigma), which were immersed in solvent for 24 hrs prior to use. Contrary to expectations, however, the use of dry ethanol actually reduced pigment uptake efficiency during reconstitution, resulting in a significant residue remaining in the vial after incubation. Spectroscopic analysis of this sample revealed that absorption intensity was less than half that seen at 21°C with standard ethanol (Fig 4.7).

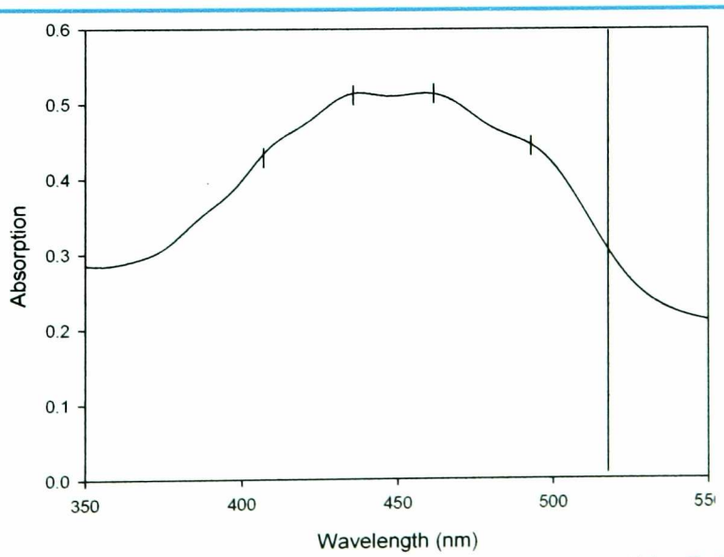

Figure 4.7 – Spectroscopic analysis of reconstituted zeaxanthin-PsbS complex using dry ethanol. Peak maxima at 1-1, 0-1 and 0-0 transitions highlighted along with the ≈405 nm shoulder (*) and the 520 nm marker (vertical line).

Absorption maxima were found at 437, 458 and 491 nm with the latter displaying a shift similar to earlier experiments. The spectrum did appear characteristically broader than the zeaxanthin control (Fig 4.1A) with a shoulder present at 408 nm. The use of acetone and CS_2 failed to produce any visible pigment uptake (data not shown).

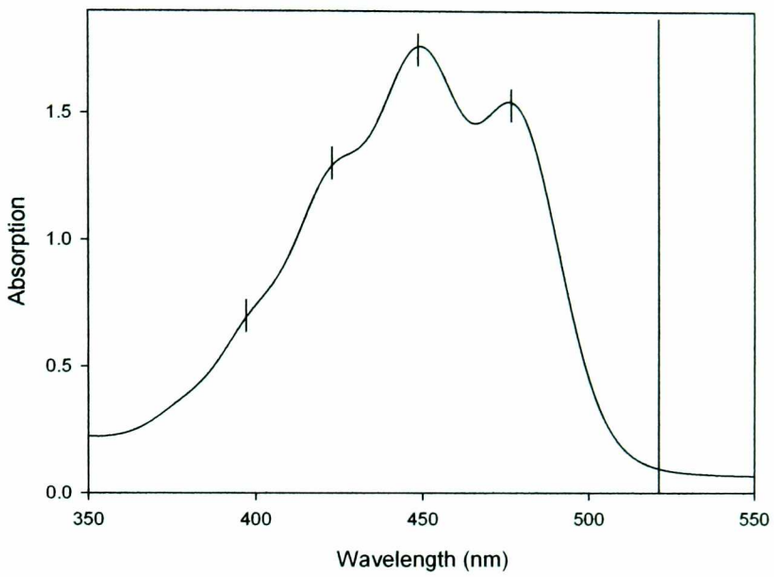

Figure 4.8 - Spectroscopic analysis of reconstituted zeaxanthin-PsbS complex using diethyl ether. Peak maxima at 1-1, 0-1 and 0-0 transitions highlighted along with the ≈405 nm shoulder (*) and the 520 nm marker (vertical line).

The key component during pigment extraction from raw materials is diethyl ether (see section 2.8 for method), employed here to rapidly dry zeaxanthin to ensure minimal water retention in the sample. The spectrum in figure 4.8 appears slightly blue-shifted, with peak maxima at 425, 455 and 486 nm and a shoulder at 396 nm, similar to that seen in the zeaxanthin control using diethyl ether (Fig 4.1D). Second derivative analysis (Fig 4.8, red trace) shows peaks at 492, 457 and 427nm corresponding to the 0-0, 0-1 and 1-1 transitions respectively. Additionally, shoulders can be seen at 405 and 384nm. No evidence of red shifted peaks can be seen.

4.4.iv Reconstitution – use of high component concentrations

Zeaxanthin concentration had been observed to have reach saturation of pigment uptake. However, it remained unclear whether this was simply due to a limitation imposed by protein concentration (and therefore density within a given sample), or whether a more complex interaction between pigment and protein was being hindered at low component concentrations. To address this issue reconstitution was performed using component concentrations ten times that used in earlier experiments.

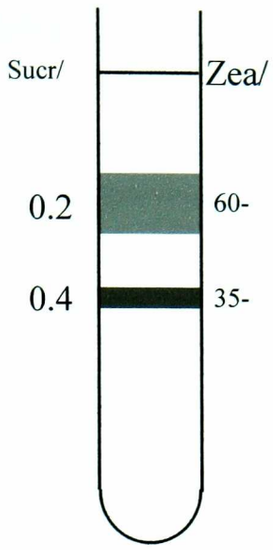

Figure 4.9 – Sucrose density gradient analysis of reconstituted PsbS. PsbS-zeaxanthin complex (grey region), minor pigment band (black region).

Reconstitution using high concentrations of each component (9 μM/ml PsbS and 14nM/ml zeaxanthin) resulted in a dramatic change in the absorption spectrum of zeaxanthin (Fig4.10, trace 1). The spectrum displayed a strong red shift, with the 0-0 absorption maximum appearing at ≈523 nm, whilst the second derivative of this spectrum shows maxima at 525, 487 and 450 nm, along with a secondary band at 536 nm (Fig4.10, trace 2).

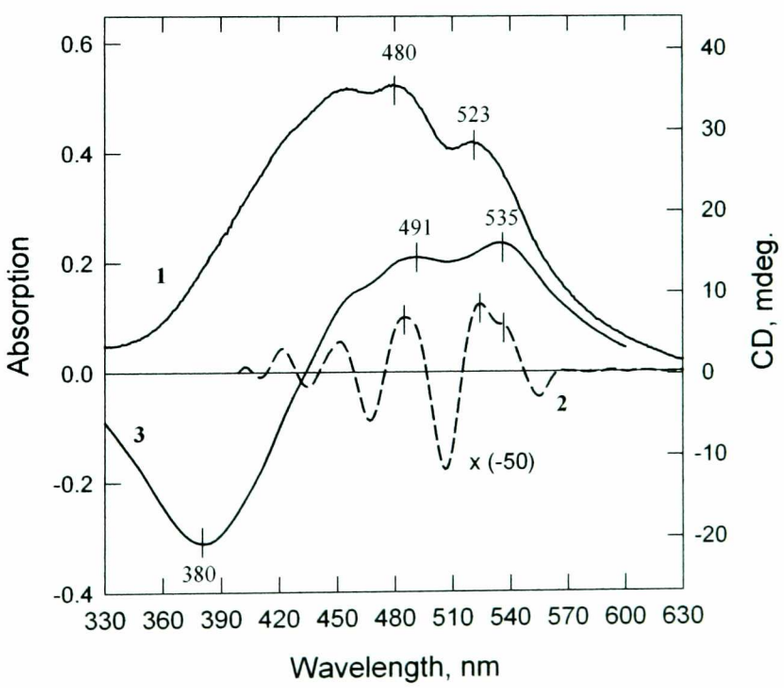

Figure 4.10 – Spectroscopic characterisation of zeaxanthin shift. Absorption spectrum of PsbS reconstituted with zeaxanthin (1), second derivative of spectrum 1 (2), CD spectrum of PsbS reconstituted with zeaxanthin (3).

The PsbS-zeaxanthin complex possessed a novel CD spectrum, which could not be observed for either constituent alone. Positive bands at 491 and 536 nm, along with a strong negative band at 380 nm can be seen (Fig 4.10, trace 3). These negative and positive symmetrical features can be attributed to the negative and positive Cotton effects of excitonically coupled pigments (Zsila et al. 2002), suggesting that two zeaxanthin molecules are interacting. The negative and positive components of this spectrum resemble those of the CD spectrum (trace 3), whilst displaying positive bands with better resolution and a clear minimum at 507 nm. The latter represents a higher excitonic component, the existence of which could be explained by the presence of a band at 525 nm, clearly seen in the second derivative absorption spectrum (trace 2). It is possible that this transition could belong to a monomeric zeaxanthin molecule bound to PsbS. The CD spectrum described above suggests that the protein is capable of significantly affecting the properties of zeaxanthin, and these CD characteristics indicate that PsbS binds zeaxanthin in this complex.

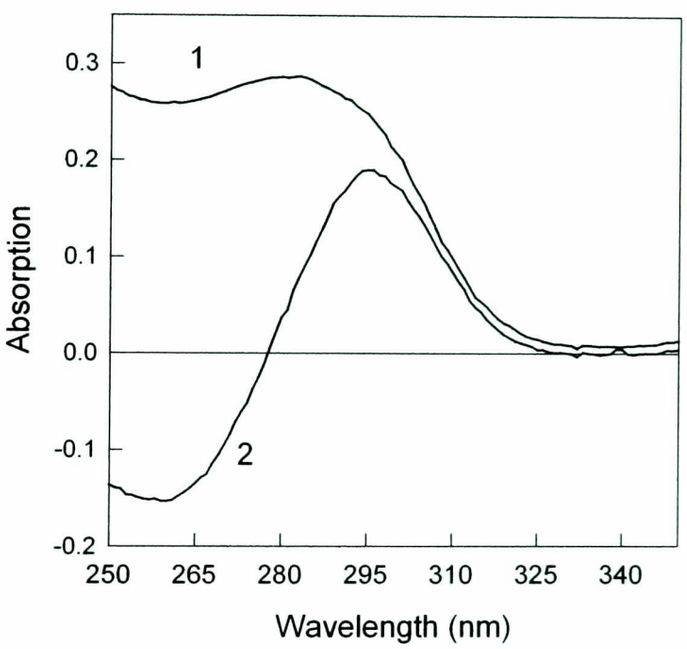

Figure 4.11 – UV absorption spectrum of PsbS reconstituted with zeaxanthin (1), and a (PsbS+zeaxanthin) – (PsbS only) absorption difference spectrum (2).

The PsbS protein itself presented an altered absorption spectrum in the presence of zeaxanthin. Analysis of the UV region of the PsbS spectrum in the absence of pigment shows an absorption band at 258 nm, arising mainly from phenylalanine (Fig 4.11). However, upon formation of a complex with zeaxanthin results in this band shifting to 280 nm (Fig 4.11, spectrum 1). The conserved nature of the corresponding difference spectrum shows that that change can be explained by a red shift in a population of phenylalanine residues in the PsbS sample (Fig 4.11,

spectrum 2). This provides further support that a specific interaction exists between PsbS and zeaxanthin.

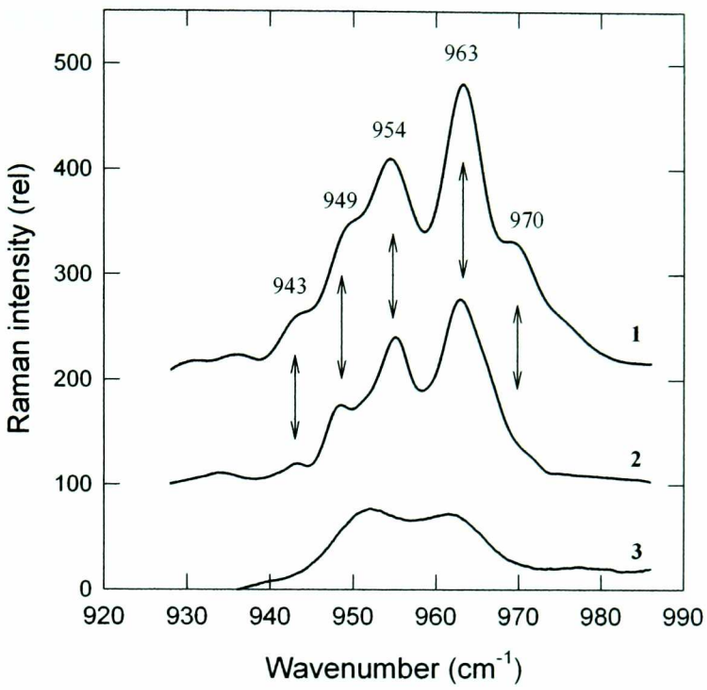

Figure 4.12 – Resonance Raman spectra of zeaxanthin in ν_4. qE-activated zeaxanthin absorbing at 535 nm (modified from (Ruban et al. 2002)) (1), zeaxanthin bound to PsbS (2), zeaxanthin in detergent-lipid micelles purified on a sucrose gradent (modified from (Ruban et al. 2002)). The arrows indicate the five main transitions assocated with zeaxanthin activation. Data provided by Dr Alexander Ruban.

A red-shifted zeaxanthin spectrum has been observed *in vivo* associated with characteristic features in the Resonance Raman spectrum (Ruban et al. 2002). The ν_4 region of the spectrum arises from wagging vibrations of various C-H groups (Robert et al. 1999), and bound red-shifted zeaxanthin *in vivo* displays five new transitions not found in zeaxanthin dissolved in detergent or solvent. This zeaxanthin "fingerprint" is shown in Fig 4.12 (spectrum 1), in comparison with the rather featureless spectrum of zeaxanthin in detergent micelles (spectrum 3). The *in vitro* PsbS-zeaxanthin complex displayed an almost identical Resonance Raman spectrum to that associated with qE (spectrum 2). The two major bands at 954 and 963 cm^{-1} were the same *in vivo* as for the PsbS-zeaxanthin complex, although the minor bands varied slightly in intensity and position in the two spectra.

4.5 Analysis of PsbS interaction of Antheraxanthin and Violaxanthin

The binding characteristics of PsbS in relation to the remaining xanthophyll cycle carotenoids, Antheraxanthin and Violaxanthin, were studied under conditions suitable for zeaxanthin binding in order to determine if the shifts in absorption spectra seen in section 4.4 were specific to that pigment.

Analysis of Violaxanthin reconstitution over the pH range from 6 – 8 resulted in maximum pigment uptake at pH 6 (Fig 4.13, trace 1) with samples incubated at pH 7 and 8 (Fig 4.13, trace 2 and 3) adopting similar absorption properties. However, pigment uptake over the chosen pH range was of a relatively low efficiency, as significant amounts of pigment remained after incubation. The peak maxima positions display little variation to the Violaxanthin control (Fig 4.1B).

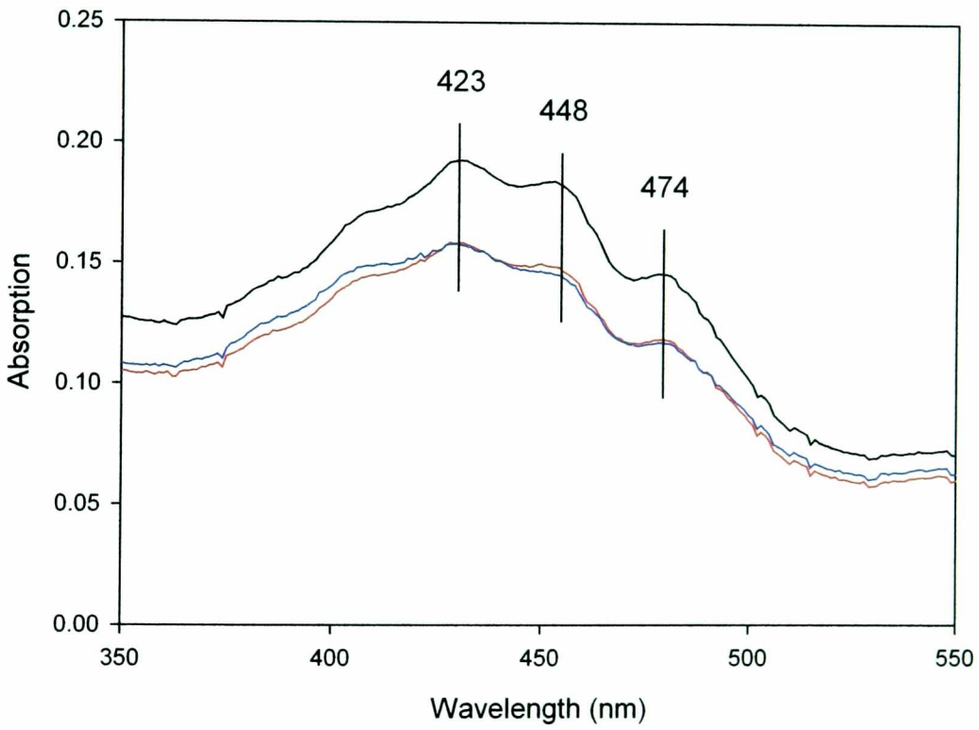

Figure 4.13 – Spectroscopic analysis of PsbS reconstitution with Violaxanthin at pH 6 (black), pH 7 (red) and pH 8 (blue).

The same pH range was employed when analysing Antheraxanthin uptake upon incubation with PsbS. Absorption efficiency was almost double that of Violaxanthin, with pH 8 proving to be the most successful (Fig 4.14, trace 1). Uptake at pH 6 and 7 appeared broadly similar (Fig 4.14, trace 2 and 3) and only marginally less than that of pH 8. Again peak maxima for all spectra identical to the control (Fig 4.1C).

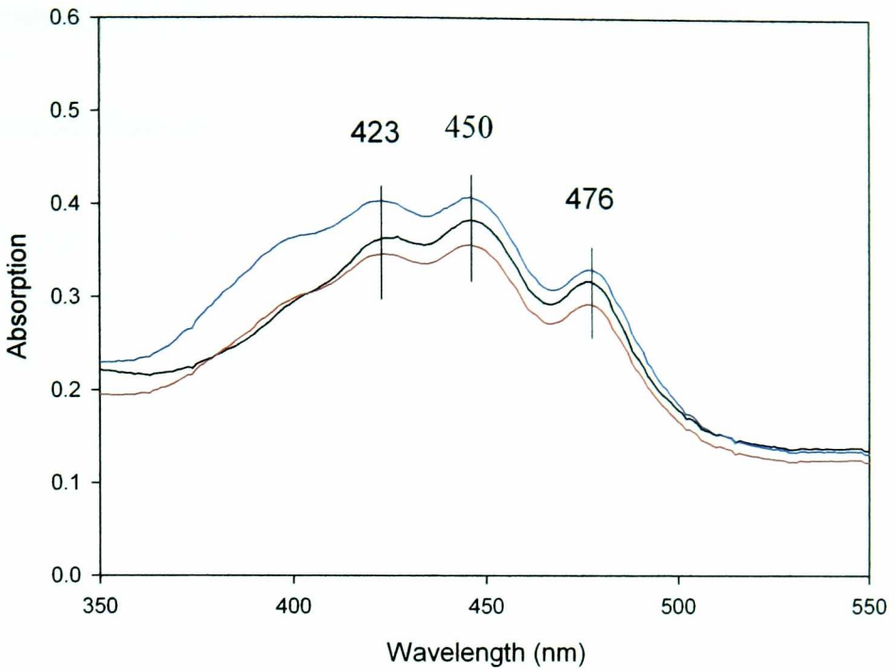

Figure 4.14 - Spectroscopic analysis of PsbS reconstitution with Antheraxanthin at pH 6 (black), pH 7 (red) and pH 8 (blue).

4.7 Analysis of reconstituted PsbS interaction with LHCII components using the *in vitro* fluorescence quenching technique

4.7.1 Introduction

Manipulating experimental conditions can reduce the fluorescence yield of chlorophyll in purified PSII light harvesting complexes, and provides a model system for investigating the mechanism of non-photochemical quenching observed in, intact, chloroplasts and leaves. Kinetic analysis has been used on data generated from isolated chloroplasts and purified LHCIIb, CP26 and CP29. This has given rise to a second-order kinetic model for the decrease in fluorescence with respect to time after the induction of quenching (Ruban et al. 2001; Wentworth et al. 2001). All pigment protein complexes of the Lhcb family have displayed a level of quenching *in vitro*, that is consistent with the extent of qE observed *in vivo* (Ruban et al. 1996) (Ruban & Horton 1999). As detailed in previous chapters, PsbS has been directly implicated with qE (Li et al. 2000) and the formation of the 535 nm shift as a result of the proteins ability to bind exogenous zeaxanthin (Aspinall-O'Dea et al. 2002), a pigment known to directly modulate the second order rate constant for isolated Lhcb proteins (Wentworth et al. 2001). In light of the work presented thus far, it was therefore possible to study the effects of the PsbS protein in relation to this model; specifically the ability of PsbS to modulate the rate of

fluorescence quenching seen for isolated Lhcb proteins in relation to pH and the presence of zeaxanthin presence.

4.7.2 Fluorescence Quenching

Isolate LHCIIb exhibits pH-dependent fluorescence quenching characteristic in isolated form (Ruban & Horton 1999) figure 4.15 (closed circle). The extent of quenching recorded 20 seconds after sample dilution into a reduced detergent medium at a specified pH. The titration appears to have two components; the first between pH 7 and 5 with the second between pH 5 and 4. The latter which accounts for most of the quenching has an approximate pKa of 4.7. In the presence of PsbS there is a small shift to 4.9 (Fig 4.15, open circle).

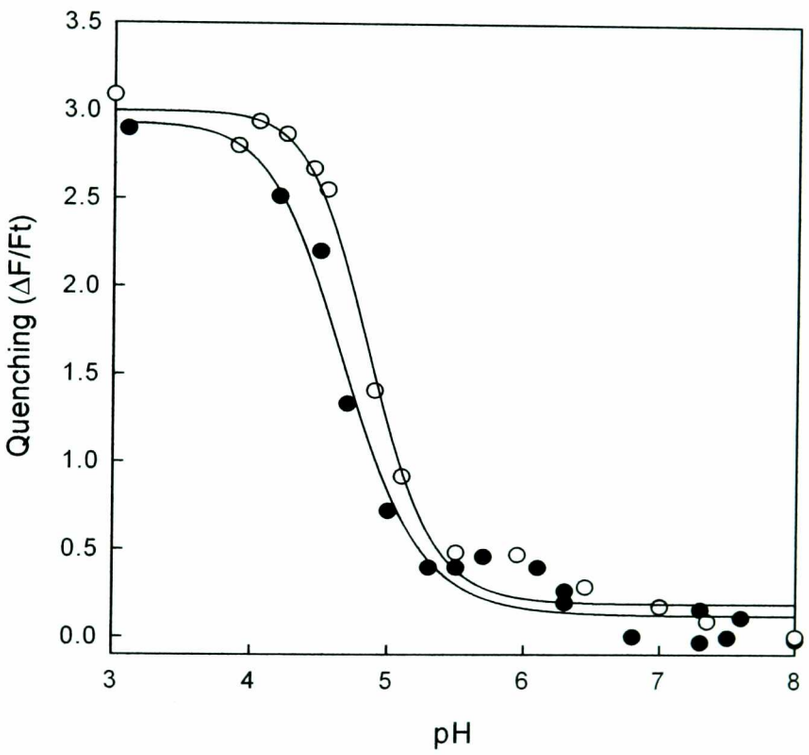

Figure 4.15 – Quenching of chlorophyll fluorescence in LHCIIb (60μg/ml final concentration chlorophyll) as a function of medium pH. (Closed Circle) the effect of reducing the detergent concentration to 6μM, (Open Circle) the effect of 5μl of buffered PsbS (1μM). Quenching was initiated by dilution of the complex into a medium containing 60μM DM at a specified pH as described in the text. Quenching was calculated as the change in fluorescence (ΔF) divided by the fluorescence intensity after 30 seconds (F_t).

The presence of zeaxanthin has previously been shown to shift the pK of LHCIIb fluorescence quenching to a higher pH (Wentworth et al. 2001), as can be seen in figure 4.18 (open circles). The control sample (closed circles) displays a similar pK to that of LHCIIb in figure 4.15,

whilst the addition of 20μM zeaxanthin causes the pKa to rise from 4.7 to 5.1. This value is increased further when LHCIIb is incubated with 5μM PsbS resulting in a pKa of 5.4.

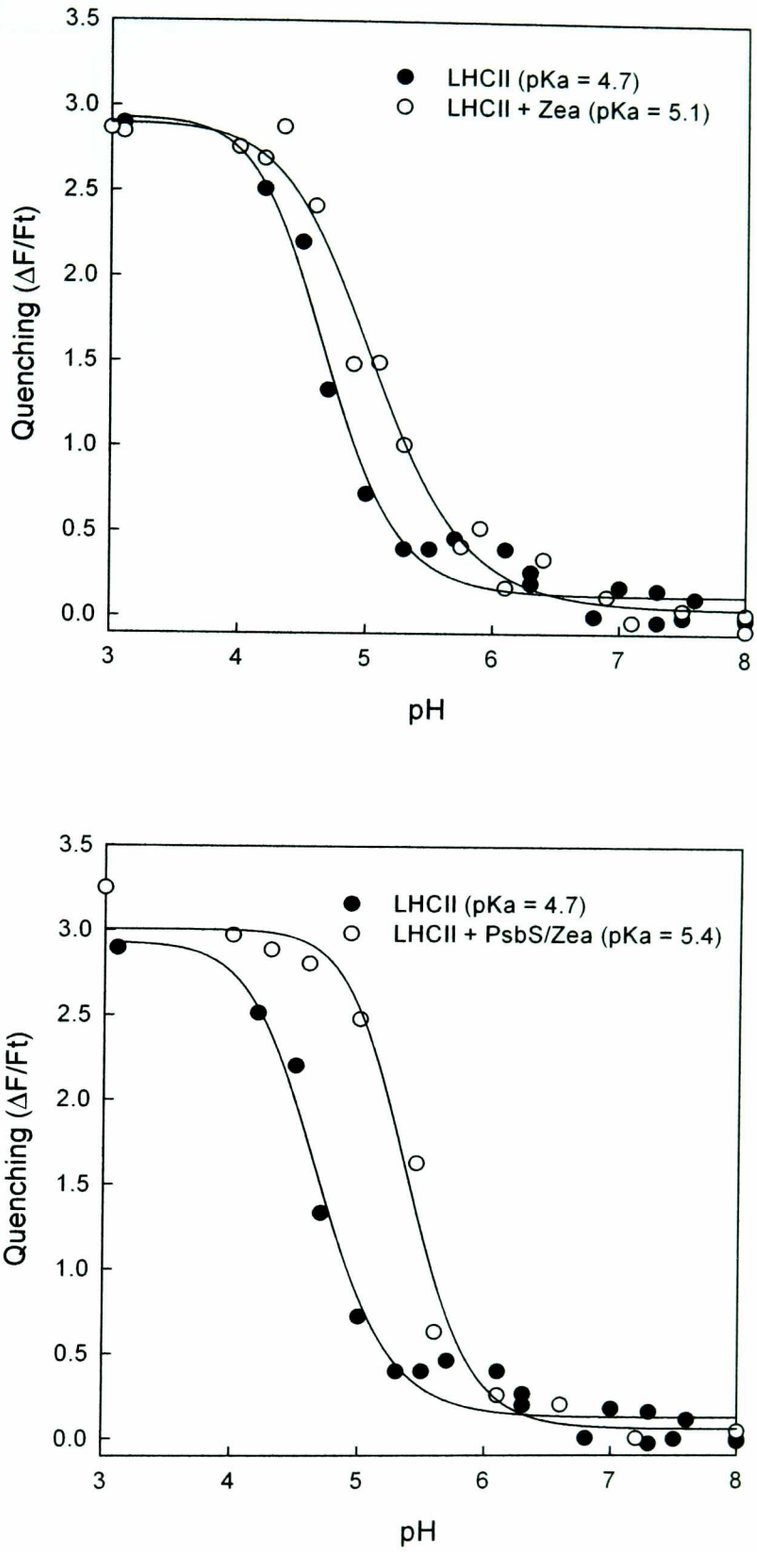

Figure 4.16 - Quenching of chlorophyll fluorescence in isolated CP26 as a function of medium pH. (Closed Circle) the effect of reducing the detergent concentration to 6μM, (Open Circle) the effect of 5μl of buffered PsbS. Quenching calculated as in Fig 4.17.

The quenching kinetics of these samples have previously been shown to display similar characteristics to qE in chloroplasts (Wentworth et al. 2001). In all cases the quenching with LHCIIb fitted a second-order reaction as evidenced by good fits to hyperbolic kinetics

and linear reciprocal plots (Figure 4.17). Both the rate constant and the maximum quenching level could be altered with the addition of zeaxanthin or zeaxanthin and PsbS, with the latter showing the highest level of quenching.

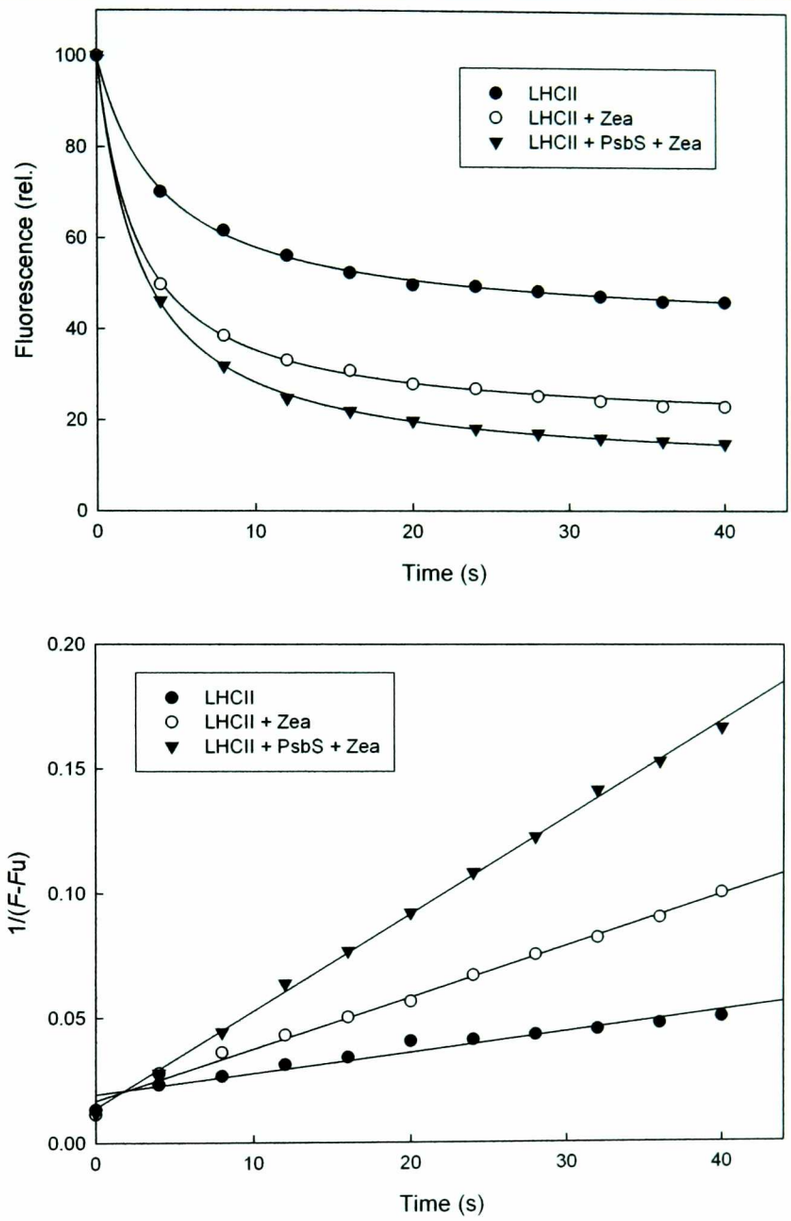

Figure 4.17 – Kinetics of chlorophyll fluorescence quenching in isolated LHCII. Upper graph, decrease in fluorescence. Data points were obtained by digitization of chart recorder traces, and the line represents the best fit generated using equation $F=1/(kt + 1/F_q) + Fu$. Lower graph, second-order reciprocal plot of the data where F is the level of fluorescence and r^2 values of 0.98 to 0.99. k is the second order rate constant; F_q is the amplitude of quenchable fluorescence; F_u is the amplitude of unquenchable fluorescence.

To determine if the increase in LHCIIb quenching observed in the presence of zeaxanthin and PsbS was the result of a hydrophobic interaction or a specific interaction between the three components, a control experiment using BSA was performed. Again, the titration appears to have two components; the first between pH 7 and 5 with the second between pH 5 and 4. The

latter, which accounts for most of the quenching, has an approximate pKa of 4.7. In the presence of BSA there is a small shift to 4.6 (Fig 4.18, open circle).

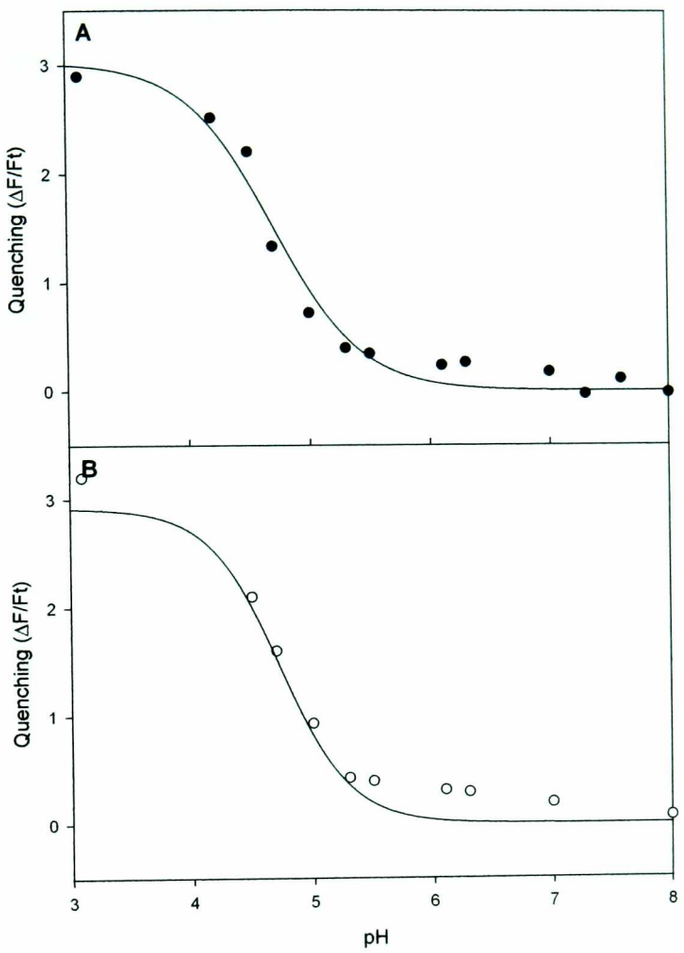

Figure 4.18 - Quenching of chlorophyll fluorescence in isolated LHCIIb as a function of medium pH. (Closed Circle) the effect of reducing the detergent concentration to 6μM, (Open Circle) the effect of 5μl of buffered BSA. Quenching calculated as in Fig 4.15.

The effect of zeaxanthin in the presence of LHCIIb was similar to that observed earlier (Fig 4.18, open circle). This value was unaffected by incubation of LHCIIb with 5μM BSA (figure 4.18, Closed triangle). The kinetic analysis of these samples showed that quenching with LHCIIb fitted a second-order reaction as evidenced by linear reciprocal plots (Figure 4.19), both displaying similar results to those seen in figure 4.17. However, it can be seen that the presence of BSA does nothing to enhance the maximum level of LHCIIb quenching in the presence of zeaxanthin, unlike PsbS.

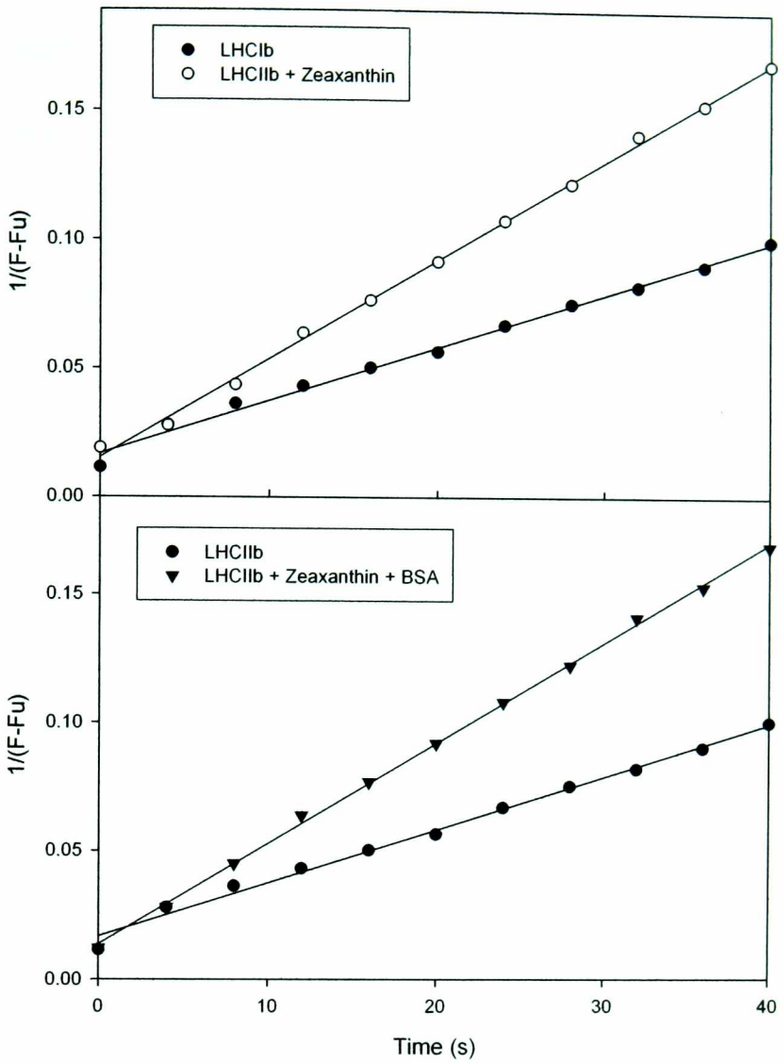

Figure 4.19 – Kinetics of chlorophyll fluorescence quenching in isolated LHCII in the presence and absence of zeaxanthin and BSA. Second-order reciprocal plot of the data where *F* is the level of fluorescence and r^2 values of 0.98 to 0.99.

Finally, spectral analysis of the sample containing quenched LHCIIb in the presence of zeaxanthin and PsbS could be seen to display a peak at 520nm, similar to that seen in Figure 4.10, along with additional peaks at 455 and 480nm (Figure 4.20). Thus, it is evident that the presence of PsbS and zeaxanthin in a heterogeneous protein environment generate a large shift in the zeaxanthin spectrum during quenching, even when component concentrations are low.

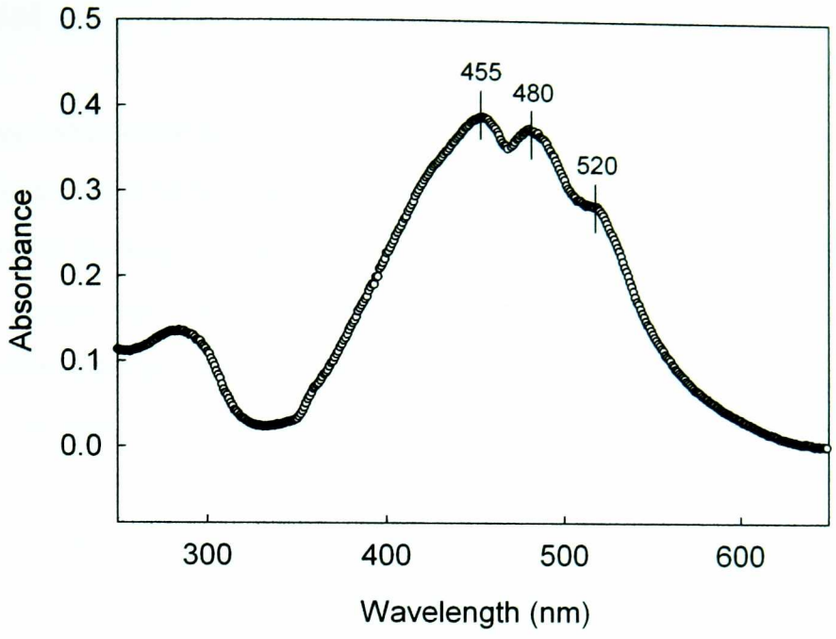

Figure 4.20 – Absorption spectrum of quenching LHCIIb in the presence of zeaxanthin and PsbS. Peak maxima shown in the visible region.

4.6 Discussion

Reconstitution of PsbS using zeaxanthin dissolved in ethanol frequently generated an unusual spectral signature. Previous studies had shown that zeaxanthin would adopt a strong peak maximum at 380 nm upon aggregation in the presence of water, resulting in a dramatic reduction in absorption between 400 and 500 nm. However, peak maxima are maintained within this range with spectral structure similar to that seen for the control. This would indicate that two populations of zeaxanthin are present in the sample; one bound to PsbS displaying a normal spectrum with a second highly aggregated species absorbing strongly at ≈380 nm. This issue was effectively overcome with the introduction the highly reproducible and robust reconstitution technique described in section 4.3. This approach requires the brief incubation of PsbS (at room temperature), with zeaxanthin deposited as a dry film on the surface of a glass tube. The latter is produced by drying zeaxanthin in oxygen free nitrogen under sonication (see Fig 4.4 for details), whilst the volume of pigment used is determined by the concentration of pigment required to achieve the required ratio (i.e. 2:1 pigment:protein) with PsbS.

The uptake of zeaxanthin by a buffered PsbS sample using this technique appears to saturate after a ratio of 3:1 is reached (Fig 4.5, trace 3). The level of increased absorption intensity seen for the 4:1 ratio (Fig 4.5, trace 4) is significantly less than that of earlier ratios (traces 1 to 3), an observation supported by data from the 5:1 ratio, which lacks any increase in absorption

intensity suggesting that the maximum zeaxanthin load for a PsbS sample of that concentration had been attained.

Temperature was also found to have a profound effect upon zeaxanthin binding with very little uptake being seen below 12°C, perhaps indicating that an energy barrier must be overcome to encourage efficient binding. Pigment absorption appeared to largely saturate above 30°C, with the maximum temperature held at 40°C in order to prevent zeaxanthin degradation. Any attempts to further enhance pigment uptake or spectral shifts using alternative solvent failed. It is unlikely this is due to zeaxanthin aggregation caused as a result of water contact, and is perhaps more readily explained in terms of an energy barrier. Drying of zeaxanthin with different solvents causes the pigment to pack together in different orientations, based on the polarity of the solvent used. As a result the packing achieved may be unfavourable for binding to a specific protein (in this case PsbS), and this may be due to an increase in the energy requirement necessary for pigment binding, hence an larger energy barrier is created. This would explain why binding appeared so inefficient using dry ethanol, at a temperature normally responsible for the most efficient uptake of pigment when using absolute ethanol. This theory would also explain the results obtained using other solvents.

Finally, reconstitution experiments were performed using high concentrations of both PsbS and zeaxanthin in order to determine if the absorption change at 535nm (Ruban et al. 1993b; Bilger & Bjorkman 1994) related to the dissipation of excitation energy in PSII in the presence of PsbS, could be achieve *in vitro*. This change is thought to result from a strong red shift in the absorption spectrum of one or two zeaxanthin molecules (Ruban et al. 2002). The shifted zeaxanthin absorption between 523 and 525 nm compared to ≈505 nm in the absence of qE, gives rise to a bind at 535 nm in the qE difference spectrum. The results of reconstitution experiments involving high component concentrations (section 4.4.iv) suggests that these 'activated' molecules are bound to PsbS as the pigment-protein complex displays a strong red shift to ≈523 nm, sufficient to generate a 535 nm band. This observation would explain why the 535 nm change is absent from the *Arabidopsis thaliana* mutant which lacks PsbS (Li et al. 2000).

The CD spectrum of the reconstituted complex has a conserved nature in relation to zeaxanthin and an altered UV-absorption spectrum for PsbS. This would suggest that the protein provides a highly polarized framework for zeaxanthin binding, which significantly affects the photochemical properties of the pigment. Zeaxanthin binding also alters the helical structure of PsbS, in which all phenylalanine residues are contained. The highest concentration of residues

can be found in the predicted fourth helix (Wedel et al. 1992; Kim et al. 1992), which may provide the binding site for zeaxanthin. The enhancement of the Resonance Raman spectrum of zeaxanthin supports the theory that a strong and specific interaction between zeaxanthin and PsbS exists, resulting in a particular pigment configuration being established. The changes in the absorbance and Resonance Raman spectra after reconstitution have the same characteristic features found *in vivo*, indicating that this *in vitro* reconstitution is similar to a process occurring *in vivo*. Analysis of the effect of PsbS upon the kinetics of fluorescence quenching in isolated light harvesting complexes indicates that in the presence of zeaxanthin this protein is capable of enhancing the rate of quenching, beyond that normally observed for zeaxanthin alone. Additionally, it is evident that low concentrations of PsbS can generate the shift in the spectrum of zeaxanthin to ~520nm in the presence of LHCIIb. This data further supports the suggested role of PsbS in qE, specifically as a prerequisite for the qE related 535nm spectral shift. A model for the role of the PsbS-zeaxanthin complex will be detailed in chapter 5.

Chapter Five

General Discussion

General Discussion

5.1 Introduction

The process of photosynthetic light harvesting in higher plants can adapt in response to altered levels of light quanta. This ability enables the plant to regulate the quantity of light energy present within the photosynthetic system and ensure that the capacity for CO_2 fixation is not exceeded. Surplus excitation energy present in the antenna system of PSII is dissipated as heat, in a process termed non-photochemical quenching, however, the mechanism of this thermal dissipation remains poorly understood. To develop a greater understanding of the key elements involved in photo-protection *Arabidopsis thaliana* mutants were isolated on the basis of impaired energy dissipation. It became evident that the PsbS protein was essential for the qE component of NPQ (Li et al. 2000), whilst light harvesting and photosynthesis were unaffected by its absence. An exhaustive analysis of this protein *in vitro* has required a new isolation technique to be established (chapter 3), which has enabled the basic properties of the protein to be uncovered whilst providing an ideal platform to study the manner in which PsbS interacts with the key regulatory components of qE, namely trans-thylakoid ΔpH, zeaxanthin and antenna complexes.

5.2 PsbS – the relationship with pH

Experiments using site-directed mutagenesis uncovered two conserved, protonatable amino acids in the PsbS protein (E122 and E226). These residues were shown to be critical elements in PsbS function (Li et al. 2002), with a double mutant at these loci displaying the most dramatic phenotype in which effectively all qE had been abolished. A single mutation was also observed to result in a 60-70% reduction in qE. Despite having such a profound effect upon the proteins function, the mutations had little effect on PsbS accumulation when compared to wild type, suggesting that the expression and stability of the protein had not been altered.

It was proposed that these residues could bind H^+ ions; whilst in contrast to the experimental evidence seen in chapter 3, PsbS was shown to bind the carboxyl modifier DCCD (Dominici et al. 2002). Such inconsistency between experimental observations is difficult to reconcile. It should be noted that the methods employed to isolate PsbS vary significantly and as a result may be responsible for such differing results. Recently however, PsbS has been shown to undergo pH-dependent structural changes involving the formation of a homodimer at high pH levels, which under high light, (hence low pH), breaks down into its constituent PsbS monomers (Bergantino et al. 2003). This conversion is reversibly induced by light with the resultant PsbS

monomer or dimer associated with the light harvesting antenna and PSII core complexes respectively. Thus, PsbS has been shown to possess protonatable residues essential for its role in qE, whilst displaying a structural dependence on pH. However, it should be noted that *in vitro* the helical structure of the protein is affected by low pH levels (chapter 3), a factor that *in vivo* may prevent PsbS from directly sensing ΔpH changes in Photosystem II. Alternatively, low pH in the thylakoid membrane may not affect PsbS in this manner because acidification is only present on the lumenal side of the membrane (hence the protein), whereas *in vitro* this effect would be applied across the entire protein.

5.3 PsbS – the relationship with the xanthophyll cycle

The evidence described in section 5.2 can be used to further explain the outcome of the reconstitution experiments detailed in chapter 4. Incubation of PsbS and zeaxanthin high concentration creates an absorbance shift in the zeaxanthin spectrum at 523 nm, which gives rise to a band at 535 nm in a calculated difference spectrum (chapter 4) attributed to the presence of activated zeaxanthin (Ruban et al. 2002), thought to arise through the formation of a head – to – head zeaxanthin dimer. At lower component concentrations this shift is difficult to detect, and, in many cases, is not present at all, even though zeaxanthin is bound. However, spectral analysis of LHCIIb in the presence of PsbS and zeaxanthin (taken after *in vitro* quenching measurements at low CMC) reveals a distinct band at ~520nm. Thus, the formation of activated zeaxanthin is possible at low concentrations of PsbS and zeaxanthin when studying heterogeneous protein populations.

It is possible to explain these results by considering the ability of PsbS to form homodimers *in vivo* (Bergantino et al. 2003). As described above, PsbS forms dimers under low light conditions when the pH level is high, and violaxanthin is the predominant xanthophyll population in the thylakoid membrane. An increase in light intensity causes the lumenal pH to drop and consequently the PsbS homodimer splits. This event correlates with an increase in violaxanthin conversion to zeaxanthin and the formation of qE and Δ535nm. Under these conditions it is proposed that zeaxanthin is bound by PsbS (Aspinall-O'Dea et al. 2002), which subsequently interacts with the light-harvesting antenna of PSII (Bergantino et al. 2003).

As a consequence, interaction between PsbS protein species is blocked in favour of heterogeneous interactions, however during reconstitution experiments PsbS is found in a homogeneous state. Thus, the rapid uptake of dried zeaxanthin by PsbS could well represent binding, however the lack of interaction between PsbS proteins prevents the formation of activated zeaxanthin and the resultant spectral shift at ~525nm. This would indicate that the

zeaxanthin dimer is formed by inter- rather than intra-protein pigment interaction. Therefore, the formation of activated pigment at high component concentrations could result from PsbS-zeaxanthin being forced to interact with each other due to the sheer quantity of complexes present in solution. Formation of the shift at ~520nm in a heterogeneous solution at low component concentration supports this hypothesis and suggests that the PsbS-zeaxanthin complex favours interaction with other protein species in PSII.

5.4 PsbS – a model for the role of PsbS in qE

Figure 5.1 describes how events could potentially unfold *in vivo*. With a reduction in lumenal pH, the xanthophyll cycle is activated through VDE resulting in violaxanthin deepoxidation. Simultaneously, PsbS-dimers monomerise and newly formed zeaxanthin is bound by PsbS preventing feedback inhibition oF VDE. It has been shown that increasing the level of PsbS expression results in elevated deepoxidation as well as NPQ (Hieber et al. 2004), supporting the theory that the thylakoid lipid phase has a limited capacity for xanthophylls, which would be responsible for negative feedback on VDE.

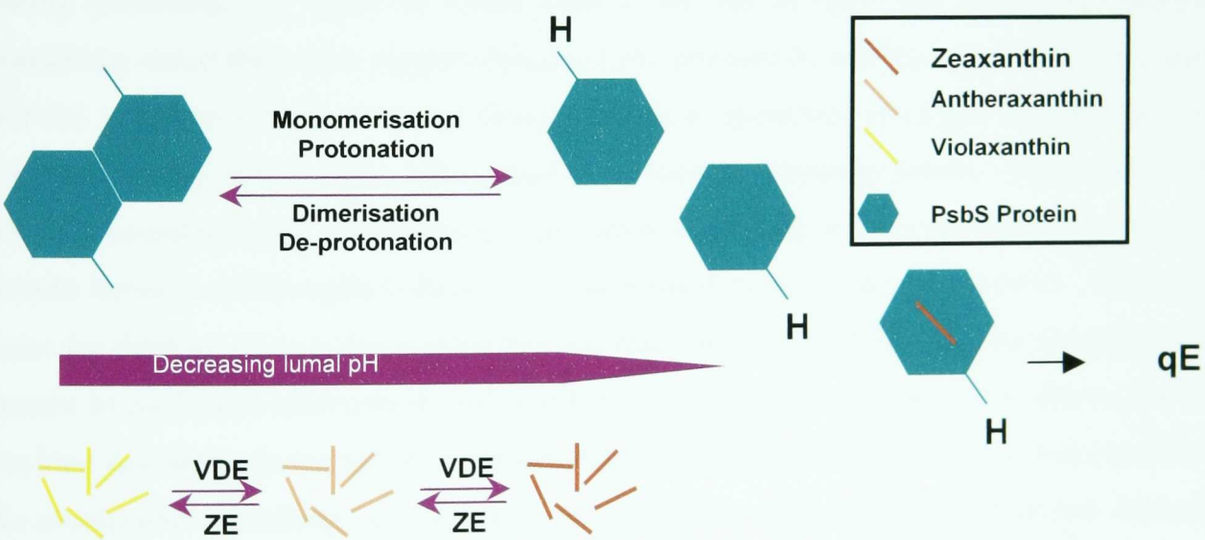

Figure 5.1 – Proposed mechanism of formation for the PsbS-Zeaxanthin complex.

The PsbS-zeaxanthin complex then performs its required function in qE; however, partly due to the absence of structural information regarding this proteins location in PSII, the mechanism of this process remains unclear. The absence of PsbS from the crystalline areas of the thylakoid membrane (Nield 2000) suggest that the protein may be present in less ordered areas of the membrane. The formation of zeaxanthin has been shown to reduce the rigidity of the thylakoid

membrane and PsbS itself may display a significantly less ordered structure compared to the rest of the Lhcb family as a result of reduced chromophore binding. It is likely that PsbS plays a key role in the effects observed as a result of zeaxanthin formation in the thylakoid membrane, and two potential functions for the protein have been suggested:

1. PsbS is the unique site of rapidly forming qE
2. PsbS is necessary to enable qE to take place efficiently

The apparent absence of pigments upon isolation of PsbS suggests that the protein is incapable of acting as the unique site of qE. There is no evidence that PsbS *in vivo* or *in vitro* is able to bind chlorophylls (Dominici et al. 2002), although that alternative reconstitution methodology, as studied in this thesis, could yield different results. The presence of PsbS is, however, important for the proper formation of qE, and may promote, or assist, conformational change in neighbouring LHC proteins resulting in quenching, enhancing the efficiency of qE. The observation that PsbS stimulates quenching of LHCII fluorescence *in vitro* is consistent with this suggestion.

PsbS has been proposed to act either directly or indirectly to dissipate excess excitation energy during quenching. A model in which PsbS is the site of ΔpH- and xanthophyll-dependent quenching, rather than other pigment-binding LHC proteins from PSII, suggests that protonation of PsbS results in a conformational change leading to quenching of singlet excited chlorophyll via direct energy transfer from chlorophyll to zeaxanthin (Demmig-Adams 1990; Owens, 1994) which is bound to PsbS. Alternatively, zeaxanthin-dependent quenching could occur within the protein between a chlorophyll dimer or a chlorophyll molecule and the protein. However, in order for PsbS to act as a direct quencher and form the site of qE it would be necessary for the protein to bind both chlorophylls and xanthophylls. Evidence reported here shows that PsbS can bind zeaxanthin in favour of antheraxanthin and violaxanthin. Nontheless, it is possible that the accelerated quenching rate observed for LHCIIb in the presence of PsbS and zeaxanthin (chapter 4) is a result of the direct quenching model as PsbS may have bound free chlorophyll pigments present in the LHCIIb preparation. However it is perhaps more likely the PsbS accelerates quenching by the introduction of 'activated' zeaxanthin.

PsbS may also act indirectly to support conformational changes and quenching that occur in adjacent LHC proteins in the PSII antenna. Evidence suggests that isolated light harvesting proteins possess intrinsic quenching capabilities (Ruban et al. 1996; Wentworth et al. 2000), similar to those seen for qE *in vivo* (Horton et al. 1996), and it is proposed that interaction between PsbS and one or more of these proteins controls the dissipation process (Horton et al.

2000). The relationship between thylakoid ΔpH and zeaxanthin, in which the latter is an allosteric regulator of qE (Ruban et al. 2001; Wentworth et al. 2001), indicates that they bind to the same protein or protein complex. The evidence presented in this thesis would suggest PsbS is an excellent candidate for this protein, and its ability to form a heterogeneous complex *in vivo* could be regulated by the protonation and binding of zeaxanthin to PsbS. According to the explanation proposed in section 5.2 such a heterogeneous complex would be essential for zeaxanthin activation. The absorbance change detected at 683 nm upon quenching of isolated light harvesting complexes, could arise *in vivo* due to the formation of such a quenching complex involving PsbS, in which activated zeaxanthin mediates thermal dissipation. It should be noted, however, that this absorbance change can occur *in vitro* in the absence of PsbS. The PsbS protein may also have a role in arranging supermolecular organisation to allow quenching to occur. The formation of a quenching complex described above would require space, and PsbS could perhaps promote the conformational change required in adjacent complexes by providing such room, prior to the formation of any complex. It has been observed when preparing PSII particles from *npq4* mutant plants, that an increased detergent concentration is required to solublise the membranes (personal communication Dr A Ruban and Dr M Wentworth). It has been suggested that the absence of PsbS results in closer packing PSII membranes forming significantly more rigid bilayer.

5.5 Conclusion

The research carried out in relation to non-photochemical quenching aims to eludicate the mechanism by which excess energy present in the light-harvesting antenna system of PSII is dissipated. This thesis has added to the understanding of the PsbS protein in relation to its interaction with the regulatory components of qE. However, every new discovery asks as many questions as it provides answers, and much work still needs to be done in order to discover the mechanism of thermal dissipation and the exact role the PsbS protein plays in this process. Characterisation of chromophore binding similar to that discussed here for xanthophyll cycle carotenoids would be an essential step forward. A structural analysis of the PsbS protein and the affect of pigment binding and protonation should be attempted using electron microscopy and FTIR, whilst further efforts should be made to locate PsbS within the thylakoid membrane. Characterisation of the PsbS effect in relation to the *in vitro* quenching model using increasingly complex protein combinations is also necessary to develop a greater understanding of the manner in which PsbS can influence adjacent protein complexes in its environment. The use of femtosecond spectroscopy (Fleming et al. 1997) could also uncover the pathway which excitation energy is passed along prior to thermal dissipation. Individually these measures will undoubtedly enhance our knowledge of photosynthesis, however, it will take a collective effort

to fully unravel not only the complete PsbS story but, more importantly, the mechanism of qE in higher plants.

Chapter Six

References

Cited Literature

Abrahams JP, Leslie AGW, Lutter R, Walker JE (1994) Structure At 2.8-Angstrom Resolution Of F1-Atpase From Bovine Heart-Mitochondria. Nature 370: 621-628

Adamska I, Funk C, Renger G, Andersson B (1996) Developmental Regulation Of The PsbS Gene Expression In Spinach Seedlings: The Role Of Phytochrome. Plant Molecular Biology 31[4], 793-802.

Adamska I (1997) Elips - Light-Induced Stress Proteins. Physiologia Plantarum 100: 794-805

Allen Jf (1992) Protein-Phosphorylation In Regulation Of Photosynthesis. Biochimica Et Biophysica Acta 1098: 275-335

Allen Jf (2003) Cyclic, Pseudocyclic And Noncyclic Photophosphorylation: New Links In The Chain. Trends In Plant Science 8: 15-19

Anderson JM, Waldron JC, And Thorne SW (1978) Chlorophyll-Protein Complexes Of Spinach And Barley Thylakoids. Spectral Characterisation Of Six Complexes Resolved By An Improved Electrophoretic Proceedure. Febs Letters 92: 227-233

Andersson B, Anderson JM (1980) Lateral Heterogeneity In The Distribution Of Chlorophyll-Protein Complexes Of The Thylakoid Membranes Of Spinach Chloroplasts. Biochimica Et Biophysica Acta 593: 427-440

Andersson B, Barber J (1996) Mechanisms Of Photodamage And Protein Degredation During Photoinhibition Of Photosystem II. In Advances In Photosynthesis (Baker, N.R Ed) Vol 5. Klewer, Dordrecht, 101-121

Andersson J, Walters RG, Horton P, Jansson S (2001) Antisense Inhibition Of The Photosynthetic Antenna Proteins CP29 And CP26: Implications For The Mechanism Of Protective Energy Dissipation. Plant Cell 13: 1193-1204

Andersson J, Wentworth M, Walters RG, Howard CA, Ruban AV, Horton P, Jansson S (2003) Absence Of The Lhcb1 And Lhcb2 Proteins Of The Light-Harvesting Complex Of Photosystem II - Effects On Photosynthesis, Grana Stacking And Fitness. Plant Journal 35: 350-361

Arvidsson PO, Bratt CE, Carlsson M, Åkerland HE (1996) Purification And Identification Of The Violoxanthin Deepoxidase As A 43 Kda Protein. Photosynthesis Research 49: 119-129

Aspinall-O'Dea M, Wentworth M, Pascal A, Robert B, Ruban A, Horton P (2002) In Vitro Reconstitution Of The Activated Zeaxanthin State Associated With Energy Dissipation In Plants. PNAS 99: 16331-16335

Balashov SP (2000) Protonation Reactions And Their Coupling In Bacteriorhodopsin. Biochimica Et Biophysica Acta-Bioenergetics 1460: 75-94

Bar-Zvi D, Tiefert Ma, Shavit N (1983) Interaction Of The Chloroplast Atp-Synthetase With The Photoreactive Nucleotide 3'-O-(4-Benzoyl)Benzoyl Adenosine 5'- Diphosphate. Febs Letters 160: 233-238

Barber J (1998) Photosystem Two. Biochimica Et Biophysica Acta-Bioenergetics 1365: 269-277

Barber J, Andersson B (1992) Too Much Of A Good Thing - Light Can Be Bad For Photosynthesis. Trends In Biochemical Sciences 17: 61-66

Barber J, Archer Md (2001) P680, The Primary Electron Donor Of Photosystem II. Journal Of Photochemistry And Photobiology A-Chemistry 142: 97-106

Barry B, Boerner RJ, De Paula JC (1994) The Use Of Cyanobacteria In The Study Of The Structure And Function Of Photosystem II. In The Molecular Biology Of Cyanobacteria (Bryant, Da Ed). Kluwer Academic, Dordrecht, 217-257

Bassi R, Caffarri S (2000) Lhc Proteins And The Regulation Of Photosynthetic Light Harvesting Function By Xanthophylls. Photosynthesis Research 64: 243-256

Bassi R, Croce R, Cugini D, Sandona D (1999) Mutational Analysis Of A Higher Plant Antenna Protein Provides Identification Of Chromophores Bound Into Multiple Sites. PNAS 96: 10056-10061

Bassi R, Dainese P (1992) A Supramolecular Light-Harvesting Complex From Chloroplast Photosystem-II Membranes. European Journal Of Biochemistry 204: 317-326

Bassi R, Giuffra E, Croce R (1996) Biochemistry And Molecular Biology Of Pigment Binding Proteins. In Light As An Energy Source And Information Carrier In Plant Physiology (RC Jennings, G Zucchelli, F Ghetti, M Crimi, Eds). Plenum Press, New York, 41-63

Bassi R, Sandona D, Croce R (1997) Novel Aspects Of Chlorophyll a/b - Binding Proteins. Physiologia Plantarum 100: 769-779

Belrhali H, Nollert P, Royant A, Menzel C, Rosenbusch JP, Landau EM, Pebay-Peyroula E (1999) Protein, Lipid And Water Organization In Bacteriorhodopsin Crystals: A Molecular View Of The Purple Membrana At 1.9 Angstrom Resolution. Structure 7: 909-917

Bergantino E, Dainese P, Cerovic Z, Sechi S, Bassi R (1995) A Posttranslational Modification Of The Photosystem-II Subunit CP29 Protects Maize From Cold Stress. Journal Of Biological Chemistry 270: 8474-8481

Bergantino E, Segalla A, Brunetta A, Teardo E, Rigoni F, Giacometti Gm, Szabo I (2003) Light- And pH-Dependent Structural Changes In The PsbS Subunit Of Photosystem II. PNAS 100: 15265-15270

Berthold D, Babcock G, Yocum C (1981) A highly resolved, oxygen-evolving photosystem II preparation from spinach thylakoid membranes. FEBS Letters 134: 231-234.

Berthold DA, Schmidt CL, Malkin R (1995) The Deletion Of PetG In Chlamydomonas-Reinhardtii Disrupts The Cytochrome bf Complex. Journal Of Biological Chemistry 270: 29293-29298

Bilger W, Bjorkman O (1994) Relationships Among Violaxanthin Deepoxidation, Thylakoid Membrane Conformation, And Nonphotochemical Chlorophyll Fluorescence Quenching In Leaves Of Cotton (Gossypium-Hirsutuml). Planta 193: 238-246.

Boekema EJ, Nield J, Hankamer B, Barber J (1998) Localization Of The 23-Kda Subunit Of The Oxygen-Evolving Complex Of Photosystem II By Electron Microscopy. European Journal Of Biochemistry 252: 268-276

Boekema EJ, Van Breemen JFL, Van Roon H, Dekker JP (2000) Arrangement Of Photosystem II Supercomplexes In Crystalline Macrodomains Within The Thylakoid Membrane Of Green Plant Chloroplasts. Journal Of Molecular Biology 301: 1123-1133

Boekema EJ, Van Roon H, Calkoen F, Bassi R, Dekker JP (1999a) Multiple Types Of Association Of Photosystem II And Its Light- Harvesting Antenna In Partially Solubilized Photosystem II Membranes. Biochemistry 38: 2233-2239

Boekema EJ, Van Roon H, Van Breemen JFL, Dekker JP (1999b) Supramolecular Organization Of Photosystem II And Its Light- Harvesting Antenna In Partially Solubilized Photosystem II Membranes. European Journal Of Biochemistry 266: 444-452

Bouvier F, Dharlingue A, Hugueney P, Marin E, Marionpoll A, Camara B (1996) Xanthophyll Biosynthesis - Cloning, Expression, Functional Reconstitution, And Regulation Of Beta-Cyclohexenyl Carotenoid Epoxidase From Pepper (Capsicum Annuum). Journal Of Biological Chemistry 271: 28861-28867

Bowlby NR, Yocum CF (1993) Effects Of Cholate On photosystem-II - Selective Extraction Of A 22 kDa Polypeptide And Modification Of Q(B)-Site Activity. Biochimica Et Biophysica Acta 1144: 271-277

Bradbury M, Baker NR (1981) Analysis Of The Slow Phases Of The Invivo Chlorophyll Fluorescence Induction Curve - Changes In The Redox State Of Photosystem-Ii Electron-Acceptors And Fluorescence Emission From Photosystem-I And Photosystem-II. Biochimica Et Biophysica Acta 635: 542-551

Brangeon J, Mustárdy L (1979) The Ontogenetic Assembly Of Intra-Chloroplastic Lamellae Viewed In 3-Dimension. Biological Cell 36: 71-80

Briantais JM, Vernotte C, Picaud M, Krause GH (1979) A Quantitative Study Of The Slow Decline In Chlorophyll *a* Fluorescence In Isolated Chloroplasts. Biochimica Et Biophysica Acta 548: 128-138

Bricker TM (1990) The Structure And Function Of CPA-1 And CPA-2 In Photosystem-II. Photosynthesis Research 24: 1-13

Bricker TM (1992) Oxygen Evolution In The Absence Of The 33 kDa Manganese-Stabilizing Protein. Biochemistry 31: 4623-4628

Bricker TM, Frankel LK (2002) The Structure And Function Of CP47 And CP43 In Photosystem II. Photosynthesis Research 72: 131-146

Bricker TM, Ghanotakis DF (1996) Introduction To Oxygen Evolution. In Oxygenic Photosynthesis The Light Reactions (Ort DR, Yocum CF, Eds) Vol 4. Kluwer, Dordrecht, 113-136

Bugos RC, Yamamoto HY (1996) Molecular Cloning Of Violaxanthin De-Epoxidase From Romaine Lettuce And Expression In Escherichia Coli. PNAS 93: 6320-6325

Bungard RA, Ruban AV, Hibberd JM, Press MC, Horton P, Scholes JD (1999) Unusual Carotenoid Composition And A New Type Of Xanthophyll Cycle In Plants. PNAS 96: 1135-1139

Burbidge A, Grieve T, Terry C, Corlett J, Thompson A, Taylor I (1997) Structure And Expression Of A cDNA Encoding Zeaxanthin Epoxidase, Isolated From A Wilt-Related Tomato (Lycopersicon Esculentum Mill). Journal Of Experimental Botany 48: 1749-1750

Büch K, Stransky H, Hager A (1995) Fad Is A Further Essential Cofactor Of The NAD(P)H And O_2 Dependent Zeaxanthin-Epoxidase. Febs Letters 376: 45-48

Caffarri S, Croce R, Breton J, Bassi R (2001) The Major Antenna Complex Of Photosystem II Has A Xanthophyll Binding Site Not Involved In Light Harvesting. Journal Of Biological Chemistry 276: 35924-35933

Carol P, Stevenson D, Bisanz C, Breitenbach J, Sandmann G, Mache R, Coupland G, Kuntz M (1999) Mutations In The Arabidopsis Gene Immutans Cause A Variegated Phenotype By Inactivating A Chloroplast Terminal Oxidase Associated With Phytoene Desaturation. Plant Cell 11: 57-68

Chain RK, Malkin R (1991) The Chloroplast Cytochrome b_6f Complex Can Exist In Monomeric And Dimeric States. Photosynthesis Research 28: 59-68

Chitnis PR (2001) Photosystem I: Function And Physiology. Annual Review Of Plant Physiology And Plant Molecular Biology 52: 593-626

Chitnis PR, Reilly PA, Nelson N (1989) Insertional Inactivation Of The Gene Encoding Subunit-II Of Photosystem-I From The Cyanobacterium Synechocystis Sp Pcc-6803. Journal Of Biological Chemistry 264: 18381-18385

Chitnis VP, Chitnis PR (1993) PsaL Subunit Is Required For The Formation Of Photosystem-I Trimers In The Cyanobacterium Synechocystis Sp Pcc-6803. Febs Letters 336: 330-334

Cleland RE, Bendall DS (1992) Photosystem-I Cyclic Electron-Transport; Measurement Of Ferredoxin-Plastoquinone Reductase-Activity. Photosynthesis Research 34: 409-418

Cramer WA, Soriano GM, Zhang HM, Ponamarev MV, Smith JL (1997) The Cytochrome b_6f Complex. Novel Aspects. Physiologia Plantarum 100: 852-862

Croce R, Canino G, Ros F, Bassi R (2002) Chromophore Organization In The Higher-Plant Photosystem II Antenna Protein CP26. Biochemistry 41: 7334-7343

Croce R, Remelli R, Varotto C, Breton J, Bassi R (1999a) The Neoxanthin Binding Site Of The Major Light Harvesting Complex (LHCII) From Higher Plants. Febs Letters 456: 1-6

Croce R, Weiss S, Bassi R (1999b) Carotenoid-Binding Sites Of The Major Light-Harvesting Complex II Of Higher Plants. Journal Of Biological Chemistry 274: 29613-29623

Davison Pa, Hunter Cn, Horton P (2002) Overexpression Of Beta-Carotene Hydroxylase Enhances Stress Tolerance In Arabidopsis. Nature 418: 203-206

Deisenhofer J, Epp O, Miki K, Huber R, Michel H (1985) Structure Of The Protein Subunits In The Photosynthetic Reaction Center Of Rhodopseudomonas-Viridis At 3A Resolution. Nature 318: 618-624

Dekker JP, Van Roon H, Boekem EJ (1999) Heptameric Association Of Light-Harvesting Complex II Trimers In Partially Solubilized Photosystem II Membranes. Febs Letters 449: 211-214

Demmig-Adams B (1990) Carotenoids And Photoprotection In Plants: A Role For The Xanthophyll Zeaxanthin. Biochimica Et Biophysica Acta 1020: 1-24

Demmig-Adams B, Adams WW (1996) The Role Of Xanthophyll Cycle Carotenoids In The Protection Of Photosynthesis. Trends In Plant Science 1: 21-26

Diner BA, Rappaport F (2002) Structure, Dynamics, And Energetics Of The Primary Photochemistry Of Photosystem II Of Oxygenic Photosynthesis. Annual Review Of Plant Biology 53: 551-580

Dominici P, Caffarri S, Armenante F, Ceoldo S, Crimi M, Bassi R (2002) Biochemical Properties Of The PsbS Subunit Of Photosystem II Either Purified From Chloroplast Or Recombinant. Journal Of Biological Chemistry 277: 22750-22758

Eggink LL, Park H, Hoober JK (2001) The Role Of Chlorophyll b - In Photosynthesis: Hypothesis. Plant Physiology 1: 2

Enami I, Tohri A, Kamo M, Ohta H, Shen JR (1997) Identification Of Domains On The 43 kDa Chlorophyll-Carrying Protein (CP43) That Are Shielded From Tryptic Attack By Binding Of The Extrinsic 33 kDa Protein With Photosystem II Complex. Biochimica Et Biophysica Acta-Bioenergetics 1320: 17-26

Engelbrecht S, Junge W (1990) Subunit-Delta Of H+-Atpases - At The Interface Between Proton Flow And ATP Synthesis. Biochimica Et Biophysica Acta 1015: 379-390

Eskling M, Arvidsson PO, Akerlund HE (1997) The Xanthophyll Cycle, Its Regulation And Components. Physiologia Plantarum 100: 806-816

Falbel TG, Staehelin LA, Adams WW (1994) Analysis Of Xanthophyll Cycle Carotenoids And Chlorophyll Fluorescence In Light Intensity-Dependent Chlorophyll-Deficient Mutants Of Wheat And Barley. Photosynthesis Research 42: 191-202

Farah J, Rappaport F, Choquet Y, Joliot P, Rochaix JD (1995) Isolation Of A Psaf-Deficient Mutant Of Chlamydomonas- Reinhardtii - Efficient Interaction Of Plastocyanin With The Photosystem-I Reaction-Center Is Mediated By The PsaF Subunit. Embo Journal 14: 4976-4984

Farber A, Young AJ, Ruban AV, Horton P, Jahns P (1997) Dynamics Of Xanthophyll-Cycle Activity In Different Antenna Subcomplexes In The Photosynthetic Membranes Of Higher Plants - The Relationship Between Zeaxanthin Conversion And Nonphotochemical Fluorescence Quenching. Plant Physiology 115: 1609-1618

Feng Y, Mccarty RE (1990) Chromatographic Purification Of The Chloroplast ATP Synthase (CF_0-CF_1) And The Role Of CF_0 Subunit-IV In Proton Conduction. Journal Of Biological Chemistry 265: 12474-12480

Frank HA, Bautista JA, Josue JS, Young AJ (2000) Mechanism Of Nonphotochemical Quenching In Green Plants: Energies Of The Lowest Excited Singlet States Of Violaxanthin And Zeaxanthin. Biochemistry 39: 2831-2837

Frank HA, Brudvig GW (2004) Redox Functions Of Carotenoids In Photosynthesis. Biochemistry 43: 8607-8615

Frank HA, Cua A, Chynwat V, Young A, Gosztola D, Wasielewski MR (1994) Photophysics Of The Carotenoids Associated With The Xanthophyll Cycle In Photosynthesis. Photosynthesis Research 41: 389-395

Funk C, Adamska I, Green B, Andersson B, Renger G (1995a) The Nuclear-Encoded Chlorophyll-Binding Photosystem-II-S Protein Is Stable In The Absence Of Pigments. Journal Of Biological Chemistry 270[50], 30141-30147. 1995a.

Funk C, Schroder W, Napiwotzki A, Tjus S, Renger G, Andersson B (1995b) The PSII-S Protein Of Higher-Plants - A New-Type Of Pigment-Binding Protein. Biochemistry 34[35], 11133-11141.

Funk C, Schroder W, Green BR, Renger G, Andersson B (1994) The Intrinsic 22 kDa Protein Is A Chlorophyll-Binding Subunit Of Photosystem-II. Febs Letters 342: 261-266

Fyfe PK, Jones MR (2000) Re-Emerging Structures: Continuing Crystallography Of The Bacterial Reaction Centre. Biochimica Et Biophysica Acta-Bioenergetics 1459: 413-421

Gau AE, Thole HH, Sokolenko A, Altschmied L, Herrmann RG, Pistorius EK (1998) PsbY, A Novel Manganese-Binding, Low-Molecular-Mass Protein Associated With Photosystem II. Molecular And General Genetics 260: 56-68

Ghanotakis DF, Tsiotis G, Bricker TM (1999) Polypeptides Of PSII: Structure And Function. In Concepts In Photobiology: Photosynthesis And Photomorphogenesis (Singhal GS, G Renger, Sopory SK, Irrgang KD, Govindjee, Eds). Narosa, New Delhi, 264-291

Ghanotakis DF, Yocum CF (1986) Characterization Of A Photosystem-II Reaction Center Complex Isolated By Exposure Of PSII Membranes To A Nonionic Detergent And High-Concentrations Of NaCl. Photosynthesis Research 10: 483-488

Giacometti G, Barbato R, Friso G, Frizzo A, Rigoni F (1992) Photosystem II Degradation Pathways After Photoinhibition Of Isolated Thylakoids. In Research In Photosynthesis (Murata N, Ed), Vol 4. Kluwer Academic Publishers, Dordrecht, 505-508

Gilmore AM, Bjorkman O (1994) Adenine-Nucleotides And The Xanthophyll Cycle In Leaves .1. Effects Of CO_2- And Temperature-Limited Photosynthesis On Adenylate Energy Charge And Violaxanthin De-Epoxidation. Planta 192: 526-536

Gilmore AM, Hazlett TL, Govindjee (1995) Xanthophyll Cycle-Dependent Quenching Of Photosystem-II Chlorophyll-a Fluorescence - Formation Of A Quenching Complex With A Short Fluorescence Lifetime. PNAS 92: 2273-2277

Gilmore AM, Shinkarev VP, Hazlett TL, Govindjee (1998) Quantitative Analysis Of The Effects Of Intrathylakoid pH And Xanathophyll Cycle Pigments On Chlorophyll a Fluorescence Lifetime Distributions And Intensity In Thylakoids. Biochemistry 37: 13582-13593

Gilmore AM, Yamamoto HY (1992) Dark Induction Of Zeaxanthin-Dependent Nonphotochemical Fluorescence Quenching Mediated By ATP. PNAS 89: 1899-1903

Giuffra E, Cugini D, Croce R, Bassi R (1996) Reconstitution And Pigment-Binding Properties Of Recombinant CP29. European Journal Of Biochemistry 238: 112-120

Gradinaru CC, Ozdemir S, Gulen D, Van Stokkum IHM, Van Grondelle R, Van Amerongen H (1998) The Flow Of Excitation Energy In LHCII Monomers: Implications For The Structural Model Of The Major Plant Antenna. Biophysical Journal 75: 3064-3077

Green BR, Durnford DG (1996) The Chlorophyll-Carotenoid Proteins Of Oxygenic Photosynthesis. Annual Review Of Plant Physiology And Plant Molecular Biology 47: 685-714

Green BR, Pichersky E (1994) Hypothesis For The Evolution Of 3-Helix Chl a/b And Chl a/c Light-Harvesting Antenna Proteins From 2-Helix And 4-Helix Ancestors. Photosynthesis Research 39: 149-162

Green BR, Pichersky E, Kloppstech K (1991) Chlorophyll-a/b-Binding Proteins - An Extended Family. Trends In Biochemical Sciences 16: 181-186

Grigorieff N, Ceska TA, Downing KH, Baldwin JM, Henderson R (1996) Electron-Crystallographic Refinement Of The Structure Of Bacteriorhodopsin. Journal Of Molecular Biology 259: 393-421

Gruszecki WI, Strzalka K (1991) Does The Xanthophyll Cycle Take Part In The Regulation Of Fluidity Of The Thylakoid Membrane. Biochimica Et Biophysica Acta 1060: 310-314

Haehnel W, Jansen T, Gause K, Klosgen RB, Stahl B, Michl D, Huvermann B, Karas M, Herrmann RG (1994) Electron-Transfer From Plastocyanin To Photosystem-I. Embo Journal 13: 1028-1038

Hager M, Biehler K, Illerhaus J, Ruf S, Bock R (1999) Targeted Inactivation Of The Smallest Plastid Genome-Encoded Open Reading Frame Reveals A Novel And Essential Subunit Of The Cytochrome *b6f* Complex. Embo Journal 18: 5834-5842

Haldrup A, Naver H, Scheller HV (1999) The Interaction Between Plastocyanin And Photosystem I Is Inefficient In Transgenic Arabidopsis Plants Lacking The PSI-N Subunit Of Photosystem I. Plant Journal 17: 689-698

Haldrup A, Simpson DJ, Scheller HV (2000) Down-Regulation Of The PSI-F Subunit Of Photosystem I (PSI) In Arabidopsis thaliana - The PSI-F Subunit Is Essential For Photoautotrophic Growth And Contributes To Antenna Function . Journal Of Biological Chemistry 275: 31211-31218

Hankamer B, Barber J, Boekema EJ (1997) Structure And Membrane Organization Of Photosystem II In Green Plants. Annual Review Of Plant Physiology And Plant Molecular Biology 48: 641-671

Hankamer B, Morris EP, Barber J (1999) Revealing The Structure Of The Oxygen-Evolving Core Dimer Of Photosystem II By Cryoelectron Crystallography. Nature Structural Biology 6: 560-564

Harrer R, Bassi R, Testi MG, Schafer C (1998) Nearest-Neighbor Analysis Of A Photosystem II Complex From Marchantia Polymorpha L. (Liverwort), Which Contains Reaction Center And Antenna Proteins. European Journal Of Biochemistry 255: 196-205

Havaux M, Gruszecki WI, Dupont I, Leblanc RM (1991) Increased Heat Emission And Its Relationship To The Xanthophyll Cycle In Pea Leaves Exposed To Strong Light Stress. Journal Of Photochemistry And Photobiology B-Biology 8: 361-370

Havaux M, Tardy F, Ravenel J, Chanu D, Parot P (1996) Thylakoid Membrane Stability To Heat Stress Studied By Flash Spectroscopic Measurements Of The Electrochromic Shift In Intact Potato Leaves: Influence Of The Xanthophyll Content. Plant Cell And Environment 19: 1359-1368

Henmi T, Yamasaki H, Sakuma S, Tomokawa Y, Tamura N, Shen MR, Yamamoto Y (2003) Dynamic Interaction Between The D1 Protein, CP43 And OEC33 At The Lumenal Side Of Photosystem II In Spinach Chloroplasts: Evidence From Light Induced Cross-Linking Of The Proteins In The Donor-Side Photoinhibition. Plant And Cell Physiology 44: 451-456

Henrysson T, Schroder WP, Spangfort M, Akerlund HE (1989) Isolation And Characterization Of The Chlorophyll-a/b Protein Complex CP29 From Spinach. Biochimica Et Biophysica Acta 977: 301-308

Hieber AD, Bugos RC, Yamamoto HY (2000) Plant Lipocalins: Violaxanthin De-Epoxidase And Zeaxanthin Epoxidase. Biochimica Et Biophysica Acta - Protein Structure And Molecular Enzymology 1482: 84-91

Hieber AD, Kawabata O, Yamamoto HY (2004) Significance Of The Lipid Phase In The Dynamics And Functions Of The Xanthophyll Cycle As Revealed By PsbS Overexpression In Tobacco And In-Vitro De-epoxidation In Monogalactosyldiacylglycerol Micelles. Plant And Cell Physiology 45: 92-102

Hobe S, Fey H, Rogl H, Paulsen H (2003) Determination Of Relative Chlorophyll Binding Affinities In The Major Light-Harvesting Chlorophyll a/b Complex. Journal Of Biological Chemistry 278: 5912-5919

Hobe S, Niemeier H, Bender A, Paulsen H (2000) Carotenoid Binding Sites In LHCIIb - Relative Affinities Towards Major Xanthophylls Of Higher Plants. European Journal Of Biochemistry 267: 616-624

Horton P, Hague A (1988) Studies On The Induction Of Chlorophyll Fluorescence In Isolated Barley Protoplasts .4. Resolution Of Non-Photochemical Quenching. Biochimica Et Biophysica Acta 932: 107-115

Horton P, Ruban A (1999) Regulation Of The Structure And Function Of The Light Harvesting Complexes Of Photosystem II By The Xanthophyll Cycle. The Photochemistry Of Carotenoids

Horton P, Ruban Av (1992) Regulation Of Photosystem-II. Photosynthesis Research 34: 375-385

Horton P, Ruban Av, Rees D, Pascal Aa, Noctor G, Young AJ (1991) Control Of The Light-Harvesting Function Of Chloroplast Membranes By Aggregation Of The LHCII Chlorophyll Protein Complex. Febs Letters 292: 1-4

Horton P, Ruban AV, Walters RG (1996) Regulation Of Light Harvesting In Green Plants. Annual Review Of Plant Physiology And Plant Molecular Biology 47: 655-684

Horton P, Ruban AV, Wentworth M (2000) Allosteric Regulation Of The Light-Harvesting System Of Photosystem II. Philosophical Transactions Of The Royal Society Of London Series B-Biological Sciences 355: 1361-1370

Huang D, Everly RM, Cheng RH, Heymann JB, Schagger H, Sled V, Ohnishi T, Baker TS, Cramer WA (1994) Characterization Of The Chloroplast Cytochrome-*b6f* Complex As A Structural And Functional Dimer. Biochemistry 33: 4401-4409

Hundal T, Virgin I, Styring S, Andersson B (1990) Changes In The Organization Of Photosystem-II Following Light- Induced D1-Protein Degradation. Biochimica Et Biophysica Acta 1017: 235-241

Ihalainen JA, Jensen PE, Haldrup A, Van Stokkum IHM, Van Grondelle R, Scheller HV, Dekker JP (2002) Pigment Organization And Energy Transfer Dynamics In Isolated Photosystem I (PSI) Complexes From Arabidopsis thaliana Depleted Of The PSI-G, PSI-K, PSI-L, Or PSI-N Subunit. Biophysical Journal 83: 2190-2201

Ishikawa Y, Nakatani E, Henmi T, Ferjani A, Harada Y, Tamura N, Yamamoto Y (1999) Turnover Of The Aggregates And Cross-Linked Products Of The D1 Protein Generated By Acceptor-Side Photoinhibition Of Photosystem II. Biochimica Et Biophysica Acta-Bioenergetics 1413: 147-158

Iwasaki T, Saito Y, Harada E, Kasai M, Shoji K, Miyao M, Yamamoto N (1997) Cloning Of Cdna Encoding The Rice 22 kDa Protein Of Photosystem II (PSII-S) And Analysis Of Light-Induced Expression Of The Gene. Gene 185: 223-229

Jansson S (1994) The Light-Harvesting Chlorophyll a/b Binding-Proteins. Biochimica Et Biophysica Acta-Bioenergetics 1184: 1-19

Jansson S (1999) A Guide To The LHC Genes And Their Relatives In Arabidopsis. Trends In Plant Science 4: 236-240

Jansson S, Andersen B, Scheller HV (1996) Nearest-Neighbor Analysis Of Higher-Plant Photosystem I Holocomplex. Plant Physiology 112: 409-420

Jegerschold C, Rutherford AW, Mattioli TA, Crimi M, Bassi R (2000) Calcium Binding To The Photosystem II Subunit CP29. Journal Of Biological Chemistry 275: 12781-12788

Jensen Pe, Rosgaard L, Knoetzel J, Scheller HV (2002) Photosystem I Activity Is Increased In The Absence Of The PSI-G Subunit. Journal Of Biological Chemistry 277: 2798-2803

Joet T, Genty B, Josse EM, Kuntz M, Cournac L, Peltier G (2002) Involvement Of A Plastid Terminal Oxidase In Plastoquinone Oxidation As Evidenced By Expression Of The Arabidopsis Thaliana Enzyme In Tobacco. Journal Of Biological Chemistry 277: 31623-31630

Johnson G, Krieger A (1994) Thermoluminescence As A Probe Of Photosystem-II In Intact Leaves - Nonphotochemical Fluorescence Quenching In Peas Grown In An Intermittent Light Regime. Photosynthesis Research 41: 371-379

Jordan P, Fromme P, Witt HT, Klukas O, Saenger W, Krauss N (2001) Three-Dimensional Structure Of Cyanobacterial Photosystem I At 2.5 Angstrom Resolution. Nature 411: 909-917

Josue JS, Frank HA (2002) Direct Determination Of The S1 Excited-State Energies Of Xanthophylls By Low-Temperature Fluorescence Spectroscopy. Journal Of Physical Chemistry A 106: 4815-4824

Kamiya N, Shen JR (2003) Crystal Structure Of Oxygen-Evolving Photosystem II From Thermosynechococcus Vulcanus At 3.7-Angstrom Resolution. PNAS 100: 98-103

Kim S, Pichersky E, Yocum CF (1994) Topological Studies Of Spinach 22 kDa Protein Of Photosystem II. Biochimica Et Biophysica Acta 1188: 339-348

Kim S, Sandusky P, Bowlby N, Aebersold R, Green B, Vlahakis S, Yocum C, Pichersky E (1992) Characterization Of A Spinach PsbS cDNA-Encoding The 22 kDa Protein Of Photosystem-II. Febs Letters 314: 67-71

Kim S, Pichersky E (2004) Psbs Sequence From Tobacco. Unpublished Work

Klukas O, Schubert WD, Jordan P, Krauss N, Fromme P, Witt HT, Saenger W (1999) Photosystem I, An Improved Model Of The Stromal Subunits PsaC, PsaD, And PsaE. Journal Of Biological Chemistry 274: 7351-7360

Kok B, Forbush B, Mcgloin M (1970) Cooperation Of Charges In Photosynthetic O_2 Evolution - I. A Linear Four Step Mechanism. Photochemistry And Photobiology 11: 457-475

Krause GH (1973) The High-Energy State Of The Thylakoid System Is Indicated By Chlorophyll Fluorescence And Chloroplast Shrinkage. Biochimica Et Biophysica Acta 292: 715-728

Krause GH, Briantais JM, Vernotte C (1981) Two Mechanisms Of Reversible Fluorescence Quenching In Chloroplasts. 5th International Congress On Photosynthesis 1, 575-585.

Krause GH, Laasch H, Weis E (1988) Regulation Of Thermal Dissipation Of Absorbed Light Energy In Chloroplasts Indicated By Energy-Dependent Fluorescence Quenching. Plant Physiology And Biochemistry 26: 445-452

Krause GH, Weis E (1991) Chlorophyll Fluorescence And Photosynthesis - The Basics. Annual Review Of Plant Physiology And Plant Molecular Biology 42: 313-349

Krauss N, Hinrichs W, Witt I, Fromme P, Pritzkow W, Dauter Z, Betzel C, Wilson KS, Witt HT, Saenger W (1993) 3-Dimensional Structure Of System-I Of Photosynthesis At 6 Angstrom Resolution. Nature 361: 326-331

Krauss N, Schubert WD, Klukas O, Fromme P, Witt HT, Saenger W (1996) Photosystem I At 4 Angstrom Resolution Represents The First Structural Model Of A Joint Photosynthetic Reaction Centre And Core Antenna, System. Nature Structural Biology 3: 965-973

Krieger A, Weis E (1993) The Role Of Calcium In The pH-Dependent Control Of Photosystem- II. Photosynthesis Research 37: 117-130

Kuhl H, Kruip J, Seidler A, Krieger-Liszkay A, Bunker M, Bald D, Scheidig AJ, Rogner M (2000) Towards Structural Determination Of The Water-Splitting Enzyme - Purification, Crystallization, And Preliminary Crystallographic Studies Of Photosystem II From A Thermophilic Cyanobacterium. Journal Of Biological Chemistry 275: 20652-20659

Kuhlbrandt W, Wang DN (1991) 3-Dimensional Structure Of Plant Light-Harvesting Complex Determined By Electron Crystallography. Nature 350: 130-134

Kuhlbrandt W, Wang DN, Fujiyoshi Y (1994) Atomic Model Of Plant Light-Harvesting Complex By Electron Crystallography. Nature 367: 614-621

Lee Cb, Rees D, Horton P (1990) Nonphotochemical Quenching Of Chlorophyll Fluorescence In The Green-Alga Dunaliella. Photosynthesis Research 24: 167-173

Lemaire C, Wollman FA (1989) The Chloroplast ATP Synthase In Chlamydomonas-Reinhardtii .1. Characterization Of Its 9 Constitutive Subunits. Journal Of Biological Chemistry 264: 10228-10234

Li XP, Gilmore AM, Niyogi KK (2002a) Molecular And Global Time-Resolved Analysis Of A PsbS Gene Dosage Effect On pH- And Xanthophyll Cycle-Dependent Nonphotochemical Quenching In Photosystem II. Journal Of Biological Chemistry 277: 33590-33597

Li XP, Phippard A, Pasari J, Niyogi KK (2002b) Structure-Function Analysis Of Photosystem II Subunit S (PsbS) In Vivo. Functional Plant Biology 29: 1131-1139

Li XP, Bjorkman O, Shih C, Grossman A, Rosenquist M, Jansson S, Niyogi K (2000) A Pigment-Binding Protein Essential For Regulation Of Photosynthetic Light Harvesting. Nature 403: 391-395

Lin ZF, Peng CL, Lin GZ, Zhang JL (2003) Alteration Of Components Of Chlorophyll-Protein Complexes And Distribution Of Excitation Energy Between The Two Photosystems In Two New Rice Chlorophyll b-Less Mutants. Photosynthetica 41: 589-595

Liu ZF, Yan HC, Wang KB, Kuang TY, Zhang JP, Gui LL, An XM, Chang WR (2004) Crystal Structure Of Spinach Major Light-Harvesting Complex At 2.72 Angstrom Resolution. Nature 428: 287-292

Ljungberg U, Akerlund HE, Andersson B (1986) Isolation And Characterization Of The 10-kDa And 22-kDa Polypeptides Of Higher-Plant Photosystem II. European Journal Of Biochemistry 158: 477-482

Lokstein H, Tian L, Polle Jew, Dellapenna D (2002) Xanthophyll Biosynthetic Mutants Of Arabidopsis Thaliana: Altered Nonphotochemical Quenching Of Chlorophyll Fluorescence Is Due To Changes In Photosystem II Antenna Size And Stability. Biochimica Et Biophysica Acta-Bioenergetics 1553: 309-319

Luecke H, Schobert B, Cartailler JP, Richter HT, Rosengarth A, Needleman R, Lanyi JK (2000) Coupling Photoisomerization Of Retinal To Directional Transport In Bacteriorhodopsin. Journal Of Molecular Biology 300: 1237-1255

Lunde C, Jensen PE, Haldrup A, Knoetzel J, Scheller HV (2000) The PSI-H Subunit Of Photosystem I Is Essential For State Transitions In Plant Photosynthesis. Nature 408: 613-615

Marin E, Nussaume L, Quesada A, Gonneau M, Sotta B, Hugueney P, Frey A, Marionpoll A (1996) Molecular Identification Of Zeaxanthin Epoxidase Of Nicotiana Plumbaginifolia, A Gene Involved In Abscisic Acid Biosynthesis And Corresponding To The ABA Locus Of Arabidopsis thaliana. Embo Journal 15: 2331-2342

Markwell JP, Thornber JP, Boggs RT (1979) Higher Plant Chloroplasts: Evidence That All The Chlorophyll Exists As Chlorophyll-Protein Complexes. PNAS 76: 1233-1235

Marr KM, Mastronarde DN, Lyon MK (1996) Two-Dimensional Crystals Of Photosystem II: Biochemical Characterization, Cryoelectron Microscopy And Localization Of The D1 And Cytochrome b_{559} Polypeptides. Journal Of Cell Biology 132: 823-833

Mauro S, Dainese P, Lannoye R, Bassi R (1997) Cold-Resistant And Cold-Sensitive Maize Lines Differ In The Phosphorylation Of The Photosystem II Subunit, CP29. Plant Physiology 115: 171-180

Mcluskey K, Prince SM, Cogdell RJ, Isaacs NW (2001) The Crystallographic Structure Of The B800-820 LH3 Light- Harvesting Complex From The Purple Bacteria Rhodopseudomonas Acidophila Strain 7050. Biochemistry 40: 8783-8789

Michel H, Deisenhofer J (1988) Relevance Of The Photosynthetic Reaction Center From Purple Bacteria To The Structure Of Photosystem-II. Biochemistry 27: 1-7

Montane MH, Kloppstech K (2000) The Family Of Light-Harvesting-Related Proteins (LHCs, ELIPs, HLIPs): Was The Harvesting Of Light Their Primary Function? Gene 258: 1-8

Morishige DT, Anandan S, Jaing JT, Thornber JP (1990) Amino-Terminal Sequence Of The 21 kDa Apoprotein Of A Minor Light-Harvesting Pigment-Protein Complex Of The Photosystem-II Antenna (LHCIId CP24). Febs Letters 264: 239-242

Morishige DT, Thornber JP (1992) Identification And Analysis Of A Barley cDNA Clone Encoding The 31-kDa LHCIIa (CP29) Apoprotein Of The Light-Harvesting Antenna Complex Of Photosystem-II. Plant Physiology 98: 238-245

Morosinotto T, Baronio R, Bassi R (2002) Dynamics Of Chromophore Binding To LHC Proteins In Vivo And In Vitro During Operation Of The Xanthophyll Cycle. Journal Of Biological Chemistry 277: 36913-36920

Mullineaux CW, Ruban AV, Horton P (1994) Prompt Heat Release Associated With ΔpH-Dependent Quenching In Spinach Thylakoid Membranes. Biochimica Et Biophysica Acta 1185: 123

Murata N, Sugahara K (1969) Control Of Excitation Transfer In Photosynthesis II. Light-Induced Decrease Of Chlorophyll *a* Fluorescence Related To Photophosphorylation System In Spinach Chloroplasts. Biochimica Et Biophysica Acta 182-192

Mustardy L, Garab G (2003) Granum Revisited. A Three-Dimensional Model - Where Things Fall Into Place. Trends In Plant Science 8: 117-122

Neubauer C, Yamamoto HY (1994) Membrane Barriers And Mehler-Peroxidase Reaction Limit The Ascorbate Available For Violaxanthin De-Epoxidase Activity In Intact Chloroplasts. Photosynthesis Research 39: 137-147

Nield J, Funk C, Barber J (2000) . Supermolecular Structure Of Photosystem II And Location Of The PsbS Protein. Philosophical Transactions Of The Royal Society Of London Series B-Biological Sciences 355[1402], 1337-1343.

Nield J, Kruse O, Ruprecht J, DA Fonseca P, Buchel C, Barber J (2000) Three-Dimensional Structure Of Chlamydomonas Reinhardtii And Synechococcus Elongatus Photosystem II Complexes Allows For Comparison Of Their Oxygen-Evolving Complex Organization. Journal Of Biological Chemistry 275: 27940-27946

Nilsson F, Andersson B, Jansson C (1990) Photosystem-II Characteristics Of A Constructed Synechocystis 6803 Mutant Lacking Synthesis Of The D1 Polypeptide. Plant Molecular Biology 14: 1051-1054

Nitschke W, Rutherford AW (1991) Photosynthetic Reaction Centers - Variations On A Common Structural Theme. Trends In Biochemical Sciences 16: 241-245

Niyogi KK, Bjorkman O, Grossman AR (1997a) Chlamydomonas Xanthophyll Cycle Mutants Identified By Video Imaging Of Chlorophyll Fluorescence Quenching. Plant Cell 9: 1369-1380

Niyogi KK, Bjorkman O, Grossman AR (1997b) The Roles Of Specific Xanthophylls In Photoprotection. PNAS 94: 14162-14167

Niyogi KK, Grossman AR, Bjorkman O (1998) Arabidopsis Mutants Define A Central Role For The Xanthophyll Cycle In The Regulation Of Photosynthetic Energy Conversion. Plant Cell 10: 1121-1134

Noctor G, Rees D, Young A, Horton P (1991) The Relationship Between Zeaxanthin, Energy-Dependent Quenching Of Chlorophyll Fluorescence, And Trans-Thylakoid pH Gradient In Isolated-Chloroplasts. Biochimica Et Biophysica Acta 1057: 320-330

Noctor G, Ruban AV, Horton P (1993) Modulation Of Delta-pH-Dependent Nonphotochemical Quenching Of Chlorophyll Fluorescence In Spinach-Chloroplasts. Biochimica Et Biophysica Acta 1183: 339-344

Noji H, Yasuda R, Yoshida M, Kinosita K (1997) Direct Observation Of The Rotation Of F-1-ATPase. Nature 386: 299-302

Norén H, Svensson P, Stefmark R, Funk C, Adamskal, Andersson B (2003) Expression Of The Early Light-Induced Protein But Not The PsbS Protein Is Influenced By Low Temperature And Depends On The Developmental Stage Of The Plant In Field-Grown Pea Cultivars. Plant Cell And Environment 26[2], 245-253.

NuβBerger S, Dörr K, Wang DN, Kühlbrandt W (1993) Lipid-Protein Interactions In Crystals Of Plant Light- Harvesting Complex. Journal Of Molecular Biology 234: 347-356

Ono T, Inoue Y (1984) Reconstitution Of Photosynthetic Oxygen Evolving Activity By Rebinding Of 33-kDa Protein To $CaCl_2$-Extracted PSII Particles. Febs Letters 166: 381-384

Owens TG (1984) Excitation Energy Transfer Between Chlorophylls And Carotenoids. A Proposed Molecular Mechanism For Non-Photochemical Quenching. In Photoinhibition Of Photosynthesis From Molecular Mechanisms To The Field. (Baker NR, Bowyer JR, Eds) Bios Scientific Publishers Ltd, Oxford, 95-107

Paolillo DJ (1970) The Three Dimensional Arrangement Of Intergranal Lamellae In Chloroplasts. Journal Of Cell Science 6: 243-255

Pascal A, Wacker U, Irrgang KD, Horton P, Renger G, Robert B (2000) Pigment Binding Site Properties Of Two Photosystem II Antenna Proteins - A Resonance Raman Investigation. Journal Of Biological Chemistry 275: 22031-22036

Paulsen H (1995) Chlorophyll a/b-Binding Proteins. Photochemistry And Photobiology 62: 367-382

Peltier G, Cournac L (2002) Chlororespiration. Annual Review Of Plant Biology 53: 523-550

Pesaresi P, Sandona D, Giuffra E, Bassi R (1997) A Single Point Mutation (E166q) Prevents Dicyclohexylcarbodiimide Binding To The Photosystem II Subunit CP29. Febs Letters 402: 151-156

Peter GF, Thornber JP (1991) Biochemical-Composition And Organization Of Higher-Plant Photosystem-II Light-Harvesting Pigment-Proteins. Journal Of Biological Chemistry 266: 16745-16754

Peterson RB, Havir EA (2003) Contrasting Modes Of Regulation Of PSII Light Utilization With Changing Irradiance In Normal And PsbS Mutant Leaves Of Arabidopsis Thaliana . Photosynthesis Research 75: 57-70

Pierre Y, Breyton C, Kramer D, Popot JL (1995) Purification And Characterization Of The Cytochrome *b6f* Complex From Chlamydomonas-Reinhardtii. Journal Of Biological Chemistry 270: 29342-29349

Pogson BJ, Niyogi KK, Bjorkman O, Dellapenna D (1998) Altered Xanthophyll Compositions Adversely Affect Chlorophyll Accumulation And Nonphotochemical Quenching In Arabidopsis Mutants. PNAS 95: 13324-13329

Polivka T, Herek JL, Zigmantas D, Akerlund HE, Sundstrom V (1999) Direct Observation Of The (Forbidden) S1 State In Carotenoids. PNAS 96: 4914-4917

Porra R, Thompson W, Kriedmann P (1989) Determination Of Accurate Extinction Coeffiecients And Simultaneous Equations For Assaying Chlorophylls a And b Extracted With Four Different Solvents: Verification Of The Concentration Of Chlorophyll Standards By Atomic Absorption Spectroscopy. Biochimica Et Biophysica Acta 975: 384-397

Quick WP, Horton P (1984) Studies On The Induction Of Chlorophyll Fluorescence In Barley Protoplasts .2. Resolution Of Fluorescence Quenching By Redox State And The Transthylakoid pH Gradient. Proceedings Of The Royal Society Of London Series B-Biological Sciences 220: 371-382

Rees D, Young A, Noctor G, Britton G, Horton P (1989) Enhancement Of The Delta-pH-Dependent Dissipation Of Excitation-Energy In Spinach-Chloroplasts By Light-Activation - Correlation With The Synthesis Of Zeaxanthin. Febs Letters 256: 85-90

Remelli R, Varotto C, Sandona D, Croce R, Bassi R (1999) Chlorophyll Binding To Monomeric Light-Harvesting Complex - A Mutation Analysis Of Chromophore-Binding Residues. Journal Of Biological Chemistry 274 : 33510-33521

Rhee KH, Morris EP, Zheleva D, Hankamer B, Kuhlbrandt W, Barber J (1997) Two-Dimensional Structure Of Plant Photosystem II At 8-Angstrom Resolution. Nature 389: 522-526

Rhee KH, Morriss EP, Barber J, Kuhlbrandt W (1998) Three-Dimensional Structure Of The Plant Photosystem II Reaction Centre At 8 Angstrom Resolution. Nature 396: 283-286

Richter ML, Patrie WJ, Mccarty RE (1984) Preparation Of The Epsilon-Subunit And Epsilon-Subunit- Deficient Chloroplast Coupling Factor-I In Reconstitutively Active Forms. Journal Of Biological Chemistry 259: 7371-7373

Rockholm DC, Yamamoto HY (1996) Violaxanthin De-Epoxidase - Purification Of A 43 kDa Lumenal Protein From Lettuce By Lipid-Affinity Precipitation With Monogalactosyldiacylglyceride. Plant Physiology 110: 697-703

Rogl H, Kuhlbrandt W (1999) Mutant Trimers Of Light-Harvesting Complex II Exhibit Altered Pigment Content And Spectroscopic Features. Biochemistry 38: 16214-16222

Ros F, Bassi R, Paulsen H (1998) Pigment-Binding Properties Of The Recombinant Photosystem II Subunit CP26 Reconstituted In Vitro. European Journal Of Biochemistry 253: 653-658

Rousseau F, Setif P, Lagoutte B (1993) Evidence For The Involvement Of PSI-E Subunit In The Reduction Of Ferredoxin By Photosystem-I. Embo Journal 12: 1755-1765

Ruban AV, Horton P (1992) Mechanism Of Delta-pH-Dependent Dissipation Of Absorbed Excitation-Energy By Photosynthetic Membranes .1. Spectroscopic Analysis Of Isolated Light-Harvesting Complexes. Biochimica Et Biophysica Acta 1102: 30-38

Ruban AV, Horton P (1994) Spectroscopy Of Nonphotochemical And Photochemical Quenching Of Chlorophyll Fluorescence In Leaves - Evidence For A Role Of The Light-Harvesting Complex Of Photosystem-II In The Regulation Of Energy-Dissipation. Photosynthesis Research 40: 181-190

Ruban AV, Horton P (1995) Regulation Of Nonphotochemical Quenching Of Chlorophyll Fluorescence In Plants. Australian Journal Of Plant Physiology 22: 221-230

Ruban AV, Horton P (1999) The Xanthophyll Cycle Modulates The Kinetics Of Nonphotochemical Energy Dissipation In Isolated Light- Harvesting Complexes, Intact Chloroplasts, And Leaves Of Spinach. Plant Physiology 119: 531-542

Ruban AV, Horton P, Young AJ (1993a) Aggregation Of Higher-Plant Xanthophylls - Differences In Absorption-Spectra And In The Dependency On Solvent Polarity. Journal Of Photochemistry And Photobiology B-Biology 21: 229-234

Ruban AV, Lee PJ, Wentworth M, Young AJ, Horton P (1999) Determination Of The Stoichiometry And Strength Of Binding Of Xanthophylls To The Photosystem II Light Harvesting Complexes. Journal Of Biological Chemistry 274: 10458-10465

Ruban AV, Pascal AA, Robert B (2000) Xanthophylls Of The Major Photosynthetic Light-Harvesting Complex Of Plants: Identification, Conformation And Dynamics. Febs Letters 477: 181-185

Ruban AV, Pascal AA, Robert B, Horton P (2001a) Configuration And Dynamics Of Xanthophylls In Light-Harvesting Antennae Of Higher Plants - Spectroscopic Analysis Of Isolated Light-Harvesting Complex Of Photosystem II And Thylakoid Membranes. Journal Of Biological Chemistry 276: 24862-24870

Ruban AV, Pascal AA, Robert B, Horton P (2002) Activation Of Zeaxanthin Is An Obligatory Event In The Regulation Of Photosynthetic Light Harvesting. Journal Of Biological Chemistry 277: 7785-7789

Ruban AV, Pesaresi P, Wacker U, Irrgang KDJ, Bassi R, Horton P (1998a) The Relationship Between The Binding Of Dicyclohexylcarbodiimide And Quenching Of Chlorophyll Fluorescence In The Light-Harvesting Proteins Of Photosystem II. Biochemistry 37: 11586-11591

Ruban AV, Phillip D, Young AJ, Horton P (1997) Carotenoid-Dependent Oligomerization Of The Major Chlorophyll a/b Light Harvesting Complex Of Photosystem II Of Plants. Biochemistry 36: 7855-7859

Ruban AV, Phillip D, Young AJ, Horton P (1998b) Excited-State Energy Level Does Not Determine The Differential Effect Of Violaxanthin And Zeaxanthin On Chlorophyll Fluorescence Quenching In The Isolated Light-Harvesting Complex Of Photosystem II. Photochemistry And Photobiology 68: 829-834

Ruban AV, Rees D, Pascal AA, Horton P (1992a) Mechanism Of Delta-pH-Dependent Dissipation Of Absorbed Excitation-Energy By Photosynthetic Membranes .2. The Relationship Between LHCII Aggregation Invitro And qE In Isolated Thylakoids. Biochimica Et Biophysica Acta 1102: 39-44

Ruban AV, Walters RG, Horton P (1992b) The Molecular Mechanism Of The Control Of Excitation-Energy Dissipation In Chloroplast Membranes - Inhibition Of Delta-pH-Dependent Quenching Of Chlorophyll Fluorescence By Dicyclohexylcarbodiimide. Febs Letters 309: 175-179

Ruban AV, Wentworth M, Horton P (2001b) Kinetic Analysis Of Nonphotochemical Quenching Of Chlorophyll Fluorescence. 1. Isolated Chloroplasts. Biochemistry 40: 9896-9901

Ruban AV, Young AJ, Horton P (1993b) Induction Of Nonphotochemical Energy-Dissipation And Absorbency Changes In Leaves - Evidence For Changes In The State Of The Light-Harvesting System Of Photosystem-II In-Vivo. Plant Physiology 102: 741-750

Ruban AV, Young AJ, Horton P (1994a) Modulation Of Chlorophyll Fluorescence Quenching In Isolated Light Harvesting Complexes Of Photosystem II. Biochimica Et Biophysica Acta 1186 : 123-127

Ruban AV, Young AJ, Horton P (1996) Dynamic Properties Of The Minor Chlorophyll a/b Binding Proteins Of Photosystem II, An In Vitro Model For Photoprotective Energy Dissipation In The Photosynthetic Membrane Of Green Plants. Biochemistry 35: 674-678

Ruban AV, Young AJ, Pascal AA, Horton P (1994b) The Effects Of Illumination On The Xanthophyll Composition Of The Photosystem-II Light-Harvesting Complexes Of Spinach Thylakoid Membranes. Plant Physiology 104: 227-234

Ruffle S, Hutchison R, Sayer RT (1998) In Phtotsynthesis: Mechanisms And Effects. (Garab G, Ed) Kluwer Academic, Dordrecht, 1013-1016

Sabbert D, Engelbrecht S, Junge W (1996) Intersubunit Rotation In Active F-ATPase. Nature 381: 623-625

Salter AH, Virgin I, Hagman A, Andersson B (1992) On The Molecular Mechanism Of Light-Induced D1-Protein Degradation In Photosystem-II Core Particles. Biochemistry 31: 3990-3998

Sandona D, Croce R, Pagano A, Crimi M, Bassi R (1998) Higher Plants Light Harvesting Proteins. Structure And Function As Revealed By Mutation Analysis Of Either Protein Or Chromophore Moieties. Biochimica Et Biophysica Acta-Bioenergetics 1365: 207-214

Sanz C, Marquez M, Peralvarez A, Elouatik S, Sepulcre F, Querol E, Lazarova T, Padros E (2001) Contribution Of Extracellular Glu Residues To The Structure And Function Of Bacteriorhodopsin - Presence Of Specific Cation- Binding Sites. Journal Of Biological Chemistry 276: 40788-40794

Sayre RT, Wrobelboerner Ea (1994) Molecular Topology Of The Photosystem-II Chlorophyll-Alpha Binding-Protein, CP43 - Topology Of A Thylakoid Membrane- Protein. Photosynthesis Research 40: 11-19

Scheller HV (1996) In Vitro Cyclic Electron Transport In Barley Thylakoids Follows Two Independent Pathways. Plant Physiology 110: 187-194

Scheller HV, Jensen PE, Haldrup A, Lunde C, Knoetzel J (2001) Role Of Subunits In Eukaryotic Photosystem I. Biochimica Et Biophysica Acta-Bioenergetics 1507: 41-60

Scheller HV, Moller BL (1990) Photosystem-I Polypeptides. Physiologia Plantarum 78: 484-494

Schelvis JPM, Vannoort PI, Aartsma TJ, Vangorkom HJ (1994) Energy-Transfer, Charge Separation And Pigment Arrangement In The Reaction-Center Of Photosystem-II. Biochimica Et Biophysica Acta-Bioenergetics 1184: 242-250

Schubert WD, Klukas O, Saenger W, Witt HT, Fromme P, Krauss N (1998) A Common Ancestor For Oxygenic And Anoxygenic Photosynthetic Systems: A Comparison Based On The Structural Model Of Photosystem I. Journal Of Molecular Biology 280: 297-314

Seidler A (1996) Intermolecular And Intramolecular Interactions Of The 33-kDa Protein In Photosystem II. European Journal Of Biochemistry 242: 485-490

Shen JR, Kamiya N (2000) Crystallization And The Crystal Properties Of The Oxygen-Evolving Photosystem II From Synechococcus Vulcanus. Biochemistry 39: 14739-14744

Shi LX, Kim SJ, Marchant A, Robinson C, Schroder WP (1999) Characterisation Of The PsbX Protein From Photosystem II And Light Regulation Of Its Gene Expression In Higher Plants. Plant Molecular Biology 40: 737-744

Shi LX, Lorkovic ZJ, Oelmuller R, Schroder WP (2000) The Low Molecular Mass PsbW Protein Is Involved In The Stabilization Of The Dimeric Photosystem II Complex In Arabidopsis thaliana. Journal Of Biological Chemistry 275: 37945-37950

Siefermann D, Yamamoto HY (1975) Properties Of NADPH And Oxygen-Dependent Zeaxanthin Epoxidation In Isolated Chloroplasts. A Transmembrane Model For The Violaxanthin Cycle. Archives Of Biochemistry And Biophysics 171: 70-77

Snyder AM, Clark BM, Robert B, Ruban AV, Bungard RA (2004) Carotenoid Specificity Of Light-Harvesting Complex II Binding Sites - Occurrence Of 9-Cis-Violaxanthin In The Neoxanthin- Binding Site In The Parasitic Angiosperm Cuscuta Reflexa. Journal Of Biological Chemistry 279: 5162-5168

Snyder S, Kohorn BD (1999) Taks, Thylakoid Membrane Protein Kinases Associated With Energy Transduction. Journal Of Biological Chemistry 274: 9137-9140

Snyder S, Kohorn BD (2001) Disruption Of Thylakoid-Associated Kinase 1 Leads To Alteration Of Light Harvesting In Arabidopsis. Journal Of Biological Chemistry 276: 32169-32176

Svensson B, Etchebest C, Tuffery P, Vankan P, Smith J, Styring S (1996) A Model For The Photosystem II Reaction Center Core Including The Structure Of The Primary Donor P-680. Biochemistry 35: 14486-14502

Takeguchi CA, Yamamoto HY (1968) Light-Induced $^{18}O_2$ Uptake By Xanthophylls In New Zealand Spinach Leaves (*Tetragonia Expansa*). Biochimica Et Biophysica Acta 153: 459-465

Testi MG, Croce R, Polverinodelaureto P, Bassi R (1996) A CK2 Site Is Reversibly Phosphorylated In The Photosystem II Subunit CP29. Febs Letters 399: 245-250

Thompson SJ, Robinson C, Mant A (1999) Dual Signal Peptides Mediate The Signal Recognition Particle Sec-Independent Insertion Of A Thylakoid Membrane Polyprotein, PsbY. Journal Of Biological Chemistry 274: 4059-4066

Thornber JP (1975) Chlorophyll-Proteins: Light-Harvestin And Reaction Centre Components Of Plants. Annual Review Of Plant Physiology And Plant Molecular Biology 26: 127-158

Thornber JP, Peter GF, Morishige DT, Gomez S, Anandan S, Welty BA, Lee A, Kerfeld C, Takeuchi T, Preiss S (1993) Light Harvesting In Photosystem-I And Photosystem-II. Biochemical Society Transactions 21: 15-18

Tomo T, Enami I, Satoh K (1993) Orientation And Nearest-Neighbor Analysis Of PsbI Gene-Product In The Photosystem-II Reaction Center Complex Using Bifunctional Cross-Linkers. Febs Letters 323: 15-18

Varotto C, Pesaresi P, Jahns P, Lessnick A, Tizzano M, Schiavon F, Salamini F, Leister D (2002) Single And Double Knockouts Of The Genes For Photosystem I Subunits G, K, And H Of Arabidopsis. Effects On Photosystem I Composition, Photosynthetic Electron Flow, And State Transitions. Plant Physiology 129: 616-624

Varotto C, Pesaresi P, Meurer J, Oelmuller R, Steiner-Lange S, Salamini F, Leister D (2000) Disruption Of The Arabidopsis Photosystem I Gene PsaE Affects Photosynthesis And Impairs Growth. Plant Journal 22: 115-124

Verhoeven AS, Adams WW, Demmig-Adams B, Croce R, Bassi R (1999) Xanthophyll Cycle Pigment Localization And Dynamics During Exposure To Low Temperatures And Light Stress In Vinca Major. Plant Physiology 120: 727-737

Vermaas WFJ, Williams JGK, Arntzen CJ (1987) Sequencing And Modification Of PsbB, The Gene Encoding The CP47 Protein Of Photosystem-II, In The Cyanobacterium Synechocystis-6803. Plant Molecular Biology 8: 317-326

Wallbraun M, Kim SY, Green BR, Piechulla B, Pichersky E (1994) Nucleotide-Sequence Of A Tomato PsbS Gene. Plant Physiology 106: 1703-1704

Walters RG, Horton P (1991) Resolution Of Components Of Nonphotochemical Chlorophyll Fluorescence Quenching In Barley Leaves. Photosynthesis Research 27: 121-133

Walters RG, Ruban AV, Horton P (1994) Higher-Plant Light-Harvesting Complexes LHCIIa And LHCIIc Are Bound By Dicyclohexylcarbodiimide During Inhibition Of Energy-Dissipation. European Journal Of Biochemistry 226: 1063-1069

Walters RG, Ruban AV, Horton P (1996) Identification Of Proton-Active Residues In A Higher Plant Light-Harvesting Complex. PNAS 93: 14204-14209

Weber N, Strotmann H (1993) On The Function Of Subunit-PsaE In Chloroplast Photosystem-I. Biochimica Et Biophysica Acta 1143: 204-210

Weber P, Fulgosi H, Sokolenko A, Karnauchov I, Andersson B, Ohad I, Herrmann RG (1998) Evidence For Four Thylakoid-Located Kinases (Garab G, Ed). Kluwer Academic Publishers, Netherlands, 1883-1886

Wedel N, Klein R, Ljungberg U, Andersson B, Herrmann R (1992) The Single-Copy Gene Psbs Codes For A Phylogenetically Intriguing 22 kDa Polypeptide Of Photosystem-II. Febs Letters 314: 61-66

Weier TE (1963) The Grana As Structural Units In Chloroplasts Of Mesophyll Of *Nicotiana Rustica* And *Phaseolus Vulgaris*. Journal Of Ultrastructure Research 8: 122-143

Weis E, Berry JA (1987) Quantum Efficiency Of Photosystem-II In Relation To Energy-Dependent Quenching Of Chlorophyll Fluorescence. Biochimica Et Biophysica Acta 894: 198-208

Wentworth M, Ruban AV, Horton P (2000) Chlorophyll Fluorescence Quenching In Isolated Light Harvesting Complexes Induced By Zeaxanthin. Febs Letters 471: 71-74

Wentworth M, Ruban AV, Horton P (2001) Kinetic Analysis Of Nonphotochemical Quenching Of Chlorophyll Fluorescence. 2. Isolated Light-Harvesting Complexes. Biochemistry 40: 9902-9908

Whitmarsh J, Pakrasi HB (1996) Form And Function Of Cytochrome b_{559}. In Oxygenic Photosynthesis The Light Reactions (Ort Dr, Yocum Cf, Eds) Vol 4. Kluwer, Dordrecht, 249-264

Widger WR, Cramer WA, Herrmann RG, Trebst A (1984) Sequence Homology And Structural Similarity Between Cytochrome- b Of Mitochondrial Complex-II And The Chloroplast-*b6f* Complex - Position Of The Cytochrome-b Hemes In The Membrane. PNAS 81: 674-678

Wraight CA, Crofts AR (1970) Energy-Dependent Quenching Of Chlorophyll *a* Fluorescence In Isolated Chloroplasts. European Journal Of Biochemistry 17: 319-327

Xiao JP, Mccarty RE (1989) Binding Of Chloroplast Coupling Factor-I Deficient In The Delta-Subunit To Thylakoid Membranes. Biochimica Et Biophysica Acta 976: 203-209

Xiong J, Subramaniam S, Govindjee (1998) A Knowledge-Based Three Dimensional Model Of The Photosystem II Reaction Center Of Chlamydomonas Reinhardtii. Photosynthesis Research 56: 229-254

Yakushevska AE, Jensen PE, Keegstra W, Van Roon H, Scheller Hv, Boekema EJ, Dekker JP (2001) Supermolecular Organization Of Photosystem II And Its Associated Light-Harvesting Antenna In Arabidopsis thaliana. European Journal Of Biochemistry 268: 6020-6028

Yakushevska AE, Keegstra W, Boekema EJ, Dekker JP, Andersson J, Jansson S, Ruban AV, Horton P (2003) The Structure Of Photosystem II In Arabidopsis: Localization Of The CP26 And CP29 Antenna Complexes. Biochemistry 42: 608-613

Yamamoto HY, Bugos RC, Hieber AD (1999) Biochemistry And Molecular Biology Of The Xanthophyll Cycle. In The Photochemistry Of Carotenoids (Frank HA, Young AJ, Cogdell RJ, Eds) Vol 8. Kluwer, Dordrecht, 271-291

Yamamoto HY, Nakayama TOM, Chichester CO (1962) Studies On The Light And Dark Interconversions Of Leaf Xanthophylls. Archives Of Biochemistry And Biophysics 97: 168-173

Yang CH, Kosemund K, Cornet C, Paulsen H (1999) Exchange Of Pigment-Binding Amino Acids In Light-Harvesting Chlorophyll a/b Protein. Biochemistry 38: 16205-16213

Yruela I, Miota F, Torrado E, Seibert M, Picorel R (2003) Cytochrome b_{559} Content In Isolated Photosystem II Reaction Center Preparations. European Journal Of Biochemistry 270: 2268-2273

Zech SG, Kurreck J, Eckert HJ, Renger G, Lubitz W, Bittl R (1997) Pulsed EPR Measurement Of The Distance Between P-680(+Center Dot) And Q(A)(-Center Dot) In Photosystem II. Febs Letters 414: 454-456

Zhang HM, Huang DR, Cramer WA (1999) Stoichiometrically Bound Beta-Carotene In The Cytochrome b_6f Complex Of Oxygenic Photosynthesis Protects Against Oxygen Damage. Journal Of Biological Chemistry 274: 1581-1587

Zouni A, Witt HT, Kern J, Fromme P, Krauss N, Saenger W, Orth P (2001) Crystal Structure Of Photosystem II From Synechococcus Elongatus At 3.8 Angstrom Resolution. Nature 409: 739-743

Zsila F, Bikadi Z, and Simonyi M (2002) Tetrahedron: Assymetry 13: 273-283

Appendix

Publications

In vitro reconstitution of the activated zeaxanthin state associated with energy dissipation in plants

Mark Aspinall-O'Dea*, Mark Wentworth*, Andy Pascal†, Bruno Robert†, Alexander Ruban*‡, and Peter Horton*§

*Robert Hill Institute, Department of Molecular Biology and Biotechnology, University of Sheffield, Western Bank, Sheffield S10 2TN, United Kingdom; †Service de Biophysique des Fonctions Membranaires, Département de Biologie Joliot Curie (DBJC)/Commissariat à l'Energie Atomique (CEA) and Unité de Recherche Associée 2096/Centre National de la Recherche Scientifique, CEA-Saclay, 91191, Gif-sur-Yvette Cedex 06, France; and ‡Departement de Biologie, Unité Mixte de Recherche 8543, Ecole Normale Superieure, 45 Rue d'Ulm, 75230, Paris Cedex 05, France

Edited by Charles J. Arntzen, Arizona State University, Tempe, AZ, and approved October 23, 2002 (received for review August 20, 2002)

Dissipation of excess light energy in plant photosynthetic membranes plays an important role in the response of plants to the environment, providing short-term balancing between the intensity of sunlight and photosynthetic capacity. The carotenoid zeaxanthin and the photosystem II subunit PsbS play vital roles in this process, but the mechanism of their action is largely unexplained. Here we report that the isolated photosystem II subunit PsbS was able to bind exogenous zeaxanthin, the binding resulting in a strong red shift in the absorption spectrum, and the appearance of characteristic features in the resonance Raman spectrum and a distinct circular dichroism spectrum, indicating pigment–protein, as well as specific pigment–pigment, interaction. A strong shift in the absorption spectrum of PsbS phenylalanine residues after zeaxanthin binding was observed. It is concluded that zeaxanthin binding to PsbS is the origin of the well known energy dissipation-related 535-nm absorption change that we showed *in vivo* to arise from activation of 1–2 molecules of this pigment. The altered properties of zeaxanthin and PsbS that result from this interaction provide the first direct indication about how they regulate energy dissipation.

Plants possess a variety of features that enable them to adjust to changes in the intensity of light encountered under natural conditions (1, 2). These features serve not only to optimize photosynthesis but to provide protection from the damaging effects of absorbed radiation. Dissipation of excess excitation absorbed by the light-harvesting antenna of plant photosystem II (PSII) provides a dynamic response to short-term changes in light intensity (3, 4). It has been shown to be an important regulatory mechanism that impacts plant fitness (5). Energy dissipation is detected as the nonphotochemical quenching of chlorophyll fluorescence (qE) and is regulated by the transthylakoid pH gradient (ΔpH) and the xanthophyll cycle, the reversible deepoxidation of violaxanthin into zeaxanthin (3, 4, 6). Zeaxanthin accumulates under conditions of excess light because of the activation of violaxanthin deepoxidase by ΔpH generated under these conditions (6). In order for zeaxanthin to carry out its role in qE, it is bound to one or more of the proteins that constitute the LHCII (light-harvesting complexes of PSII)–PSII macromolecular complex (7, 8). This binding, which has the characteristics of an allosteric regulator of qE (9, 10), depends on or is stimulated by the increase in thylakoid ΔpH (11). Formation of qE is correlated with an absorption change, wavelength maximum $\approx$535 nm (12, 13), which we showed recently to be caused by an unusually large red shift in the absorption spectrum of one to two molecules of zeaxanthin to $\approx$525 nm (14). This absorption change was considered to arise from binding to the specific site in PSII involved in regulating qE, which was suggested to be on the PsbS subunit. PsbS has an obligatory role in qE (15), and it therefore has been suggested to be the site at which protons and/or zeaxanthin bind. To date, however, the evidence that PsbS can bind any pigments is still controversial (16, 17); there is certainly no evidence that PsbS can bind zeaxanthin, and therefore the identity of this key binding site of zeaxanthin is unknown.

One obstacle to the elucidation of the role of PsbS is its extreme hydrophobicity, which leads to problems of aggregation when isolated by using established methods of fractionation of thylakoid membranes (17). Here we describe a rapid procedure for preparing PsbS from spinach PSII membranes that yields a pure, soluble protein, amenable to the study of pigment binding *in vitro*. It was found that the PsbS preparation, when mixed with zeaxanthin, was able to bind this pigment. Moreover, after interaction with PsbS, zeaxanthin showed a strong red shift in its absorption spectrum and the appearance of a characteristic resonance Raman (RR) spectrum almost identical to those observed after qE formation *in vivo*. Hence, the activated state that gives rise to the 535-nm change, and which is a key event in the dissipation of excitation energy in plants, has been reconstituted *in vitro*.

Methods

PSII membrane fragments were prepared from spinach thylakoid membranes essentially as described (18). For PsbS preparation, the PSII membrane fragments (2 mg of total chlorophyll) were extracted with 1% *n*-dodecyl β-D-maltoside (DM), incubated on ice for 50 min, stirred occasionally, and centrifuged at 10,000 $\times$ *g* for 20 min. The pellet was extracted with 0.5% sodium cholate (Sigma), pH 7.0/250 mM NaCl (19), incubated in the dark on ice with vigorous stirring for 5 min, and centrifuged at 10,000 $\times$ *g* for 10 min. The supernatant was passed through a Sephadex G-25 column, and eluted fractions containing PsbS were stored in a solution of elution buffer (25 mM Hepes, pH 8.0/0.01% DM). The protein concentration was determined from the absorption spectra of the sample by using the OD of phenylalanine at 275 nm and taking into account the phenylalanine-to-protein ratio in PsbS. Protein samples were solubilized and separated by 15% denaturing SDS/PAGE using standard procedures (20). Proteins were transferred to a poly(vinylidene difluoride) membrane (Hybond-P, Amersham Pharmacia) in a Mini Trans-Blot transfer cell (Bio-Rad) at 30 mA for 12 h. Membranes were probed with an antibody raised in rabbit against a 12-aa synthetic peptide (GDRGRFVDEPTT) that was completely specific to spinach PsbS. The primary antibody was detected by using a horseradish peroxidase-labeled secondary antibody using an ECL Plus kit (Amersham Pharmacia). Chemiluminescence was detected on Hyperfilm ECL (Amersham Pharmacia) photographic film and developed for 20 min. Zeaxanthin was purified from orange peppers and dried onto the surface of a glass tube under a stream of N_2. Binding of zeaxanthin to PsbS was achieved by adding 1 ml of 9 μM PsbS solution to a glass tube containing 14 nmol of dried zeaxanthin and mixing for 30 s with sonication in an ultrasonic bath.

This paper was submitted directly (Track II) to the PNAS office.

Abbreviations: PSII, photosystem II; ΔpH, transthylakoid proton gradient; qE, nonphotochemical quenching dependent on ΔpH;LHCII, light-harvesting complexes of PSII; RR, resonance Raman; DM, *n*-dodecyl β-D-maltoside; CD, circular dichroism.

§To whom correspondence should be addressed. E-mail: p.horton@shef.ac.uk.

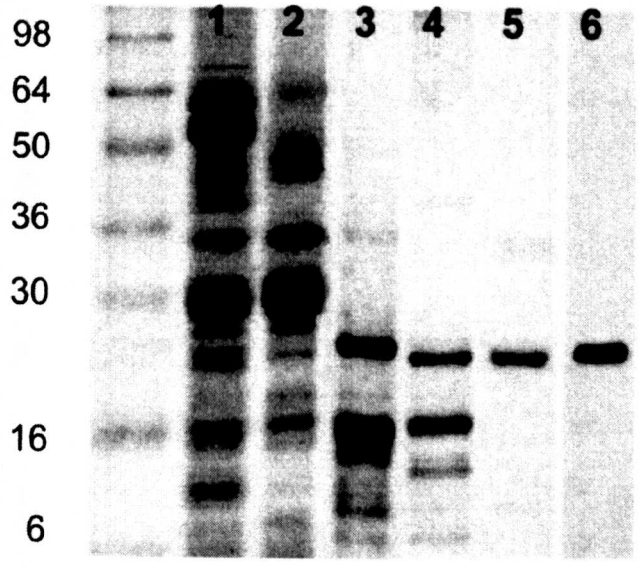

Fig. 1. Purification of PsbS. Silver-stained SDS polyacrylamide gel showing spinach thylakoids (lane 1), PSII membrane fragments (lane 2), pellet after extraction with DM (lane 3), supernatant after extraction with cholate (lane 4), and after passing down a Sephadex G-25 column (lane 5). A Western blot of lane 5 with anti-PsbS antibody is shown in lane 6. Molecular weight markers (See Blue, Invitrogen) are shown in the far-left lane.

Sucrose-gradient centrifugation was carried out as described with a DM concentration of 0.3% (8). Absorption spectra were recorded by using a Cary 500 spectrophotometer at room temperature. Circular dichroism (CD) spectra were obtained by using a Jasco J810 spectropolarimeter. RR spectra were recorded as described (14).

Results

Extraction of PSII membrane fragments (Fig. 1, lane 2) with DM leaves a pellet enriched in a protein that has an apparent molecular mass of 22 kDa (lane 3). Treatment of this sample with cholate, shown to be useful for extracting PsbS (19), brings about solubilization of many of the proteins in the DM pellet, with some apparent enrichment of this 22-kDa protein (lane 4). This cholate extract was passed through a Sephadex G-25 column, yielding a sample that was assessed to be 90% pure in this protein from observation of the silver-stained gel (lane 5). The protein reacts with an antibody raised against a PsbS peptide (lane 6) that does not crossreact with any other PSII protein. We conclude that this represents a highly purified preparation of PsbS. The absorption spectrum of this PsbS preparation shows that it contained no bound pigment; if the absorption spectrum shown in Fig. 2*A* is extended into the visible region, there is no recorded absorption from either carotenoid or chlorophyll. In contrast, a sample of LHCII at the same protein concentration would give an OD of ≈20 in the red region of the spectrum.

Spectroscopic analysis was used to further establish the purity of the PsbS preparation. The published amino acid sequence of spinach PsbS indicates the presence of 17 phenylalanines and 1 tyrosine (21, 22). By using the extinction coefficients at 257 and 274 nm of 0.19×10^5 and 1.25×10^5 $M^{-1} \cdot m^{-1}$, respectively, a theoretical absorption ratio of phenylalanine to tyrosine of 2.5 is predicted. The absorption spectrum of the PsbS preparation was deconvoluted to show the contributions from phenylalanine and tyrosine (Fig. 2*A*), and these data gave a phenylalanine/tyrosine ratio of 2.0. A very minor contribution from tryptophan (not present in the PsbS sequence) at 288 nm is evident, but given

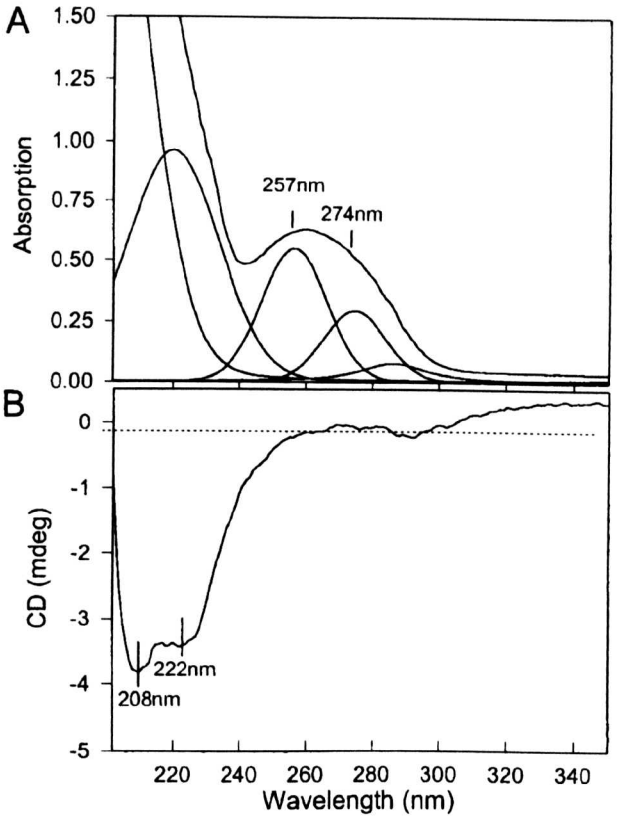

Fig. 2. Absorption (*A*) and CD (*B*) spectra of the preparation of purified PsbS. The absorption spectrum was deconvoluted, revealing the bands at 257 and 274 nm arising from phenylalanine and tyrosine, respectively.

the large extinction coefficient of this amino acid, the level of contamination by other proteins would appear to be minimal. The CD spectrum of the PsbS preparation shows the presence of a secondary α-helical structure with characteristic minima at 208 and 222 nm (Fig. 2*B*), providing evidence that the protein was not denatured and suggesting that it had been isolated in a native form.

We tested whether purified PsbS would bind zeaxanthin. For this, zeaxanthin deposited as a dry film on the surface of a glass tube was washed with a solution of PsbS. (This procedure was found to be more satisfactory than mixing zeaxanthin dissolved in ethanol with the PsbS preparation, although qualitatively similar results were obtained with both methods.) The mixture then was analyzed by sucrose-gradient centrifugation, and it was found that 60% of the zeaxanthin was located in the PsbS-containing band at ≈0.3 M sucrose. Very little free carotenoid was detected. It was concluded that PsbS was able to bind zeaxanthin to form a PsbS–zeaxanthin complex. We estimated the molar ratio of zeaxanthin/PsbS to be ≈2:1 in this complex.

Zeaxanthin dissolved in ethanol has a characteristic absorption spectrum with maxima at 482, 454, and 428 nm (Fig. 3*A*, trace 1). The positions of these maxima can be shifted depending on the polarity of the solvent, the 0–0 transition at 482 nm in ethanol shifting to 511 nm in CS_2 (14). When zeaxanthin and PsbS are mixed, the absorption spectrum of zeaxanthin was altered dramatically; there was a strong red shift, with the 0–0 absorption maximum position appearing at ≈523 nm (Fig. 3*B*, trace 1). The derivative spectrum shows maxima at 525, 487, and 450 nm, with evidence of a secondary band at ≈536 nm (Fig. 3*B*, trace 2). It should be noted that mixing of zeaxanthin with the

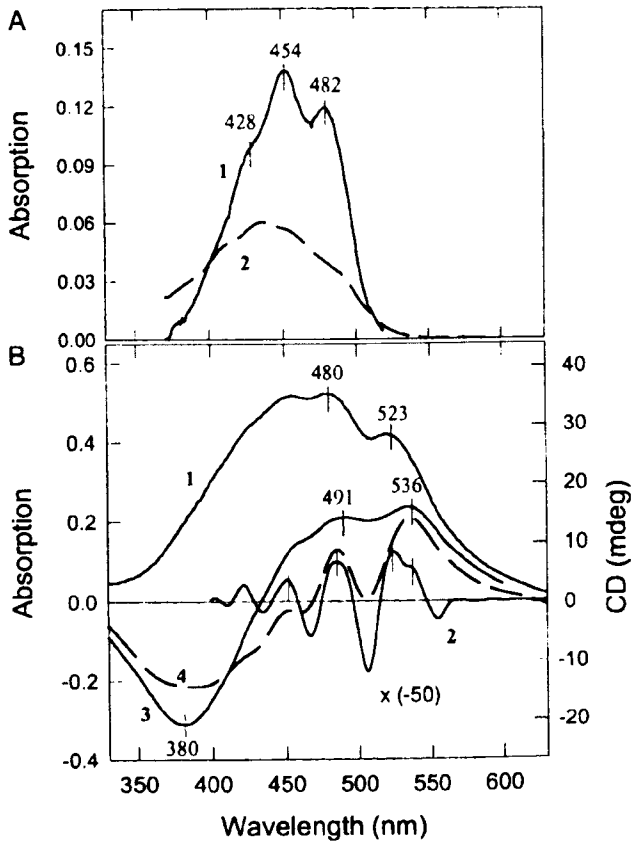

Fig. 3. (*A*) Absorption spectra of zeaxanthin in ethanol (1) and in detergent buffer used in reconstitution experiments (2). (*B*) 1, Absorption spectrum of PsbS reconstituted with zeaxanthin; 2, second derivative of spectrum 1; 3, CD spectrum of PsbS reconstituted with zeaxanthin; 4, simulated CD spectrum of two excitonically coupled zeaxanthin molecules with the higher and lower exciton components at 507 and 536 nm, respectively.

aqueous buffer minus PsbS causes a quite different effect (Fig. 3*A*, trace 2): the appearance of the slightly blue-shifted bands, arising probably from some aggregation of zeaxanthin, similar to that described (23). A spectrum the same as trace 2 was obtained when zeaxanthin was mixed with BSA dissolved in buffer (not shown). Under the same reconstitution conditions, there was no evidence of formation of a complex between violaxanthin and PsbS; there was no difference between the absorption spectra of violaxanthin mixed with PsbS and with the detergent buffer alone.

The PsbS–zeaxanthin complex displayed a CD spectrum not found for either constituent alone. There were positive bands at 491 and 536 nm and a strong negative band at 380 nm (Fig. 3*B*, trace 3). These negative and positive symmetrical features can be attributed to the negative and positive Cotton effects of excitonically coupled pigments (24), suggesting that two zeaxanthin molecules are interacting. Indeed, because the CD spectrum has a differential nature, it can be modeled by using two shifted-absorption spectra. Fig. 3*B* (trace 4) represents the difference between spectrum 1 and the same spectrum with a 15-nm blue shift. It is clear that both the negative and positive parts resemble those of the CD spectrum (trace 3). The only difference is that the positive group of bands is better resolved, and there is a clear minimum at 507 nm, the higher excitonic component. This difference could be due to a presence of the band at 525 nm, which is seen clearly in the second derivative absorption spectrum (trace 2). This transition could belong to a monomeric zeaxanthin bound to the protein. These features of the CD spectrum demonstrate that PsbS can exert strong effects on the properties of zeaxanthin, indicative of binding.

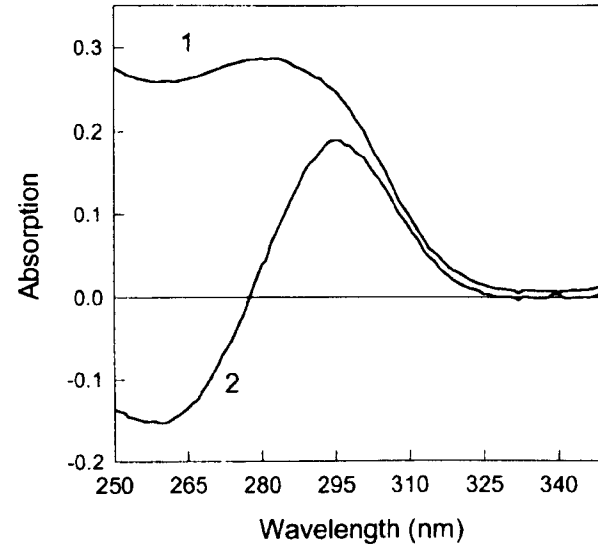

Fig. 4. UV absorption spectrum of PsbS reconstituted with zeaxanthin (1) and a (PsbS + zeaxanthin) (PsbS only) absorption difference spectrum (2).

It was noted also that the absorption spectrum of PsbS in the UV region was altered by the presence of zeaxanthin; the absorption band at 258 nm, arising mainly from phenylalanine (see Fig. 2*A*), was shifted to 280 nm (Fig. 4, spectrum 1). The conserved nature of the corresponding difference spectrum shows that the change can be explained by a red shift in a population of phenylalanine residues in the PsbS sample (Fig. 4, spectrum 2). This is further evidence of a rather specific interaction between zeaxanthin and PsbS.

In vivo, the appearance of the red-shifted zeaxanthin was associated with characteristic features in the RR spectrum (14). The ν_4 region of the RR spectrum arises from wagging vibrations of various C–H groups (25), and bound red-shifted zeaxanthin *in vivo* displays five new transitions not found in zeaxanthin dissolved in detergent or solvent. This zeaxanthin "fingerprint" is shown in Fig. 5 (spectrum 1), in comparison with the rather featureless spectrum of zeaxanthin in detergent micelles (spectrum 3). The *in vitro* PsbS–zeaxanthin complex displayed an almost identical RR spectrum to that associated with qE (spectrum 2). The two major bands at 954 and 963 cm^{-1} were the same *in vivo* and for the PsbS–zeaxanthin complex, although the minor bands varied slightly in intensity and position in the two spectra.

Discussion

The dissipation of excitation energy in PSII, qE, correlates strongly to an absorption change at 535 nm (12, 13). Recently we showed that the 535-nm change could be explained by a strong red shift in the absorption spectrum of one to two molecules of zeaxanthin (14). The appearance of red-shifted zeaxanthin absorbing at 523–525 nm, compared with ≈505 nm in the absence of qE, gives rise to a band at 535 nm in the qE difference spectrum. Here we provide evidence to support the hypothesis that this "activated" zeaxanthin is bound to PsbS, because we successfully reconstituted a zeaxanthin–PsbS complex that shows a similarly strong red shift to ≈523 nm. This shift was found to be sufficient to give rise to a 535-nm band in a difference spectrum calculated by subtracting an absorp-

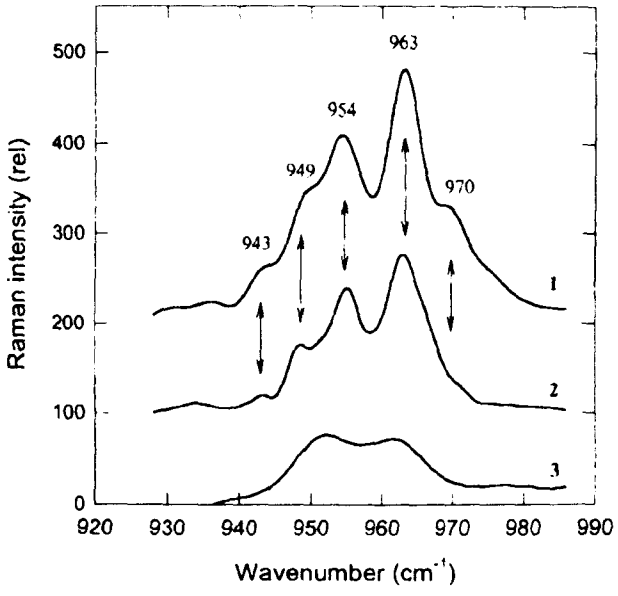

Fig. 5. RR spectra of zeaxanthin in ν_4. 1, qE-activated zeaxanthin absorbing at 535 nm (modified from ref. 14). 2, zeaxanthin bound to PsbS obtained as described for Fig. 3; and 3, zeaxanthin in detergent-lipid micelles purified on a sucrose gradient (modified from ref. 14). The arrows indicate the five main transitions associated with zeaxanthin activation.

tion spectrum of "nonactivated" zeaxanthin, simulated by using a spectrum recorded in CS_2 as described (14). Therefore, these data represent the first direct link between zeaxanthin and PsbS, which both play vital roles in qE (6, 15). The data also provide an explanation of why the 535-nm change is absent in the *npq4* mutant of *Arabidopsis*, which lacks this protein (15).

The zeaxanthin–PsbS complex has several important features. In addition to the large red shift in the absorption spectrum of zeaxanthin, there is a strong CD spectrum of zeaxanthin with a conserved nature and an alteration in the UV-absorption spectrum of the protein. These features indicate that PsbS provides a highly polarizing environment that strongly affects the photophysical properties of zeaxanthin and, conversely, that zeaxanthin binding alters the structure of PsbS, precisely the helical regions, which contain all the phenylalanine residues. Specifically, it is in the predicted fourth helix, present in PsbS but not in the Lhcb proteins (21, 22), that numerous phenylalanine residues are found, suggesting that this region of the protein provides the binding site for zeaxanthin. Violaxanthin does not appear to bind to this site. *In vivo*, zeaxanthin is bound to all the Lhcb proteins (7, 8), and *in vitro* zeaxanthin can induce fluorescence quenching in these proteins (26–28). However, thus far we have not observed any red shifts in the absorption spectra of zeaxanthin bound to these proteins (29). It is interesting that in *Chlamydomonas*, mutation of the Lhcbm1 protein results in a loss of qE (30). It is possible that in this organism, the much weaker qE (compared with higher plants) is controlled by zeaxanthin binding to LHCII.

The features of the CD spectrum of the zeaxanthin–PsbS complex can be interpreted as resulting from two processes. First, there is an excitonic interaction between two bound zeaxanthin molecules (507- and 535-nm components of a splitting), consistent also with the upper estimate of two molecules bound (both *in vitro* and *in vivo*). Second, there is binding of a single pigment with absorption shifted to ≈520 nm. The presence of these two effects indicates some heterogeneity in the binding stoichiometry in the complex. The enhancement of the RR spectrum of zeaxanthin provides further compelling evidence of a strong and specific interaction between zeaxanthin and PsbS, which establishes a particular configuration of the bound zeaxanthin. Moreover, the changes in the absorption and RR spectrum after reconstitution of the zeaxanthin–PsbS complex have the same features found *in vivo*, suggesting that the binding of zeaxanthin to PsbS *in vitro* is mimicking a similar process occurring *in vivo*.

These conclusions add considerably to the understanding of the chain of events that lead to energy dissipation in PSII under excess light conditions. The two factors that control this process are the thylakoid ΔpH and the deepoxidation of violaxanthin to zeaxanthin. The interaction between these factors, in which zeaxanthin is an allosteric activator of qE (9, 10), suggests that they bind to the same protein or protein complex. Recently, evidence has been obtained that certain carboxyl amino acids on PsbS are essential for qE formation (31). Here we show that PsbS can bind zeaxanthin, and the features of this binding are consistent with a similar binding associated with *in vivo* qE (14), suggesting that the qE-associated activation of zeaxanthin arises because of its binding to PsbS. We should point out that zeaxanthin binding to PsbS *in vitro* was not pH-dependent (data not shown). We suggest that *in vivo*, binding is prevented by structural constraints imposed by the local environment in the thylakoid membrane. A conformational change in PsbS induced by protonation of these carboxyl amino acids would be necessary then for zeaxanthin binding.

The subsequent event, how the protonated PsbS–zeaxanthin complex is able to interact with the antenna chlorophyll to bring about dissipation of excited states, of course, is not resolved. However, given the abundant evidence of the intrinsic quenching capabilities of isolated light-harvesting proteins (26–28) and the similarities between this process and *in vivo* qE (3), the most favored hypothesis is that an interaction between PsbS and one or more of these proteins controls the dissipation process (32). We suggest that this interaction is controlled in turn by the protonation and binding of zeaxanthin to PsbS. The successful reconstitution of PsbS and zeaxanthin reported here should enable further testing of this hypothesis.

This work was supported by a grant from the United Kingdom Biotechnology and Biological Sciences Research Council (to P.H.) and grants from the Joint Infrastructure Fund and Joint Research Equipment Initiative (to the Department of Molecular Biology and Biotechnology, University of Sheffield).

1. Björkman, O. & Demmig-Adams, B. (1995) in *Ecophysiology of Photosynthesis: Ecological Studies*, eds. Schulze, E. D. & Caldwell, M. M. (Springer, Berlin), pp. 14–47.
2. Horton, P., Murchie, E. H., Ruban, A. V. & Walters, R. G. (2001) *Novartis Found. Symp.* **236**, 117–134.
3. Horton, P., Ruban, A. V. & Walters, R. G. (1996) *Annu. Rev. Plant Physiol. Plant Mol. Biol.* **47**, 655–684.
4. Niyogi, K. K. (1999) *Annu. Rev. Plant Physiol. Plant Mol. Biol.* **50**, 333–360.
5. Külheim, C., Ågren, J. & Jansson, S. (2002) *Science* **297**, 91–93.
6. Demmig-Adams, B. (1990) *Biochim. Biophys. Acta* **1020**, 1–24.
7. Ruban, A. V., Young, A. J., Pascal, A. A. & Horton, P. (1994) *Plant Physiol.* **104**, 227–234.
8. Ruban, A. V., Lee, P. J., Wentworth, M. W., Young, A. J. & Horton, P. (1999) *J. Biol. Chem.* **274**, 10458–10465.
9. Ruban, A. V., Wentworth, M. & Horton, P. (2001) *Biochemistry* **40**, 9896–9901.
10. Wentworth, M., Ruban, A. V. & Horton, P. (2001) *Biochemistry* **40**, 9902–9908.
11. Gilmore, A. M., Shinkarev, V. P., Hazlett, T. L. & Govindjee (1998) *Biochemistry* **37**, 13582–13593.
12. Ruban, A. V., Young, A. J. & Horton, P. (1993) *Plant Physiol.* **102**, 741–750.
13. Bilger, W. & Björkman, O. (1994) *Planta* **193**, 238–246.

14. Ruban, A. V., Pascal, A. A., Robert, B. & Horton, P. (2002) *J. Biol. Chem.* **277,** 7785–7789.
15. Li, X.-P., Björkman, O., Shih, C., Grossman, A. R., Rosenquist, M., Jansson, S. & Niyogi, K. K. (2000) *Nature* **403,** 391–395.
16. Funk, C., Schroder, W. P., Napiwotzki, A., Tjus, S. E., Renger, G. & Andersson, B. (1995) *Biochemistry* **34,** 11133–11141.
17. Dominici, P., Caffarri, S., Armenante, F., Ceoldo, S., Crimi, M. & Bassi, R. (2002) *J. Biol. Chem.* **277,** 22750–22758.
18. Berthold, D. A., Babcock, G. T. & Yocum, C. F. (1981) *FEBS Lett.* **134,** 231–234.
19. Bowlby, N. R. & Yocum, C. F. (1993) *Biochim. Biophys. Acta* **1144,** 271–277.
20. Laemmli, U. K. (1970) *Nature* **227,** 680–685.
21. Kim, S., Sandusky, P., Bowlby, N. R., Aebersold, R., Green, B. R., Vlahakis, S., Yocum, C. F. & Pichersky, E. (1992) *FEBS Lett.* **314,** 67–71.
22. Wedel, N., Klein, R., Ljungberg, U., Andersson, B. & Herrmann, R. G. (1992) *FEBS Lett.* **314,** 61–66.
23. Ruban, A. V., Horton, P. & Young, A. J. (1993) *J. Photochem. Photobiol. B* **21,** 229–234.
24. Zsila, F., Bikadi, Z. & Simonyi, M. (2002) *Tetrahedron: Assymetry* **13,** 273–283.
25. Robert, B. (1999) in *The Photochemistry of Carotenoids*, eds. Frank, H., Young, A., Britton, G. & Cogdell, R. (Kluwer, Dordrecht, The Netherlands), pp. 189–201.
26. Ruban, A. V., Young, A. J. & Horton, P. (1994) *Biochim. Biophys. Acta* **1186,** 123–127.
27. Ruban, A. V., Young, A. J. & Horton, P. (1996) *Biochemistry* **35,** 674–678.
28. Wentworth, M., Ruban, A. V. & Horton, P. (2000) *FEBS Lett.* **471,** 71–74.
29. Ruban, A. V., Pascal, A., Lee, P. J., Robert, B. & Horton, P. (2002) *J. Biol. Chem.* **277,** 42937–42942.
30. Elrad, D., Niyogi, K. K. & Grossman, A. R. (2002) *Plant Cell* **14,** 1801–1816.
31. Li, X.-P., Phippard, A., Pasari, J. & Niyogi, K. K. (2002) *Funct. Plant Biol.* **29,** 1131–1139.
32. Horton, P., Ruban, A. V. & Wentworth, M. (2000) *Philos. Trans. R. Soc. London B* **355,** 1–10.